UNIVERSIDAD POLITÉCNICA DE MADRID

ESCUELA TÉCNICA SUPERIOR DE
INGENIEROS DE MINAS Y ENERGÍA

BIODIESEL AND BIOKEROSENES:

PRODUCTION, CHARACTERIZATION, SOOT & PAH EMISSIONS

Autor:

ALBERTO LLAMAS LOIS
Ingeniero de Minas

Madrid 2015

DEPARTAMENTO DE ENERGÍA Y COMBUSTIBLES

ESCUELA TÉCNICA SUPERIOR DE INGENIEROS DE MINAS Y ENERGÍA

BIODIESEL AND BIOKEROSENES:

PRODUCTION, CHARACTERIZATION, SOOT & PAH EMISSIONS

Autor:

ALBERTO LLAMAS LOIS
Ingeniero de Minas

Directores:

LAUREANO CANOIRA LÓPEZ
Dr. En Ciencias Químicas

MARÍA JESÚS GARCÍA MARTÍNEZ
Dra. Ingeniera de Minas

Madrid 2015

TABLE OF CONTENTS

Chapter I: INTRODUCTION

Chapter II: MATERIALS AND METHODS

Chapter III: RESULTS AND DISCUSION

Chapter IV: CONCLUSIONS

Resumen:

Con el objetivo de consolidar el trabajo en biocombustibles del grupo de investigación al que pertenece el autor, esta tesis doctoral se centra en el desarrollo de las técnicas necesarias para continuar con la investigación del grupo.

En esta tesis se ha estudiado la producción de FAME de diferentes fuentes de aceites y grasas no comestibles: camelina, ricino, jojoba, linaza, aceite de freír usado y grasa animal. Estos FAME se han caracterizado para determinar su idoneidad como combustibles.

En esta tesis se muestra la producción y posterior destilación de FAME a partir de aceite de palma, babassú y coco. Los esteres que resultan de este proceso son compuestos saturados de cadena corta que tienen propiedades similares a las del keroseno. El autor sugiere utilizarlos hasta una cierta cantidad en mezclas de keroseno fósil como biokeroseno.

El autor también ha estudiado el uso de la glicerina como materia prima en la industria química para la producción de 1,3-ditertbutoxypropan-2-ol, un aditivo para mejorar la calidad de la ignición.

La combustión de materia orgánica conlleva a la formación de hollín. La tendencia a formar hollín de mezclas de compuestos oxigenados con keroseno. En esta tesis también se han caracterizado los PAH, precursores del hollín, a partir de la combustión de FAME y FAEE de diferentes materias primas.

Abstract:

Targeting the consolidation of the work from the author's research group on biofuels, this PhD thesis is focused on developing the necessary techniques to continue with the group's research.

In this thesis the production of FAME from different non-edible sources of oils and fats: camelina, castor oil, jojoba, linseed, waste frying oil and animal fat, has been studied. These FAME have been characterized in order to assess their suitability as fuels.

The author has also studied use of bioglycerol, the main by-product in biodiesel production, as a chemical feedstock for the production of 1,3-ditertbutoxypropan-2-ol, a recognized ignition quality improver.

In this thesis, production and further distillation of FAME from palm kernel, babassu and coconut oils is reported. The esters mixtures resulting from this process are saturated low carbon number compounds which have similar properties to those of kerosene. Therefore, the author suggests to use them up to a certain amount in fossil kerosene as biokerosene blends.

The combustion of organic matter leads to soot formation. The sooting tendency of oxygenated blends with fossil kerosene is studied. The soot precursors, PAH, from the combustion of FAME and FAEE from different feedstocks are also characterized in this thesis.

TABLE OF CONTENTS

1 INTRODUCTION

This doctoral thesis has been carried out under the "Investigación, Modelización y Análisis del Riesgo en Medio Ambiente" (Research, Modelling, and Environmental Risk Assessment) Master's doctorate program. Focusing in setting up a research laboratory centred on biofuels within the former department of Chemical Engineering and Fuels (Universidad Politécnica de Madrid), now included in the new department of Energy and Fuels. Therefore, the path that has been followed was to create a general work that would allow the development of quality research, encompassing the main issues related to the environmental aspects of biofuel production and use, not solely focusing on one aspect.

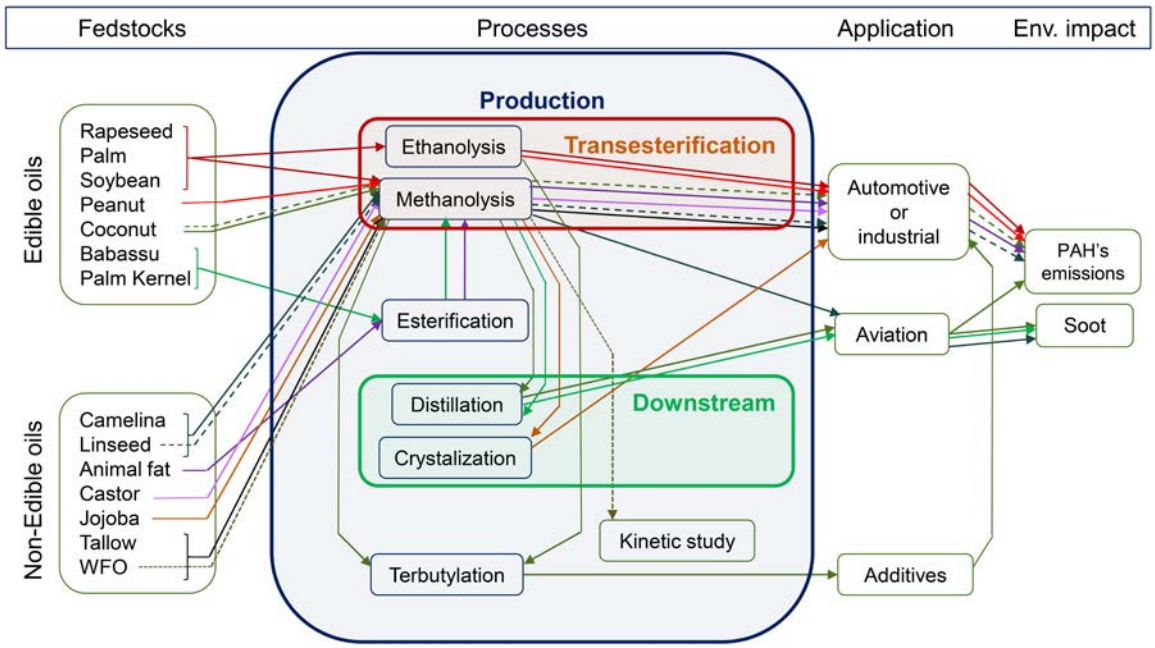

Figure 1. Outline of the goals of the thesis.

Within this benchmark, the work is based on this environmental approach required by the doctorate program, the topics (outlined in Figure 1) that have been studied are:

- the production of biodiesel from non-edible sources that could be used in internal combustion engines.
- the production of biokerosenes from Fatty Acid Methy Esters (FAME).
- the PAH and soot emissions produced in the combustion of FAME and FAEE.
- and the production of additives from bioglycerol.

Concerning FAME from non-edible sources, the production of FAME from low grade animal fat that could be mixed with soybean oil FAME fulfilling the specifications has been studied. Additionally, biodiesel production from commonly used raw materials, waste frying oil (WFO) and horse tallow was accomplished. The transesterification of waste frying oil has been studied with more detail and the kinetic parameters of the processes could be studied.

Then, the collaboration with biofuels manufacturers such as Combustibles Ecológicos Biotel S.L., opened the path to study less commonly used materials. It began with the development of a method of producing biodiesel from jojoba oil-wax - a plant native to Mexico - and the evaluation of its properties as a fuel. The production of a biofuel from castor oil (*Ricinus communis*) has been studied as well.

The manufacturing of biokerosene from coconut, palm kernel, babassu (a coconut species from Brazil and Africa); linseed and camelina meeting most of the specifications required for use in aircraft engines has been carried out in order to extend the use of biofuels for the aviation sector.

Once the production angle was dealt with. The author proceeded with the characterization of biodiesel and biokerosene in order to assess their suitability as biofuels and in blends with fossil fuels.

Additionally, the synthesis of additives for improving the behaviour of biodiesel in combustion engines, and the characterisation of exhaust emissions has also been studied. Specifically, the work was new production routes for additives from by-products of the manufacturing process

This step was to consider the most important by-product of the biodiesel manufacture: glycerine. A new synthetic route for the production of 1,3-di-tert. butoxypropan-2-ol as an additive to fossil diesel or biodiesel was studied in order to provide a new process where glycerine could be used as a feedstock. 1,3-di-tert. butoxypropan-2-ol is also a good cetane number improver.

The next step was the characterisation of exhaust emissions from combustion engines. To cover this field, research was performed in collaboration with other laboratories. There were two areas of focus:

- the Polycyclic aromatic hydrocarbons (PAHs) emissions, and
- the development of a new method for the study of PAHs produced during combustion

This additional focus was given to the study of PAHs since they are the most dangerous compounds from the human health risk point of view

This kind of research needs the collaboration of much greater laboratories than that of the author. Therefore, a new much simpler method for the study of the compounds produced during combustion of biodiesel was developed.

THIS WORK HAS ALLOWED TO DEVELOP MODELS THAT EXPLAIN THE PAH'S PRODUCED FROM BIODIESEL DEPENDING ON THE BIODIESEL TYPE AND ON THE COMBUSTION CONDITIONS.

The approach followed in this doctoral thesis has a clear advantage allowing formative work in many fields related to the production and development of biofuels, and as a further result setting up a research laboratory in which to develop the teaching of biofuels in new degrees of Energy Engineering. On the other hand, it has led to a more succinct level of analysis in the final result than what is usual in a work of this kind, the decision was taken out of the belief that the benefits of this approach justify the chosen path.

2 BIODIESEL

Biodiesel is defined as "a fuel comprised of monoalkylesters of long chain fatty acids derived from vegetable oils or animal fats" (1). The first time the term "biodiesel" showed up was in (Wang, 1988) (2) and, since in 1983 M. Mittelbach (3) proved the viability of the transesterification products as fuel, the usage of this term has been more and more restricted to the mono alkyl methyl esters. Transesterification (also called alcoholysis) of triglycerides for biodiesel manufacture has been extensively studied in the past few years in the author's research group (4, 5, 6) and others (7, 8, 9, 10, 11, 12). FAME from vegetable oils have shown promise as biodiesel, as the result of improved viscosity, volatility and combustion behaviour relative to triglycerides, while maintaining its cetane number (around 50). FAME biodiesel is also compatible with conventional diesel, and the two can be blended in any proportion, although the ignition quality of the blends remains essentially the same as that of the conventional diesel (13). Transesterification (also called alcoholysis) of triglycerides has been studied intensively by numerous investigators (14), and more than a dozen US Patents, the most mentioned being that of Bradshaw and Meuly(15), and many European processes have been issued (16).

Biodiesel, considered as "a substitute for, or an additive to diesel fuel that is derived from the oils and fats of plants and animals" (17) has found favour in the markets of Europe and United States in the past years. Currently, renewable biodiesel fuels are the most promising alternative to partly replace fossil diesel fuel consumption. The European Union Council in 2007 had set an objective to secure motor biofuels a market share of 10% of total motor fuel consumption by 2020 and has issued Directive 28/2009/EC, (18) which mandates the use of biofuels in a percentage to 10 % in 2020 (calculated on the basis of energy content) for all transportation fuels marketed within the member states, and it is expected that a significant portion of this amount will be biodiesel due to the growing "dieselisation" of the fuel markets in some European countries. This directive that sets down its specifications is already transposed to most countries and does not only specify this objective but sets a number of sustainability conditions. In a similar way, the US Department of Energy estimates that up to 50 % of the total diesel fuel consumption could be replaced with biodiesel (19).

However the global economic scenario in the last years is holding back the biodiesel production in most European countries since the financial aids are disappearing in many of them.

THE MAIN ADVANTAGES OF USING THIS ALTERNATIVE FUEL ARE ITS RENEWABILITY, BETTER QUALITY EXHAUST GAS EMISSIONS (AS IT DOES NOT CONTAIN SULPHUR), ITS BIODEGRADABILITY AND, GIVEN THAT ALL THE ORGANIC CARBON PRESENT IS INVOLVED IN A CLOSE CARBON CYCLE, IT DOES NOT CONTRIBUTE TO A RISE IN THE LEVEL OF CARBON DIOXIDE IN THE ATMOSPHERE, AND CONSEQUENTLY TO THE GREENHOUSE EFFECT (16).

Consequently, the production and use of biodiesel fuels was expected to noticeably increase in the next years. Although, since late 2007, and mainly during 2008 (20) biofuels have been subjected to great controversy which is still present on the scientific literature (21) due mainly to food crops competition and high producing prices derived from the feedstock price rises.

However, the 2008 food crisis is still being discussed and the causes are not clearly correlated to energy vs food crops competition since the low stocks seemed not an important cause of the crisis (22). Shenggen attributes the rises in food price to the reach of underlying macroeconomic phenomena that affected all sorts of commodities. The argument against the oilseeds that are the object of this work is weakened if we consider that the rise in the demand of energy crops affected maize much more than it affected oilseeds.

Tyner points also in the same direction (23) and attributes the steep rise in food prices to many factors that include global supply and demand trends, regional or commodity specific supply disruptions, changes in the value of the US$, macroeconomic issues such as recession or financial crisis, trade policy changes, and biofuels.

While Ji and Fan (24) assure that crude oil market volatility affects in a greater way than any other the volatility of every other commodity. Eccleston argues about the possibility of having reached a peak food (25), a similar concept to peak oil, i.e. a maximum of the crop production per inhabitant curve. In the last 20 years, rice and wheat production have stayed practically stable, as have other vegetables and fruits (21) while maize and oilseed production have sharply increased to the detriment of animal feed crops. Taheripour, Hurt and Tyner's opinion is that the biofuels boom and higher feed prices have slowed growth rates in the world's livestock sector. That effect is expected to diminish as corn ethanol production will not grow significantly in the future. Although, direct and indirect land use change will still be an issue. Therefore, these and many other authors (26, 27) claim that food, energy and biofuel policies must respond to this situation.

Biodiesel can be synthesized from a variety of feedstocks, including vegetable oils, animal fats and used cooking oils. Usually, refined vegetable oils are the main feedstock for biodiesel production. However, in the last few years, the prices of these refined vegetable oils (soybean, rapeseed, palm and others) have been increasing steadily (28), making the biodiesel production from these feedstock unprofitable in many locations. Waste greases such as used cooking oil and animal fats can also be used as feedstock because of their availability and low cost (29, 30, 31, 32, 33, 34, 35, 36) and (37).

As it has been mentioned previously, in case that these increasing quantities of biodiesel fuels come from non-used vegetable oils, it has been recently claimed that the biodiesel promotion could derive in a shortage of raw materials for feed purposes and a steep rise of food prices, which could lead to poverty in some regions (38, 39). This situation could be avoided by the use of second generation biodiesel fuels (i.e. from wastes, agricultural residues or non-food crops (40, 41, 42) but their associated technology is currently being developed. Therefore, different less valuable feedstock should be considered, such as waste cooking oils/fats (known in the literature as yellow and brown greases (43, 44)) and animal fats collected from supermarkets, slaughterhouses, etc. Both greases and animal fats represent a large share of the total oil and fat production, and their potential is increasing continuously (29) .

Due to the alleged competition of biodiesel from edible oils in the food crops market, both, edible oils and other sources are treated separately when it comes to biodiesel. Hence, this work will consider them separately.

3 BIODIESEL FROM NON-EDIBLE SOURCES

3.1 Biodiesel from low grade animal fat.

Animal fats have also been used without transformation to improve the rheological properties of fuel-oil (45). The use of these waste greases to produce biodiesel opens a route to recycle this waste that otherwise would finish in the drain or could only be sold as feedstock for the soap industry. Moreover, animal fats are considered low quality feedstock compared to refined vegetable oils because of their free fatty acids (FFA) content that may increase up to 15 % wt. by contrast with refined soybean oil which typically contains less than 0.5 % wt. FFA. In 2007, the price of this yellow animal fat was around 419 € / t(28) by contrast with the soybean oil of 780 € / t [(28) and has increased till the current prices in 2012 (between 700 € / t and 710 € / (28) t for animal fat and 931 € / t for soybean oil (28). Soybean oil reached its historical maximum price in €, 941 € / t on February 2011. This increase in the prices of animal fat, and also of WFO, the price of which has risen from practically free to 820 € / t (28) in 2012 finds its ground in its commercial use as biodiesel feedstock. Because of this price difference, the use of waste animal fat feedstock for biodiesel production could be a reasonable way to lower the overall biodiesel production costs. Moreover, the quality, engine performance and emissions of harmful compounds originated from animal-fat-derived biodiesel have already been evaluated (46, 47), and so has the safety of a biodiesel production process using prion-contaminated animal fat as a feedstock (48, 49).

Regarding the animal fats, these are classified into three categories, according to their health risk level, by the Regulation 1774/2002 (50). Most of the animal fats used by different industries fall into category number 3, which is free of risk and has the wider availability. Another commonly-used classification is based on the free fatty acids (FFA) content of the animal fats, distinguishing low, medium and high grade (or quality) fat. High grade animal fats, with a very low FFA content (below 2%), are used for human and animal (mainly livestock) food and cosmetics industry. Their high prices (above 750 €/ton) prevent them from being used as biodiesel feedstock. Medium grade fats have 3-5% FFA content and a sell price of 625 €/ton, approximately, and they are mainly used for poultry fodder production. Finally, low grade animal fats, with a FFA content above 5% and a sell price of 600 €/ton, approximately, are used in both the fodder and biodiesel industry. Sometimes, biodiesel manufacturers also use blends of medium and low grade animal fats as feedstock in order to reduce their FFA content. It should be noticed that during the production process of rendered animal fats, composed by several stages such as crushing, cooking, draining, filtering and depuration, the sulphur content of the animal fat product is progressively reduced. But only after the final depuration stage the sulphur (which may occur during the pre-treatment) content is low enough for biodiesel production, as this compound is limited in fuel quality normative.

Moreover, the current high prices of most vegetable oils have encouraged the use of low-priced waste sources in biodiesel plants. In fact, lately, most of the Spanish biodiesel plants that used vegetable oils as their raw material had no choice than to stop their production as a consequence of the high market prices (51). Only those plants that use waste-cooking oils and/or animal fats, apart from those which purchased large quantities of vegetable oils when prices were lower, are currently able to produce biodiesel fuels in Spain with a final sell price similar to that of fossil diesel fuel.

With regard to sustainability, the Directive for the promotion of the use of energy from renewable sources (18), approved by the European Commission, establishes a mandatory minimum reduction of greenhouse gas emissions of 35% with respect to petroleum diesel fuel.

The default value initially considered for this relative saving is 77% in the case of both waste cooking oil and animal fats biodiesel fuels, while the typical value (obtained in the Directive by reducing in 40% the CO_2 emissions of the production processes) rises up to 83%. These values are the highest among all the raw materials contemplated in the Directive, which constitutes a considerable advantage for both waste cooking oils and animal fats.

Encinar et al. (52) studied the transesterification from high FFA (between 4% and 14%) animal fats both via alkali and acid catalysis and with and without pre-esterification. Their results showed fairly good biodiesel yields (between 89 % for the acid catalyst and 97 % for the alkali catalyst) when they used pre-esterification, they achieved a reduction to 0.5 % of FFA. Dias et al. (53) produced biodiesel from mixtures of vegetable and waste oils and animal fat; their production yields varied from 81.7 to 88.8 wt. % and fulfilled the European quality standards. They modelled the composition and some properties of the final product from the mixture composition and showed an optimum of at least 12 % usage of lard in a soybean oil /lard mixture. Morales et al. (54) produced biodiesel from low-grade oils and fats via acid catalysis using arenesulfonic acid-functionalized SBA-15 silica providing yields close to 80 % in a simultaneous esterification and transesterification. The high concentrations of unsaponifiable matter in these particular feedstocks reacted with the catalyst and deactivated it, turning its recuperation and reutilisation more difficult, but a previous washing in presence of a cationic exchange resin and following drying of the raw materials improved the FAME yield in the second use of the catalyst. García et al. (55) compared the ethanolysis and methanolysis of low free fatty acids (< 1 % wt.) animal fat (tallow, crude lard and commercial lard) using sodium ethoxyde and methoxyde respectively. They achieved good conversion yields between 78 % and 87 % and the biodiesel reached most of the EN 14 214 specifications.

Several advantages and disadvantages of the production and use of biodiesel from animal fats have been pointed out in the literature. Biodiesel fuels from animal fats are typically more saturated than those from vegetable oils (56, 57), involving the following properties:

- a higher cetane number that reduces the amount of fuel burnt in the premixed fraction of the combustion process
- lowering the combustion noise and NOx formation, and
- better oxidation stability improvement when additives are added to meet biodiesel fuel quality requirements.

On the other hand, animal fats have commonly:

- a high content of free fatty acids, so a previous esterification process is usually needed to reduce it before entering the transesterification reactor, and
- poor cold flow properties that could prevent them from being used in cold climates.

TO OVERCOME THE DISADVANTAGES MENTIONED, BLENDING ANIMAL FATS WITH VEGETABLE OILS IS AN ALTERNATIVE.

3.2 Biodiesel from tallow and used vegetable oil.

Bio-fuels large-scale production is often criticized because it could turn agricultural production away from food crops, especially in developing countries. The basic argument is that energy-crop programs compete with food crops and thus could cause food shortages and price increase. Recently, following the cost increase of food items around the world these critiques have increased. Therefore, and also because of the benefit in the reduction of liquid waste and the subsequent burden off sewage treatment, biodiesel from waste frying oils (WFOs) seems like an interesting approach (37). Furthermore, regarding the European Directive, 28/2009/EC, there's a bonus on the calculation of the CO_2 emissions concerning the biodiesel coming from waste sources such as animal fat and waste oils, this bonus benefits the global LCA (Life cycle analysis) result following the directive. The main benefit in using waste animal fat and oil probably is its cost since it is a much cheaper feedstock than conventional and edible oils. Once the main problems concerning biodiesel from WFO production, i.e. free fatty acids (FFA) and polymerized triglycerides are dealt with, Kulkarni and Dalai (58) stated that this FAME implies even better engine performance and less emissions than reference diesel fuel when tested on commercial diesel engines based on the result from works such as (59, 60).

The mean consumption of edible oils in Spain is shown in Table 1; most of these oils are used in frying pans or fryers, and, after a variable time of use, are discarded. The waste frying oil was mostly thrown through the home drain, with the water pollution that this current practice implies. Moreover, as more than 80% (Table 1) of the oil is consumed at home, the control of this disposal behaviour is very difficult. In most parts of the world edible oils are used in frying pans or fryers and after a variable time of use are discarded. These waste frying oils have different properties from those of refined and crude vegetable oils. The presence of heat and water accelerates the hydrolysis of triglycerides and increases the content of free fatty acids (FFA) in the oil (61). The FFA and water content have significant negative effects on the transesterification reaction (62).

In Spain, edible vegetable oil consumption is approximately 800 ML y^{-1}. Most of this oil (70 %) is olive oil that is mainly used for deep-frying processes. According to the Spanish National Institute of Statistics, about 74 ML of waste olive oil are collected per year, which is an approximate value since most of the household waste frying oil is thrown through the drainage. In this way, transesterification of waste olive oil to produce biodiesel could decrease the waste disposal problem.

Many residential villages in Spain have launched pioneering programs to recover all the waste frying oil in wasted oil containers (capacity 500 L); the containers are emptied and cleaned twice a week, and the used oil is transported to a factory for processing.

Table 1: Consumption of edible oils in Spain

Oils	Home ML	Restaurants ML	Institutions ML	Total	Home (%)	Restaurants (%)	Institutions (%)
Olive	360.59	34.67	6.82	402.08	89.68	8.62	1.70
Sunflower	247.01	67.72	28.25	342.98	72.02	19.74	8.24
Corn	4.36	0.36	0.00	4.73	92.28	7.72	0.00
Seeds	16.67	5.35	0.38	22.39	74.42	23.87	1.71
Soybean	2.65	1.11	0.00	3.76	70.45	29.55	0.00
Other	24.74	3.03	0.01	27.78	89.08	10.90	0.02
Total	656.02	112.24	35.46	803.72	81.62	13.96	4.41

Form the Statistical Yearbook of Spanish Ministry of Agriculture, Fisheries and Food, Official Statistics of Spain

On the other hand, the consumption of animal fats such as tallow is in very big decline as a result of a change in the feeding habits of the population (Table 2) and the soap industry cannot take up all the exceeding animal fats produced.

Table 2: Tallow uses in Spain

	ML
Animal feeding	140.0
Industrial uses	375.0
Transformation	30.8
Human consumption	125.0
Total uses	670.8

Form the Statistical Yearbook of Spanish Ministry of Agriculture, Fisheries and Food, Official Statistics of Spain

Although the alkali catalysed transesterification involves a number of problems when dealing with high free fatty acids and water (both are commonly presented in WFO) due to soap formation, its usage is widely spread. The most common alkali catalysts are NaOH and KOH and there are many studies published related to WFO and those two catalysts (63, 64, 65, 66). Dorado et al. (67) carried out the transesterification of WFO (palm oil and Brazilian hydrogenated fat with 5.12% FFA, Spanish olive oil with 2.24% FFA and a mixture of several other German vegetable oils with 1.28% FFA), using KOH as catalyst. A two-step transesterification process was carried out using a stoichiometric amount of methanol and the necessary amount of KOH and sufficient quantity of KOH to neutralize the FFA. It was concluded that a two-step transesterification process without any costly purification steps is a good method for biodiesel production from WFO of different origins with FFA less than 3%. Çayli and Küsefoglu (68) have compared one-step and two-step base-catalysed room temperature transesterification reaction of waste frying oil, the two-step process showed higher yields and better (reduced) alcohol and catalyst usage. Dorado et al. and Encinar et al. (69, 70) compared catalytic activities from NaOH and KOH and the best results (best biodiesel properties and a quicker reaction) showed up for KOH. Leung and Guo (71) compared $NaOCH_3$, NaOH and KOH. Saifuddin and Chua (72) investigated the effect of microwave irradiation on the biodiesel from WFO production and Chen et al. (73) recently published a work where they improved the yield in transesterification of WFO by microwave heating using $NaOCH_3$ as a catalyst. Gan et al. (74) studied the esterification of free fatty acids in waste frying oil with methanol in the presence of ferric sulphate/active carbon catalyst and the effects on the conversion of FFA of different temperature, methanol/FFA mole ratio and amount of catalyst.

Knothe et al. (75) shows that differences between WFO and virgin crude oil are not always very noticeable. However, in some cases, the products of decomposition caused by frying deplete oil quality and should be pretreated. Common pretreatments are found in Kularkani and Dalai's review (58), e.g.: steam evaporation, column chromatography, neutralisation, film vacuum evaporation and vacuum filtration.

Kularkani and Dalai's review (58) work also regarded acid WFO. Zhang (76) proposed an empirical first order kinetics for the acid WFO catalysis and afterwards Zheng (77) showed that it is a pseudo-first order reaction. The catalytic activities of different $H2SO_4$ and HCl in the WFO transesterification are compared in Al-Widyan and Al-Shyoukh's work (78). To avoid the saponification derived from alkali catalysis and the slow reaction time when using acid transesterification, Lepper among other authors (79, 80, 81) have carried out two steps alkali-acid reactions but this method deals with the problem of separating the catalyst after both steps.

Hancsok et al. and other authors (81, 82, 83) report enzymatic catalysis of WFO biodiesel using lipases where reactions are insensitive to water content from WFO. Marchetti et al. (84) pointed out the main advantages and disadvantages of using lipases as a catalyst. Among the advantages are:

- the possibility of regeneration and the reuse of the immobilized residue since it can be left in the reactor
- the high concentrations allowed and thus the long activation of the lipases
- the better thermal stability of the enzyme
- the immobilisation of the lipase protects it from the solvent and prevents the enzyme particles getting together and an easier separation of the catalyst.

On the other hand, the disadvantages are:

- the volume of the oil molecule which reduces the initial activity
- the number of support enzyme is not uniform and biocatalysts are more expensive than natural enzymes.

On their review, Enweramadu and Mbarawa (85) sorted a list of the most relevant variables influencing the final yield concerning oil transesterification in general, but applicable to WFO: FFA and water content in the oil, reaction temperature, molar alcohol to oil ratio, catalyst employed, type of alcohol, concentration of catalyst, reaction time, stirring intensity and the use of co-solvents.

3.2.1 Kinetics of the transesterification of waste olive oil.

Although the literature concerning the production of biodiesel has increased dramatically in the past recent years (7, 8), the data related to the kinetics of transesterification are rather scarce: Freedman et al. (9) presented the kinetics and final state of methano-, ethano- and butanolysis of cottonseed, peanut, soybean and sunflower oils catalysed by sodium hydroxide and methoxide or sulphuric acid. Mittelbach and Trathnigg (10) studied the kinetics of methanolysis of sunflower oil catalysed with KOH. Bikou et al. (86) described the effect of water on the kinetics of cotton oil ethanolysis catalysed by KOH. Diasakou et al. (11) studied the kinetics of the non-catalytic transesterification of soybean oil at 220 and 230 ºC. Kusdiana and Saka (87) described the kinetics of transesterification of rapeseed oil to biodiesel fuel in supercritical methanol without any catalyst, and Komers et al. (12) described the kinetics and mechanism of the KOH catalysed methanolysis of rapeseed oil for biodiesel production. Moreover, Boocock et al. (88) have studied the kinetics of methoxide base-catalysed methanolysis of soybean oil at 40°C. As said before, the same team on (77) and on (89) proposed a fist order kinetics and a pseudo-first order kinetics respectively for acid catalysed transesterification of waste frying oil.

3.3 Biodiesel from Jojoba oil wax.

Jojoba (*Simmondsia chinensis*) is a perennial shrub that grows naturally in the Sonora desert (Mexico) and in the South-West of the USA. Jojoba is now cultivated in some countries: Argentina (2.0 kt y^{-1}), Israel (1.1 kt y^{-1}), USA (1.0 kt y^{-1}) and some Mediterranean and African lands are the main seed producers (data are for the campaign 2002-03). In the early 2000s there were 7930 ha of Jojoba planted in the world (90).

The Jojoba seed has a nut-shaped form and is around 1-2 cm long, with red-brown to dark-brown colour. This seed contains between 45-55 % wt. of Jojoba oil-wax, a golden liquid that can be obtained by cold pressing or solvent extraction (91). Unlike vegetable oils and animal fats, Jojoba oil is not a triglyceride, but a mixture of long chain esters (97-98 %wt.) of fatty acids and fatty alcohols, and therefore is more properly referred to as a wax; however, Jojoba oil-wax is the term in general use. Jojoba oil-wax contains minor amounts of free fatty acids and alcohols, phytosterols, tocopherols, phospholipids and trace amounts of a triacylglycerol which have been carefully analysed (92). These minor constituents have also an economical interest and a pilot-scale plant for their extraction has been built (93).

Jojoba oil-wax has a low chemical reactivity and a very high normal boiling point (398 ºC) that gives this product very important physico-chemical properties and uses. One of the first uses of the

Jojoba oil-wax in the 1970's was the substitution of the sperm whale oil, when whale hunting was banned worldwide, but it has many other uses in cosmetics, pharmaceuticals, dietetic foods, animal feeding, lubrication, polishing and gardening (94). The structure of the Jojoba oil-wax is shown in figure 2.

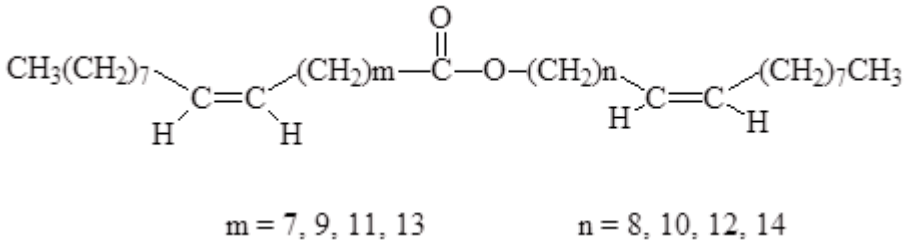

Figure 2. General chemical structure of the Jojoba oil-wax components.

Transesterification (also called alcoholysis) of triglycerides for biodiesel manufacture has been extensively studied in the past few years (4), but the transesterification of Jojoba oil-wax has received much less attention (95). Selim et al. (96) have published a paper on the combustion of Jojoba methyl esters in an indirect injection diesel engine.

Moreover, the feasibility of the commercial use of Jojoba methyl ester as biodiesel is strongly dependant of the added value (around 0.84 € kg^{-1}) (97) obtained for the fatty alcohols produced as secondary products in the transesterification process, since the maximum price of the Jojoba oil-wax for making the process economically attractive is 0.75 € kg^{-1} (98), far less than the actual market price of the Jojoba oil-wax in USA (1.89 € kg^{-1}), although a much lower price of 0.80 € kg^{-1} has been reported in Egypt (99).

3.4 Biodiesel from castor oil.

In the last few years, the prices of refined vegetable oils (soybean, rapeseed, palm and others) have been increasing steadily (28), making the biodiesel production from these feedstock unprofitable in many locations. Castor oil (the oil extracted from the plant *Ricinus communis L.*, popularly known as castor bean, castor oil plant, higuerilla, mamona, mamoeira, palma Christi) has been a feedstock in great demand by the pharmaceutical and chemical industries (100). However, the use of castor oil as a biodiesel feedstock would be feasible only if the castor oil prices currently paid (825 €/t) (28) decreased considerably.

Implementing castor oil for biodiesel will not be easy due to its properties based on its composition. Berman et al. (101) concluded that due to its high ricinoleic acid content (Figure 3) its use is limited to 10% in diesel blends and stated that castor oil biodiesel does not meet itself many ASTM requirements such as viscosity. Scholz and Da Silva (100) stated that it should be taken into account in small-scale farming structures since castor requires a large amount of hand labour, although it might be a more interesting option in a future. Da Silva et al. (102) suggested that most problems for castor oil biodiesel finding its way through in Brazil were related to the castor plant production. Pradhan et al. (103) sketched an optimisation of reactive extraction of castor oil from the seed in order to produce biodiesel. Finally, Lavanya et al. (104) screened various *Ricinus* genotypes for biodiesel production in India.

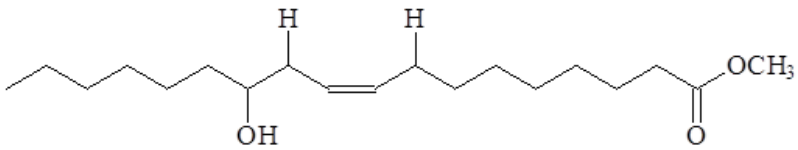

Figure 3. Methyl Ricinoleate

The data on the transesterification of castor oil are rather scarce in the recent literature if they are compared with the general literature on biodiesel: Silva et al. (105, 106), Plentz- Meneghetti et al. (107, 108, 109), De Oliveira et al. (110), as well as other authors (111, 112) have studied the alcoholysis of castor oil using classical catalysts and have evaluated the influence of different reaction parameters in the yield of FAME and FAEE; Hincapie et al. (113) compared conventional with in situ transesterfication using n-hexane as cosolvent, and Pena et al. (114) studied the effect of catalyst and cosolvent . Pereira-Fagundes et al. (115) have studied the production of FAME from castor oil and the rheological properties of its blends with fossil diesel fuel; Conceiçao et al. have carried out the synthesis and the thermoanalytical (116) and rheological (117) characterisation of FAME from castor oil as well as its oxidative behaviour (118) and this researcher with others have also made dynamic calculations on the thermal stability of the raw oil and the FAME and FAEE derived from this oil, Conceiçao et al. and other authors (119, 120, 121, 122) also studied these parameters. Varma and Madras (123) have carried out the synthesis of castor oil FAME in supercritical CO_2. Encinar et al. (124) tried transesterification under ultrasonic irradiation while Pradhan et al. (103) studied transesterification of castor oil by microwave and ultrasound radiation using a SrO catalyst. Coelho et al. (125) studied the influence of variables in the purification of castor oil biodiesel. Jeong and Park among other authors (126, 127, 128) developed different process optimisations for castor oil transesterification. Panwar et al. (122, 129, 130) discussed the performance of castor oil biodiesel blends in diesel engines.

4 BIOKEROSENE: PRODUCTION AND PROPERTIES OF THEIR BLENDS WITH FOSSIL KEROSENE

The aviation companies are facing three problems that argue in favour of biofuels:

- rising cost of traditional fuel
- price volatility
- environmental concerns.

According to the International Air Transport Association (IATA), the global market for jet fuel represents a 10 % slice of all transportation fuels (242 billion L /year). The cost of conventional jet fuels has been soaring; in 2010, airlines spent $ 139 billion in jet fuel, an 11 % increase over the precedent years, but the fuel itself was 30 % more expensive, however gains in jet fuel hedging and efficiency overcame part of this increase. Jet fuel costs represent around 30 % of operating expenses for airlines on average, up from 14 % in 2003. A typical great airline consumes 41 million L a day, at a cost of $ 35 million / day ($ 25000 / minute). An increase of one dollar in the crude barrel price costs this company some additional $ 100 million a year (131).

The world economy is strongly dependent on oil prices, and the main oil reserves are located in social and politically unstable countries which causes great fluctuations in the crude oil and petroleum products prices. From January 2003 to July 2008, the jet fuel price increased 462 %, reaching $ 3.89 / gallon. Due to the world economic crisis, the jet fuel price dropped to $1.26 /gallon in February 2009, but since then this price has been steadily increasing, and it was $ 3.09 / gallon in January 2012. These fluctuations and the very foreseeable future ones have led to many countries try to develop a diversified fuel market less dependent of the crude oil imports (132).

The literature on the production and use of biofuels for the aviation sector is still scarce and in some cases contradictory. Dunn (133) studied the properties of a fuel obtained blending 10- 30 % vol. of soybean FAME with JP-8 and JP-8+100. Dagault and Gail (134) examined the oxidation behaviour of a blend of 20 % vol. rapeseed FAME with Jet-A1. Korres et al. (135) compared the behaviour of the jet fuel JP-5 against fossil diesel and animal fat biodiesel in a diesel engine. Wagutu et al. (136) prepared six biofuels from jatropha, croton, calodendrum, coconut, sunflower and soybean, and they concluded among other findings that the coconut FAME is the biofuel that approaches most closely to the fossil jet fuel properties.

On the Bio-SPK (Synthetic paraffinic kerosene) issue, Kinder and Rhams (137) reported the hydrotreating and isomerisation of vegetable oils to produce a kerosene range of hydrocarbons, which had a very similar chemical composition to the fossil jet fuel. In this technology, the oil, once refined, was hydrogenated to remove the oxygen atoms and to saturate the olefinic double bonds which increased the heating value of the fuel and its thermal and oxidative stability; the ulterior isomerisation and cracking of the diesel range paraffins yielded a typical kerosene fraction called Bio-SPK. Some blends of 50 % vol. of Bio-SPK with Jet-A1 have been tested in air flights of three different companies.

The American Society for Testing Materials has published recently the approved methods for the production of alternative jet fuels that are basically the Fischer-Tropsch hydroprocessed synthesized paraffinic kerosene (FT-SPK) and the hydroprocessed esters and fatty acids (HEFA). The actual situation of the production of renewable jet fuels, including the feedstock, the jet fuel input and the technology used is summarized in table 3 (131).

The actual situation of the production of renewable jet fuels, including the feedstock, the jet fuel input and the technology used has been clearly summarized recently (131), with a predominance of the HEFA technology over the alcohol-to-jet or pyrolysis-to-jet and FT technologies. Moreover, Chuck et al have investigated different jet biofuels and very interestingly they have calculated the payload range of them (138). Another research team has evaluated some blends for use as jet biofuels in the tropics (139) and also some authors have reviewed the current situation in aviation biofuels in the frame of the European ITAKA group (140). More recently, a work has been published on blends of sesquiterpanes and 5-methylundecane, generated from biomass sugars by a combination of fermentation and chemical catalysis, which may allow for their production at industrially relevant scales and that shows good properties as jet fuel (141).

Table 3: Renewable jet fuels

COMPANY	FEEDSTOCK	JET FUEL INPUT	TECHNOLOGY	PARTNERS
ENERGY CROP FIRMS				
Agrisoma Biosciences	Carinata	Vegetable oil	HEFA	UOP
SG Biofuels	Hybrid jatropha	Vegetable oil	HEFA	Bunge; Flint Hills Resources
AltAir Fuels	Camelina	Vegetable oil	HEFA	UOP; Boeing
BIOFUELS FIRMS				
Amyris	Cane sugar	Biofarnesene	Direct fermentation	Total
Gevo	Corn sugar; cellulose	Isobutyl alcohol	Alcohol-to-jet	U.S. Air Force Research Lab
KiOR	Biomass	Hydrocarbon	Pyrolysis-to-jet	Hunt Refining
Lanzatech	Waste gas; lignin	Ethanol	Alcohol-to-jet	Swedish Biofuels; Boeing; Virgin Atlantic
Sapphire Energy	Sunlight; CO2	Algal oil	HEFA	Boeing
Solazyme	Cane sugar	Algal oil	HEFA	Dynamic Fuels; United; U.S. Navy
Virent	Sugar; cellulose	Hydrocarbon	Unknown	Shell; U.S. Department of Energy
REFINING FIRMS				
Neste Oil	Camelina; jatropha; animal fat	Vegetable oil; fats	HEFA	Lufthansa
Rentech	Forest waste	Synthesis gas	Fischer-Tropsch	Ontario government

5 PRODUCTION OF ADDITIVES DERIVED FROM GLYCEROL

Since 2000 the production of biodiesel has been increasing exponentially due to the aim of governments to meet Kyoto protocol and for other environmental reasons (142). The rise in biodiesel production brought about a subsequent increase of that of bioglycerol, by-product from the former. The bioglycerol excess enters in an already saturated market, which has led to a dramatic reduction of the economic value of glycerol as raw material (143).

The final destiny of this bioglycerol excess resulting from biodiesel production has traditionally been energetic valorisation (144) by joint combustion with methane to generate electrical power. This application is not considered to be optimum, as it does not generate a significant economic benefit.

Alternative applications of bioglycerol are under investigation in industrial chemistry (145, 146, 147) for its conversion into valuable chemicals. One of the bioglycerol derivatives that has received much attention is glycerol carbonate (148, 149, 150, 151, 152, 153, 154). Acrolein could also be obtained from bioglycerol on HZSM-5 zeolite (155). Bioglycerol could be also a valuable feedstock for industrial microbiology (156).

One of these possible applications of bioglycerol is the transformation into oxygenated additives for fuels, as 1,3-di-tert-butoxypropan-2-ol. Octyl nitrate (prepared by esterification of 2-ethyl-1-hexanol with nitric acid) is an additive currently added (from 10 to 1000 mg L-1) to conventional diesel fuel to enhance its cetane number and its combustion properties. Ether additives of glycerol are compatible with diesel and biodiesel fuels (157, 158) and are also excellent additives for these fuels (159, 160). These additives are mixed with biodiesel for different purposes, such as to increase the energetic efficiency of the fuel and its stability and to lower the emissions (161). Oxygenated additives improve the combustion by reducing the amount of air needed in the process and therefore lowering the nitrogen oxides in the resulting exhaust gases. A Japanese patent (162) has been issued on the use of 1,3-di-tert-butoxypropan-2-ol as a diesel additive in 0.2-10.0 % vol. to improve the combustion and to lower the particulate and VOC's emissions.

Tertbutylation of bioglycerol with isobutylene or terc-butanol has been referred in the literature using ion-exchange resins (163, 164, 165, 166, 167, 168), zeolites (167, 168, 169, 170), mesostructured silicas (171) and other catalysts (172, 173, 174, 175). According to these authors, the bioglycerol conversion producing tert-butyl oxygenated additives using acidic catalysts reaches to about 50%. However, some years ago the author tried to etherify bioglycerol with pure isobutylene over Amberlyst-15 catalyst in a fixed-bed experimental reactor without any success. He obtained only the trimerisation of isobutylene with good yield and selectivity, but the bioglycerol was recovered totally unchanged (176).

6 PAH and soot emissions.

6.1 PAH Occurrence during combustion of biodiesel from various feedstocks

The European legislators may eventually require oil companies to take actions that ensure concomitant reduction in aromatic emissions. PAH are produced in combustion processes from fossil and renewable fuels. It is important to understand the mechanisms that lead to the formation of these aromatic compounds during the combustion. (177) PAHs are the contaminants of most concern regarding the aromatic emissions and they are considered as the major pollutants generated from engines (178). The burning of fossil fuels is the main source of anthropogenic PAH emission (179), specifically, exhaust emission is the most important contributor for PAH in urban areas (180, 181).

PAHs are hydrocarbons with a fused ring structure containing several benzene rings that may carry alkyl substituents. PAH occurrence in exhaust gases may be driven by:

a) survival, the fuel PAH may survive the combustion process, retaining the original carbon skeleton
b) pyrosynthesis during combustion from lower molecular weight aromatic compounds, the PAH isolated in the exhaust emissions could be produced by a process whereby fragments of partially destroyed compounds could recombine to produce the new PAH, and others having the same structures as those from the fuel, destroyed in the combustion process from various fuel sources (177, 182);
c) pyrolysis of unburned fuel and lubricating oil: the pyrolysis products were shown to accumulate in motor oil, raising the amount of PAHs from undetectable in fresh oil to substantial amounts in used oil (e.g., 190 $\mu g\ g^{-1}$ phenanthrene, 650 $\mu g\ g^{-1}$ methylphenanthrenes, and 50 $\mu g\ g^{-1}$ chrysene)(183).

When the temperature exceeds 500 ºC, carbon–carbon bonds are broken to form free radicals. These radicals combine to form etylene and 1, 3-butadiene which further condenses with aromatic ring structures, that are resistant to thermal degradation (181). In their review, Ravindra et al. (180) discussed about PAH source attribution and referred that three possible mechanisms suggested of PAH formation during combustion, i.e. slow Diels–Alder condensations, rapid radical reactions, and ionic reaction mechanism. However, the radical formation mechanism is favoured as the combustion process within the internal combustion engine has to occur very rapidly. It seems that gaseous hydrocarbon radicals rearrange quickly, providing the mechanism of PAHs formation and growth. The addition of

hydrocarbon radicals to lower molecular weight PAHs then leads, via alkyl PAHs, to the formation of higher PAHs. Recently, Lima et al. (183) reviewed and discussed some of the factors (type of fuel, amount of oxygen, and temperature) that affect the production and environmental fate of combustion-derived PAHs. While PAHs are present at ambient temperature in air, both as gas and associated with particles, the lighter PAHs, such as phenanthrene, are found almost exclusively in gas phase whereas the heavier PAHs, such as Benzo[a]pyrene, are almost totally adsorbed on particles (181).

Karavalakis (181, 182) sketched an alternative Diels-Alder reaction between two FAME compounds that is consistent with the analyses done in this thesis. However the large size of FAME molecules suggests that this is a less probable mechanism.

Regarding PAH and biodiesel combustion, many works have been published (178, 181, 184, 185, 186, 187), but few of them have studied its relation with the biodiesel composition (181, 188, 189, 190) and not one of them compared the combustion products depending on the alcohol group, FAME or FAEE. This thesis describes the production of PAH in the combustion of FAME and FAEE with different pure oxygen pressures in a bomb calorimeter, and it correlates the amount and type of PAH produced with the fatty acid profile of the biodiesel.

6.2 Biokerosene soot emissions:

Airplane emissions have a great global impact due to the height of emission. Carbon dioxide, water and nitrogen and sulphur oxides, sulphates and airborne particles have different effects depending of the height of emission. At ground level, these emissions have only local or regional effects, but the emissions at flight height could have an impact in the global atmosphere leading to global warming. According to the Aerial Transport Action Group (191), the 2092 world airlines transport actually more than two billion passengers per year in a fleet of around 23000 airplanes, with a prevision of double number of passengers for the year 2031 (192). Transport in general is responsible of the 23 % of world greenhouse gas emissions, and the aviation sector shares 12 % of the total carbon dioxide emissions (670 Mt in 2012) while road transport accounts for 74 %. The emissions of an airplane turbine are the result of the combustion process of the jet fuel, and it is here where the use of more efficient fuels with less carbon content could diminish these emissions without the need to modify substantially these turbines. Plane's emissions at large airports are important sources of local air pollution including fine particulate matter which can increase people's risk of heart disease and asthma (193).

On the other hand, on December 20th 2006 the European Commission approved a law proposal to include the civil aviation sector in the European market of carbon dioxide emission rights [European Union Emissions Trading System, EUETS). On July 8th 2009, the European Parliament and Council agreed that all flights leaving or landing in the EU airports starting from January 1st 2012 should be included in the EUETS. On November 19th 2008, the EU Directive 2008/101/CE (194) included the civil aviation activities in the EUETS, and this directive was transposed by the Spanish law 13/2010 of July 5th 2010 (195). Thus, in 2012 the aviation sector should reduce their emissions a 3 % of the mean values registered in the period 2004- 2006, and for 2013 these emissions should reach 5 % of the mean values for that same period. Trying to face this situation, the aviation companies are seriously planning the use of alternative jet fuels to reduce their greenhouse gas emissions and to lower their costs. However, some US airlines have issued a lawsuit before the European Court of Justice based on the fact that this EU action violates a long-standing worldwide aviation treaty, the Chicago convention of 1944, and also the Chinese, Indian and Russian airlines have rejected to pay the EU carbon dioxide tax (196).

On September 22nd 2012, the US Senate passed unanimously a law (S. 1956) that would authorize the Transportation Department to prohibit US airlines from participating in the EU's cap-and–trade system for greenhouse gas emissions; also, the House of Representatives passed a measure (H.R. 2594) similar to the above (197).

The International Civil Aviation Organisation (ICAO), A United Nations agency that regulates air travel, in its Global Framework Alternative Air Fuels (GFAAF) initiative and resolution A37-19 propose a 2 % increase in the air fuel efficiency for 2020, and an additional 2 % from 2020 to 2050, calculated on the basis of fuel volume per ton-km transported (198).

In Spain, The Biokerosene Spanish Initiative propose to fabricate 200,000 t / year of biokerosene in 2020 (2-4 % of total fuel consumption) (199) in the frame of the European program Enterprise 2020.

Moreover, the USA Departments of Agriculture and Energy and the Navy will invest a total of up to $150 million over three years to spur production of aviation and marine biofuels for commercial and military applications (200). Trying to face this situation, the aviation companies are considering seriously the use of alternative jet fuels to reduce greenhouse gas emissions and to lower their costs. However, these alternative jet fuels should fulfil a set of extraordinarily sensible properties to guarantee the safety of passengers and planes during the flights (201).

Some authors have approached the jet fuel alternatives from biological sources from a totally different perspective, that is, the use of the Fischer-Tropsch (FT) synthesis and the synthetic paraffinic kerosenes of biological origin (Bio-SPK). On the former issue, Hileman et al. (202) analyzed the chemical composition and the energy content of different jet fuels, showing that the biokerosene obtained by FT synthesis or hydrotreating of renewable oils can reduce the energy expenditure of planes by 0.3 %. Cottineau (203) claimed that UOP has developed a biokerosene from jatropha that surpasses the properties of actual jet fuels. World News (204) referred to the construction of two pilot plants in France based in the PRENFLO process from Udhe which were due to come on stream in 2012 to produce biodiesel and biokerosene from syngas, obtained from biomass by FT technology (205).

However, alternative jet fuels included in Table 3 (section 4, page 19) have a common drawback: they lack of oxygen in their molecular structures, since fatty acid methyl esters (FAME) is not approved as an additive for jet fuel. The maximum allowable level is 50 mg/kg, which is accepted by approval authorities as the functional definition of "Identified Incidental Material" (206). The presence of oxygen in a fuel has two main advantages:

a) it reduces the carbon content of the fuel, which in turn would reduce its carbon footprint and,
b) it reduces also the soot formation (emission) of the fuel.

Numerous studies both experimental and numerical confirmed that oxygenated fuel additives reduce soot formation in engines (207). Moreover, a study has found that particulate matter emissions from a plane's engine can fall by almost 40 % when researchers blend jet fuel with alternative fuels.

7 OBJECTIVES AND SCOPE

7.1 Production of FAME from non-edible sources.

Several sources of non-edible fats and oils have been submitted to transesterification. Once the Biodiesel was obtained, it has been characterized to assess its suitability as a fuel in internal combustion engines.

- *Biodiesel from waste*

1 *Producing* FAME from low grade animal fat and mixing it with soybean oil FAME to achieve a product that meets the specifications.

Different mixtures of waste animal fat and soybean oil as feedstock for biodiesel production have also been studied, since the biodiesel obtained exclusively from animal fat could hardly meet the EN 14214 or ASTM D6751 standards specifications, and some parameters of the biodiesel obtained with each one of these mixtures as feedstock have been analysed.

2 *Producing* FAME from waste frying oil (WFO) and tallow.

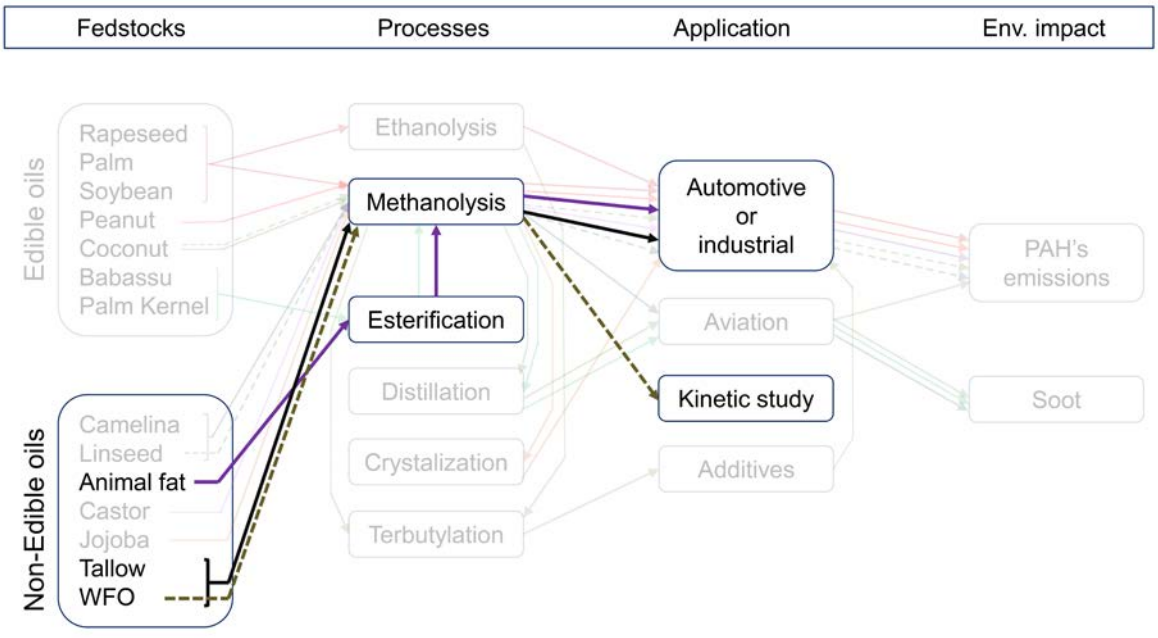

Figure 4a. Production of FAME from waste

A more specific objective related to the WFO transesterification is

2.1 Calculating the kinetics parameters of the transesterification of waste frying oil.

- *FAME from non-edible plants.*

3 *Reporting* the methods of transesterification with methanol of Jojoba oil-wax with acid and basic catalysis, and the procedure of separation of methyl jojoboate (the fraction rich in FAME) from jojobyl alcohol (the fatty alcohols rich fraction) by crystallisation. A preliminary evaluation of some properties of methyl jojoboate as a diesel fuel (viscosity, density, cold filter plugging point and higher heating value) will also be reported.

4 *Producing* FAME from castor oil that could be blended with fossil diesel fuel for its use as a fuel in internal combustion engines.

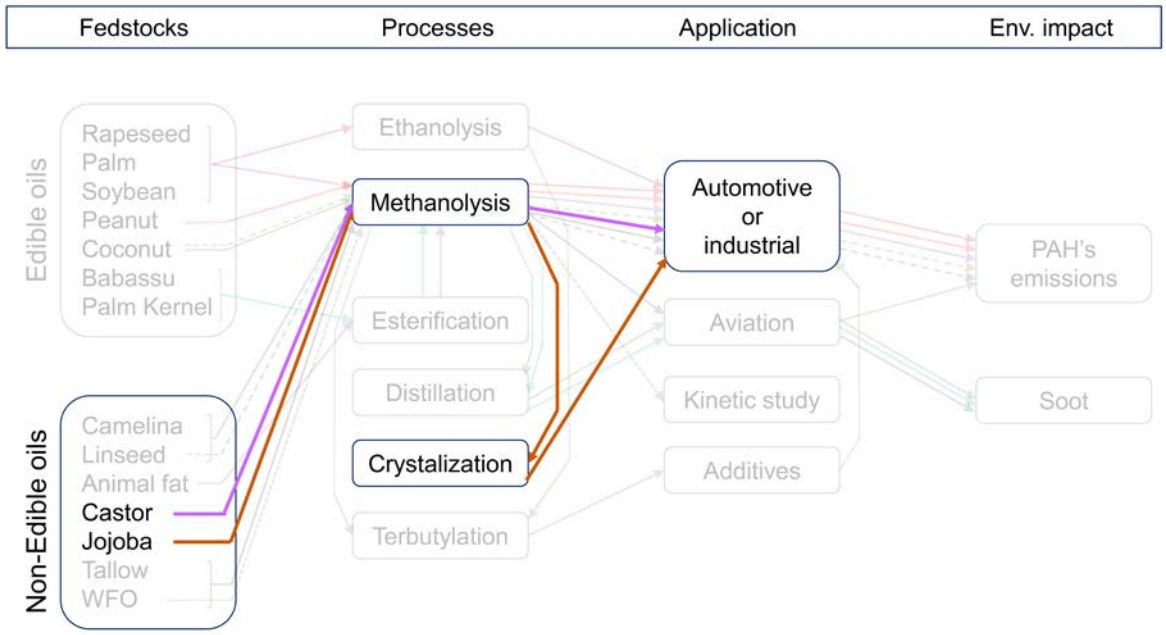

Figure 4b FAME from non-edible plants

This work deals with the transesterification of castor oil with methanol to produce FAME that could be blended with fossil diesel fuel for its use as a fuel in internal combustion engines. We intently avoid the name of biodiesel for the FAME obtained from the transesterification of castor oil, since the extremely high viscosity and high water content of this FAME discard its use in pure form as a fuel in internal combustion engines.

7.2 Production of biokerosenes.

5 *Producing* FAME from oil and distillate FAME from babassu, coconut and palm kernel oil and mixing them with fossil kerosene in order to develop a new product that could meet the specifications and partially replace fossil kerosene on a jet engine.

6 *Producing* biodiesel from linseed and camelina oil to study the sooting tendency of these non-edible highly unsaturated FAME, intended for use in blended form in aviation turbine engines.

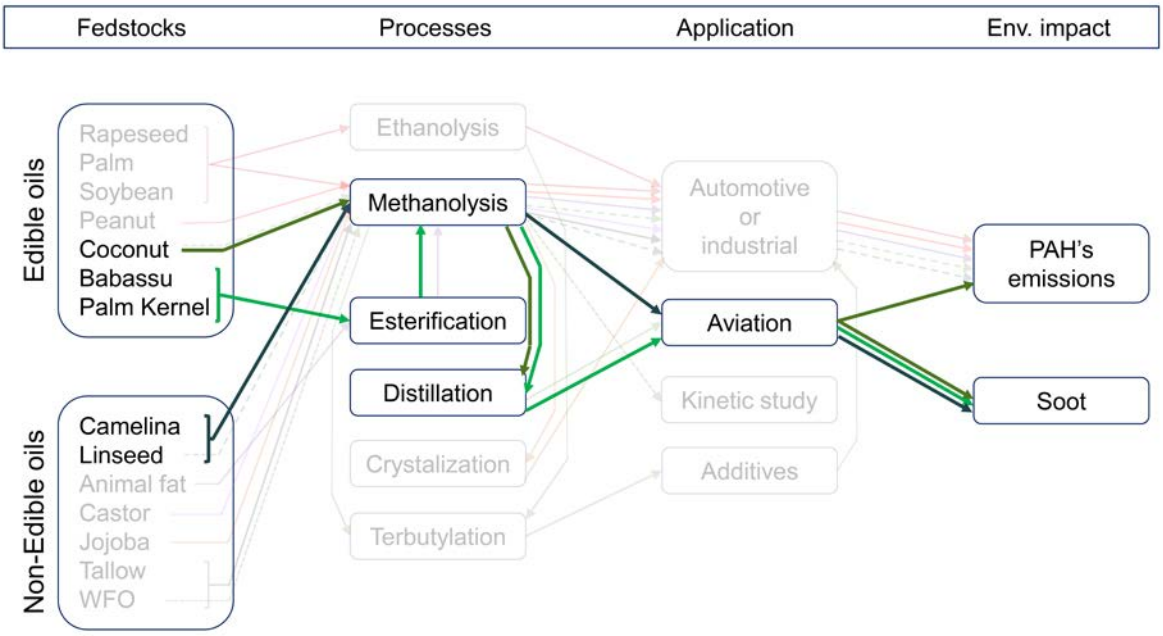

Figure 4c *Production of biokerosenes*

Two different approaches have been followed to obtain a fuel suitable for aviation.

a) FAME from oils rich in saturated short chain fatty acids: coconut, palm kernel and babassu, a palm popular in Brazil were synthesized [17], and then the fraction which approaches the distillation range of fossil kerosene, that is, from 175-185 °C to 240-275 °C at atmospheric pressure, was separated by vacuum distillation. Since this pure biokerosene did not meet the different aviation jet fuel standards, blends containing 5, 10 and 20 % vol. of biokerosene with fossil kerosene with and without additives, were tested together with pure biokerosene. The bottom fraction of the FAME distillation of babassu, coconut and palm kernel, which can reach up to 50 % of the FAME, has also been tested in order to check if it accomplishes by itself the EN 14213 standard for heating biodiesel, or needs to be blended with other

FAME to find this application. Another use of this bottom fraction could be as a marine transport biofuel.

b) FAME from camelina oil and linseed oil very rich in unsaturated methyl esters (84.0 % wt.) were blended without previous distillation at 5,10 and 20 % vol. with fossil kerosene without additives. The excellent cold flow behaviour of these unsaturated methyl esters suggested direct blending without previous distillation.

7.3 Production of additives from glycerol

7 *Describing* a new synthetic route for the production of 1,3-di-tert-butoxypropan-2-ol as an additive for fossil diesel or biodiesel, different from the etherification process of glycerol with isobutylene or tert-butanol.

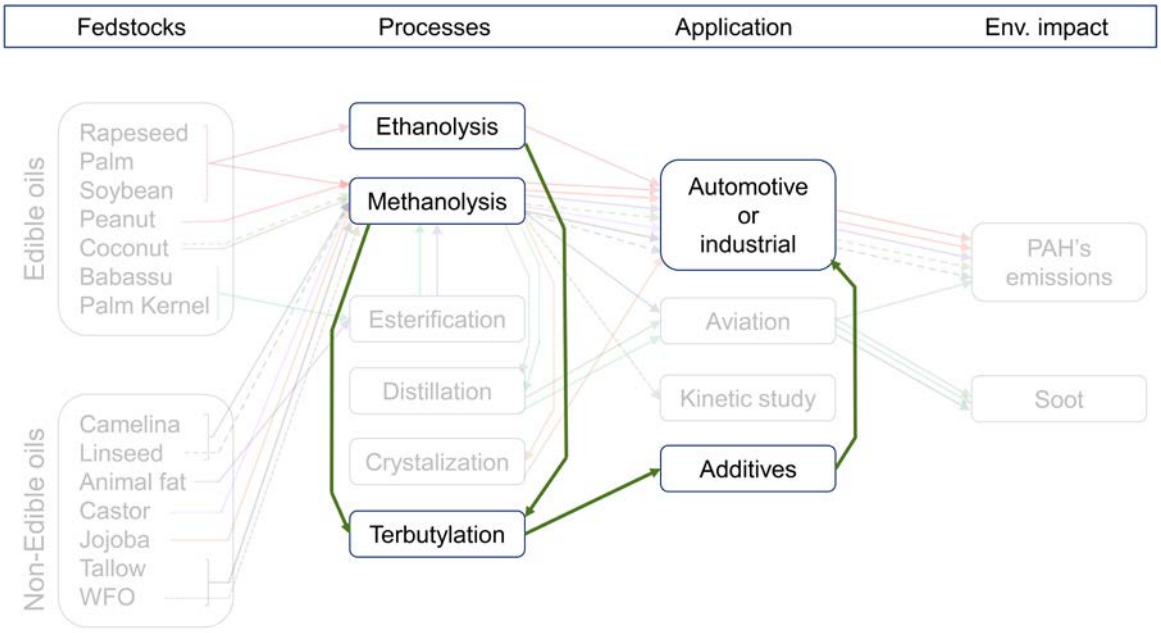

Figure 4d Production of additives from glycerol

On the subject of biodiesel's main by-product, glycerol, the aim of this work is to describe a new synthetic route for the production of 1,3-di-tert-butoxypropan-2-ol as an additive for fossil diesel or biodiesel, different from the etherification process of glycerol with isobutylene or tert-butanol. Solvay has recently developed a process to obtain epichlorohydrin from bioglycerol (208, 209, 210), instead of the classical route from propylene, (view Scheme 1). In this Thesis, the synthesis of 1,3-ditert-butoxypropan-2-ol in a three steps process is described, starting from epichlorohydrin and tert-butanol as raw materials, (view

Scheme 2). Since terc-butanol is obtained by hydration of isobutylene, and epichlorohydrin is obtained from bioglycerol in the Solvay route, the process described could be considered as an alternative, however longer, to the direct etherification of bioglycerol with isobutylene to obtain 1,3-di-tert-butoxypropan-2-ol, that, otherwise never reaches quantitative results. Our process converts completely the starting compounds to 1,3-di-tert-butoxypropan-2-ol.

1) The first step consists of obtaining 1-chloro-3-tert-butoxypropan-2-ol (chlorohydrin ether) **1** by reaction of epichlorohydrin with tert-butanol, catalysed by boron trifluoride etherate.
2) The second step is the reaction of the chlorohydrin ether **1** obtained in the first step with a strong basic solution of 50 % wt. sodium hydroxide to obtain 3-tert-butoxypropylene-1,2-oxide (glycidyl ether) **2**.
3) Finally, the third step consists in the oxirane ring opening reaction of the glycidyl ether **2** with tert-butanol, testing different catalysts (perchloric acid, potassium hydroxide, sodium tert-butoxide and boron trifluoride etherate) to synthesize 1,3-di-tert-butoxypropan-2-ol **3**.

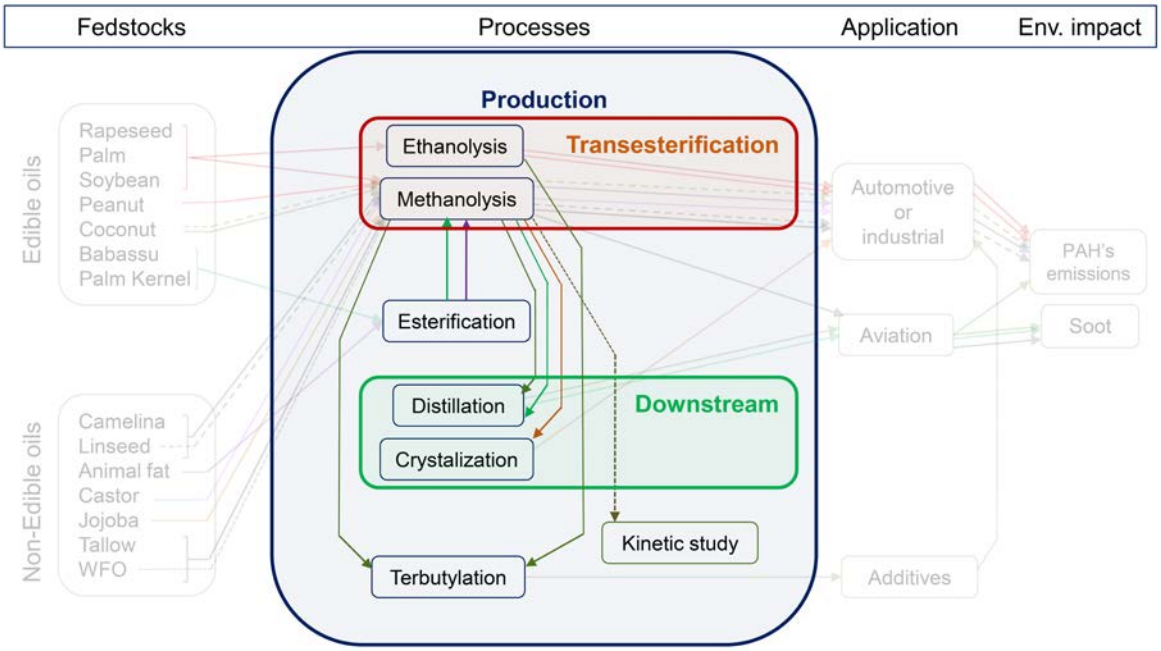

Figure 4e Processes encompassed in these thesis

Figure 4e highlights the processes encompassed within this thesis, gathering: the transesterification process which is the base of the work, downstream processes needed for the biokerosene production and the separation of the FAME and alcohol phases from the Jojoba raw product and finally the terbutilation of epichlorohydrin from which an additive with an added value is obtained from bioglycerol, biodiesel production's main by-product.

4)

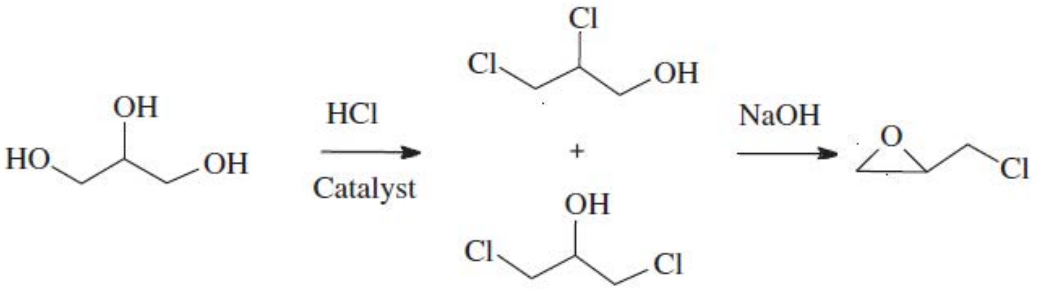

Scheme 1. *Solvay process for the synthesis of epichlorohydrin from bioglycerol through dichloropropanols mixture.*

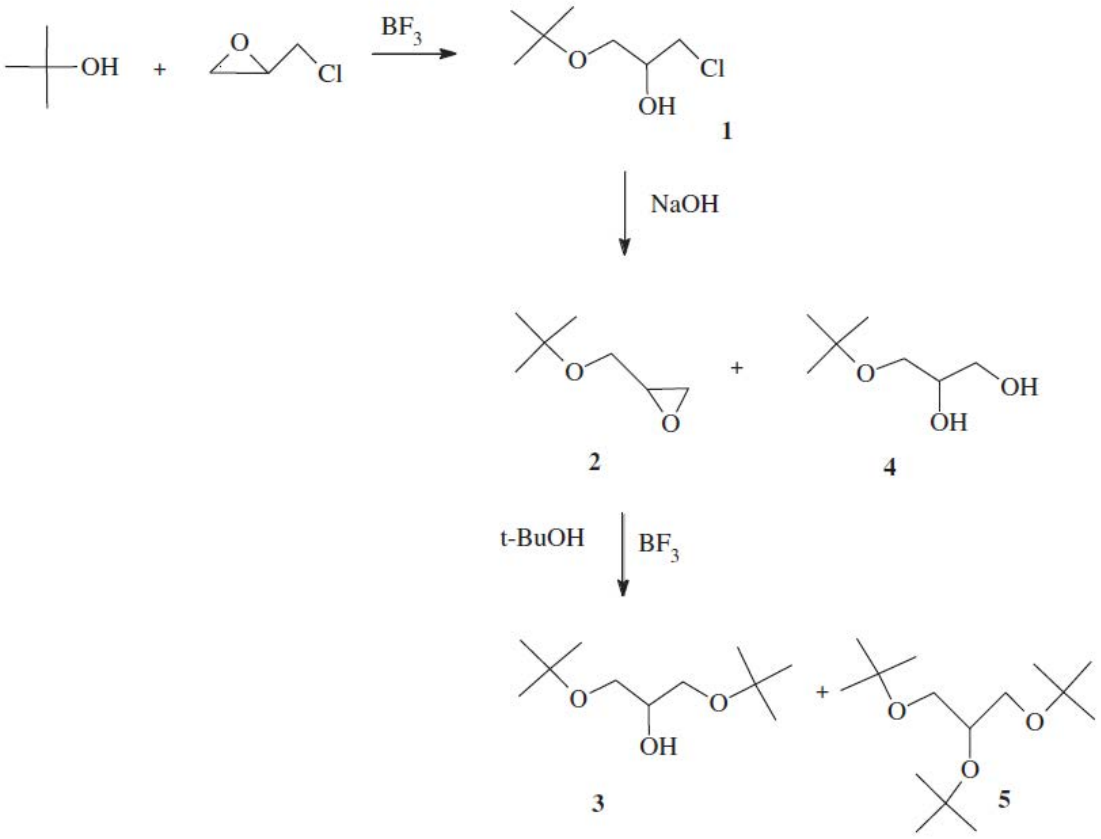

.

Scheme 2. *Process for the synthesis of 1,3-di-tert-butoxypropan-2-ol from epichlorohydrin and tert-butanol.*

7.4 PAH and soot emissions.

- *PAH emissions.*

8 *Developing* a method to measure the PAHs originated during the combustion of biodiesel samples in a bomb calorimeter.

8.1 *Producing* biodiesel: FAME, and FAEE (Fatty Acid Ethyl Esters) from different edible oils to study their behavior during combustion. Tranesterifying soybean, rapeseed and palm oil into FAME and FAEE as well as peanut FAME.

8.2 *Producing* biodiesel from linseed oil to study the PAH formation from non-edible highly unsaturated FAME.

Biodiesel have been processed and characterized from several feedstocks (i.e. tallow, palm, rapeseed, soy-bean, coconut, peanut and linseed oils) to obtain FAME and FAEE and a method to measure the PAHs originated during their combustion in a bomb calorimeter has been developed. The tests have been carried out under different oxygen pressure conditions, and samples have been cleaned from the bomb after each one of these tests. The samples have been prepared for GC-MS analysis, where PAH quantities among some other combustion products have been assessed.

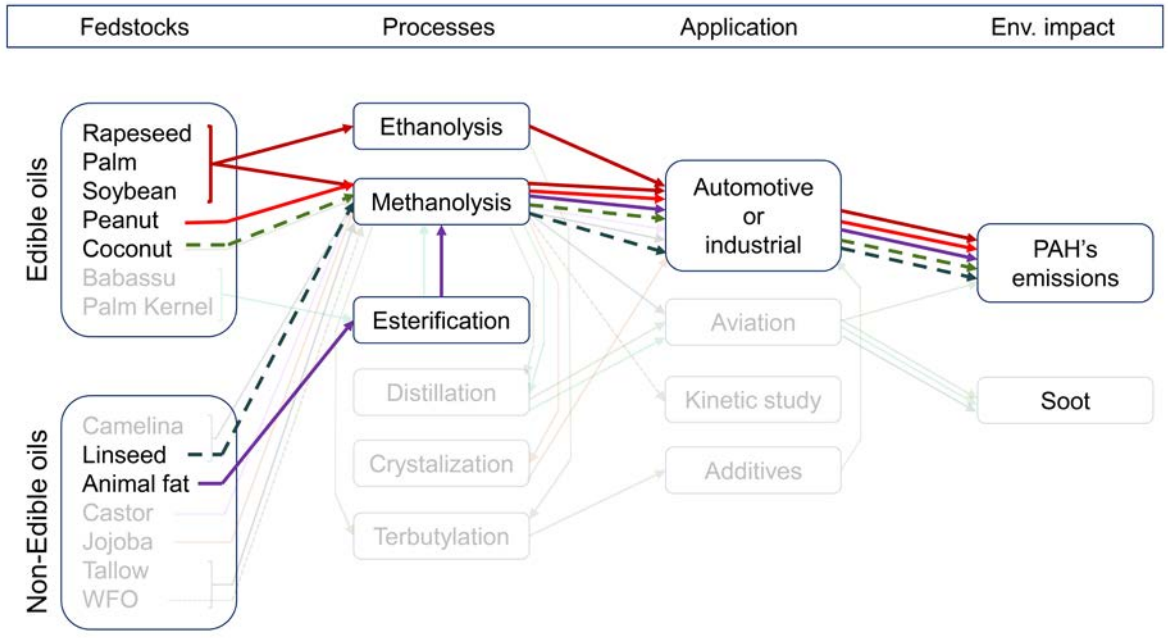

Figure 4f PAH emissions

9 *Obtaining* statistical relationships between the measured amounts of 16 PAH of concern and the composition (oil and type of alcohol) used to obtain the biodiesel, and also the oxygen pressure during combustion.

This work shows statistical relations obtained between the measured amounts of 16 PAH of concern and the composition (oil and type of alcohol) used to obtain the biodiesel, and also the oxygen pressure during combustion.

In order to achieve these two objectives, first some specific objectives had to be accomplished. Biodiesel from several edible and non-edible oils and fats had to be produced, characterization was needed to assess the suitability of these fuels and blends.

- *Sooting Tendency*

10 *Comparing* the sooting tendency of FAME from different feedstocks that could be blended with fossil kerosene.

Another objective of this thesis chapter is to quantify the potential of FAME blends to reduce the sooting tendency of kerosenes making FAME blends an option as aviation fuels, which is at least worthy to be considered.

9 REFERENCES

1. *BS EN 14214:2008+A1:2009 - Automotive Fuels. Fatty Acid Methyl Esters (FAME) for Diesel Engines. Requirements and Test Methods – BSI British Standards...*

2. WANG, R. Development of Biodiesel Fuel. *Taiyang- Neng Xuebao*, 1988, vol. 9. pp. 434-436.

3. MITTELBACH, M. and REMSCHMIDT, C. *Biodiesel: The Comprehensive Handbook*. Graz, Austria: Martin Mittelbach, 2004.

4. ALCANTARA, R., et al. Catalytic Production of Biodiesel from Soy-Bean Oil, used Frying Oil and Tallow. *Biomass and Bioenergy*, 2000, vol. 18, no. 6. pp. 515 - 527.

5. CANOIRA, L., ALCÁNTARA, R., JESÚS GARCÍA-MARTÍNEZ, M. and CARRASCO, J. Biodiesel from Jojoba Oil-Wax: Transesterification with Methanol and Properties as a Fuel. *Biomass and Bioenergy*, 2006, vol. 30, no. 1. pp. 76 - 81.

6. CANOIRA, L., et al. Nitration of Biodiesel of Waste Oil: Nitrated Biodiesel as a Cetane Number Enhancer. *Fuel*, 2007, vol. 86, no. 7-8. pp. 965 - 971.

7. MA, F. and HANNA, M.A. Biodiesel Production: A review1Journal Series #12109, Agricultural Research Division, Institute of Agriculture and Natural Resources, University of Nebraska–Lincoln.1. *Bioresource Technology*, 1999, vol. 70, no. 1. pp. 1 - 15.

8. MEHER, L., VIDYASAGAR, D. and NAIK, S. Technical Aspects of Biodiesel Production by Transesterification—a Review. *Renewable and Sustainable Energy Reviews*, 2006, vol. 10, no. 3. pp. 248 - 268.

9. FREEDMAN, B., BUTTERFIELD, R.O. and PRYDE, E.H. Transesterification Kinetics of Soybean Oil 1. *Journal of the American Oil Chemists' Society*, 1986, vol. 63, no. 10. pp. 1375 - 1380.

10. MITTELBACH, M. and TRATHNIGG, B. Kinetics of Alkaline Catalyzed Methanolysis of Sunflower Oil. *FETT Wissenschaft Technologie/FAT Science Technology*, 1990, vol. 92, no. 4. pp. 145 - 148.

11. DIASAKOU, M., LOULOUDI, A. and PAPAYANNAKOS, N. Kinetics of the Non-Catalytic Transesterification of Soybean Oil. *Fuel*, 1998, vol. 77, no. 12. pp. 1297 - 1302.

12. KOMERS, K., SKOPAL, F., STLOUKAL, R. and MACHEK, J. Kinetics and Mechanism of the KOH? Catalyzed Methanolysis of Rapeseed Oil for Biodiesel Production. *European Journal of Lipid Science and Technology*, 2002, vol. 104, no. 11. pp. 728-737.

13. CLARK, S.J., WAGNER, L., SCHROCK, M.D. and PIENNAAR, P.G. Methyl and Ethyl Soybean Esters as Renewable Fuels for Diesel Engines. *Journal of the American Oil Chemists Society*, 1984, vol. 61, no. 10. pp. 1632 - 1638.

14. K.S. MARKLEY. *Fatty Acids, their Chemistry, Properties, Production, and Uses.* 2d completely rev. and augm. ed. ed. New York: Interscience Publishers, 1960 worldcat.

15. *PREPARATION OF DETERGENTS.* UNITED STATES: US PATENT, 1944. US 2360844 A.

16. BONDIOLI, P., et al. Storage Stability of Biodiesel. *Journal of the American Oil Chemists' Society*, 1995, vol. 72, no. 6. pp. 699 - 702.

17. STOURNAS, S., LOIS, E. and SERDARI, A. Effects of Fatty Acid Derivatives on the Ignition Quality and Cold Flow of Diesel Fuel. *Journal of the American Oil Chemists' Society*, 1995, vol. 72, no. 4. pp. 433 - 437

18. *Directive 2009/28/EC of the European Parliament and of the Council of 23 April 2009 on the Promotion of the use of Energy from Renewable Sources and Amending and Subsequently Repealing Directives 2001/77/EC and 2003/30/EC - LexUriServ.Do.*

19. *Biofuels for Transportation: The Road from Research to the Marketplace.*. Washington D.C.: U.S. Department of Energy (National Renewable Energy Laboratory), NREL. , 1993.

20. TOLLEFSON, J. Energy: Not Your Father's Biofuels. *Nature*, 2008, vol. 451, no. 7181. pp. 880-883.

21. TAHERIPOUR, F., HURT, C. and TYNER, W.E. Livestock Industry in Transition: Economic, Demographic, and Biofuel Drivers. *Animal Frontiers*, April 01, 2013, vol. 3, no. 2. pp. 38-46.

22. SHENGGEN FAN, D.H. Reflections on the Global Food Crisis: How did it Happen? how has it Hurt? and how can we Prevent the Next One?. *Research Report of the International Food Policy Research Institute*, 2010, no. 165 . pp. 1-140.

23. TYNER, W.E. Biofuels and Food Prices: Separating Wheat from Chaff. *Global Food Security*, Volume 2, Issue 2, July 2013, Pages 126–130.

24. JI, Q. and FAN, Y. How does Oil Price Volatility Affect Non-Energy Commodity Markets?. *Applied Energy*, 1, 2012, vol. 89, no. 1. pp. 273-280.

25. ECCLESTON, C.H. Peak Food?. *Environmental Quality Management*, 2009, vol. 18, no. 3 . pp. 9-17.

26. RABINOVICH, M. White Biotech and the Financial Crisis. *Biotechnology Journal*, 2009, vol. 4, no. 8. pp. 1117-1123.

27. WEBB, P. Medium- to Long-Run Implications of High Food Prices for Global Nutrition. *The Journal of Nutrition*, January 01, 2010, vol. 140, no. 1. pp. 143S-147S.

28. *Agra Informa Ltd.* The Public Ledger. Agra Informa Ltd. November 19, 2007., 2007.

29. CANAKCI, M. The Potential of Restaurant Waste Lipids as Biodiesel Feedstocks. *Bioresource Technology*, 20060118, Jan, 2007, vol. 98, no. 1. pp. 183-190 ISSN 0960-8524; 0960-8524. DOI 10.1016/j.biortech.2005.11.022.

30. NEBEL, B.A. and MITTELBACH, M. Biodiesel from Extracted Fat Out of Meat and Bone Meal. *European Journal of Lipid Science and Technology*, 2006, vol. 108, no. 5. pp. 398 - 403.

31. AHN, E., HILBER, T., MITTELBACH, M. and SCHMIDT, E. *Experience of Truck Fleets with BioDiesel made from Animal Fats as Compared to Rapeseed Oil Methyl Ester.* Aus tin, TX ed. , Nov. 7 - 12 2004, 2004.

32. DEMIRBAS, A. and KARSLIOGLU, S. Biodiesel Production Facilities from Vegetable Oils and Animal Fats. *Energy Sources, Part A: Recovery, Utilisation, and Environmental Effects*, 2007, vol. 29, no. 2. pp. 133 - 141.

33. HAAS, M.J., SCOTT, K.M., FOGLIA, T.A. and MARMER, W.N. The General Applicability of in Situ Transesterification for the Production of Fatty Acid Esters from a Variety of Feedstocks. *Journal of the American Oil Chemists' Society*, 2007, vol. 84, no. 10. pp. 963 - 970.

34. MA, F., CLEMENTS, L.D. and HANNA, M.A. Biodiesel Fuel from Animal Fat. Ancillary Studies on Transesterification of Beef Tallow†. *Industrial & Engineering Chemistry Research*, 1998, vol. 37, no. 9. pp. 3768 - 3771.

35. MUNIYAPPA, P.R., BRAMMER, S.C. and NOUREDDINI, H. Improved Conversion of Plant Oils and Animal Fats into Biodiesel and Co-Product. *Bioresource Technology*, 1996, vol. 56, no. 1. pp. 19 - 24.

36. TASHTOUSH, G.M., AL-WIDYAN, M.I. and AL-JARRAH, M.M. Experimental Study on Evaluation and Optimisation of Conversion of Waste Animal Fat into Biodiesel. *Energy Conversion and Management*, 2004, vol. 45, no. 17. pp. 2697 - 2711.

37. *Outlook for U.S. Agricultural Trade.* USDA - AES-. 02-21-2008,

38. *Biofuel Expansion: Challenges, Risks and Opportunities for Rural Poor People.* International Fund for Agricultural Development IFAD.

39. ZABANIOTOU, A., IOANNIDOU, O. and SKOULOU, V. Rapeseed Residues Utilisation for Energy and 2nd Generation Biofuels. *Fuel*, 2008, vol. 87, no. 8-9. pp. 1492 - 1502.

40. ABU-JRAI, A., et al. Effect of Gas-to-Liquid Diesel Fuels on Combustion Characteristics, Engine Emissions, and Exhaust Gas Fuel Reforming. Comparative Study. *Energy & Fuels*, 2006, vol. 20, no. 6. pp. 2377 - 2384.

41. SZYBIST, J.P., KIRBY, S.R. and BOEHMAN, A.L. NOx Emissions of Alternative Diesel Fuels A Comparative Analysis of Biodiesel and FT Diesel. *Energy Fuels*, 05/14; 2013, 2005, vol. 19, no. 4. pp. 1484-1492.

42. GOODRUM, J. Rheological Characterisation of Animal Fats and their Mixtures with #2 Fuel Oil. *Biomass and Bioenergy*, 2003, vol. 24, no. 3. pp. 249 - 256.

43. KINAST, J.A. *Production of Biodiesels from Multiple Feedstocks and Properties of Biodiesels and Biodiesel/Diesel Blends: Final Report NREL/SR-510-31460.* National Renewable Energy Laboratory. , 2003

44. N.Y. KADO and P.A. KUZMICKY. *Bioassay Analyses of Particulate Matter from a Diesel Bus Engine using various Biodiesel Feedstock Fuels: Final Report; Report 3 in a Series of 6 - NREL/SR-510-31463.* . National Renewable Energy Laboratory 2003;NREL. February 2003

45. LEBEDEVAS, S., et al. Use of Waste Fats of Animal and Vegetable Origin for the Production of Biodiesel Fuel:? Quality, Motor Properties, and Emissions of Harmful Components. *Energy & Fuels*, 2006, vol. 20, no. 5. pp. 2274 - 2280.

46. WYATT, V.T., et al. Fuel Properties and Nitrogen Oxide Emission Levels of Biodiesel Produced from Animal Fats. *Journal of the American Oil Chemists' Society*, 2005, vol. 82, no. 8. pp. 585 - 591.

47. SEIDEL, B., et al. Safety Evaluation for a Biodiesel Process using Prion-Contaminated Animal Fat as a Source. *Environmental Science and Pollution Research International*, Mar, 2006, vol. 13, no. 2. pp. 125-130

48. BENSON, T.J., ZAPPI, M., FRENCH, T. and HERNANDEZ, R. *Production of Biodiesel from Wastes Associated with Meat Butchering Processes.* AICHE Conference proceedings 2005.

49 EUROPEAN PARLIAMENT AND OF THE COUNCIL. *REGULATION (EC) of THE EUROPEAN PARLIAMENT AND OF THE COUNCIL of 3 October 2002 Laying Down Health Rules Concerning Animal by-Products Not Intended for Human Consumptio.* REGULATION ed. , of 3 October 2002, 2002

50. MIRALLES, R. Biocarburantes En España: Una Crisis En La Encrucijada. Info APPA, 2008, vol. 26. pp. 16-18.

51. ENCINAR, J.M., SANCHEZ, N., MARTINEZ, G. and GARCIA, L. Study of Biodiesel Production from Animal Fats with High Free Fatty Acid Content. *Bioresource Technology*, Volume 102, Issue 23, 2011 Pages 10907–10914

52. DIAS, J.M., ALVIM-FERRAZ, M.C.M. and ALMEIDA, M.F. Mixtures of Vegetable Oils and Animal Fat for Biodiesel Production: Influence on Product Composition and Quality. *Energy & Fuels*, 2008, vol. 22, no. 6. pp. 3889 - 3893.

53. MORALES, G., et al. Low-Grade Oils and Fats: Effect of several Impurities on Biodiesel Production Over Sulfonic Acid Heterogeneous Catalysts. *Bioresource Technology*, Volume 102, Issue 23, 2011 Pages 9571–9578

54. GARCÍA, M., et al. Methanolysis and Ethanolysis of Animal Fats: A Comparative Study of the Influence of Alcohols. *Chemical Industry and Chemical Engineering Quarterly*, 2011, vol. 17, no. 1. pp. 91 - 97.

55. GRABOSKI, M.S. and MCCORMICK, R.L. Combustion of Fat and Vegetable Oil Derived Fuels in Diesel Engines. *Progress in Energy and Combustion Science*, 1998, vol. 24, no. 2. pp. 125-164.

56. ARANDA MORAES, M.S., et al. Tallow Biodiesel: Properties Evaluation and Consumption Tests in a Diesel Engine. *Energy and Fuels*, 2008, vol. 22, no. 3 pp. 1949-1954.

57. KULKARNI, M.G. and DALAI, A.K. Waste Cooking OilAn Economical Source for Biodiesel: A Review. *Industrial & Engineering Chemistry Research*, 2006, vol. 45, no. 9. pp. 2901-2913

58. DORADO, M.P., et al. Exhaust Emissions from a Diesel Engine Fueled with Transesterified Waste Olive Oil☆. *Fuel*, 7, 2003, vol. 82, no. 11. pp. 1311-1315.

59. MITTELBACH, M. and TRITTHART, P. Diesel Fuel Derived from Vegetable Oils, III. Emission Tests using Methyl Esters of used Frying Oil, 1988, vol. 65, no. 7 ISSN 0003-021X.

60. MARMESAT, S., RODRIGUES, E., VELASCO, J. and DOBARGANES, C. Quality of used Frying Fats and Oils: Comparison of Rapid Tests Based on Chemical and Physical Oil Properties. *International Journal of Food Science & Technology*, 2007, vol. 42, no. 5. pp. 601 - 608.

61 CANAKCI, M. and ÖZSEZEN, A.N. Evaluating waste cooking oils as alternative diesel fuel. *Gazi university Journal of Science*, 2005, vol. 18, no. 1. pp. 81 - 91.

62. ARQUIZA, A.C., BAYUNGAN, M.C. and TAN, R. *Production of Biodiesel and Oleochemicals from used Frying Oil.* University of Philippines, Los Baños, 2000.

63. FELIZARDO, P., et al. Production of Biodiesel from Waste Frying Oils. *Waste Management (New York, N.Y.)*, 2006, vol. 26, no. 5. pp. 487-494.

64. LEUNG, Y.C. and CHEN, G.Y. *Biodiesel Production using Waste Cooking Oil from Restaurant.* HKUST., Symposium on Energy Engineering in the 21st century (SEE 2000), 2000

65. GUO, Y., LEUNG, Y.C. and KOO, C.P. *A Clean Biodiesel Fuel Produced from Recycled Oils and Grease Trap Oils.* Better air quality in Asian and Pacific rim cities, BAQ 2002 ed. Hong Kong Polytechnic University, December 2002

66. M. P. Dorado, et al. AN ALKALI CATALYZED TRANSESTERIFICATION PROCESS FOR HIGH FREE FATTY ACID WASTE OILS, 2002, vol. 45, no. 3. pp. 525.

67. ÇAYLI, G. and KÜSEFOGLU, S. Increased Yields in Biodiesel Production from used Cooking Oils by a Two Step Process: Comparison with One Step Process by using TGA. *Fuel Processing Technology*, 2008, vol. 89, no. 2. pp. 118 - 122.

68. DORADO, M.P., BALLESTEROS, E., MITTELBACH, M. and LÓPEZ, F.J. Kinetic Parameters Affecting the Alkali-Catalyzed Transesterification Process of used Olive Oil. *Energy & Fuels*, 2004, vol. 18, no. 5. pp. 1457 - 1462.

69. ENCINAR, J.M., GONZÁLEZ, J.F. and RODRÍGUEZ-REINARES, A. Biodiesel from used Frying Oil. Variables Affecting the Yields and Characteristics of the Biodiesel. *Industrial & Engineering Chemistry Research*, 2005, vol. 44, no. 15. pp. 5491 - 5499.

70. LEUNG, D.Y.C. and GUO, Y. Transesterification of Neat and used Frying Oil: Optimisation for Biodiesel Production. *Fuel Processing Technology*, 2006, vol. 87, no. 10. pp. 883 - 890..

71. SAIFUDDIN, N. and CHUA, K.H. Production of Ethyl Ester (Biodiesel) from used Frying Oil: Optimisation of Transesterification Process using Microwave Irradiation. *Malaysian Journal of Chemistry*, 2004, vol. 6, no. 1 pp. 77 - 82.

72. CHEN, K., LIN, Y., HSU, K. and WANG, H. Improving Biodiesel Yields from Waste Cooking Oil by using Sodium Methoxide and a Microwave Heating System. *Energy*, 2012, vol. 38, no. 1. pp. 151 - 156.

73. GAN, M., et al. The Kinetics of the Esterification of Free Fatty Acids in Waste Cooking Oil using Fe2(SO4)3/C Catalyst. *Chinese Journal of Chemical Engineering*, 2009, vol. 17, no. 1. pp. 83 - 87.

74. Knothe Gerhard, Dunn Robert O. and Bagby Marvin O. Fuels and Chemicals from BiomassAmerican Chemical Society, 05/01, 1997 *Biodiesel: The use of Vegetable Oils and their Derivatives as Alternative Diesel Fuels*, pp. 172-208

75. ZHANG, Y. Biodiesel Production from Waste Cooking Oil: 1. Process Design and Technological Assessment. *Bioresource Technology*, 2003, vol. 89, no. 1. pp. 1 - 16.

76. ZHENG, S., KATES, M., DUBÉ, M.A. and MCLEAN, D.D. Acid-Catalyzed Production of Biodiesel from Waste Frying Oil. *Biomass and Bioenergy*, 2006, vol. 30, no. 3. pp. 267 - 272.

77. AL-WIDYAN, M.I. and AL-SHYOUKH, A.O. Experimental Evaluation of the Transesterification of Waste Palm Oil into Biodiesel. *Bioresource Technology*, 2002, vol. 85, no. 3. pp. 253 - 256.

78. LEPPER H, F.L. *Process for the Production of Fatty Acid Esters of Short-Chain Aliphatic Alcohols from Fats and/Or Oils Containing Free Fatty Acids. US PATENT* US: US 4608202 A August 26, 1986.

79. M. Canakci and J. Van Gerpen. BIODIESEL PRODUCTION FROM OILS AND FATS WITH HIGH FREE FATTY ACIDS, 2001, vol. 44, no. 6. pp. 1429.

80. HANCSÓK, J., KOVÁCS, F. and KRÁR, M. Production of Vegetable Oil Fatty Acid Methyl Esters from used Frying Oil by Combined Acidic/Alkali Transesterification. *Petroleum & Coal*, 2004, vol. 46, no. 3. pp. 36 - 44.

81. WU, W.H., FOGLIA, T.A., MARMER, W.N. and PHILLIPS, J.G. Optimizing Production of Ethyl Esters of Grease using 95% Ethanol by Response Surface Methodology. *Journal of the American Oil Chemists' Society*, 1999, vol. 76, no. 4. pp. 517 - 521.

82. HSU, A., JONES, K., MARMER, W.N. and FOGLIA, T.A. Production of Alkyl Esters from Tallow and Grease using Lipase Immobilized in a Phyllosilicate Sol-Gel. *Journal of the American Oil Chemists' Society*, 2001, vol. 78, no. 6. pp. 585 - 588.

83. MARCHETTI, J.M., MIGUEL, V.U. and ERRAZU, A.F. Possible Methods for Biodiesel Production. *Renewable and Sustainable Energy Reviews*, 2007, vol. 11, no. 6. pp. 1300 - 1311.

84. ENWEREMADU, C.C. and MBARAWA, M.M. Technical Aspects of Production and Analysis of Biodiesel from used Cooking oil—A Review. *Renewable and Sustainable Energy Reviews*, 2009, vol. 13, no. 9. pp. 2205 - 2224.

85. BIKOU, E., LOULOUDI, A. and PAPAYANNAKOS, N. The Effect of Water on the Transesterification Kinetics of Cotton Seed Oil with Ethanol. *Chemical Engineering & Technology*, 1999, vol. 22, no. 1. pp. 70-75.

86. KUSDIANA, D. and SAKA, S. Kinetics of Transesterification in Rapeseed Oil to Biodiesel Fuel as Treated in Supercritical Methanol. *Fuel*, 2001, vol. 80, no. 5. pp. 693 - 698.

87. BOOCOCK, D.G.B., KONAR, S.K., MAO, V. and SIDI, H. Fast One-Phase Oil-Rich Processes for the Preparation of Vegetable Oil Methyl Esters. *Biomass and Bioenergy*, 1996, vol. 11, no. 1. pp. 43 - 50.

88. ZHENG, S. *Biodiesel Production from Waste Frying Oil: Conversion Monitoring and Modeling.* MASc thesis, ed. Department of Chemical Engineering, University of Ottawa, 2003.

89. *International Jojoba Export Council*. Available from: http://www.ijec.net/.

90. ABU-ARABI, M.K., ALLAWZI, M.A., AL-ZOUBI, H.S. and TAMIMI, A. Extraction of Jojoba Oil by Pressing and Leaching. *Chemical Engineering Journal*, 2000, vol. 76, no. 1. pp. 61 - 65.

91. BUSSON-BREYSSE, J., FARINES, M. and SOULIER, J. Jojoba Wax: Its Esters and some of its Minor Components, *Journal of the American Oil Chemists' Society*, September 1994, Volume 71, Issue 9, pp 999-1002

92. ABBOTT, T.P., et al. Pilot-Scale Isolation of Simmondsin and Related Jojoba Constituents. *Industrial Crops and Products*, 1999, vol. 10, no. 1. pp. 65 - 72.

93. Shani, A. The Struggles of Jojoba. [Ben-Gurion Univ. of the Negev,Beersheba (Israel)].

94. SHANI, A., LURIE, P. and WISNIAK, J. Synthesis of Jojobamide and Homojojobamide. *Journal of the American Oil Chemists' Society*, 1980, vol. 57, no. 3. pp. 112 - 114.

95. SELIM, M.Y.E., RADWAN, M.S. and ELFEKY, S.M.S. Combustion of Jojoba Methyl Ester in an Indirect Injection Diesel Engine. *Renewable Energy*, 2003, vol. 28, no. 9. pp. 1401 - 1420.

96. *Oleochemicals.*.Chem Systems. , 2001

97. CARRASCO, J. *Obtención De Biodiesel Por Transesterificación De Aceite-Cera De Jojoba.* MSc Thesis. ed. School of Mines. Polytechnic University of Madrid, 2004.

98. EL MOGUY, N. *Jojoba: The Green Gold Hope for the Egyptian Desert Development United Nations: Economic and Social Commission for Western Asia. Report of the Experts Group Meeting Manama (Bahrain).* , 10-12 June 2002.

99. SCHOLZ, V. and DA SILVA, J.N. Prospects and Risks of the use of Castor Oil as a Fuel. *Biomass and Bioenergy*, 2//, 2008, vol. 32, no. 2. pp. 95-100.

100. BERMAN, P., NIZRI, S. and WIESMAN, Z. Castor Oil Biodiesel and its Blends as Alternative Fuel. *Biomass and Bioenergy*, 2011, vol. 35, no. 7. pp. 2861 - 2866..

101. DA SILVA CÉSAR, A. and OTÁVIO BATALHA, M. Biodiesel Production from Castor Oil in Brazil: A Difficult Reality. *Energy Policy*, 2010, vol. 38, no. 8. pp. 4031 - 4039.

102. PRADHAN, S., MADANKAR, C.S., MOHANTY, P. and NAIK, S.N. Optimisation of Reactive Extraction of Castor Seed to Produce Biodiesel using Response Surface Methodology. *Fuel*, 2012, vol. 97. pp. 848 - 855.

103. LAVANYA, C., MURTHY, I.Y.L.N., NAGARAJ, G. and MUKTA, N. Prospects of Castor (Ricinus Communis L.) Genotypes for Biodiesel Production in India. *Biomass and Bioenergy*, 2012, vol. 39. pp. 204 - 209.

104. LIMA DA SILVA, N., MACIEL, M., BATISTELLA, C. and FILHO, R. Optimisation of Biodiesel Production from Castor Oil, *Applied Biochemistry and Biotechnology* 2006, vol. 130, no. 1-3. pp. 405-414

105. SILVA LIMA, N., WOLF MACIEL, M.R., BATISTELLA, C.B. and Maciel Filho. *Biodiesel Production - Application of Response Surface Methodology to Optimize Castor Oil Ethanolise.* , 2006 Conference: International Congress of Chemical and Process Engineering, CHISA

106. MENEGHETTI, S.M.P., et al. Ethanolysis of Castor and Cottonseed Oil: A Systematic Study using Classical Catalysts. *Journal of the American Oil Chemists' Society*, 2006, vol. 83, no. 9. pp. 819 - 822.

107. MENEGHETTI, S.M.P., et al. Biodiesel from Castor Oil:? A Comparison of Ethanolysis Versus Methanolysis. *Energy & Fuels*, 2006, vol. 20, no. 5. pp. 2262 - 2265.

108. MENEGHETTI, S.M., et al. Biodiesel Production from Vegetable Oil Mixtures: Cottonseed, Soybean, and Castor Oils. *Energy Fuels*, 2007., vol. 21, no. 6. pp. 3746-3747 ISSN 0887-0624.

109. OLIVEIRA, D., et al. Optimisation of Alkaline Transesterification of Soybean Oil and Castor Oil for Biodiesel Production, 2005, vol. 122, no. 1-3. pp. 553-560 ISSN 0273-2289.

110. BARBOSA, D.d.C., SERRA, T.M., MENEGHETTI, S.M.P. and MENEGHETTI, M.R. Biodiesel Production by Ethanolysis of Mixed Castor and Soybean Oils. *Fuel*, 2010, vol. 89, no. 12. pp. 3791 - 3794.

111. SOUSA, L.L., LUCENA, I.L. and FERNANDES, F.A.N. Transesterification of Castor Oil: Effect of the Acid Value and Neutralisation of the Oil with Glycerol. *Fuel Processing Technology*, 2010, vol. 91, no. 2. pp. 194 - 196.

112. HINCAPIÉ, G., MONDRAGÓN, F. and LÓPEZ, D. Conventional and in Situ Transesterification of Castor Seed Oil for Biodiesel Production. *Fuel*, 2011, vol. 90, no. 4. pp. 1618 - 1623.

113. PEÑA, R., et al. Transesterification of Castor Oil: Effect of Catalyst and Co-Solvent. *Industrial and Engineering Chemistry Research*, 2009, vol. 48, no. 3. pp. 1186-1189.

114. PEREIRA FAGUNDES, F., et al. Optimisation of the Biodiesel Production from Castor Oil and Influence of the Temperature on the Rheological Behavior of its Blends with Diesel Fuel. , *Applied Biochemistry and Biotechnology*, 113-16 771-780 2008.

115. CONCEIÇÃO, M.M., et al. Thermoanalytical Characterisation of Castor Oil Biodiesel. *Renewable and Sustainable Energy Reviews*, 2007, vol. 11, no. 5. pp. 964 - 975.

116. CONCEIÇÃO, M.M., et al. Rheological Behavior of Castor Oil Biodiesel. *Energy & Fuels*, 2005, vol. 19, no. 5. pp. 2185 - 2188.

117. CONCEIÇÃO, M.M., et al. Thermal and Oxidative Degradation of Castor Oil Biodiesel. *Energy & Fuels*, 2007, vol. 21, no. 3. pp. 1522 - 1527.

118. CONCEIÃ§Ã£O, M., et al. Dynamic Kinetic Calculation of Castor Oil Biodiesel, 2007, vol. 87, no. 3. pp. 865-869 ISSN 1388-6150.

119. THOMAS, T.P., BIRNEY, D.M. and AULD, D.L. Viscosity Reduction of Castor Oil Esters by the Addition of Diesel, Safflower Oil Esters and Additives. *Industrial Crops and Products*, 2012, vol. 36, no. 1. pp. 267 - 270.

120. FARIAS, R.M.C., et al. Evaluation of the Thermal Stability of Biodiesel Blends of Castor Oil and Passion Fruit. *Journal of Thermal Analysis and Calorimetry*, 2011, vol. 106, no. 3 pp. 651-655.

121. PANWAR, N.L., et al. Performance Evaluation of a Diesel Engine Fueled with Methyl Ester of Castor Seed Oil. *Applied Thermal Engineering*, 2010, vol. 30, no. 2-3. pp. 245 - 249..

122. VARMA, M.N. and MADRAS, G. Synthesis of Biodiesel from Castor Oil and Linseed Oil in Supercritical Fluids. *Industrial & Engineering Chemistry Research*, 2007, vol. 46, no. 1. pp. 1 - 6.

123. ENCINAR, J.M., GONZÁLEZ, J.F. and PARDAL, A. Transesterification of Castor Oil Under Ultrasonic Irradiation Conditions. Preliminary Results. *Fuel Processing Technology*, 11, 2012, vol. 103, no. 0. pp. 9-15.

124. COÊLHO, D.G., ALMEIDA, A.P., SOLETTI, J.I. and DE CARVALHO, S.H.V. Influence of Variables in the Purification Process of Castor Oil Biodiesel. *Chemical Engineering Transactions*, 2011, vol. 24. pp. 829-834.

125. JEONG, G. and PARK, D. Optimisation of Biodiesel Production from Castor Oil using Response Surface Methodology. *Applied Biochemistry and Biotechnology*, 2009, vol. 156, no. 1-3. pp. 1 - 11.

126. RAMEZANI, K., ROWSHANZAMIR, S. and EIKANI, M.H. Castor Oil Transesterification Reaction: A Kinetic Study and Optimisation of Parameters. *Energy*, 2010, vol. 35, no. 10. pp. 4142 - 4148.

127. THOMAS, T.P., BIRNEY, D.M. and AULD, D.L. Optimizing Esterification of Safflower, Cottonseed, Castor and used Cottonseed Oils. *Industrial Crops and Products*, 2013, vol. 41. pp. 102 - 106.

128. LÓPEZ-ARENAS, T., ACA-ACA, G., SÁNCHEZ-DAZA, O. and SALES-CRUZ, M. *Viscosity Prediction of Compounds Derived from Castor Oil. Parameter Optimisation.* , 2011. 21st European Symposium on Computer Aided Process

129. VALENTE, O.S., et al. Fuel Consumption and Emissions from a Diesel Power Generator Fuelled with Castor Oil and Soybean Biodiesel. *Fuel*, 2010, vol. 89, no. 12. pp. 3637 - 3642.

130. BOMGARDNER, M.M. Flying the Green Skies with Biofuels: With Test Flights Behind them, Airlines Push for More Production of Biobased Jet Fuel. *Chemical and Engineering News*, 2012, vol. 90, no. 24 pp. 18-21.

131. *Biofuels International - Home.*. Available from:http://www.biofuels-news.com/.

132. R. O. Dunn. ALTERNATIVE JET FUELS FROM VEGETABLE OILS, 2001, Transactions of the ASABE. Vol. 44(6): 1751–1757.

133. DAGAUT, P. and GAIL, S. Kinetics of Gas Turbine Liquid Fuels Combustion: Jet-A1 and Bio-Kerosene. , *A.S.M.E. paper* 2007.

134. KORRES, D.M., et al. Aviation Fuel JP-5 and Biodiesel on a Diesel Engine. *Fuel*, 2008, vol. 87, no. 1. pp. 70 - 78.

135. WAGUTU, A., et al. Indigenous Oil Crops as a Source for Production of Biodiesel in Kenya. *Bulletin of the Chemical Society of Ethiopia*, 2009, vol. 23, no. 3.

136. KINDER, J.D. and RAHMES, T. *Evaluation of Bio-Derived Synthetic Paraffinic Kerosenes (Bio-SPK).* The Boeing Company .Sustainable Biofuels Research & Technology Program. , 2009

137. CHUCK, C.J. and DONNELLY, J. The Compatibility of Potential Bioderived Fuels with Jet A-1 Aviation Kerosene. *Applied Energy*, 4/1, 2014, vol. 118, no. 0. pp. 83-91.

138. HONG, T.D., et al. A Study on Developing Aviation Biofuel for the Tropics: Production process—Experimental and Theoretical Evaluation of their Blends with Fossil Kerosene. *Chemical Engineering and Processing: Process Intensification*, 12, 2013, vol. 74, no. 0. pp. 124-130.

139. CHIARAMONTI, D., PRUSSI, M., BUFFI, M. and TACCONI, D. Sustainable Bio Kerosene: Process Routes and Industrial Demonstration Activities in Aviation Biofuels. *Applied Energy*, 12/31, 2014, vol. 136, no. 0. pp. 767-774.

140. HARVEY, B.G., MERRIMAN, W.W. and KOONTZ, T.A. High-Density Renewable Diesel and Jet Fuels Prepared from Multicyclic Sesquiterpanes and a 1-Hexene-Derived Synthetic Paraffinic Kerosene. *Energy Fuels*, 2015, vol. 29, no. 4 pp. 2341-2436.

141. C. SMITH. *Biodiesel Revolution Gathering Momentum.* , 2004 http://www.straight.com/news/biodiesel-revolution-gathering-momentum.

142. RAHMAT, N., ABDULLAH, A.Z. and MOHAMED, A.R. Recent Progress on Innovative and Potential Technologies for Glycerol Transformation into Fuel Additives: A Critical Review. *Renewable and Sustainable Energy Reviews*, 2010, vol. 14, no. 3. pp. 987 - 1000.

143. GALAN, M., et al. From Residual to Useful Oil: Revalorisation of Glycerine from the Biodiesel Synthesis. *Bioresource Technology*, 2009, vol. 100, no. 15. pp. 3775 - 3778.

144. ZHENG, Y., CHEN, X. and SHEN, Y. Commodity Chemicals Derived from Glycerol, an Important Biorefinery Feedstock. *Chemical Reviews*, 2010, 110 (3), pp 1807–1807.

145. SABOURIN-PROVOST, G. and HALLENBECK, P.C. High Yield Conversion of a Crude Glycerol Fraction from Biodiesel Production to Hydrogen by Photofermentation. *Bioresource Technology*, 2009, vol. 100, no. 14. pp. 3513 - 3517.

146. GARCÍA, E., et al. New Class of Acetal Derived from Glycerin as a Biodiesel Fuel Component. *Energy & Fuels*, 2008, vol. 22, no. 6. pp. 4274 - 4280..

147. OCHOA-GÓMEZ, J.R., et al. Synthesis of Glycerol Carbonate from Glycerol and Dimethyl Carbonate by Transesterification: Catalyst Screening and Reaction Optimisation. *Applied Catalysis A: General*, 2009, vol. 366, no. 2. pp. 315 - 324.

148. ILHAM, Z. and SAKA, S. Dimethyl Carbonate as Potential Reactant in Non-Catalytic Biodiesel Production by Supercritical Method. *Bioresource Technology*, 2009, vol. 100, no. 5. pp. 1793 - 1796.

149. KIM, S.C., et al. Lipase-Catalyzed Synthesis of Glycerol Carbonate from Renewable Glycerol and Dimethyl Carbonate through Transesterification. *Journal of Molecular Catalysis B: Enzymatic*, 2007, vol. 49, no. 1-4. pp. 75 - 78.

150. CLIMENT, M.J., et al. Chemicals from Biomass: Synthesis of Glycerol Carbonate by Transesterification and Carbonylation with Urea with Hydrotalcite Catalysts. the Role of Acid-Base Pairs. *Journal of Catalysis*, 2010, vol. 269, no. 1 pp. 140-149.

151. ARESTA, M., DIBENEDETTO, A., NOCITO, F. and FERRAGINA, C. Valorisation of Bio-Glycerol: New Catalytic Materials for the Synthesis of Glycerol Carbonate Via Glycerolysis of Urea. *Journal of Catalysis*, 2009, vol. 268, no. 1. pp. 106 - 114.

152. ARESTA, M., DIBENEDETTO, A., NOCITO, F. and PASTORE, C. A Study on the Carboxylation of Glycerol to Glycerol Carbonate with Carbon Dioxide: The Role of the Catalyst, Solvent and Reaction Conditions. *Journal of Molecular Catalysis A: Chemical*, 2006, vol. 257, no. 1-2. pp. 149-153.

153. FABBRI, D., BEVONI, V., NOTARI, M. and RIVETTI, F. Properties of a Potential Biofuel obtained from Soybean Oil by Transmethylation with Dimethyl Carbonate. *Fuel*, 2007, vol. 86, no. 5-6. pp. 690 - 697.

154. JIA, C., et al. Small-Sized HZSM-5 Zeolite as Highly Active Catalyst for Gas Phase Dehydration of Glycerol to Acrolein. *Journal of Catalysis*, 2010, vol. 269, no. 1. pp. 71 - 79.

155. DA SILVA, G.P., MACK, M. and CONTIERO, J. Glycerol: A Promising and Abundant Carbon Source for Industrial Microbiology. *Biotechnology Advances*, 2009, vol. 27, no. 1. pp. 30 - 39.

156. NOUREDDINI, H., DAILEY, W.R. and HUNT, B.A. Production of Ethers of Glycerol From Crude Glycerol - The By-Product of Biodlesel Production. *Chemical and Biomolecular Engineering Research and Publications: Papers in Biomaterials*, 1998, vol. 18. pp. 1 - 18.

157. NOUREDDINI, H. System and Process for Producing Biodiesel Fuel with Reduced Viscosity and a Cloud Point below Thirty-Two (32) Degrees Fahrenheit. 2001. *Chemical and Biomolecular Engineering Research and Publications. Papers in Biomaterials*

158. LIPKIN, D. *FUEL FOR COMPRESSION IGNITION ENGINES.* US: , 1940. US PATENT US 2221839.

159. OLAH, G.A. *CLEANER BURNING AND CETANE ENHANCING DIESEL FUEL SUPPLEMENTS.* 1996. US PATENT US 5520710 A

160. PIEL, W.J., KARAS, L.J. and KESLING JR., H.S. *Chemical use in Reformulated Fuels and Potential Impact on the Petrochemical Industry.* , 1994 American Chemical Society. Division of Petroleum Chemistry. Impact of reformulated fuels. Symposium, Washington DC vol. 39, 4, pp. 493-527

161. JAPANESE PATENT Japan: , 1995. ISBN JP07082576.

162. ADI, G., et al. Soy-Biodiesel Impact on NOx Emissions and Fuel Economy for Diffusion-Dominated Combustion in a Turbo - Diesel Engine Incorporating Exhaust Gas Recirculation and Common Rail Fuel Injection. *Energy and Fuels*, 2009, vol. 23, no. 12 [pp. 5821-5829.

163. OZBAY, N., OKTAR, N., DOGU, G. and DOGU, T. Conversion of Biodiesel by-Product Glycerol to Fuel Ethers Over Different Solid Acid Catalysts. *International Journal of Chemical Reactor Engineering*, 2010, vol. 8

164. FRUSTERI, F., et al. Catalytic Etherification of Glycerol by Tert-Butyl Alcohol to Produce Oxygenated Additives for Diesel Fuel. *Applied Catalysis A: General*, 2009, vol. 367, no. 1-2. pp. 77 - 83.

165. KLEPÁCOVÁ, K., MRAVEC, D., KASZONYI, A. and BAJUS, M. Etherification of Glycerol and Ethylene Glycol by Isobutylene. *Applied Catalysis A: General*, 2007, vol. 328, no. 1. pp. 1 - 13.

166. KIJEŃSKI, J., JAMRÓZ, M.E. and TĘCZA, W. Studies of Utilisation of Glycerol in Organic Synthesis. Part 2. Conversion of Glycerol to its Tert-Butyl Ethers. , 2007 *Przemysł Chem*., 2007, 86(4), 282-285.

168. KLEPÁCOVÁ, K., MRAVEC, D. and BAJUS, M. Etherification of Glycerol with Tert-Butyl Alcohol Catalysed by Ion-Exchange Resins. *Chemical Papers*, 2006, vol. 60, no. 3. pp. 224 - 230.

169. KLEPÁCOVÁ, K., MRAVEC, D. and BAJUS, M. Tert-Butylation of Glycerol Catalysed by Ion-Exchange Resins. *Applied Catalysis A: General*, 2005, vol. 294, no. 2. pp. 141 - 147.

170. E. A. BARSA AND B. M. STEINMETZ, “Preparation of glycerol tert-butyl ethers,” *US Patent* 0240086 A1, 2009..

171. MELERO, J.A., et al. Acid-Catalyzed Etherification of Bio-Glycerol and Isobutylene Over Sulfonic Mesostructured Silicas. *Applied Catalysis A: General*, 2008, vol. 346, no. 1-2. pp. 44 - 51.

172. BOZ, N. and DOGU, T. Reflux?Recycle?Reactor for High Yield and Selectivity in TAME and TAEE Production. *AIChE Journal*, 2005, vol. 51, no. 2. pp. 631-640.

173. DOGU, T., et al. DRIFT Studies for the Reaction and Adsorption of Alcohols and Isobutylene on Acidic Resin Catalysts and the Mechanism of ETBE and MTBE Synthesis. *Industrial & Engineering Chemistry Research*, 2001, vol. 40, no. 23. pp. 5044 - 5051.

174. BEHR, A. and OBENDORF, L. Development of a Process for the Acid-Catalyzed Etherification of Glycerine and Isobutene Forming Glycerine Tertiary Butyl Ethers. *Engineering in Life Sciences*, 2002, vol. 2, no. 7. pp. 185-189.

175. MACHO, V., KAVALA, M. and KOLIESKOVA, Z. Tert-Butyl Ethers of Polyhydric Alcohols. *Neftekhimiya (Pet Chem)*, 1979, vol. 19. pp. 821-827.

176. ALCÁNTARA, R., et al. Trimerisation of Isobutene Over Amberlyst-15 Catalyst. *Reactive and Functional Polymers*, 2000, vol. 45, no. 1. pp. 19 - 27.

177. RHEAD, M.M. and HARDY, S.A. The Sources of Polycyclic Aromatic Compounds in Diesel Engine Emissions?. *Fuel*, 2003, vol. 82, no. 4. pp. 385 - 393.

178. BORRÁS, E., TORTAJADA-GENARO, L.A., VÁZQUEZ, M. and ZIELINSKA, B. Polycyclic Aromatic Hydrocarbon Exhaust Emissions from Different Reformulated Diesel Fuels and Engine Operating Conditions. *Atmospheric Environment*, 2009, vol. 43, no. 37. pp. 5944 - 5952.

179. TAVARES, M., et al. Emission of Polycyclic Aromatic Hydrocarbons from Diesel Engine in a Bus Station, Londrina, Brazil. *Atmospheric Environment*, 2004, vol. 38, no. 30. pp. 5039 - 5044.

180. RAVINDRA, K., SOKHI, R. and VANGRIEKEN, R. Atmospheric Polycyclic Aromatic Hydrocarbons: Source Attribution, Emission Factors and Regulation. *Atmospheric Environment*, 2008, vol. 42, no. 13. pp. 2895 - 2921.

181. KARAVALAKIS, G., et al. The Impact of Soy-Based Biodiesel on PAH, Nitro-PAH and Oxy-PAH Emissions from a Passenger Car Operated Over Regulated and Nonregulated Driving Cycles. *Fuel*, 2010, vol. 89, no. 12. pp. 3876 - 3883.

182. KARAVALAKIS, G., BOUTSIKA, V., STOURNAS, S. and BAKEAS, E. Biodiesel Emissions Profile in Modern Diesel Vehicles. Part 2: Effect of Biodiesel Origin on Carbonyl, PAH, Nitro-PAH and Oxy-PAH Emissions. *The Science of the Total Environment*, 20101129, Nov 29, 2010

183. LIMA, A.L.C., FARRINGTON, J.W. and REDDY, C.M. Combustion-Derived Polycyclic Aromatic Hydrocarbons in the Environment - A Review. *Environmental Forensics*, 2005, vol. 6, no. 2 pp. 109-131. S.

184. CORRÊA, S.M. and ARBILLA, G. Aromatic Hydrocarbons Emissions in Diesel and Biodiesel Exhaust. *Atmospheric Environment*, 2006, vol. 40, no. 35. pp. 6821 - 6826.

185. FONTARAS, G., et al. Effects of Biodiesel on Passenger Car Fuel Consumption, Regulated and Non-Regulated Pollutant Emissions Over Legislated and Real-World Driving Cycles. *Fuel*, 2009, vol. 88, no. 9. pp. 1608 - 1617.

186. LAI, J.Y.W., LIN, K.C. and VIOLI, A. Biodiesel Combustion: Advances in Chemical Kinetic Modeling. *Progress in Energy and Combustion Science*, 2011, vol. 37, no. 1. pp. 1 - 14.

187. TSAI, J.H., et al. PM, Carbon, and PAH Emissions from a Diesel Generator Fuelled with Soy-Biodiesel Blends. *Journal of Hazardous Materials*, 20100304, Mar 4, 2010

188. BAKEAS, E., KARAVALAKIS, G., FONTARAS, G. and STOURNAS, S. An Experimental Study on the Impact of Biodiesel Origin on the Regulated and PAH Emissions from a Euro 4 Light-Duty Vehicle. *Fuel*, 2011, vol. 90, no. 11. pp. 3200 - 3208.

189. KARAVALAKIS, G., BAKEAS, E., FONTARAS, G. and STOURNAS, S. Effect of Biodiesel Origin on Regulated and Particle-Bound PAH (Polycyclic Aromatic Hydrocarbon) Emissions from a Euro 4 Passenger Car. *Energy*, 2011, vol. 36, no. 8. pp. 5328 - 5337.

190. BALLESTEROS, R., HERNÁNDEZ, J.J. and LYONS, L.L. An Experimental Study of the Influence of Biofuel Origin on Particle-Associated PAH Emissions. *Atmospheric Environment*, 2010, vol. 44, no. 7

191. *Beginner's Guide to Aviation Biofuels.* ATAG (Air Transport Action Group):. 2009 Available from: http://www.enviro.aero/content/upload/file/beginnersguide_biofuels_webres.pdf.

192. *Global Market Forecast 2012-2031.* Airbus. , 2012 Available from: http://www.airbus.com/company/market/forecast/.

193. Alternative Jet Fuels Cut Particulate emissions. *Chemical and Engineering News*, 2011, vol. 89, no. 47. pp. 2.

194. *2008/101/EC OF THE EUROPEAN PARLIAMENT AND OF THE COUNCIL of 19 November 2008 Amending Directive 2003/87/EC so as to Include Aviation Activities in the Scheme for Greenhouse Gas Emission Allowance Trading within the Community.* DIRECTIVE ed. , .2009

195. *Disposición 10706 Del BOE 163 De 2010 - BOE-A-2010-10706.*

196. HOGUE, C. Unfriendly Skies. *Chemical and Engineering News*, 2011, vol. 89, no. 42

197. *Chemical and Engineering News*, 2012, vol. 90, no. 40. pp. 42.

198. *Home.* http://www.icao.int/Pages/default.aspx.

199. *Europa Press.* , online version July 8th 2012.

200. *Administration Pushes Biofuels Production | Concentrates Concentrates | Concentrates | Chemical & Engineering News.*

201. *ASTM D4054-09 Standard Practice for Qualification and Approval of New Aviation Turbine Fuels and Fuel Additives.* ASTM International West Conshohocken, Pennsylvania.

202. HILEMAN, J.I., DONOHOO, P.E. and STRATTON, R.W. Energy Content and Alternative Jet Fuel Viability. *Journal of Propulsion and Power*, 2010, vol. 26, no. 6. pp. 1184 - 1196.

203. COTTINEAU, J. Green Chemistry. Bio Motor Fuels. the Aviation Industry Unveils Bio-Kerosine. *Info Chimie Magazine*, 2008, vol. 45, no. 490 [viewed 15 June 2013]. pp. 27.

204. World News: France: The BTL Chain. *Hydrocarbon Engineering*, 2010, vol. 15, no. 4 pp. 8. Available from:

205. Uhde's Prenflo Process to be Part of Joint R&D Project BioTfueL in France. *Chemical Engineering*, 2010, vol. 117, no. 4 pp. 79.

206. *ASTM D7566 20. Standard Specification for Aviation Turbine Fuel Containing Synthesized Hydrocarbons.* ASTM International West Conshohocken, Pennsylvania.

207. BARRIENTOS, E.J., LAPUERTA, M. and BOEHMAN, A.L. Group Additivity in Soot Formation for the Example of C-5 Oxygenated Hydrocarbon Fuels. *Combustion and Flame*, 2013, vol. 160, no. 8. pp. 1484-1498.

208. REISCH, M.S. and TULLO, A.H. Government Policy Concentrates *Chemical and Engineering News*, 2006, vol. 84, no. 51. pp. 30-35.

209. VILLORBINA, G., et al. Combining AlCl3·6H2O and an Ionic Liquid to Prepare Chlorohydrin Esters from Glycerol. *Tetrahedron Letters*, 6/10, 2009, vol. 50, no. 23. pp. 2828-2830.

210. LUO, Z., YOU, X. and ZHONG, J. Design of a Reactive Distillation Column for Direct Preparation of Dichloropropanol from Glycerol. *Industrial & Engineering Chemistry Research*, 2009, vol. 48, no. 24. pp. 10779-10787.

TABLE OF CONTENTS

1 FEEDSTOCK AND REAGENTS

The edible oils oils used in this thesis are the following:

1. The soybean oil[1] was of commercial edible grade.

2. The soybean oil[2] used for the animal fat/soybean oil mixtures and for the combustion in the bomb calorimeter was supplied by Combustibles Ecologicos Biotel SL.

3. Rapeseed, crude babassu oil, crude palm kernel oil, and palm oils were supplied by Combustibles Ecologicos Biotel SL.

4. Refined coconut oil bought from Across Organics.

5. Peanut oil used in this work was for edible use available in supermarkets.

Other oils and Fats are:

1. The waste frying oil for transesterification, amidation and nitration (waste oil: 1, 2 and 3) was originally a mixture (50% v/v) of olive oil and sunflower oil, supplied by the catering service of the School of Mines.

2. The tallow was supplied by the Madrid City Council slaughterhouse, and was free of meat.

3. The animal fat used for the animal fat/soybean oil mixtures and for the combustion in the bomb calorimeter was supplied by Valgrasa.

4. The castor oil was supplied by Cailà & Parés, s.a.

5. The Jojoba oil wax was supplied by EIEC Complex SL.

6. Yellow animal fat was supplied by Combustibles Ecologicos Biotel SL.

7. Linseed oil was bought from Fisher Scientific.

8. Camelina seeds were supplied by the Laboratory of Fuels and Petrochemistry of the Gomez-Pardo Foundation.

Hydrocarbons used in this thesis.

1. Kerosene of fossil origin has been used to prepare the blends with biokerosene: one of them was a straight-run atmospheric distillation cut (hydrotreated) kerosene without any additives and the other one was a commercial Jet A1 kerosene and it contains additives; both samples of fossil kerosene were obtained from the Spanish Company Logistica de Hidrocarburos (CLH).

2. Fossil diesel used for the nitrated WFO FAME and the castor oil FAME blends was of commercial use purchased in a petrol station.

Other reagents used in this thesis:

All the reagents used in this work were of commercial grade and were used without further purification.

1. Dichloromethane of technical grade was purchased from Panreac. For the Camelina seed extraction, dichloromethane of HPLC grade (Merck) was used.

2. Methanol was of synthesis grade, and it was purchased from Scharlau.

3. Absolute ethanol were of commercial grade (Panreac)

4. p-Toluensulphonic acid, used as catalyst for the esterification reaction of the crude oils, was of synthesis grade, and it was purchased from Scharlau.

5. The molecular sieve was of technical purity, and it was purchased from Scharlau.

6. The catalytic solution of sodium methoxide 25 wt % in methanol was purchased from Acros Organics.

7. Magnesium silicate Magnesol D-60 was kindly supplied by The Dallas Group of America.

8. Silicagel 60-230 mesh (0.060 -0.230 mm) was purchased from Aldrich and was activated before use.

9. Oxygen for the combustion pump was of 99.99% purity.

10. Tert-butanol, epichlorohydrin, nitrogen, sodium hydroxide, perchloric acid, potassium hydroxide, metallic sodium, boron trifluoride etherate, dichloromethane, sodium m, tetrahydrofuran (THF), 37 wt.% hydrochloric acid, anhydrous sodium sulphate, toluene and petroleum ether (b.p. 40–70 °C) were of commercial grade.

2 EXPERIMENTAL EQUIPMENT

2.1 Experimental equipment used in the transesterification.

2.1.1 Reactors.

1. A three necked 250 mL round bottomed glass flask, partially immersed in an oil bath heated by a magnetic stirring plate Bunsen MC-8, with temperature and stirring power regulations, was used for lower scale of reagents.

2. A 2.0 L glass tank reactor (22 cm height x 10 cm o.d.) (see Fig. 5a and 5b) equipped with a glass anchor-shaped stirrer powered by a Heidolph RZR 2050 engine, a type K thermocouple, a water reflux condenser and funnel, surrounded by a 220 V heating jacket controlled by a proportional integral derivative (PID) temperature controller device TC-10 from the Instituto de Catálisis y Petroleoquímica (Madrid). The device has three top B-29 inlets for: reagents, stirrer and the thermocouple and one bottom outlet for the discharge of products.

Figure. 5a. Picture of the 2 L reactor used in the transesterification experiments.

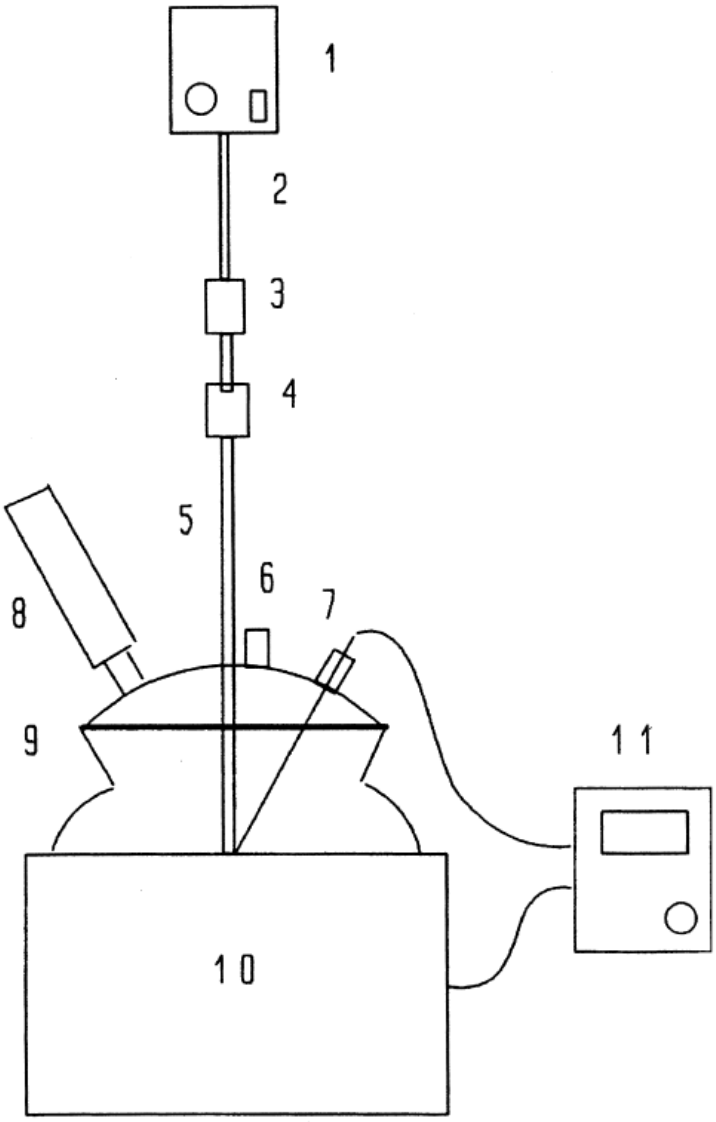

Figure. 5b. Scheme of the 2 L reactor used in the transesterification experiments. 1. Stirrer engine. 2. Stirrer steel bar. 3. Coupling device. 4. Stirrer lubricant reservoir. 5. Glass stirrer. 6. Funnel. 7. Thermocouple. 8. Water condenser. 9. Glass tank reactor. 10. Heating mantle. 11. PID temperature controller.

3. A 5.0 L cylindrical glass tank reactor (42 cm height x 21 cm o.d.) equipped with: a glass jacket for the circulation of the heating fluid (hot water heated in a bath SELECTA model Unitronic S-320-200), a KPG type Teflon stirrer powered by an IKA RW 20DZM engine, a double jacket water reflux condenser, three top B-29 inlets for reagents and a type K thermocouple, and one bottom outlet for the discharge of products. (Fig. 6)

Figure. 6. *5L reactor.*

4. A 50.0 L HDPE reactor bought from Bioking (The Netherlands) (60 cm high x 29 cm width x 29 cm long) equipped with: a heating resistance, a level control device, a pump for the stirring of the reaction mass, and nine manual 2.54 cm i.d. valves to control the circulation of fluids within the reactor and with the three auxiliary HDPE decantation tanks (Fig. 7).

Figure. 7. *50 L reactors. On the left the one used for the wet wash, on the right the transesterification reactor.*

2.2 Other equipment.

Some of the reactions were carried out in the following equipment.

- A 1 L Soxhlet extractor.
- A 1L autoclave Burton-Coblin from Autoclave Engineers.

Other experimental procedures have been carried out in the following equipment

- *Centrifuge.*

ORTO model tornax that can accommodate four round bottomed glass tubes of 180 mL (110mm height x 60 mm o.d.), with variable stirring speed between 1000 and 6000 rpm, and automatic control of the centrifugation time between 1 and 60 minutes.

ORTOALRESA model Digtor 20 that can accommodate four round bottomed glass tubes of 650 mL (120 mm height x 95 mm o.d.), with variable stirring speed until 3800 rpm, and automatic control of the centrifugation time. (Fig.8)

Figure. 8. ORTOALRESA model Digtor 20 Centrifuge

- *Distillation apparatus.*

The distillated fraction of the biodiesel fuel was obtained by fractional distillation using a 41 cm long × 3.5 cm outer diameter Vigreux column. The distillation was carried out using a rotary vacuum pump.

- *Combustion apparatus.*

The combustion tests for the determination of the PAH were carried out in an automatic bomb calorimeter LECO AC300.

2.3 Characterisation equipment.

The characterisation equipment will be described in this section.

2.3.1 Infrared equipment.

Two infrared instruments were used to follow up the raw materials conversion into biofuels.

- *Infrared spectrophotometer*

The infrared absorption spectra were registered in a dispersive infrared spectrophotometer Foxboro, model Miran 980, with a single beam. The spectra were registered as thin films between sodium chloride disks, scanning in 3 min from 4000 to 690 cm^{-1}. The spectra were acquired and stored in a PC, using a data acquisition board Keithley, model DAS 801, and the software Easyest.

- *Fourier Transform Infrared Spectrophotometer (FT-IR)*

The control of the reactions was monitored in a Fourier Transform Infrared Spectrophotometer Bruker model Vector 22, using a cell for liquids of 0.01 mm of optical pathway, with potassium bromide windows in tetracloroethylene as a solvent.

2.3.2 Gas chromatography equipment.

- *Gas chromatography, flame ionisation detector GC-FID*

- *Hewlett-Packard 5840 GC*

A Hewlett-Packard 5840 GC, equipped with a capillary column of acidified polyethylene glycol (25 m x 0.53 mm x 1 μm). The detector was a flame ionisation detector (FID), and the carrier gas helium (5 mL/min).

- *Hewlett Packard 5890*

Hewlett Packard 5890 GC with a Carbowax 20 M capillary column (25 m x 0.32 mm x 0.3 μm) was used to analyze the reaction products. The detector was a FID. Helium was the carrier gas.

Gas chromatography, Mass spectrometry detector

- *Varian CP-3800 GC*

The gas chromatography-mass spectrometry analyses were carried out in a Varian CP-3800 GC, equipped with a CP-8400 automatic injector.

- *GC-MS HP-6890/MSD-5973*

The gas chromatography-mass spectrometry analyses were determined in a GC-MS HP-6890/MSD-5973 system, with an automated system of sample injection. The column was a 5% diphenylpolydimethylsiloxane AT-5 from Alltech (25m x 0.25mm x 0.20 μm), and helium was used as the carrier gas. This technique was needed for the analysis of the species in the 1,3 ditertbutoxy-propan-2-ol reaction and in the PAH assessment.

- *GC 7890 - MS 5975*

The analysis were carried out via automatic Agilent PTV injector in a gas chromatograph / mass spectrometer system (GC-MS) Agilent GC 7890 - MS 5975, equipped with a capillary column HP5MS (30 m x 0.250 mm x 0.25 μm).

2.3.3 Other characterisation equipment used

- *^1H NMR*

Spectra were recorded on a Bruker WP 200SY spectrometer at 200.13 MHz using $CDCl_3$ as solvent and $SiMe_4$ as internal standard.

- *Coulometer*

The water content of the biodiesel samples was measured in a Karl-Fischer automatic titration apparatus Methrom model 756 KF or model 831.

- *Rancimat*

The oxidative stability of the biodiesel was determined in the automatic equipment Methrom model 743.

- *Viscosimeter*

The kinematic viscosity at 40 ºC of the biodiesel was determined in a viscosimeter Proton 4378, using tubes Turbiscan model 9506 of Polyscience, immersed in a bath Tamson model TV 2000. A Cannon Fenske Afora 5354/2B model was used for other determinations.

- *Elemental analyzer*

The sulfur content of the biodiesel was determined in an Oxford Lab-X3000 X-ray fluorescence spectrophotometer, the CHNS content in a LECO CHN-600 elemental analyzer and a LECO CHNS-932.

- *The metal content*

(Na, K, Ca, and Mg) of the biodiesel was determined in a Philips PU 9100X atomic absorption spectrophotometer, using Conostan Multi Element Standard S-21.

- *Bomb calorimeter*

The higher heating value (HHV) of the biodiesel was determined in a Leco AC-300 *Bomb calorimeter*, using benzoic acid tablets as the external standard. The same equipment was used for the formation of PAH.

- *Acidity*

The acidity index of the biodiesel was analyzed in an apparatus Methrom model 702 Titrino.

- *Flash point*

The flash point of the biodiesel was measured in a Pensky Martens apparatus PMA2 and a PMA4 from SurBerlin. Other measurements were determined with a Herzog 1088 model.

- *Cold-Filter Plugging Point (CFPP)*

The CFPP of the biodiesel was analyzed with the automatic apparatus of ISL model FPP 5G.

- *Cloud point (CP) and Pour point (PP)*

CP and PP of the fuels were analyzed with an ATPM apparatus.

- *High Frequency Reciprocating Rig (HFRR) test (wear scar)*

The wear scar of the fuels was measured in a PCS Instrument that works in the following operating conditions: frequency 10 to 200 Hz; stroke length 20 μm to 2.0 mm; load 0.1 to 1.0 kg with supplied weights; maximum friction force dependent on amplitude - maximum 10.0 N; temperature: ambient to 150°C (400°C with high power heater option); standard upper specimen 6.0 mm diameter ball; standard lower specimen 10.0 mm diameter x 3.0 mm thick disc.

- *Density*

Density of the fuels has been measured at different temperatures both with a pycnometer and with a digital density meter DMA 48 (Anton Paar GmbH).

- *Smoke point*

The smoke point was determined using an Analis 47551 apparatus.

3 EXPERIMENTAL PROCEDURES

3.1 Feedstock pretreatment.

3.1.1 Biodiesel from low grade animal fat.

The high FFA acid content of the waste animal fat (Table 13, Chapter III, section 2.2) renders it inadequate for the most traditional direct one-step base-catalyzed transesterification process to biodiesel due to soap formation. However, an indirect multistep process allows the use of these feedstocks with high FFA concentrations by first carrying out an acid-catalyzed esterification of the FFA before the base-catalyzed triglyceride transesterification (80, 211, 212, 213). Moreover, the low quality of the animal fat used as feedstock in this study poses other problems that need to be addressed in the production process. The higher nitrogen and sulfur contents of the animal fat (Tables 13 and 14, Chapter III, section 2.2) indicate that still some protein and phosphoglycerides (usually called gums) remain in the feedstock; the phosphoglycerides are essential constituents of the animal cell membranes and they concentrate in the lipids fraction. For this reason, a degumming process to eliminate the phosphoglycerides has been proposed as the first step of this multistep process. The degumming method with 60 wt % orthophosphoric acid has been taken from the literature among the existing ones (214, 215, 216, 217, 218, 219, 220, 221, 222, 223) , and it produces between 3 and 5 wt % gums, which are separated by centrifugation, depending on the quality of the fat.

The esterification of the FFA was carried out at 60 °C with stirring (600 rpm) using a molar ratio of 6:1 methanol/oil-fat with acid catalysis. Among the acids of choice to catalyse this esterification of the FFA, concentrated hydrochloric acid (ca. 35 wt. %) would introduce an undesirable amount of water in the reaction. Concentrated sulphuric acid (ca. 95 wt. %) does not give this problem, but some sulphate groups could add to the double bonds of the triglycerides, increasing the already high sulphur content of the fat. In fact, the use of concentrated sulphuric acid as catalyst in this step (in 0.35-2.00 wt. % of the oil-fat) produces a biodiesel with a high sulphur content of 49-388 mg/kg (the feedstock animal fat had roughly this same sulphur concentration, but it was mixed with 50 vol % soybean oil with no appreciable sulphur content). For this reason, we have chosen a strong organic acid, p-toluenesulfonic acid (p-TsOH; pKa = -6.5) (0.5 wt. % of the oil-fat), as the catalyst for our esterification process, although the reaction time to lower the acidity index of the feedstock to ca. 0.6° increased to around 4 h, in contrast to the catalysis by 2 wt. % concentrated sulphuric acid that was completed at the same level in 1 h. With this

esterification catalyst, the sulphur content of the final biodiesel could be substantially reduced in this multistep process to 34.5-49.5 mg/kg, depending on the sulphur content of the animal fat, and obviously out of specifications. The water produced in this esterification step and the acid catalyst need to be eliminated from the reaction medium, since we usually do not evaporate the methanol and use the reaction mixture in the next transesterification step; this could be done in three different ways with similar success:

(a) The first was chemically, by adding a 30 wt. % excess over the stoichiometric of freshly calcined calcium oxide,(213) to form calcium hydroxide; this method also neutralized the p-TsOH catalyst. The calcium salts formed need to be separated by centrifugation, and occasionally the biodiesel should be treated with magnesium silicate to lower the excessive calcium content.

(b) The second way was by adsorption of the reaction water on a 4 Å molecular sieve (10 wt. % oil-fat), which could be easily removed by filtration. In this alternative, the p-TsOH catalyst needs to be neutralized in the transesterification step using an excess of sodium methoxide.

(c) The third method was by overnight decantation of the upper methanol-water-acid catalyst phase from the lower oil/fat phase (80). This method has the important drawback that the methanol in the upper phase has to be distilled fractionally and returned to the reaction medium.

3.1.2 Biodiesel production from coconut, palm kernel, babassu and camelina oils.

Crude palm kernel oil has an acidity index of 2.18° (4.32 mg KOH/g) and a water content of 442 ppm, and thus, the esterification step described previously for the low grade animal fat was pertinent to reduce the acidity to (0.14 mg KOH/g).

Cameline seeds are very small dark-yellow grains of elliptical shape (2.09 mm × 1.14 mm). Whole seeds of cameline were dried overnight at 105 °C in an oven, and the seeds were extracted with dichloromethane in a 1 L Soxhlet extractor for 24 h. After elimination of the solvent, the oil extracted amounts only to 6% wt. of the dried seeds, and since higher oil yield have been reported for this seed in the literature (224) the seeds were gently ground in an iron mortar, repeating the extraction procedure afterward. The amount of extracted oil from the grounded seeds increased to 31.4 wt. %, closer to the reported values.

Crude babassu and cameline oils needed a previous step of esterification, since their acidity numbers were 7.96 and 3.96 mg KOH/g oil, respectively; after the esterification, their acidity numbers

decreased to 0.24 and 1.58 mg KOH/g oil, respectively. After the esterification step, babassu oil was dried over 4 Å molecular sieve (8 wt. % of sieve based on the weight of oil) due to its high water content (984.1 ppm), which would produce the formation of soaps, and it was filtered prior to transesterification.

Cameline oil was essentially dry due to the previous drying of the seeds.

3.2 Transesterificaction.

3.2.1 Biodiesel from low grade animal fat.

For this biodiesel, sodium methoxide (1 wt. % of the oil-fat) was always used as the basic catalyst, as is usual in our processes;(4, 5, 6) the sodium methoxide (ca. 30 wt. %) was solved in the amount of methanol necessary to reach the 7.5:1 molar ratio of methanol-fat used in this step, and it was added to the reaction mixture from the precedent esterification step. The advance of the transesterification was followed by Fourier transform infrared (FT-IR) spectroscopy (225). Usually, the transesterification was completed in 60 min with quantitative yield.

3.2.2 Biodiesel from soybean oil, WFO and horse tallow.

In this section the transesterification of the waste olive oil is described, the other two Feedstock went through a similar procedure. In a 2.0 L glass reactor (see Fig. 5) equipped with a glass anchor-shaped stirrer, a type K thermocouple, a water condenser and funnel, and surrounded by a heating mantle controlled by a proportional integral derivative (PID) temperature controller device, 873 mL (702 g, 0.80 mol) of waste frying oil and 244 mL (6 mol) of methanol were placed. The temperature was raised to 60 °C and the mixture was stirred at 600 rpm. When this temperature was reached, sodium methoxide (7 g, 0.13 mol, 1% wt. of oil, prepared recently from sodium metal and anhydrous methanol) was added; the temperature increased by two to three degrees, decreasing later to 60 °C by the action of the PID controller. Samples of 10 mL (8 g) were taken from the reaction mixture at regular intervals, typically 10 min, neutralized, and analysed by gas chromatography (GC, see below). When the conversion of the oil was quantitative, as determined by the GC, the heating mantle was switched off. The mixture was then allowed to cool in the reactor and was neutralized with the stoichiometric amount of concentrated hydrochloric acid (11.5 mL, 35% wt.), appearing as two distinct phases after switching off the stirrer. These two phases were decanted using the bottom outlet of the reactor. The excess methanol in both phases was evaporated at vacuum, and 580 g of biodiesel, 17 g of glycerine water interface and 200 mL

of methanol were recovered. The interface was composed of glycerine, water and sodium chloride. Biodiesel, was a clear, light yellow liquid.

3.2.3 Kinetic experiment.

For the production of biodiesel from waste olive oil it had been used the method of transesterification with methanol and basic catalyst (sodium methoxide) in the following conditions: molar ratio methanol / oil: 7.85 /1; temperature: 60 °C; stirring speed: 600 rpm approx.; amount of catalyst from 1.4 to 2.8 % wt. of the oil. The total quantity of the oil 760 mL (700 g) was placed in the reactor with part of the methanol, 155 mL (120.9 g, 3.78 mol). The stirring and the heating were switched on and the temperature begins to rise until the 60 °C according to the controller programming. The rest of the methanol, 100 mL (78 g, 2.44 mol) was used for the preparation of the catalyst by reaction with 4.35 g (0.189 mol) of metallic sodium. After the total dissolution of the sodium, the catalyst was added to the reactor were the desired temperature was already achieved. A slight increase of temperature to 64 °C was observed after the addition of the catalyst which was soon controlled by the PID to 60°C. The reactor was then left for the time specified for the reaction. After this time had passed, the heating and the stirring were switched off and one hour after the refrigerating water was also switched off, and the two phases were decanted overnight. After the distillation of the methanol in both phases, the glycerine phase was neutralised with 14.5 mL of concentrated (37 % wt.) hydrochloric acid. The biodiesel phase was neutralised in a decanting funnel with two washings with diluted aqueous solution of hydrochloric acid, and afterwards it was washed with diluted aqueous solution of sodium chloride and three times with water. The biodiesel was then dried with anhydrous sodium sulphate and filtered.

The kinetics experiments have been carried out following the procedure described above. From the three different samples provided by the School of Mines, the one used for this experiment was the third one. Samples of 10 mL were taken at 2, 5, 10, 15, 25, 40 and 60 minutes and were immediately neutralised with 1:1 hydrochloric acid (2 mL). Methanol was evaporated from the sample using a rotary evaporator and 10 mL of THF were added, in order to avoid a biphasic system, and this solution was then dried with anhydrous sodium sulphate. The amount of biodiesel taken for the sample (around 200 mg accurately weighed) was used for the analysis of free glycerol, and mono-, di- and triglycerides according to the standard EN 14105 [18] (instead of the 100 mg to balance for the addition of the THF). The Fatty Acids Methyl Esters (FAME) content was calculated from the above analyses and the mass balance in each kinetic sample.

3.2.4 Biodiesel from jojoba oil wax.

- *Transesterification of jojoba oil-wax to methyl jojoboate with acid catalysis*

In a 1L round bottomed flask, 0.4 L of methanol (316 g, 9.87 mol) were cooled in an ice-salt-water bath, and 23 mL of acetyl chloride (25 g, 0.32 mol) added drop wise so that the inside temperature was kept below 5 °C. The addition took 25 min. This solution was then added to 49.2 mL (42.4 g, 0.072 mol) of Jojoba oil-wax and 40 mL of toluene placed in a 1.0 L cylindrical glass tank reactor, and the mixture was refluxed at 62 °C for 4 h with vigorous stirring (600 rpm). This procedure was used to generate dry hydrochloric acid plus acid acetic acid.

On cooling, it was poured into 0.6 L of distilled water. The organic phase was decanted, and the aqueous phase was extracted with petroleum ether (b.p. 30–70 °C). The organic phases were combined, washed with 0.1M sodium carbonate solution, saturated sodium chloride solution (three times) and dried over anhydrous sodium sulphate. Evaporation of the solvent in a rotary evaporator left 43.2 g (97% isolated yield, 97% gas chromatography conversion) of a mixture of methyl jojoboate and jojobyl alcohol in an approximately 1:1 ratio. IR: 1745 cm^{-1} (C=O), 3649 cm^{-1} (O–H).

- *Transesterification of jojoba oil-wax to methyl jojoboate with basic catalysis*

Freshly cut sodium metal (0.736 g, 0.032 mol) was added in small pieces to 50mL of methanol (39.5 g, 1.23 mol) placed in a glass flask in a hood over a period of about 30 min. The solution obtained was then poured over 200 mL of Jojoba oil-wax (172.4 g, 0.293 mol) and 100mL of methanol (78.7 g, 2.46 mol), placed in a 1.0 L autoclave Burton-Coblin from Autoclave Engineers. The autoclave was closed, and the mixture was heated at 65 °C with stirring at 600 rpm for a 4 h period. On cooling at room temperature, the autoclave was opened and the mixture was neutralized adding concentrated hydrochloric acid (2.8 mL, 0.032 mol) with vigorous stirring. The excess methanol was evaporated under vacuum, and the crude product was dried with anhydrous sodium sulphate and filtered, yielding 163.4 g (90% isolated yield, 100% gas chromatography conversion) of a mixture of methyl jojoboate and jojobyl alcohol in an approximately 1:1 ratio. IR: 1745 cm^{-1} (C=O), 3649 cm^{-1} (O–H).

3.2.5 Biodiesel from castor oil.

The only parameter that could cause any problem during the transesterification process is the high water content (1920 mg/kg) and the high hygroscopic character of this oil (226). However, we proceeded further in our research without any drying of the oil.

The transesterification of castor oil with methanol was carried out in two scales, 1.5 and 50.0 L reactors with basic catalysis. A commercial solution of sodium methoxide 25 wt.% in methanol was always used as the basic catalyst. The advancement of the transesterification was followed by FT-IR spectroscopy (227), taking aliquots every 2 min at the beginning of the reaction, later every 5–10 min and finally every 30 min: the lower G-Phase was decanted, the upper phase was dissolved in tetrachloroethylene, and the absorbance of the peaks at 1436 cm^{-1} and 1465 cm^{-1} was checked against a calibration plot made with standards of pure castor FAME and pure castor oil. Methanol does not interfere with this analytical method. Usually, the transesterification was completed in 60 min with quantitative yield.

3.2.6 Biodiesel from coconut, palm kernel, babassu and camelina oils.

Transesterification of coconut and palm kernel oils were carried out following our experimental procedure previously described in 3.2.3. Refined coconut oil has an acidity index of 0.6° (1° is equivalent to 1 % wt. of free oleic acid. In the units of acidity for biodiesel or kerosene, 10 is equivalent to 1.98 mg KOH/g, that is, to simplify the calculus, 1° = 2 mg KOH/g), and a water content of 411 ppm. The previous esterification step was unnecessary with this feedstock.

Transesterification of babassu and camelina oils was carried out following the experimental procedure previously described in 3.2.3.

3.2.7 Biodiesel from various feedstocks used in the combustion tests.

FAME and FAEE from coconut, peanut, soybean, rapeseed, linseed and palm oil and animal fat have been produced. Degumming, esterification (if necessary) and transesterification of oils/fats have been carried out in the 2 L reactor following the method previously described in section 3.2.3 for the low grade animal fat using a 6:1 methanol: oil ratio instead.

3.3 Purification

3.3.1 Biodiesel from low grade animal fat.

The upper biodiesel phase was separated from the lower G-phase by centrifugation, and the methanol remaining in the biodiesel was eliminated by vacuum distillation. Two alternative ways of biodiesel purification were used in this work: (a) the "wet wash" and (b) the "dry wash" with magnesium silicate, brand name Magnesol D60.41

(a) The "wet" wash consists of a neutralizing step with a 1 wt. % citric acid solution, a washing step with 3 wt. % sodium chloride solution, and three consecutive washing steps with deionized water, followed by dehydration with a 4 Å molecular sieve.

(b) The "dry" wash consists in the treatment of the biodiesel with 2 wt. % magnesium silicate at 77 °C, with stirring at 800 rpm for 30 min, leaving the adsorbent decanting overnight, and filtering it afterward through a 0.45 μm filter.

3.3.2 Biodiesel from Jojoba oil wax.

- *Separation of methyl jojoboate from jojobyl alcohol*

The mixture of methyl jojoboate and jojobyl alcohol (43 g, 50 mL) was dissolved in low boiling point petroleum ether (b.p. 30–70 °C, 100 mL) in a volumetric ratio 1:2, and the solution was left overnight in the freezer at -18 °C. An abundant white solid crystallized that was quickly filtered at vacuum while cooling using a water pump. The mother liquors were concentrated in a rotary evaporator, yielding 23.8 g (55.3%) of an oil, the FAME mixture methyl jojoboate. Its GC-MS analysis showed a composition of 79% FAME mixture (51.5% of methyl-cis-11-eicosenoate, C 20:1, and 14.5% of methyl-cis-13-docosenoate, C 22:1), and 21% fatty alcohols (11.6% of cis-11-eicosen-1-ol), see table 19 4th column (Chapter III section 2.4).

The solids filtered in the Büchner funnel were left at room temperature and they melted slowly (20 h) to yield after vacuum concentration in a rotary evaporator 17.9 g of an oily product (41.6% yield), the fatty alcohols rich fraction jojobyl alcohol, its composition was also determined by GC-MS showed a composition of 28% FAME mixture (18.33% of methylcis-11-eicosenoate, C 20:1) and 72% fatty alcohols (26.1% of cis-11-ecosen-1-ol, 35.75% of cis-13-docosen-1-ol, and 8.0% of 15-tetracosen-1-ol, Table 19, 5th column, Chapter III section 2.4). A small amount of oily solids (0.638 g, 1.6% yield) did not

melt at room temperature, and this oily white solid was also analysed by GC-MS (Table 19, 6th column, chapter III section 2.4).

A different separation method based in the vacuum distillation of the crude transesterification product was totally unsuccessful, since only a very small amount of light cracked products could be distilled.

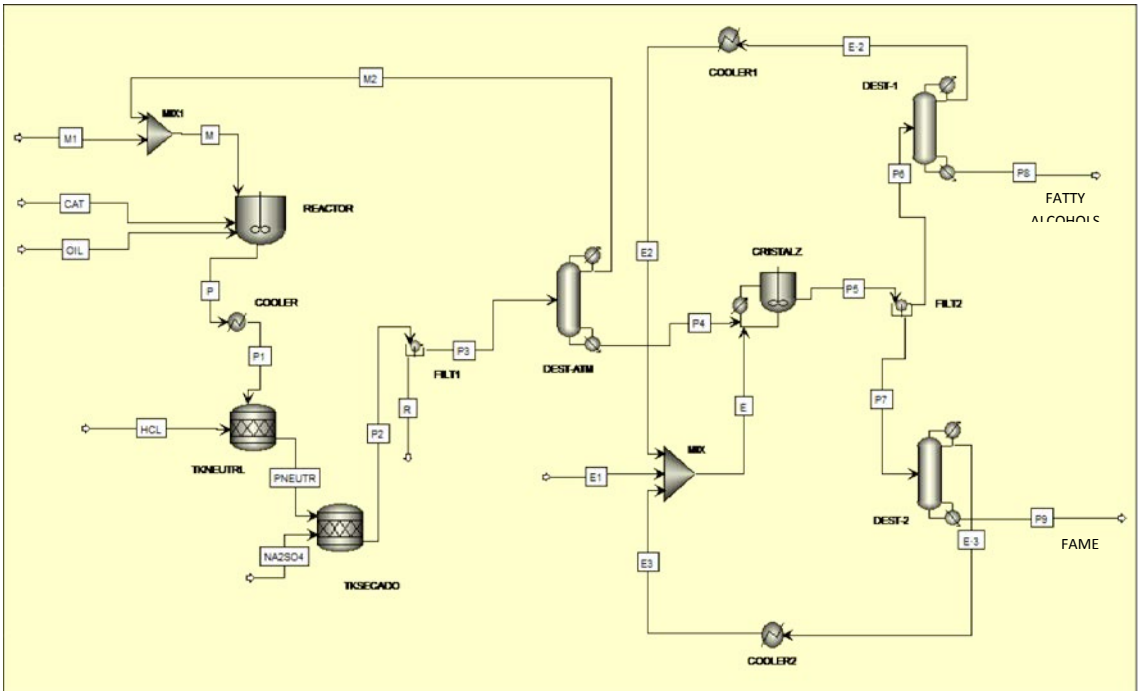

Fig. 9. Block diagram of the batch transesterification process of Jojoba oil-wax with methanol, catalyzed with sodium methoxide. From left to right: M1 = fresh methanol feed; M2 = recycled methanol; M = methanol feed to the reactor; CAT = catalyst feed; OIL = Jojoba oil-wax feed; Pn = Products of the different unit operations; TKNEUTRL =neutralization tank; HCL = hydrochloric acid 35 wt%; TKSECADO = drying tank; Na2 · SO4 =anhydrous sodium sulphate; FILT1 = filter 1; R = residual solids (NaCl and Na2SO4 ·nH2O); DEST-ATM = distillation column for the recovery of methanol; E1 = fresh petroleum ether; E2 = recycled petroleum ether from the fatty alcohols mixture; E3 =recycled petroleum ether from the FAME mixture; CRISTALZ ¼ crystallizator; E =petroleum ether feed to the crystallizator; FILT2 = filter for FAME and fatty alcohols separation; DEST-1 and DEST-2 = distillation columns for the recovery of petroleum ether; P8 = fatty alcohols mixture (42% yield); P9 = FAME mixture (55% yield).

Fig. 9 shows a block diagram of the process of transesterification of Jojoba oil-wax with basic catalysis, including the steps of methanol recovery from the reaction and of petroleum ether recovery from the cryogenic crystallization.

3.3.3 Biodiesel from castor oil.

The upper FAME phase was separated from the lower G-phase by centrifugation (1.5 L reactor) or decantation (50 L reactor). In all the experiments it is noticeable that a small amount of G-phase separated (around 35 mL in the 1.5 L reactor and at around 1.8 L in the 50 L reactor, see Table 21, chapter III section 2.5). In the transesterification of other oils, the G-phase usually contains most of the unused methanol and the FAME contains only 3–5 % vol. of methanol, but this is not the case with the FAME of castor oil which retains most of the methanol due to its association with the methyl ricinoleate by hydrogen bonds. Thus, the methanol remaining in the FAME was eliminated although not completely by vacuum distillation. Two alternative ways of FAME purification were tried in this work: the "wet wash" and the "dry wash". The "wet wash" consists of a neutralizing step with a 1 wt.% citric acid solution, a washing step with 3 wt.% sodium chloride solution, and three consecutive washing steps with deionized water, followed by dehydration with 4 A molecular sieve. However, the FAME forms an emulsion with the aqueous phase of the neutralisation step that cannot be separated by decantation or centrifugation (see Fig. 10), so this "wet wash" purification method is unpractical using castor oil as feedstock for FAME production. The "dry wash" consists in the treatment of the FAME with:

(a) A 2–4 wt.% of magnesium silicate Magnesol D-60 at 77 °C, with stirring at 800 rpm for 30 min, leaving the adsorbent decanting overnight, and filtering it afterwards through a 0.45 mm filter (227)

(b) A 10 wt.% of Amberlite BD-10 at room temperature, with stirring at 800 rpm for 2 h, leaving the adsorbent to decant, and filtering it afterwards through a 0.45 mm filter.

Figure 10. Graphical summary of the experimental troubles found in the production of FAME from castor oil: Irreversible emulsions formation in the "wet wash" purification method.

3.4 Distillation of biodiesel from coconut, babassu, and palm kernel to produce biokerosenes.

The biokerosene fraction of the FAME's was obtained by fractional distillation of the coconut, and babassu and palm kernel biodiesel fuels using a 41 cm long - 3.5 cm o.d. Vigreux column. The coconut biokerosene (CBK100) distilled between 47 and 114 °C at 2 torr (2.67 h Pa) with a yield of 81.8 wt.% based on the coconut FAME, and leaving 12.6 wt.%. yield of a bottom fraction (coconut bottom) that was also characterized. The palm kernel biokerosene (PBK100) distilled between 35 and 113 °C at 2 torr (2.67 h Pa) with a yield of 40.8% based on the palm kernel FAME, and leaving a 58.6% yield of a bottom fraction (palm kernel bottom) that was also analysed. And the babassu biokerosene fraction distilled between 47 and 124 °C at 2 torr (2.67 hPa) yielding 73.3 wt. % with respect to the babassu biodiesel fuel and 19.4 wt. % yield of a bottom fraction (babassu bottom)

The cameline biokerosene (CAM100) and linseed biokerosene (LIN100) were used without previous distillation.

3.5 Additives derived from glycerol.

- *1-Chloro-3-tert-butoxypropan-2-ol synthesis **1** (chlorohydrinether)*

Tert-butanol (4 mol, 296 g) and 5 wt.%. of boron trifluoride etherate (0.104 mol, 14.2 g) were mixed in the stirred tank reactor. The mixture was maintained at ca. 80 °C. At this temperature, epichlorohydrin (1 mol, 92.5 g) was added dropwise to the reactor in a period of 2 h. After addition was finished, the reaction mixture was stirred for an additional 20 h until the reaction was completed, as observed by thin layer chromatography (TLC). The mixture was then cooled at room temperature and diluted with water. The solution was exhaustively extracted with dichloromethane. The combined extracts were washed with brine and dried with anhydrous sodium sulphate and finally, the dichloromethane was evaporated in vacuum. The crude 1-chloro-3-tert-butoxypropan-2-ol **1** (pure by GC and ^{1}H-NMR) was used without further purification (144.8 g, 87%, bp 56–7 °C 80torr). ^{1}H-NMR δ 1.17 (s, 9H); 2.67 (δ, 1H) 3.4–4.0 (m, 5H).

- *Tert-butoxypropylene-1,2-oxide **2** (tert-butyl glycidyl ether) synthesis*

The chlorohydrin ether **1** obtained in the precedent procedure (1.03 mol, 172 g) was introduced in the reactor under N_2 atmosphere and cooled in an ice bath to approximately 5 °C. Addition of NaOH (50 wt.% aqueous, 1.275 mol) was carried out dropwise during a 1 h period, keeping the mixture stirred at 5 °C. Stirring at room temperature was kept until the reaction was complete by TLC (approximately 15 h). Water was added to the reaction mixture and the phases separated. The aqueous phase was exhaustively extracted with dichloromethane, and the combined organic phases were washed with water until neutral pH, then washed with brine and dried with anhydrous sodium sulphate. The solvent was removed by evaporation in vacuum. 3-Tert-butoxypropylene-1,2-oxide **2** was vacuum distilled as a colorless oil (102 g, 76.3%; 66–67 °C25 torr; lit. bp 152 °C760 torr (228)). ^{1}H-NMR: δ 1.17 (s, 9 H); 2.7 (m, 2H); 3.13 (m, 1H); 3.50 (m, 2H). 3-Tert-butoxypropane-1,2-diol **4** was also vacuum distilled as a colorless oil (36.1 g, 23.7%; 94.2–97.2 °C 0.075 torr). ^{1}H-NMR: δ 1.14 (s, 9 H); 3.36 (dd, 1 H, J = 9.2 Hz, J = 5.8 Hz); 3.38 (dd, 1 H, J = 9.2 Hz, J = 4.4 Hz); 3.54 (s, 2H, OH); 3.56 (dd, 1 H, J = 11.3 Hz, J = 5.7 Hz); 3.63 (dd, 1 H, J = 11.3 Hz, J = 3.7 Hz); 3.74 (m, 1 H).

- *1,3-Di-tert-butoxypropan-2-ol* Four different alternative catalysts have been checked:

A) Perchloric acid catalyst:

A mixture of tert-butanol (4 mol, 296 g) and 72 wt.% perchloric acid (0.01 mol, 1.00 g) was introduced in the 2 L reactor and heated at 80 °C. Once this temperature was reached, tert-butyl glycidyl ether **2** (1 mol, 130 g) was added dropwise during a 1 h period.The mixture was stirred for 15 additional hours, until all the reagent **2** was consumed as observed by GC. The resulting mixture was cooled and neutralized with aqueous 0.5 M sodium carbonate solution. The excess tert-butanol and water were evaporated in vacuum. 1,3-Ditert-butoxypropan-2-ol **3** was obtained in a 25.8% yield by GC.

B) Potassium hydroxide catalyst:

A mixture of tert-butanol (0.3 mol, 22.2 g) and potassium hydroxide (0.025 mol, 1.4 g) was placed in a magnetically stirred 250 mL three necked flask. The flask was heated to 80 °C in an oil bath. Once the temperature was reached and the potash lenses were dissolved, tert-butyl glycidyl ether **2** (0.1 mol, 13.0 g) was added dropwise during 1 h period. The mixture was kept stirred for an additional hour, until a conversion higher than 50% of the starting material **2** was observed by GC. The resulting mixture was cooled and neutralized with 0.6 mL of 1.12 M sulphuric acid. The excess tert-butanol and water were evaporated in vacuum. 1,3-Di-tert-butoxypropan-2-ol **3** was obtained only in a 3.8% yield by GC.

C) Sodium tert-butoxide catalyst:

Sodium tert-butoxide catalyst: A mixture of terbutanol (0.3 mol, 22.2 g) and metallic sodium (0.013 mol, 0.3 g) was placed in a magnetically stirred 250 mL three necked flask. The flask was heated to 80 °C until all sodium was dissolved. Later, tert-butyl glycidyl ether **2** (0.1 mol, 13.0 g) was added dropwise during 1 h period. The mixture was stirred at the same temperature for five additional hours, until the conversion of the starting compound **2** was quantitative as observed by GC. The resulting mixture was cooled and neutralized with 0.6 mL of 1.12 M sulphuric acid. The excess tert-butanol and water were evaporated in vacuum. 1,3-Ditert- butoxypropan-2-ol **3** was obtained only in a 4.1% yield by GC.

D) Boron trifluoride etherate catalyst

A mixture of tert-butanol(4 mol, 296 g) and boron trifluoride etherate (0.01 mol,1.42 g) was placed in a mechanically stirred 2 L tank reactor.The reactor was heated at 80 _C. Tert-butyl glycidyl ether **2** (1 mol, 130 g) was added dropwise during 1 h period. Temperature and stirring were kept for an additional 15 h period, until the conversion of the compound **2** was quantitative by GC. The mixture was then cooled at room temperature and diluted with water. The solution was exhaustively extracted with dichloromethane. The combined extracts were washed with brine and dried with anhydrous sodium sulphate and finally, the dichloromethane was evaporated in vacuum. 1,3-Di-tert-butoxypropan-2-ol **3** was purified by vacuum distillation (107.3 g, 52.6% yield) ^{1}H-NMR: δ 0.98 (s, 18 H); 2.81 (s, 1H, OH); 3.16 (dd, 2 H, J = 9.0 Hz, J = 5.8 Hz); 3.20 (dd, 2H, J = 9.0 Hz, J = 5.3 Hz); 3.56 (m, 1 H, CH). MS (70 eV): 186 (M^{+}-18), 171 (M^{+} -18-15), 147 (M^{+}-57), 133, 117, 112, 100, 87, 75, 57 (base peak), 41, 29. A small impurity of 1,2,3-tri-tert-butoxypropane 5 was present in the distillate. ^{1}H-NMR: δ 1.15 (s, 18 H); 1.19 (s, 9 H); 3.16 (dd, 2 H, J = 9.2 Hz, J = 5.3 Hz); 3.36 (dd, 2 H, J = 9.2 Hz, J = 5.8 Hz); 3.59 (m, 1 H). MS (70 eV): 261 (M^{+} + 1), 186, 173, 133, 130, 117, 87, 75, 57 (base peak). Higher heating value = 32.503 MJ kg-1; lower heating value = 29.955 MJ kg-1 (229).

4 OTHER EXPERIMENTAL PROCEDURES: COMBUSTION OF BIODIESEL

4.1 PAH analysis.

The higher heating values of FAME and FAEE were measured in an automatic calorimetric pump LECO AC300, burning 1.0 g of biofuel under different pure oxygen pressures: 689.5 kPa (100 psi), 1379.0 kPa (200 psi), 2068.4 kPa (300 psi) and 2757.9 kPa (400 psi). Once the combustion test has finished, the sample crucible and the bomb were thoroughly rinsed with dichloromethane and the combined dichloromethane extracts were passed through a Pasteur pipette half filled with silica-gel to eliminate soot particles.

In the test at 200, 300 and 400 psi of oxygen pressure, the test was repeated three times without changing nor cleaning the crucible and the bomb, in order to recover a higher amount of post-combustion products. In the test at 100 psi, the test was carried out only once, the crucible and the bomb were washed separately with dichloromethane, recovering the soot particles present in both devices, and the separated extracts were passed through silica-gel in the same way as described above. These recovering methods for PAH were taken into account when quantifying the total amount of PAH produced from each feedstock.

4.2. Smoke point and Oxygen extended sooting index of biokerosenes

Smoke point is defined as the height in millimetres of the highest flame produced without smoking soot breakthrough when the fuel is burned in a specific test lamp (230). Numerous studies (231, 232, 233) defined the sooting tendency of fuels and blends as inversely proportional to their smoke point. Consequently, a minimum value is required in jet fuel standards (min. twenty-five mm). A standard smoke point lamp as specified by ASTM D1322 (230) was used for the smoke point measurements. A blackpainted steel frame surrounding the apparatus was used to control air flow during the measurements. For each fuel, the smoke points were measured three times and averaged, and the standard deviation was obtained. Previously, the method was calibrated in accordance with ASTM D1322 using two standard reference fuel blends. The first blend, composed of 15% (v/v) toluene and 85% (v/v) 2,2,4-trimethylpentane (iso-octane), led to a smoke point of 25 mm, and the second blend, composed of 40% (v/v) toluene and 60% (v/v) 2,2,4-trimethylpentane, led to a smoke point of 15 mm. The comparison of

the measured smoke points and those reported in the standard led to a correction factor of 1.006. The ambient temperature and relative humidity of the test site were monitored to make sure that fluctuations of environmental conditions did not affect the smoke points of the blends. The ambient temperature ranged from 21 to 25 °C, and the relative humidity ranged from 47 to 57%. All tests were performed at atmospheric pressure (around 93.5 kPa).

5 CHARACTERISATION SUMMARY

The following tables 4a through 9b summarize the characterisation methods and standard procedures carried out in the Madrid School of Mines laboratory and other partner laboratories (1) and (2) to assess the properties of the products used in this work as well as the ones from their blends with fossil kerosene.

(1) Laboratory of Fuels and Petrochemistry

Tecnogetafe Scientific Park c/ Erik Kandel s/n

28906 – Getafe Spain

(2) Grupo de combustibles y motores

ETS Ingenieros Industriales

Universidad de Castilla La Mancha

Avenida Camilo José Cela s/n

13071 - Ciudad Real, Spain

Table 4a: Edible oils characterisation

Property	Standard-Method	Soybean oil	Palm kernel oil	Babassu oil	Coconut oil
Acidity index (°)	ISO 660	x	x	x	x
Elemental analysis (CHN)	ASTM D5291	x			
Gas chromatography analysis		x			
Sulphur Content	ASTM D4294	x			

Table 4b: Non edible fats and oils characterisation

Property	Standard-Method	WFO	Tallow	Animal fat	Animal fat mixed with soybean oil	Jojoba oil-wax	Castor oil	Camelina oil
Acidity index (°)	ISO 660	x	x	x	x		x	x
Cold Filter Plugging Point… (CFPP, °C)	EN 116					x		
Colour (Gardner)	AOCS Td 1a 64						x	
Density at 15 °C (kg /m^3)	ASTM D 4052					x		
Density at 15 °C (g/cm^3)	ASTM D1298	x						
Elemental analysis (CHN)	ASTM D5291			x	x		x	
Gas chromatography analysis (m/m%)		x	x			x	x	
Iodine index (g I_2/100 g)	ISO 3961						x	
Kinematic viscosity at 40 °C (mm^2/s)	ASTM D 445					x		
Refraction index (20 °C)	UNE 55015						x	
Saponification index (mg KOH/g)	ISO 3657						x	
Sulphur Content	ASTM D4294			x	x			
Water content (mg/kg)	ISO 662						x	

Table 5a: FAME from edible oils chemical properties

Property	Standard-Method	Soybean FAME	Palm FAME	Rapeseed FAME	Peanut FAME
Acidity index (mg KOH/g)	EN ISO 660/2000	x			
Calcium, mg/kg		x			
Composition Other	GC-MS	x			
Conversion	FT-IR	x			
Elemental analysis	ASTM D5291	x			
Ester content (% m/m)	EN 14 103	x			
Ester profile	EN 14103	x	x	x	x
Fat and oil derivatives (m/m%)	EN 14105	x			
Group I metals (mg/kg)	EN 14109	x			
Group II metals (mg/kg)	EN 14538	x			
iodine index, mg of I_2/100 g	ISO 3961	x	x	x	x
Iodine value	fom FAME profile	x			
Methanol (m/m%)	EN 14110	x			
Phosphorous content (mg/kg)	EN 14 107	x			
Oxidative stability (h)	EN 14112	x			
Sulphur content, mg/kg	ASTM D4294	x			
Total contamination (mg/kg)	EN 12662	x			
Water content (mg/kg)	ASTM D1774	x			

Table 5b: FAME from edible physical and combustion properties

Property	Standard-Method	Soybean FAME	Palm FAME	Rapeseed FAME	Peanut FAME
Cetane Index	ASTM D-4737	x			
Cetane number	from FAME profile	x	x	x	x
Cloud point(°C)	ASTM D2500	x	x	x	x
Cold Filter Plugging Point (CFPP, °C)	EN 116	x	x	x	x
Colour and aspect	ASTM D1500	x	x	x	x
Copper strip corrosion (class)	ASTM D 130	x			
Density at 15 °C (g/cm^3)	ASTM D1298	x			
Density at 23 °C (kg/m^3)	EN ISO 3675	x	x	x	x
Distillation curve	ASTM D-86	x			
Flash point (°C)	EN ISO 3679	x			
Higher heating value, MJ/kg	ASTM D240	x			
Kinematic viscosity at 40 °C (mm^2 /s)	ASTM D 445	x	x	x	x
Kinematic viscosity at 40 °C (mm^2 /s)	EN ISO 3104	x			
Lower heating value (MJ/kg)	ASTM D240-modified	x	x	x	x
Lower Heating Value (LHV)(MJ/kg)		x			
Pour point(°C)	ASTM D2500	x	x	x	x

Table 5c: FAME from edible oils chemical properties

Property	Standard-Method	Palm kernel FAME	Babassu FAME	Coconut FAME	Palm kernel distillate	Babassu distillate	Coconut distillate	Palm kernel bottom	Babassu bottom	Coconut bottom
Acidity (mg KOH/g)	EN ISO 14104				x	x			x	
Elemental composition	ASTM D5291				x	x	x		x	
Ester profile	EN 14103	x	x	x	x	x	x	x	x	x
Water content (mg/kg)	ASTM D1774					x			x	
Water content (mg/kg)	EN ISO 12937						x			

Table 5d: FAME from edible physical and combustion properties

Property	Standard-Method	Palm kernel FAME	Babassu FAME	Coconut FAME	Palm kernel distillate	Babassu distillate	Coconut distillate	Palm kernel bottom	Babassu bottom	Coconut bottom
Cloud point(°C)	ASTM D2500					x			x	
Cold Filter Plugging Point (CFPP, °C)	EN 116				x	x	x		x	
Colour and aspect	ASTM D1500				x	x	x		x	
Copper strip corrosion (class)	ASTM D 130				x	x	x		x	
Density at 15 °C (g/cm^3)	ASTM D1298								x	
Density at 15 °C (kg /m^3)	ASTM D 4052				x	x	x			
Density at 23 °C (kg/m^3)	EN ISO 3675					x	x			
Flash point (°C)	EN ISO 3679				x	x			x	
Freezing point (°C)	ASTM D2386				x					
Higher heating value, MJ/kg	ASTM D240				x	x	x	x	x	x
Kinematic viscosity at 40 °C (mm^2 /s)	ASTM D 445				x	x	x			
Kinematic viscosity at 40 °C (mm^2 /s)	EN ISO 3104								x	
Lower heating value (MJ/kg)	ASTM D4809				x	x	x			
Lower heating value (MJ/kg)	ASTM D240*				x	x	x	x	x	x
Lubricity (mm), HFRR test	EN ISO 12156						x			
Oxidative stability (h)	EN 14112				x	x	x			
Pour point(°C)	ASTM D2500					x			x	
Smoke point (mm)	ASTM D1322				x	x	x			

Table 5e: FAME from non-edible oils and fats characterisation

Property	Standard-Method	Waste Frying oil FAME	Tallow FAME	Animal fat FAME	Animal fat mixed with soybean FAME	Jojoba oil-wax crude FAME	Methyl jojoboate	Castor FAME
Acidity index (mg KOH/g)	EN ISO 660/2000	x		x	x			x
Calcium, mg/kg				x	x			
Composition Other	GC-MS	x		x	x	x	x	
Conversion	FT-IR			x	x	x		
Elemental analysis	ASTM D5291	x		x	x			x
Ester content (% m/m)	EN 14 103			x	x			
Ester profile	EN 14103	x	x	x	x			x
Fat and oil derivatives (m/m%)	EN 14105	x		x	x			x
Group I metals (mg/kg)	EN 14109			x	x			x
Group II metals (mg/kg)	EN 14538			x	x			
iodine index, mg of I_2/100 g	ISO 3961			x	x			x
Iodine value	from FAME profile			x	x			
Methanol (m/m%)	EN 14110			x	x			x
Oxidative stability (h)	EN 14112			x	x			
Phosphorous content (mg/kg)	EN 14107			x	x			
Soaps content (m/m% sodium oleate)	Titration	x						x
Sulphated ash, (m/m%)	ASTM D 482	x						x
Sulphur content, mg/kg	ASTM D4294			x	x			x
Total contamination (mg/kg)	EN 12662	x		x	x			x
Water and Sediments	ASTM D 1796	x						
Water content (mg/kg)	ASTM D1774			x	x			
Water content (mg/kg)	EN ISO 12937							x

Table 5f: FAME from non-edible oils and fats physical and combustion properties

Property	Standard-Method	Waste Frying oil FAME	Tallow FAME	Animal fat FAME	Animal fat mixed with soybean FAME	Jojoba oil-wax crude FAME	Methyl jojoboate	Castor FAME
Cetane Index	ASTM D-4737	x	x					
Cetane number	from FAME profile			x	x			
Cloud point(°C)	ASTM D2500	x		x				
Cold Filter Plugging Point (CFPP, °C)	EN 116	x		x	x	x	x	x
Colour and aspect	ASTM D1500		x					
Copper strip corrosion (class)	ASTM D 130	x						
Copper strip corrosion (class)	ASTM D 130	x		x	x			x
Density at 15 °C (g/cm^3)	ASTM D1298	x	x	x	x			x
Density at 15 °C (kg /m^3)	ASTM D 4052	x				x	x	
Distillation curve	(ASTM D-86)	x	x					
Flash point (°C)	EN ISO 3679	x		x	x			
Freezing point (°C)	ASTM D2386	x						x
Higher heating value, MJ/kg	ASTM D 2382					x	x	
Higher heating value, MJ/kg	ASTM D240	x		x	x			
Kinematic viscosity at 40 °C (mm2 /s)	ASTM D 445			x	x	x	x	
Kinematic viscosity at 40 °C (mm2 /s)	EN ISO 3104	X		x	x			x
Lower Heating Value (LHV)(MJ/kg)				x	x			
Lubricity (mm), HFRR test	EN ISO 12156							x
Pour point(°C)	ASTM D2500			x				x

Table 5g: FAME from non-edible oils and fats physical and combustion properties

Property	Standard-Method	Lineseed FAME	Camelina FAME
Elemental analysis	ASTM D5291		x
Ester profile	EN 14103	x	x
iodine index, mg of I_2/100 g	ISO 3961	x	
Oxidative stability (h)	EN 14112		x

Table 5h: FAME from non-edible oils and fats chemical properties

Property	Standard-Method	Lineseed FAME	Camelina FAME
Cetane number	from FAME profile	x	
Cloud point(°C)	ASTM D2500	x	x
Cold Filter Plugging Point (CFPP, °C)	EN 116	x	x
Colour and aspect	ASTM D1500	x	x
Copper strip corrosion (class)	ASTM D 130		x
Density at 15 °C (kg /m^3)	ASTM D 4052		x
Density at 23 °C (kg/m^3)	EN ISO 3675	x	
Higher heating value, MJ/kg	ASTM D240		x
Kinematic viscosity at 40 °C (mm2 /s)	ASTM D 445	x	
Lower Heating Value (MJ/kg)	ASTM D240-modified	x	x
Lower Heating Value (MJ/kg)	ASTM D4809		x
Pour point(°C)	ASTM D2500	x	x
Smoke point (mm)	ASTM D1322		x

Table 6: FAEE characterisation

Property	Standard- Method	Palm FAEE	Soybean FAEE	Rapeseed FAEE
Cetane number	from FAEE profile	x	x	x
Cloud point (°C)	ASTM D-2500	x	x	x
Cold Filter Plugging Point (CFPP, °C)	EN 116	x	x	x
Colour and aspect	ASTM D1500	x	x	x
Density at 15 °C (kg /m^3)	EN ISO 12185	x	x	x
Ester profile	EN 14103	x	x	x
Higher heating value, MJ/kg	ASTM D240	x	x	x
Iodine value	fom FAEE profile	x	x	x
Kinematic viscosity at 40 °C (mm^2 /s)	EN ISO 3104	x	x	x
Oxidative stability (h)	EN 14112	x	x	x

Table 7: Tert-butyl ethers of bioglycerol characterisation

Property	Standard-Method	Tert-butyl ethers of bioglycerol
Cold Filter Plugging Point (CFPP, °C)	IP 309	x
Density at 15 °C (kg /m^3)	ASTM D-4052	x
Flash point (°C)	EN ISO 3679	x
Higher heating value, MJ/kg		x
Kinematic viscosity at 40 °C (mm^2 /s)	EN ISO 3104	x
Kinematic viscosity at 40 °C (mm^2 /s)	ASTM D-445	x
Thin layer chromatography (TLC)		x

Table 8a: Blends with fossil fuels characterisation

Property	Standard-Method	Palm kernel biokerosene and Jet A1	Babassu biokerosene and Jet A1	Palm kernel biokerosene and fossil kerosene	Babassu biokerosene and fossil kerosene	Coconut biokerosene and fossil kerosene
Acidity (mg KOH/g)	EN ISO 14104		x	x	x	
Cloud point(°C)	ASTM D2500		x		x	
Cold Filter Plugging Point (CFPP, °C)	EN ISO 116			x	x	x
Colour and aspect	ASTM D1500	x	x	x	x	x
Copper strip corrosion, class	ASTM D130	x	x	x	x	
Density at 15 °C (g/cm^3)	ASTM D1298	x	x	x	x	
Density at 23 °C (kg/m^3)	EN ISO 3675		x			x
Elemental composition	ASTM D5291	x	x	x	x	x
Flash point (°C)	EN ISO 3679	x	x	x	x	
Freezing point (°C)	ASTM D2386	x		x		x
Higher heating value (MJ/kg)	ASTM D240	x	x	x	x	x
Lower heating value (MJ/kg)	ASTM D240b-modified	x	x	x	x	x
Lower heating value (MJ/kg)	ASTM D4809	x	x	x	x	x
Lubricity (mm), HFRR test	EN ISO 12156					x
Oxidative stability (h)	EN 14112		x		x	x
Pour point(°C)	ASTM D2500		x		x	
Smoke point (mm)	ASTM D1322	x	x	x	x	x
Viscosity at 40 °C (mm^2/s)	EN ISO 3104	x	x		x	x
Water content (mg/kg)	ASTM D1774		x		x	
Water content (mg/kg)	EN ISO 12937					x

Table 8b: Blends with fossil fuels characterisation

Property	Standard-Method	Castor FAME and fossil diesel	Camelina FAME and fossil kerosene
Acidity (mg KOH/g)	EN ISO 14104	x	
Aromatic hydrocarbons content (m/m%)		x	
Cloud point(°C)	ASTM D2500		x
Cold Filter Plugging Point (CFPP, °C)	EN ISO 116	x	x
Colour and aspect	ASTM D1500		x
Copper strip corrosion, class	ASTM D130		
Density at 15 °C (g/cm^3)	ASTM D1298	x	x
Elemental analysis	ASTM D5291	x	x
Flash point (°C)	EN ISO 3679		
Higher heating value (MJ/kg)	ASTM D240	x	x
iodine index, mg of I2/100 g	ISO 3961		
Lower heating value (MJ/kg	ASTM D240b-modified		x
Lower heating value (MJ/kg	ASTM D4809	x	x
Lubricity (mm), HFRR test	EN ISO 12156	x	
Oxidative stability (h)	EN 14112	x	x
Pour point(°C)	ASTM D2500		x
Smoke point (mm)	ASTM D1322		x
Viscosity at 40 °C (mm^2/s)	EN ISO 3104	x	
Water content (mg/kg)	ASTM D1774	x	x

6 CHARACTERISATION METHODS

6.1 Infrared Spectrophotometry

6.1.1 Transesterification control

1 Animal fat/soybean oil transesterification

The advance of the animal fat and soybean and castor oil transesterification was followed by Fourier transform infrared (FT-IR) spectroscopy in a FT-IR Bruker Model Vector 22, using a cell for liquids of 0.1 mm optical pathway, with potassium bromide windows in tetrachloroethylene as solvent (225). Jojoba oil wax transesterification was controlled using the same equipment but using 1,1,2-trichlorotrifluoro ethane solution using a cell for liquids with potassium bromide windows and a 0.1mm Teflon spacer, or in film between potassium bromide disks.

The advancement of the transesterification was followed by FT-IR spectroscopy (225), taking aliquots every 2 min at the beginning of the reaction, later every 5–10 min and finally every 30 min: the lower G-Phase was decanted, the upper phase was dissolved in tetrachloroethylene, and the absorbance of the peaks at 1436 cm^{-1} and 1465 cm^{-1} was checked against a calibration plot made with standards of pure castor FAME and pure castor oil. Methanol does not interfere with this analytical method.

- *Infrared spectrophotometry data treatment.*

This calibration has been set up for both the castor oil and the multi species animal fat.

(1) Equipment

The analysis have been carried out using a Bruker Vector 22 FT-IR spectrophotometer, using a circular cell with a 0.1 mm optical path and potassium bromide windows. Spectroscopic quality tethrachloretilene (Merk) was used as solvent.

(2) Procedure

First, the absorption in the infrared region of the initial and final species of the biodiesel synthesis reaction has been studied. The chosen method is mid infrared absorption spectrophotometry. Figure 11.1 shows the complete spectra of biodiesel and fat.

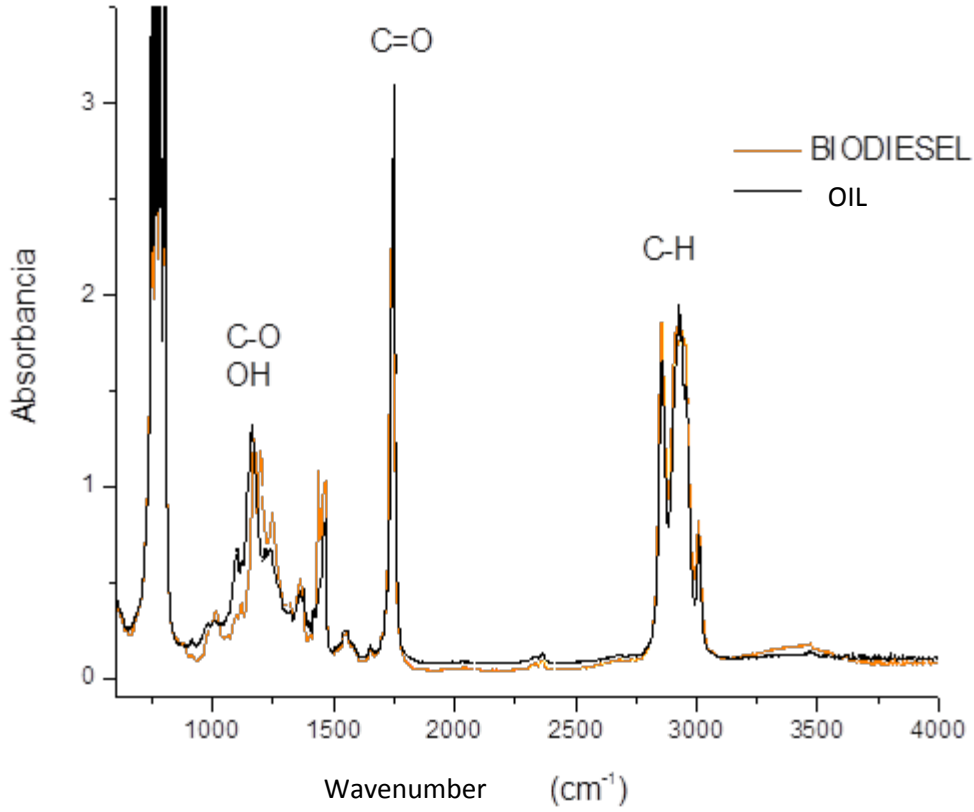

Figure 11.1. Fat and biodiesel IR spectra.

This spectrum can be divided in four regions for a better understanding.

Great absorption peaks in the 1000-1250 cm^{-1} region corresponding to the tension vibrations of the ester C-O as shown in Figure 11.2.

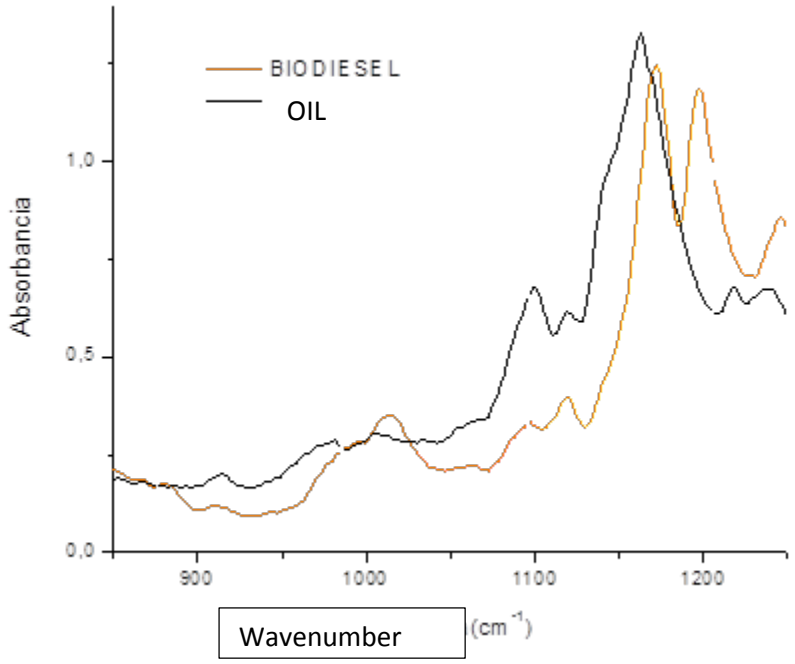

Figure 11.2. *Fat and biodiesel IR spectra. 800-1300 cm^{-1} region.*

Two peaks, one around 1436 cm^{-1} and another one around 1465 cm^{-1} can be observed in the region between 1250 and 1600 cm^{-1} (Figure 11.3). These bands correspond to the CH_2 and CH_3 flexion vibrations. The ratio between the peaks 1436 and 1465 cm^{-1} is different for the biodiesel and the fat as it can be observed in figure 11.3. Therefore the occurrence or absence of methyl esters in the mixture can be determined from it, as well as de degree of advancement. If the 1465 cm^{-1} and the 1436 cm^{-1} bands are related to the CH_2 and the CH_3 group flexion vibrations respectively the difference on the two intensities can be explained based on the increase of the amount of the methyl group in the reaction product.

In figure 11.3 another two absorption bands in the 1350 –1375 cm^{-1} region can be also observed. The 1375 cm^{-1} peak appears on the fat curve but not on the biodiesel one, whereas the 1360 cm^{-1} peak appears on the ester curve but not on the fat one. These bands can be related to the methyl and methylene flexion vibration respectively. The ratio between these two peaks could also be used during the reaction, however, the ratio 1465/1436 cm^{-1} was used instead, since those two peaks are more intense

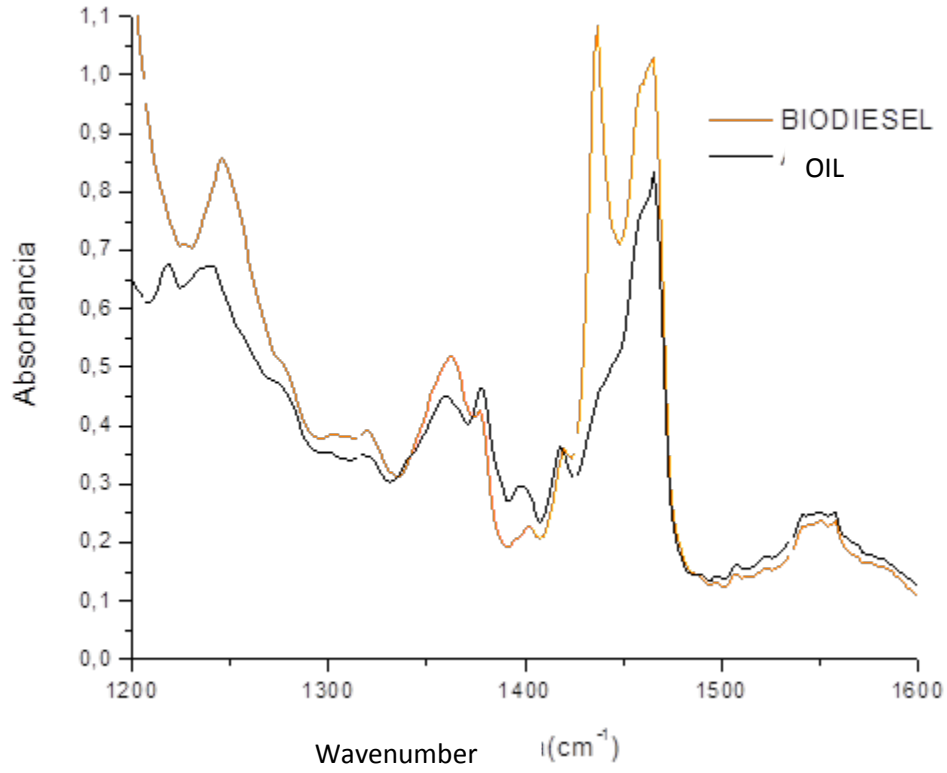

Figure 11.3. Fat and biodiesel IR spectra.1200-1600 cm^{-1} region.

There is only one peak occurring in the region between 1600 and 2000 cm^{-1} (Figure 11.4). This peak around 1750 cm^{-1} relates to the carbonyl group (C=O) tension vibration. A shift can be observed between the peak from each one of the species, this shift can be used to identify the species.

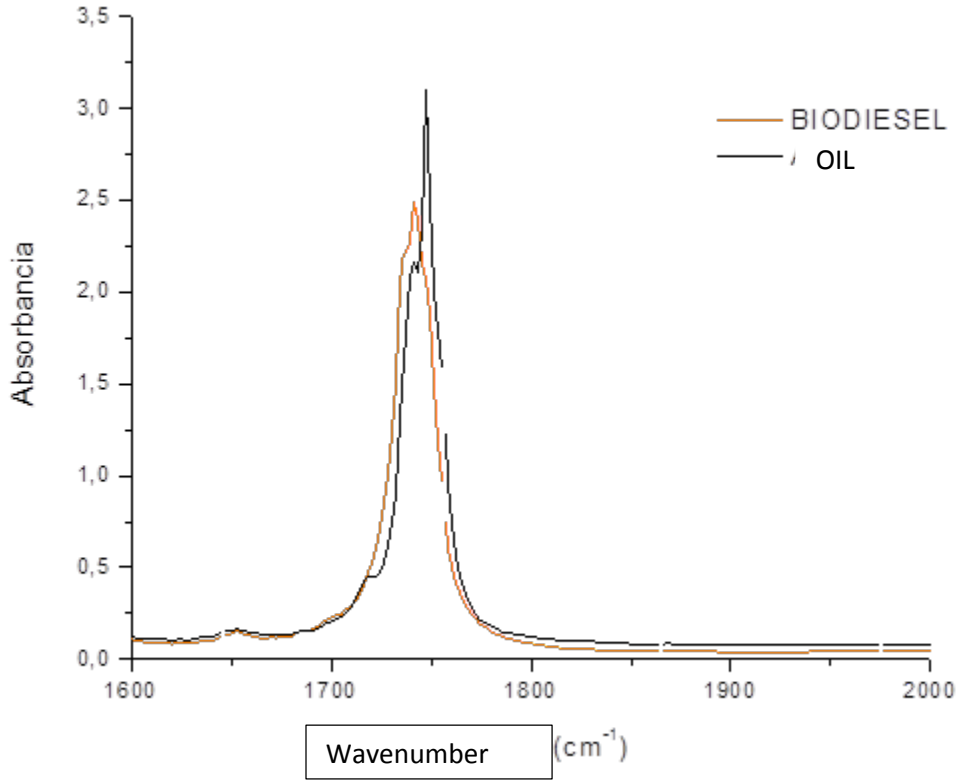

Figure 11.4. Fat and biodiesel IR spectra. 1600-2000 cm^{-1}region.

Finally, in the region between 2000 and 3200 cm^{-1} (Figure 11.5) several peaks occur close to the 2800-3000 cm^{-1} area. These peaks relate to the tension vibrations of the CH bonds.

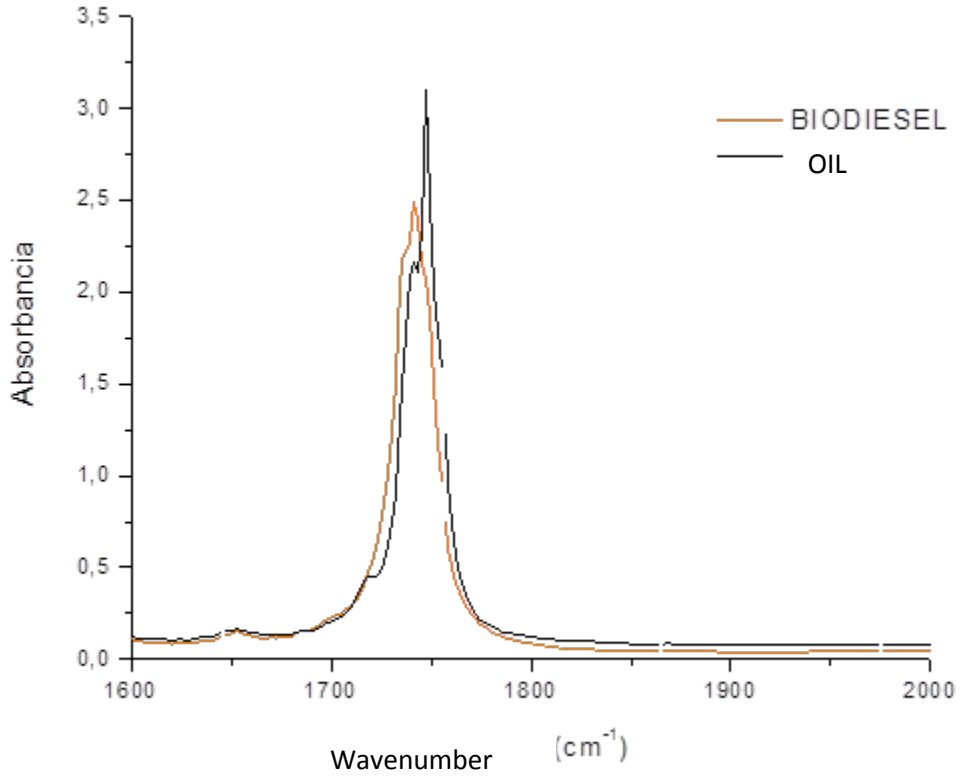

Figure 11.5. *Fat and biodiesel IR spectra. 2000-3600 cm^{-1}region.*

- *Infrared spectroscopy calibration curve.*

Once the method to assess the amount of biodiesel is selected, the ratio between the peaks 1465 and 1436 cm^{-1} is registered and their variation depending on the amount of biodiesel and fat is studied. In order to achieve that, mixtures of animal fat and biodiesel from animal fat were prepared, and their spectra were analysed. These data were used for the calibration.

These simple mixtures were prepared in the following proportions: 100% biodiesel, 90%-10%, 80%-20%, 70%-30%, 60%-40%, 50%-50%, 40%-60%, 30%-70%, 20%- 80% y 100% animal fat.

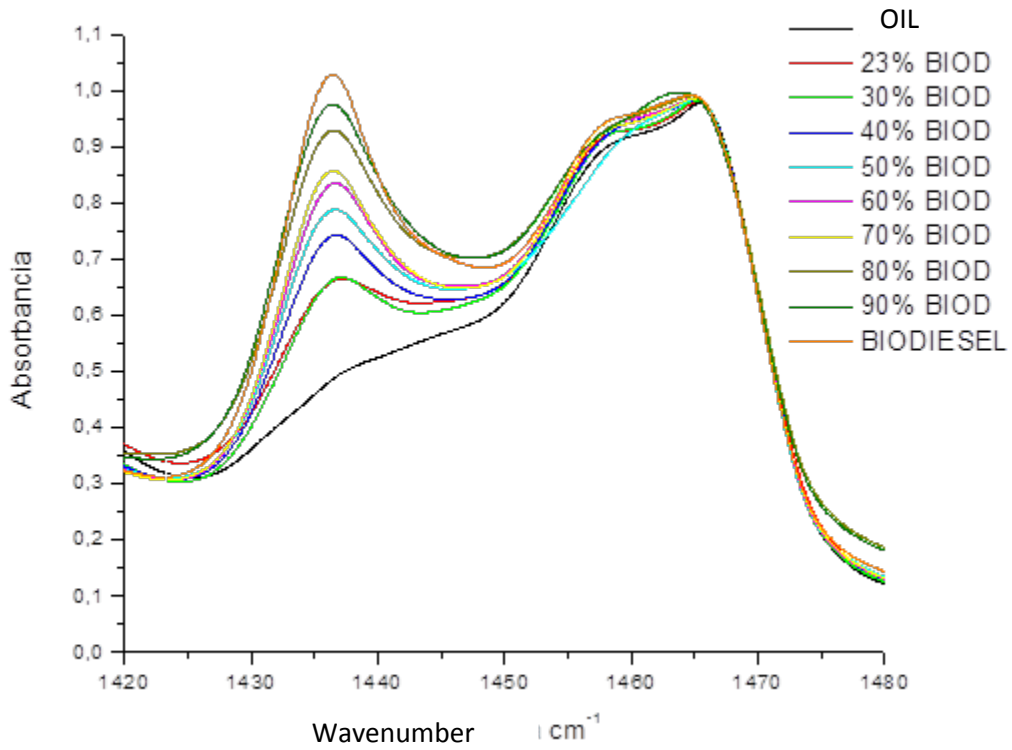

Figure 11.6. IR Spectra of the samples used in the calibration.

Figure 11.6 shows that the increasing amount of biodiesel involves an increase on the 1436 cm^{-1} absorption band. Thus, the 1436 cm^{-1} peak intensity can be related to the biodiesel amount in the mixture simple.

Figure 11.7 shows the correlation of the IR absorbance of the sample at 1436 cm^{-1} and the amount of biodiesel, the numeric data are displayed on the Table 9.

Table 9: FT-IR calibration curve

% Biodiesel	Abs. 1465 cm-1	Abs. 1436 cm-1	Ratio
100	1,41	1,45	1,03
90	1,41	1,38	0,98
80	1,31	1,20	0,92
70	1,12	0,98	0,88
60	1,32	1,04	0,79
50	1,14	0,83	0,72
40	1,19	0,84	0,70
30	1,18	0,74	0,63
20	1,03	0,60	0,58
10	0,95	0,48	0,51
0	1,24	0,60	0,49

The results can be fitted using a linear regression using the following equation:

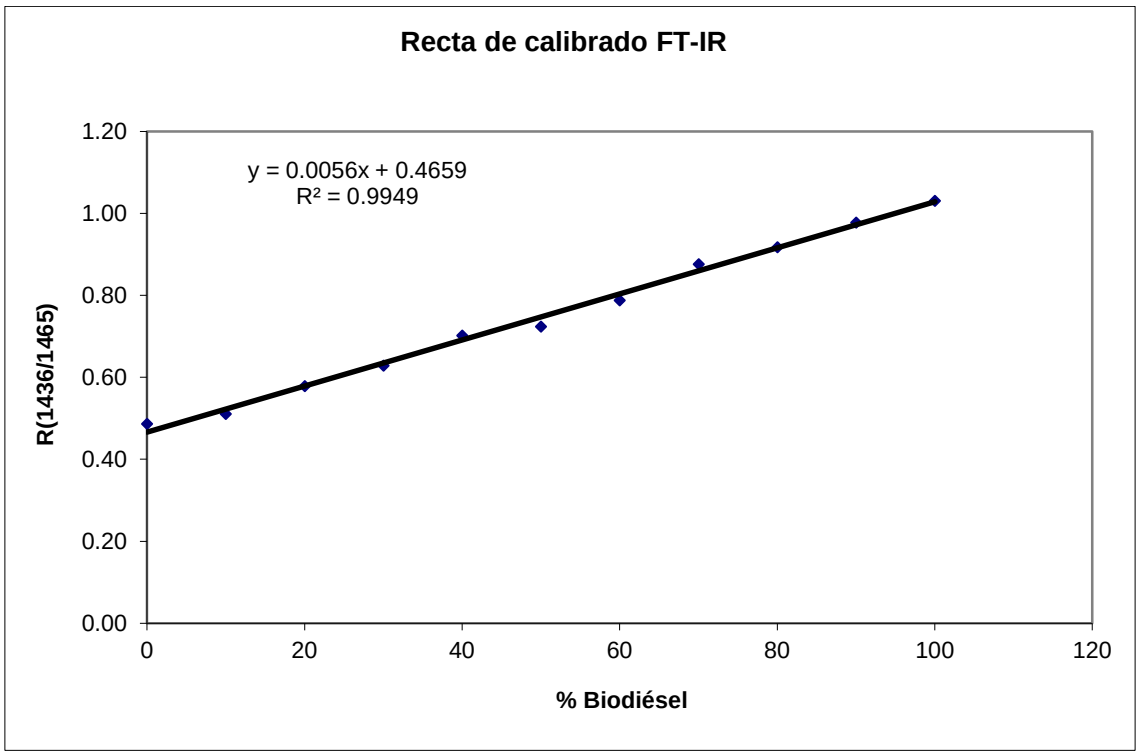

Figure 11.7. Linear fit. Calibration FT-IR

Y = 0.0056 X + 0.4659

X = (% wt. biodiesel in sample) Y = R = Absorbance 1436 cm^{-1} / Absorbance 1465 cm^{-1})

6.2 Gas chromatography

6.2.1 Transesterification control

Gas chromatography Flame ionisation detector GC-FID

- *Transesterification of soybean oil, waste frying oil and tallow.*

The fatty acid compositions of these fats and oils were determined by a well-established GC procedure (235). Standards of the methyl esters of the fatty acids were prepared from the acids by esterification with methanol (235) and a standard mixture of these esters was injected in the GC for identification and quantification purposes. Standards and samples (0.050 g dissolved in 10 mL of n-hexane) were injected (1 µl) in a Hewlett-Packard 5840 GC, equipped with a capillary column of acidified polyethylene glycol (25 m x 0.53 mm x 1 µm). The GC oven was kept at 180 °C for 2 min, heated at 4°C/min up to 200 °C, where it was kept for 10 min. The detector was a flame ionisation detector (FID), and the carrier gas helium (5 mL/min). The analysis of biodiesel by GC was carried out by dissolving 0.050 g of the biodiesel sample in 10 mL of n-hexane, and injecting 1 µl of this solution into the GC, in the same conditions as above. The content of biodiesel for each sample was quantified by comparing the FID counts for each methyl ester of the GC sample of biodiesel with the FID counts of each methyl ester in the standard mixture of FAMEs, averaging out these relationships for all the methyl esters.

The conversion of oil or fat in each experiment was calculated from the content in methyl esters of biodiesel as analysed by GC, and the mean molecular weight of biodiesel/oil (Mw). The mean molecular weight of biodiesel was calculated averaging the individual molecular weights (Mwi) of each constituent methyl ester, according to the biodiesel fatty acid methyl ester analysis (wi). The factor three appears in this formula since each triglyceride molecule yields three methyl ester molecules.

$$Conversion\ (\%) = \frac{\frac{weight\ biodiesel}{Mw\ of\ biodiesel \times 3} \times \text{content in biodiesel } \%}{\frac{weight\ oil}{Mw\ of\ oil}}$$

Mw = mean molecular weight

$$Mw = \sum Mw_i \times \chi_i$$

The analysis of biodiesel by GC was carried out by dissolving 0.050 g of the biodiesel sample in 10 ml of n-hexane, and injecting 1 μl of this solution in the GC, in the same conditions written in the precedent paragraph.

The content of biodiesel of each sample was quantified by comparison of the FID counts for each methyl ester of the GC sample of biodiesel with the FID counts of each methyl ester in the standard mixture of FAME's ,averaging out these relationships for all the methyl esters.

The conversion of oil in each experiment was calculated from the content in methyl esters of biodiesel, and the material balance of the experiment;

- *Animal fat transesterification*

All the gas chromatography analyses were carried out in a Varian CP-3800 GC, equipped with a CP-8400 automatic injector.

All the biodiesel samples prepared from mixtures of animal fat and soybean oil as feedstocks are in the ranges established by the EN 14214 and ASTM D6751 standards, indicating that the process described in this thesis reaches very good mono-, di-, and triglyceride conversion values, and that both biodiesel purification methods are also adequate.

- *Castor oil transesterification*

All the gas chromatography analyses were carried out in a Varian CP-3800GC, equipped with a CP-8400 automatic injector.

Gas chromatography Mass spectrometer detector GC-MSD

- *WFO transesterification*

For one of the WFO analysis of the biodiesel of the content in glycerol and mono-, di- and triglycerides according to the European standard EN 14105 (236) it has been used a gas chromatograph Hewlett Packard HP 6890 series GC system, connected with a mass spectrometer Hewlett Packard 5973 Mass Selective Detector, with an automated system of sample injection.

- *Jojoba oil wax transesterification*

The gas chromatography-mass spectrometry analyses were determined in a GC-MS HP-6890/MSD-5973 system. The sample was dissolved in dichloromethane and 4 mL of this solution were injected in the splitless mode at 275 °C in the injection port using an automatic injector. The column was a 5% diphenylpolydimethylsiloxane AT-5 from Alltech (25m x 0.25mm x 0.20 μm), and helium was used as the carrier gas at a constant column head pressure of 4.0 psi. The gradients used were as follows: 60 °C (1 min), heating at 6.00 °C min-1 to 300 °C, 10 min at 300 °C, and leaving 15 min between runs. The mass selective detector MSD-5973 was set at 70 eV of accelerating voltage in the ion source. Mass spectra were matched against the Wiley 275 mass spectral library for the identification of compounds, using the software Chemstation from Hewlett-Packard.

The Fig. 12 shows a chromatogram of the crude transesterification product obtained in the GC-MS instrument.

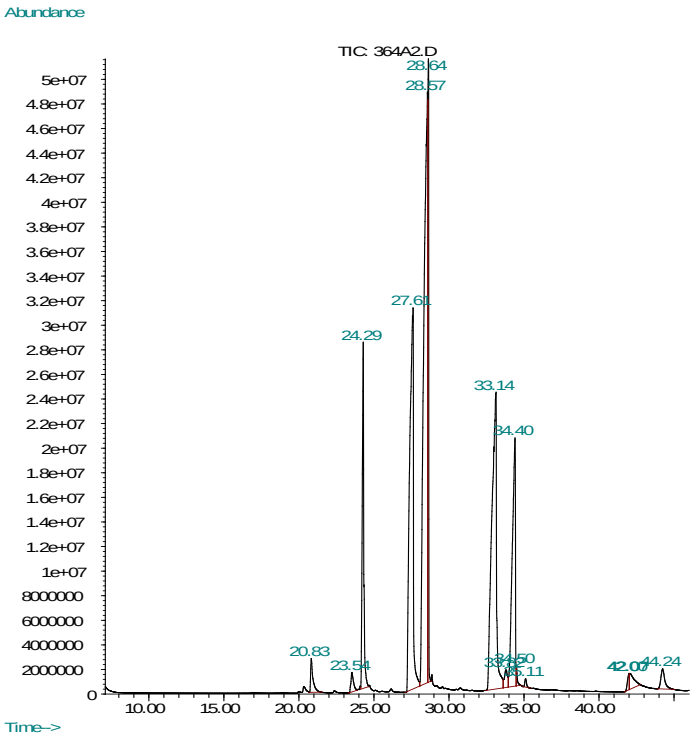

Figure. 12. *Gas chromatogram of the crude product of the transesterification of Jojoba oil-wax.*

6.2.2 Etherification control

- *Glycerol etherification (1,3-ditertbutylglycerol)*

Gas-chromatograph (GC): a Hewlett Packard 5890 GC with a Carbowax 20 M capillary column (25 m -0.32 mm - 0.3 μm) was used to analyze the reaction products. The detector was a FID. Helium was the carrier gas and the column head pressure was set to 6 psi (40.8 kPa). GC settings were as follows: initial temperature 100 °C; initial time 4 min.; heating rate 4 °C/min; final temperature 200 °C; final time 10 min.

The technical quality of the final product 1,3-di-tert-butoxypropan-2-ol has been tested by GC-MS. Using a Mass spectrometer VG AUTOSPEC: Spectra of electronic impact: 70 eV; m/z scan from 50 to 800 Da; resolution 1000. Analytical column of the GC: Supelcowax: (30 m - 0.25 mm - 0.25 μm). Column head pressure: 22.4 psi (152.3 kPa) with helium flow of 2.16 mL/min. Sample Amount: 0.2 μL. GC settings were as follows: initial temperature 50 °C; initial time 1 min; medium temperature 200 °C; medium time 5 min; final temperature 250 °C; final time 20 min. Heating rate 10 °C/min.

6.2.3 PAH analysis

All dichloromethane extracts were concentrated to 1 mL in a rotary evaporator, and they were analysed without any further handling. Concentrated samples were charged with an internal standard (Decafluorobiphenyl) and injected in the split mode (1 μL, three times) via automatic Agilent PTV injector in a gas chromatograph / mass spectrometer system (GC-MS) Agilent MS 7890 - GC 5975, equipped with a capillary column HP5MS (30 m x 0.250 mm x 0.25 μm). The analytical program was: initial temperature 60 ºC, initial time 2 min, rate 5 ºC/min during 10 min, final temperature 110 ºC, final time 60 min. The column head pressure was 8.2317 psi (56.76 kPa) and the analysis was carried out at constant flow (1mL/min).

Mass spectrometer ionizing chamber was set at 70 eV in the electronic impact mode (EI), and the scan and simultaneous ion monitoring (SIM) modes of the software ChemStations from Agilent were used, scanning from 70 to 500 Da. The PAH analysed and their characteristic ions were summarized in the results and they are included in the EPA list of concern compounds; these PAH were quantified using calibration curves with standards of the 16 PAH of concern from Aldrich.

7 REFERENCES

211. - ISA K. MBARAKA , KYLE J. MCGUIRE , AND BRENT H. SHANKS Acidic Mesoporous Silica for the Catalytic Conversion of Fatty Acids in Beef Tallow. *Ind. Eng. Chem. Res.,* 2006, 45 (9), pp 3022–3028

212. CANAKCI, M. and VAN GERPEN, J. A Pilot Plant to Produce Biodiesel from High Free Fatty Acid Feedstocks. *ASABE*, July 30-August 1, 2001, 2001.

213. - EDGAR LOTERO , YIJUN LIU , DORA E. LOPEZ , KAEWTA SUWANNAKARN , DAVID A. BRUCE , AND JAMES G. GOODWIN , JR Synthesis of Biodiesel Via Acid Catalysis. *Ind. Eng. Chem. Res.,* 2005, 44 (14), pp 5353–5363

214. - YINGYING ZHANG, YIWEN YANG, QILONG REN & HAILIANG Quantification of Soybean Phospholipids in Soybean Degummed Oil Residue by HPLC with Evaporative Light Scattering Detection. *Journal of Liquid Chromatography & Related Technologies* Volume 28, Issue 9, 2005 pp1333-1343

215. WANG, Y. and LIN, C. Variation of Peroxide Value in Water-Degummed and Alkali-Refined Soy Oil during Bleaching Under Nitrogen Stream. *Separation and Purification Technology*, 8, 2006, vol. 51, no. 1. pp. 64-71.

216. LIN, H. and LIN, C. Kinetics of Adsorption of Free Fatty Acids from Water-Degummed and Alkali-Refined Soy Oil using Regenerated Clay. *Separation and Purification Technology*, 8, 2005, vol. 44, no. 3. pp. 258-265.

217. ZHANG, W., HE, H., FENG, Y. and DA, S. Separation and Purification of Phosphatidylcholine and Phosphatidylethanolamine from Soybean Degummed Oil Residues by using Solvent Extraction and Column Chromatography. *Journal of Chromatography B*, 12/25, 2003, vol. 798, no. 2. pp. 323-331.

218. HOLSER, R.A. Properties of Refined Milkweed Press Oil. *Industrial Crops and Products*, 9, 2003, vol. 18, no. 2. pp. 133-138.

219. ROSSI, M., GIANAZZA, M., ALAMPRESE, C. and STANGA, F. The Role of Bleaching Clays and Synthetic Silica in Palm Oil Physical Refining. *Food Chemistry*, 8, 2003, vol. 82, no. 2. pp. 291-296

220. YEN, G. and WU, S. Reduction of Mutagenicity of the Fumes from Cooking Oil by Degumming Treatment. *LWT - Food Science and Technology*, 2, 2003, vol. 36, no. 1. pp. 29-35

221. INDIRA, T.N., et al. Water Degumming of Rice Bran Oil: A Response Surface Approach. *Journal of Food Engineering*, 2, 2000, vol. 43, no. 2. pp. 83-90

222. IWUOHA, C.I., UBBAONU, C.N., UGWO, R.C. and OKEREKE, N.U. Chemical and Physical Characteristics of Palm, Palm Kernel and Groundnut Oils as Affected by Degumming. *Food Chemistry*, 1996, vol. 55, no. 1. pp. 29-34.

223. MCDONNELL, K.P., WARD, S.M. and TIMONEY, D.J. Hot Water Degummed Rapeseed Oil as a Fuel for Diesel Engines. *Journal of Agricultural Engineering Research*, 1, 1995, vol. 60, no. 1. pp. 7-14.

224. DORADO, M.P. - Biofuels Refining and Performance McGraw-Hill ed., New York: - McGraw Hill Professional, Access Engineering, 2008 *Raw Materials to Produce Low-Cost Biodiesel.* , pp. 107

225. REYMAN, D. and RODRIGUEZ-GAMERO, M. *Biodiesel Synthesis Assisted by Ultrasounds: FT-IR and GC Analysis.* Universidad Autónoma de Madrid, 2007.

226. SCHOLZ, V. and DA SILVA, J.N. Prospects and Risks of the use of Castor Oil as a Fuel. *Biomass and Bioenergy*, 2008, vol. 32, no. 2 pp. 95-100.

227. CANOIRA, L., et al. Biodiesel from Low-Grade Animal Fat: Production Process Assessment and Biodiesel Properties Characterisation. *Industrial and Engineering Chemistry Research*, 2008, vol. 47, no. 21 pp. 7997-8004.

228. - DENNIS M. DISHONG , CRAIG J. DIAMOND , MICHAEL I. CINOMAN , GEORGE W. GOKEL Crown Cation Complex Effects. 20. Syntheses and Cation Binding Properties of Carbon-Pivot Lariat Ethers. - *J. Am. Chem. Soc.*, 1983, 105 (3), pp 586–593

229. LAPUERTA, M. *Unpublished Results.* Universidad de Castilla La Mancha: , 2010.

230. *ASTM International. ASTM D 1322-08. Standard Test Method for Smoke Point of Kerosine and Aviation Turbine Fuel;* ASTM International West Conshohocken, Pennsylvania. 2008.

231. MINCHIN, S.T. Luminous Stationary Flames: The Quantitative Relationship between Flame Dimensions at the Sooting Point and Chemical Composition, with Special Reference to Petroleum Hydrocarbons. *J. Inst. Petrol. Technol.*, 1931, vol. 17, no. 88. pp. 102-120.

232. CLARKE, A.E., HUNTER, T.G. and GARNER, F.H. The Tendency to Smoke of Organic Substances on Burning. *J. Inst. Pet.*, 1946, vol. 32. pp. 627-642.

233. GILL, R.J. and OLSON, D.B. Estimation of Soot Thresholds for Fuel Mixtures. *Combustion Science and Technology*, 09/01; 2015/03, 1984, vol. 40, no. 5-6. pp. 307-315

234. KEMP, W. *Practical Organic Chemistry.* London: McGraw-Hill, 1967

235. *EN 14105 Fat and Oil Derivatives - Fatty Acid Methyl Esters (FAME) - Determination of Free and Total Glycerol and Mono-, Di-, Triglyceride Contents.*

TABLE OF CONTENTS

1 INTRODUCTION

In this chapter, two different strategies have been followed. Some of the results have been discussed in the classic way of a PhD work, whereas the most recent published results have been included in the form of the articles from the journals where these results were reported. This second approach, apart from being widely accepted in many universities, implies the added advantage of dealing with reports that have been peer reviewed by leading experts in the field before being accepted in journals placed all in the Q1 quartile of the corresponding category of the Thomson Reuters' Journal Citation Report.

2 FEEDSTOCK CHARACTERIZATION, PRETREATMENT, TRANSESTERIFICATION AND PURIFICATION

2.1 Ester profiles.

Most of the properties of the biofuels reported in this PhD thesis depend strongly on their ester profiles since the properties depending on the production have been under control in most cases. The ester profiles of every oil and fat produced in this thesis are showed at the beginning of the results section in order to compare them (Table 10, 11 and 12).

Table 10: Ester profiles of FAME from edible oils

Ester	*Soybean*	*Soybean[2]*	*Palm*	*Soybean[3]*	*Rapeseed*	*Coconut[1]*	*Peanut*	*Palm kernel*	*Babassu*	*Coconut[2]*	*Palm kernel*	*Babassu*	*Coconut*	*Palm kernel*	*Babassu*	*Coconut*
Profile	FAME1	FAME2	FAME	FAME	FAME	FAME	FAME	FAME	FAME	FAME	distillate	distillate	distillate	bottom	bottom	bottom
C6:0																
C8:0		0.02				0.1			3.91	8.3	3.6	13.27	17.3			
C10:0		0.03				8.8			3.3	3	3.5	11.27	7			
C12:0			0.3			32.2		56.6	20.85	55.5	90.8	69.46	66.7	19	21.91	16.3
C14:0	0.1	0.07	1			20.5		15	31.33	14.9	2.1	5.58	8.9	19.7	34.08	46.1
C16:0	11.4	10.59	46	13.6	5.1	10.9	10.1	8.5	18	6.4		0.61	0.1	9.9	19.84	26
C16:1																
C18:0	3.2	3.82	9.7	6.9	9.2	2.9	2.9	1.7	5.51	2.5				12.8	6.18	2.2
C18:1	21.8	24.96	33.5	24.9	59.6	8.3	57.6	17.1	12.54	7.5				32.7	13.25	8.7
C18:2	54.9	63.11	9.1	49	17.7	2.4	26.3	1.1	0.21	1.9				5.9	0.22	0.7
C18:3	8.3	6.47		5.2	6.6				3.45						3.58	
C20:0	0.2	0.38	0.3	0.4	0.5		1.4		0.19						0.19	
C20:1		0.05			1.4		1.7		0.72						0.75	
C22:0		0.047														
C22:1		0.03														
C24:1																

Table 11: Ester profiles of FAME from non-edible oils

Ester	*Jojoba oil-wax*	*Methyl*	*Castor*	*Lineseed*	*Camelina*	*Tallow*	*Animal fat*	*WFO*	*WFO*	*WFO*	*Animal fat*
Profile	crude FAME	jojoboate	FAME	FAME	FAME	FAME	FAME	FAME3,1	FAME,3,2	FAME3,3	FAME
C6:0											
C8:0							0.11				
C10:0							0				
C12:0					1.1						
C14:0				1	0.5	5.4	2.52				1.9
C16:0	1.08	1.27	1.25	6.9	6.2	32.8	28.35	10.4	12.1	12.8	25.4
C16:1	0.21					4.3					
C18:0	7.22	9.51	1.31	4.5	3.1	4.1	15.74				15.5
C18:1	0.04		3.81	21.3	17.5	35.1	42.19	72	33.7	53	43.9
C18:2			5.27	17.3	19.1	15.7	9.43	16	54.2	33	8.9
C18:3			0.81	49.1	33.6		0.6	1.7		1	0.5
C20:0	0.23		0.05		1.6	0.5	0.16				
C20:1	37.55	51.46	0.38		17.3		0.86				0.9
C22:0	0.29		0.01				0.01				
C22:1	11.15	14.49	0.01				0.01				
C24:1	1.07	1.96									
C18:1-OH			87.1								

Table 12: Ester profiles of FAEE from edible oils

Ester Profile	*FAEE Palm*	*FAEE Rapeseed*	*FAEE Soybean*
C6:0			
C8:0			
C10:0			
C12:0	0.3		
C14:0	1		
C16:0	46	5.1	13.6
C16:1			
C18:0	9.7	9.2	6.9
C18:1	33.5	59.6	24.9
C18:2	9.1	17.7	49
C18:3		6.6	5.2
C20:0	0.3	0.5	0.4
C20:1		1.4	
C22:0			
C22:1			
C24:1			
C18:1-OH			

- The reason why the ester profiles of the produced FAME does not agree with the FAEE is that sodium methoxide was used as catalyst leaving significant amounts of FAME in the sample that were hindered in the GC analysis by the FAEE peaks.

2.2 Animal fat

As a result of the previous esterification process using *p*-toluenesulfonic acid (0.5 wt % of the oil-fat) as a catalyst, described in the experimental section 3.1.1, the sulfur content of the final biodiesel could be substantially reduced in a multistep process to 34.5-49.5 mg/kg, depending on the sulfur content of the animal fat, and obviously out of specifications.

In the experimental section 3.1.1, three methods are described to eliminate the residual water occurred during the esterification process. All three methods produce practically the same quantitative yields of oil-fat with an acidity index acceptable for transesterification (Table 13).

Table 13: Acidity index of the feedstock before and after esterification and elemental analysis of the feedstock[1]

Animal fat /soybean oil (% vol.)	Acidity index initial (EN ISO 660/2000)	Acidity index after esterification (EN ISO 660/2000)	% C	% H	% N
100/0	13.6	1.7	76.51	12.36	0.26
80/20	10.4	0.5	76.72	12.28	0.24
60/40	6.8	0.6	76.93	12.20	0.23
50/50	7.2	0.6	77.04	12.16	0.22
40/60	4.8	0.3	77.14	12.12	0.21
0/100	0.5	-	77.56	11.96	0.18

[1]*Mean value of four replicate analysis. The values have been determined for the pure soybean oil and animal fat and deduced for the mixtures. The sulphur (S) content of the animal fat is 380.9 mg/kg and below the method's detection limit (5mg/kg) for the pure soybean oil.*

For the transesterification, sodium methoxide (1 %wt. of the oil-fat) was always used as the basic catalyst as it is usual in our processes (4, 5, 6); the sodium methoxide (*ca.* 30% wt.) was solved in the amount of methanol necessary to reach the 7.5:1 molar ratio methanol-fat used in this step, and it was added to the reaction mixture from the precedent esterification step. The advance of the transesterification was followed by FT-IR spectroscopy as described in chapter II section 6.1.1. (225). Usually, the transesterification was completed in 60 minutes with quantitative yield (see Figure 13).

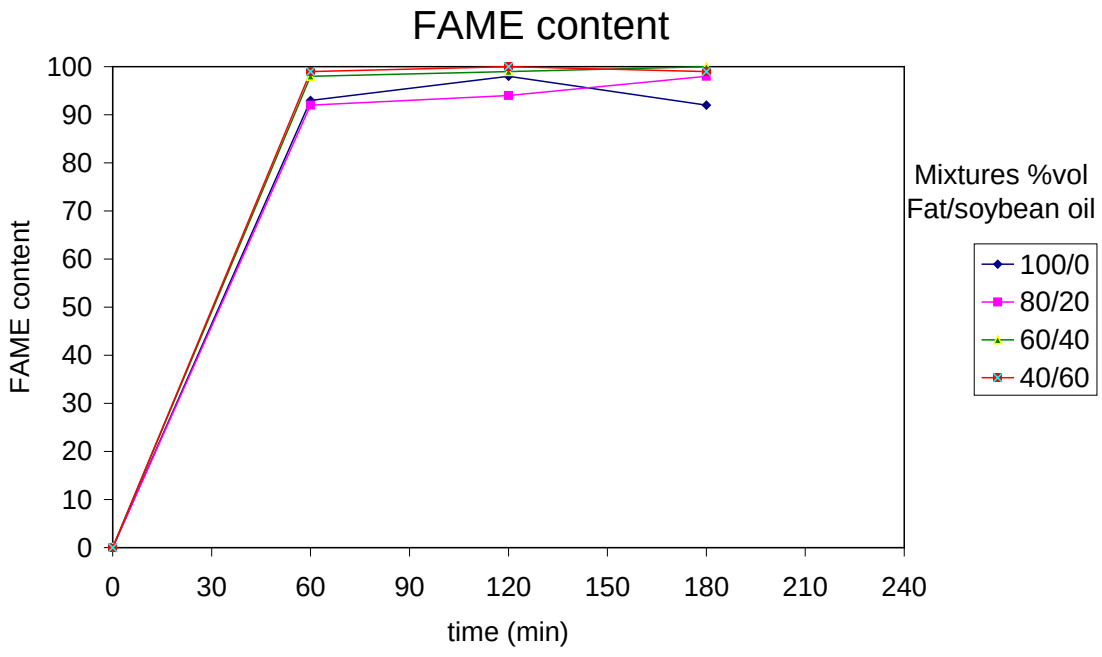

Figure 13. FAME content evolution vs. time in the transesterification reaction

- *Purification*

The purification process is described in chapter II section 3.3.1. The results affected by the purification method for a feedstock of 50% vol. animal fat-soybean oil are summarized in Table 14. A little better biodiesel yield was observed in the "wet" wash purification process, but the rest of the parameters were almost identical; only the oxidative stability of the biodiesel, the total contamination (EN 12662), and the sulfur content (out of specifications for both methods) were slightly better for the "dry" wash. When using solid adsorbents (magnesium silicate or molecular sieve) for the purification process of biodiesel, a thorough filtration step through a 0.45 μm filter needs to be added to the production process scheme to account for the particle contamination problem.

Table 14: Comparison of "dry" and "wet" purification methods for biodiesel from animal fat-soybean oil 50 %vol feedstock.

Parameter	*"Dry" wash*	*"Wet" wash*
Monoglycerides, *%m/m*	0.37	0.40
Diglycerides, *%m/m*	0.09	0.08
Triglycerides, *%m/m*	0.02	0.02
Free glycerol, *%m/m*	0.019	0.010
Total glycerol, *%m/m*	0.13	0.13
Acidity index, *mg KOH/g*	0.45	0.16
Water content, *mg/kg*	334	321
Oxidative stability 110 ºC, *h*	5.11	3.86
Sulphur content, *mg/kg*	34.5	49.5
Ester content, *%m/m*	95.2	91.2
Iodine index, *mg I_2/100g*	97.5	94.8
Total contamination, *mg/kg*	103.0	155.9
Calcium, *mg/kg*	n.d.	4.5
Biodiesel yield, *%*	75	81

Table 15 summarizes the performance of three different size reactors for this biodiesel production process, showing improved biodiesel yields and EQ factors with the increasing size of the reactor.

Table 15: Comparison of the Performance of Three Different Size Reactors for the Same Feedstock, Animal Fat-Soybean Oil, 50 vol %

	1.5 L reactor	*5.0 l reactor*	*50.0 L reactor1*
Feedstock	1.0 L (0.9 kg)	3.0 L (2.7 kg)	30 L (27 kg)
Biodiesel	0.659 L (0.560 kg)	2.35 L (2.02 kg)	29 L (25 kg)
Biodiesel yield, %	62.2	74.8	92.5
Gums	27.0 g	81 g	-
Salts	63.4 g	51 g	0.98 kg
G-phase	147.0 g	630 g	6.5 kg
Interfaces	48.4 g	210 g	-
Environmental Quotient, EQ	0.51	0.48	0.30

[1]*Process realized without degumming or calcium oxide addition*

Since a few years back, the environmental suitability of a chemical process is measured by the environmental quotient factor EQ (237), where E represents the quotient between the weight of byproducts and the weight of desired product, and Q represents the quality of the byproducts (e.g., for neutralization salts such as sodium chloride or calcium sulfate Q = 1, but for heavy metals salts, Q ranges from 10^2 – 10^3 depending of the salt toxicity). The generally accepted values for EQ are: less than 0.1 for the oil refining industry (10^6-10^8 t/y of production capacity), between 1-5 for the commodities industry (10^4-10^6 t/y of production capacity), between 5-50 for the fine chemicals industry (10^2-10^4 t/y of production capacity) and between 25-100 for the pharmaceutical industry (10-10^3 t/y of production capacity). The EQ factor for a typical biodiesel production process from vegetable oils as feedstock is:

$$EQ = E = \frac{112\ kg_{glycerol} + 30\ kg_{gums} + 16\ kg_{salts}}{1000\ kg_{biodiesel}} = 0.158$$

That approaches the value of the oil refining industry (the Q value is always 1 since the byproducts lack toxicity). The EQ values of our process for the three reactors used are summarized in Table 15. These values, although acceptable because the biodiesel could be considered still a commodity, are much higher than those of the oil refining industry with which the biodiesel should be competitive.

None of the biodiesel samples prepared from mixtures of animal fat and soybean oil gives an ester content higher than 96.5 %wt. as it is compulsory. The explanation to this fact is that the biodiesel produced from animal fats or their mixtures contains methyl heptadecanoate, an odd carbon atom number FAME which is used as the internal standard in this determination, producing a bias in all these analyses. The ester content of the biodiesel samples increases asymptotically with the increase in the soybean oil content of the feedstock as can be seen in Figure 14a. Thus, a modified method such as the one proposed by Mittelbach *et al* (238) that takes into account the natural content of methyl

heptadecanoate should be used in this determination when the biodiesel comes from animal fats or mixtures containing them as feedstock.

Table 16: FAME profiles of the biodiesel from mixtures of animal fat-soybean oil feedstock

		Animal fat /soybean oil (% vol)					
Esters profile, % m/m		*100/0*	*80/20*	*60/40*	*50/50*	*40/60*	*0/100*
Methyl octanoate	*C8:0*	0.11	0.08	0.05	0.01	0.05	0.02
Methyl decanoate	*C10:0*	0.00	0.00	0.01	0.05	0.00	0.03
Methyl myristate	*C14:0*	2.52	1.41	1.04	0.80	1.20	0.07
Methyl palmitate	*C16:0*	28.35	22.97	20.33	17.52	16.18	10.59
Methyl stearate	*C18:0*	15.74	14.02	10.70	8.90	8.23	3.82
Methyl oleate	*C18:1*	42.19	38.76	35.50	34.10	33.49	24.96
Methyl linoleate	*C18:2*	9.43	19.94	28.71	33.39	35.98	53.11
Methyl linolenate	*C18:3*	0.60	1.70	2.71	3.80	3.62	6.47
Methyl arachnidate	*C20:0*	0.16	0.22	0.27	0.31	0.34	0.38
Methyl eicosenoate	*C20:1*	0.86	0.82	0.60	0.50	0.55	0.05
Methyl behenate	*C22:0*	0.01	0.02	0.03	0.30	0.34	0.47
Methyl eructate	*C22:1*	0.01	0.05	0.06	0.00	0.06	0.03

Figure 14b and table 16 show the FAME profiles of biodiesel for the main constituents vs. the animal fat content in the feedstock. Methyl oleate, palmitate and stearate increase linearly with the animal fat content, whereas linoleate decreases abruptly and linolenate decreases also but smoothly. Saturated FAME have high advantageous cetane numbers and oxidative stability, but possess poor cold flow properties. Unsaturated, especially polyunsaturated FAME have lower melting points, which are desirable for improved low-temperature properties, but also have low cetane numbers and reduced oxidative stability, which are undesirable for a diesel fuel. Methly oleate has been suggested and studied as a prime component of modified (genetic or others modifications) biodiesel fuels (239, 240) . The amounts of methyl oleate and methyl linoleate equals at around 50 % vol. of animal fat in the feedstock (see Figure 14b), while the amount of methyl linolenate is below the upper admitted limit in all cases. Thus, 50 % vol animal fat could be a good mixture as feedstock.

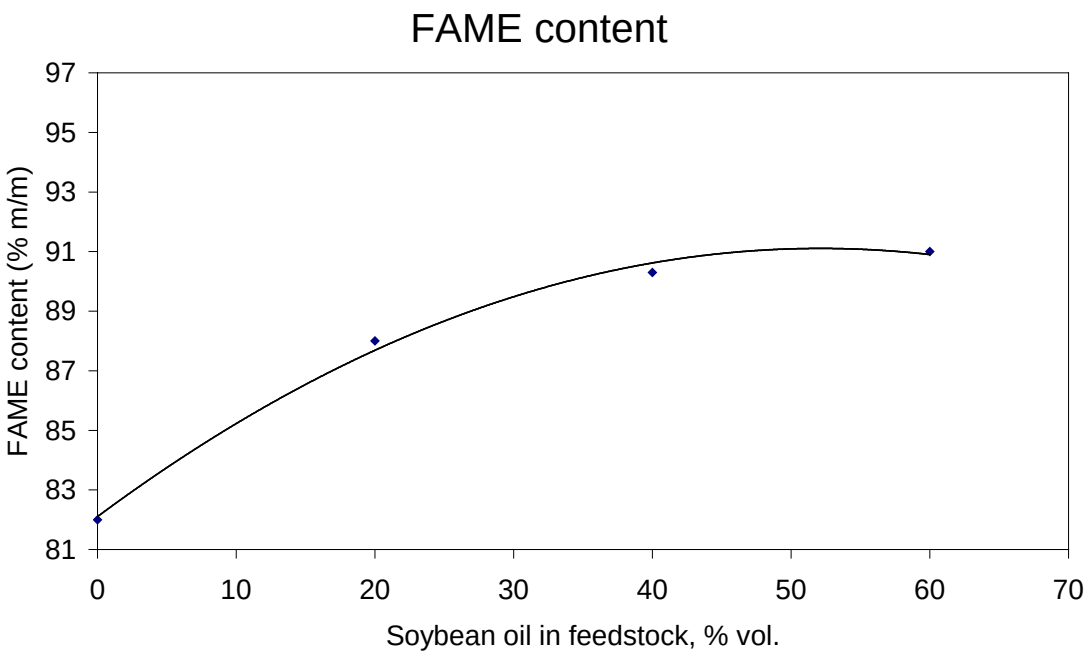

Figure 14a. *FAME profiles of biodiesel vs. animal fat content in the feedstock .*

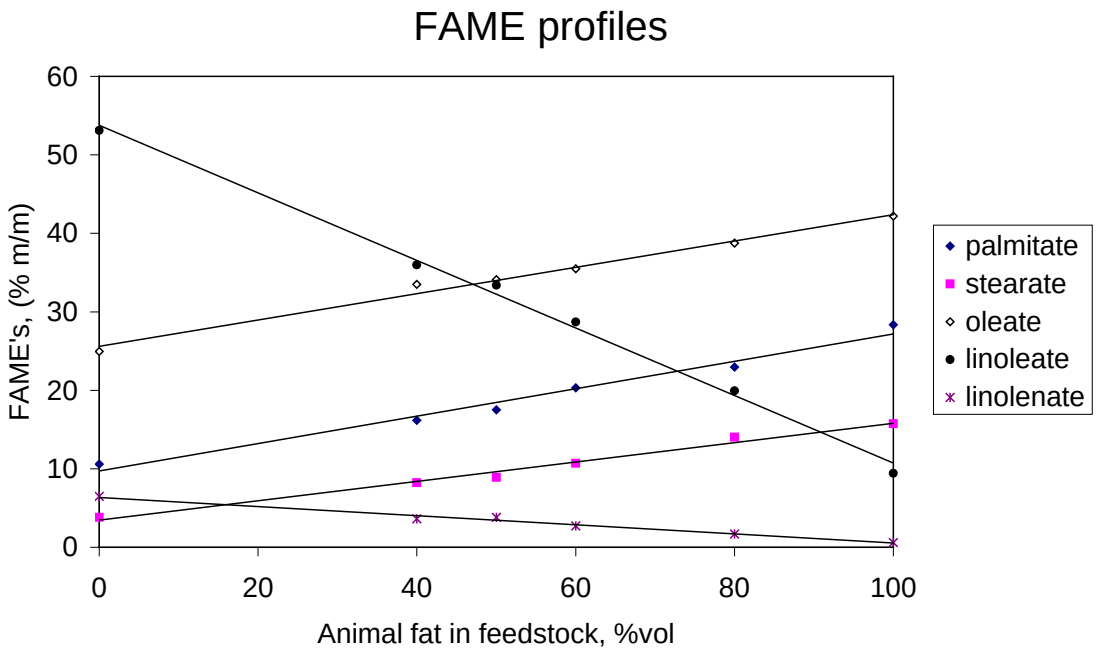

Figure 14b. *FAME content of biodiesel vs. soybean oil in the feedstock*

2.3 Soybean oil, WFO and horse tallow

The fatty acid composition of the soy-bean oil, waste frying oil and tallow are given in the summary table 10 and 11 at the beginning of this section. The oils show a high grade of unsaturation (oleic+linoleic acids 80% wt.), while in the tallow the predominance of the saturated acids is higher. The acidity indices of the soy-bean oil and the waste frying oil are 0.53° and 0.47° respectively, which allows the use of basic catalysts in the transesterification process (241) . The tallow, supplied by the Madrid City Council slaughterhouse, had an acidity index of 6.8° which is a limiting condition for the use of basic catalysis (241).

The transesterification of soy-bean oil with methanol was carried out following the procedure described in chapter II section 3.2.1(241)(242)(242)(242)(242)(243)(242)(243)(243)(213)(213)(213). Since the reagents constitute a biphasic system, the transesterification of soy-bean oil was carried out at two randomly chosen stirring speeds 360 and 600 rpm, (Fig. 15). At the lower speed, the oil conversion reached only 12% after 8 h of reaction, whereas at 600 rpm the oil conversion was complete in less than 2 h. This result shows that an efficient mixing of the reagents is essential to reach a high conversion of the oil in a short reaction time.

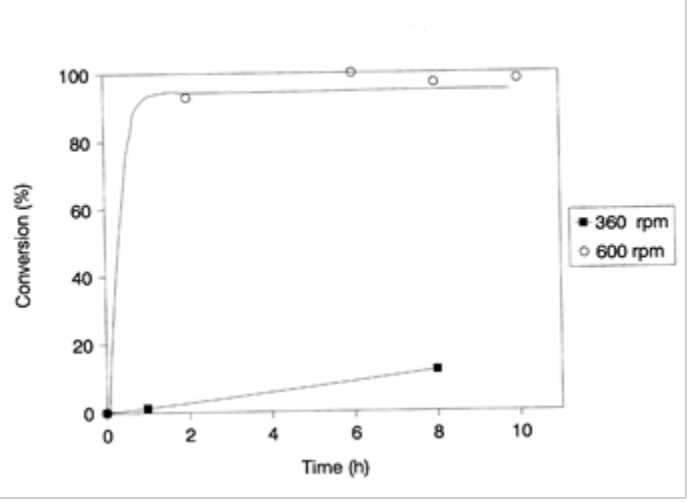

Fig. 15. Transesterification of soy-bean oil with methanol using stirring speeds of 360 or 600 rpm.

In the literature (241), it has also been reported that basic catalysis (with low volumes of catalyst, typically 0.1%) could only be applied when the acidity index of the oils and fats is below approx. 0.5° (1mg KOH/g).In order to attest this, we carried out the transesterification of tallow (the only sample with an acidity index higher than 0.5°) using both acid and basic catalysis (Fig. 16). In the acid catalysis process using 1% wt. H_2SO_4 (the other conditions remaining the same as above), the fat conversion

reached only 13% conversion after 48 h of reaction, since acidic processes are substantially slower than basic ones. When 1% wt. of sodium methoxide was used as catalyst, the transesterification of tallow proceeded quantitatively in less than 3 h showing that the acidity index of the fat was not a critical factor when using this basic catalyst amount (1% wt.).

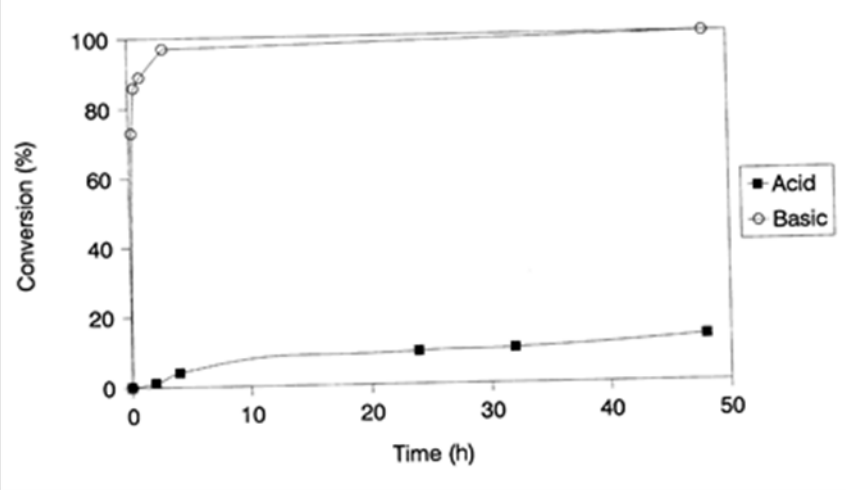

Fig. 16. Transesterification of tallow with methanol using either acid or base catalysis.

Fig. 17 shows the oil conversion vs time for the three oils/fats studied, after optimization of the reaction conditions (molar ratio methanol: oil is 7.5; temperature 60 °C; catalyst 1% sodium methoxide; stirring 600 rpm). It could be seen that the conversion is quantitative after about a 30 min reaction time for the three oils/fats. With a view to exploring a continuous process, it was also interesting the possibility of catalyst reuse. We decanted the lower glycerin and methanol phase, without neutralization, in an experiment with waste frying oil, as described in the experimental section 3.2.1, eliminated the methanol under vacuum, and used the glycerin residue to catalyze a new transesterification of fresh waste frying oil with methanol. The result is summarized in Fig. 17; the reused catalyst showed a slightly longer induction period than the original one, but at the end of about 1 h the conversions for both were similar. The basic catalyst was then without appreciable loss of catalytic activity.

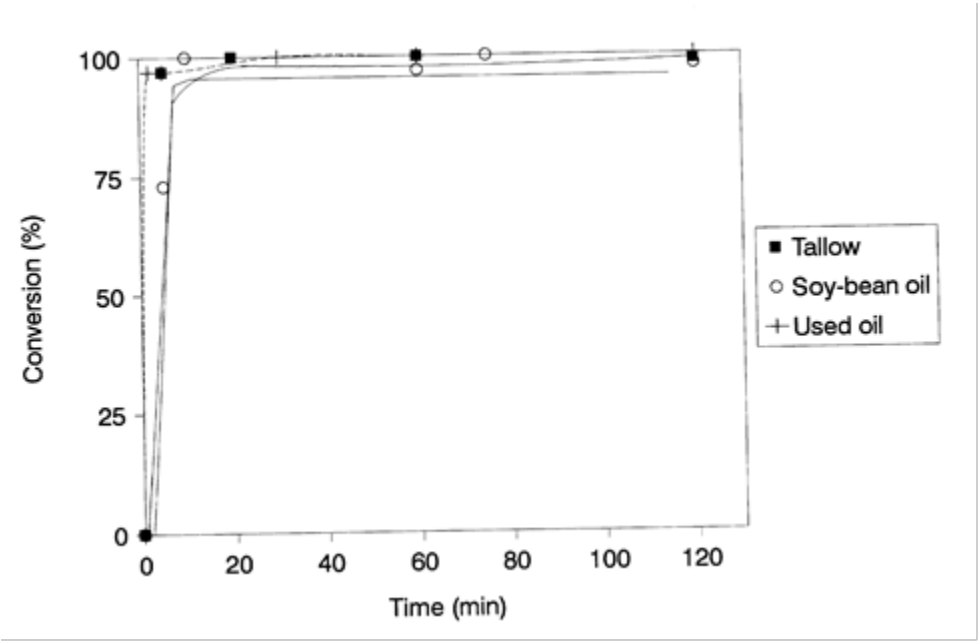

Fig. 14. Transesterification of either fats/oils with methanol over time.

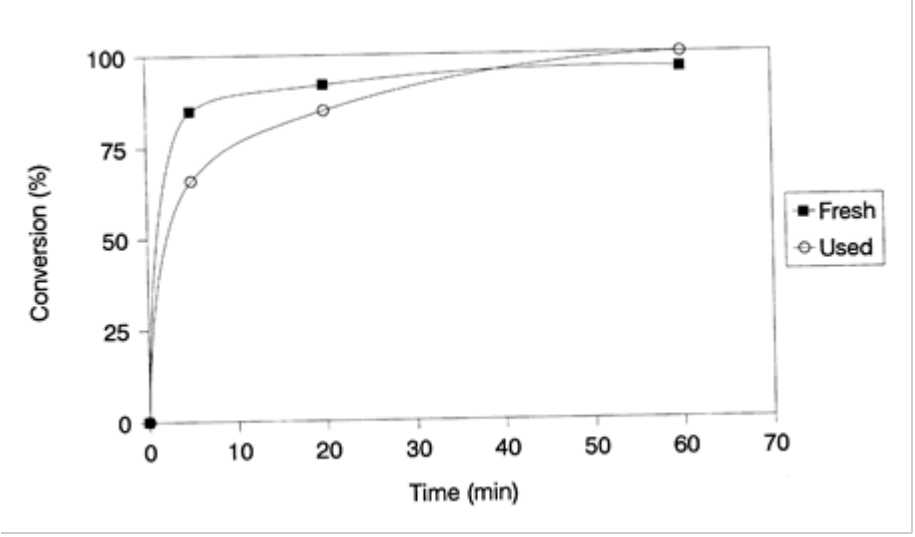

Fig. 17. Transesterification of waste frying oil with methanol using recycled or new catalyst.

Waste frying oil has been studied more deeply, another two batches have been submitted to transesterification and the kinetic parameters from one of them has been calculated.

The density and acidity of the three different waste olive oils used are shown in Table 17. The biodiesel obtained from WFO was analysed by GC using a previously described procedure (chapter II section 6), and the FAME composition of biodiesel matches perfectly the fatty acids composition of the parent waste oils as summarised in Table 14. The FAME content of the samples obtained after the procedure described before was always higher than 97 % wt., and the conversion was calculated after the equation described in the experimental section 6.2.1. For these waste oils, the conversion is quantitative after one hour approximately, ranging from 93% to 98%.

Table 17. Acidity index and density of waste oils.

Sample	*Acidity index (%)*	*Density (g cm-3)*
Waste oil 1	0.25	0.912
Waste oil 2	0.60	0.890
Waste oil 3	0.57	0.916

Figure 18 shows the conversion of the transesterification reaction of two different samples of waste frying oil vs. time.

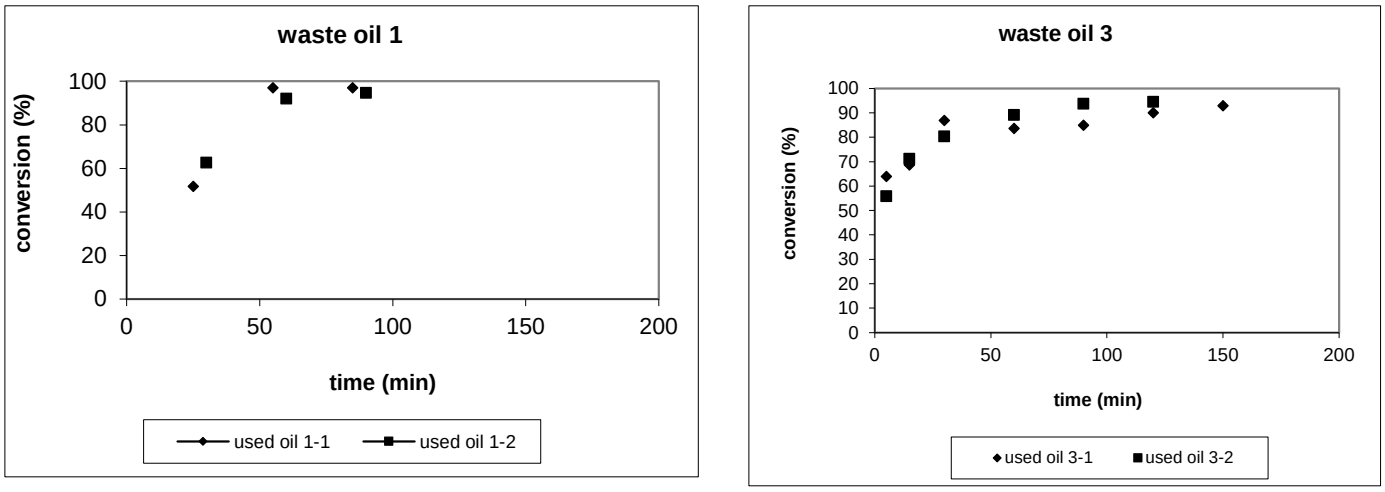

Figure 18. Conversion vs. time in the transesterification reaction of waste oils

2.3.1 WFO Kinetic experiment.

The transesterification reaction rate is much higher than it was originally estimated. As it is shown in the kinetic analysis in Table 18, after the first 10 min of the addition of the catalyst to the reactor, an almost quantitative conversion of triglycerides (TG) to FAME and glycerol takes place. All the time that the reactor is left running after this initial time, the reactions that take place are reversible reactions, and the reaction mixture is slowly moving towards the equilibrium

Table 18 Concentration of mono-, ditriglycerides, FAME, glycerol and methanol vs. time in the kinetic experiments.

Time (minutes)	*Glycerol G, % wt.*	*Monoglycerides MG, % wt.*	*Diglycerides DG, % wt.*	*Triglycerides TG, % wt.*	*FAME, % wt.*
0	0	0	0	100	0
2	7.34	0.08	0.10	19.35	71.14
5	9.08	0.59	0.14	1.17	88.67
10	9.27	0.35	0.08	0.00	90.09
15	9.24	0.45	0.08	0.00	90.01
25	9.24	0.48	0.08	0.00	89.98
40	9.26	0.38	0.07	0.00	90.07
60	9.23	0.50	0.08	0.00	89.97
Time (minutes)	*MeOH, χm*	*[MG], χm*	*[DG], χm*	*[TG], χm*	*[FAME], χm*
0	0,2226	0	0	0,7726	0
2	0,2462	0,0006	0,0008	0,1582	0,5385
5	0,2327	0,0048	0,0012	0,0095	0,6820
10	0,2317	0,0028	0,0007	0,0000	0,6935
15	0,2317	0,0037	0,0007	0,0000	0,6928
25	0,2317	0,0039	0,0006	0,0000	0,6927
40	0,2317	0,0032	0,0006	0,0000	0,6933
60	0,2317	0,0041	0,0007	0,0000	0,6925

χ_m = *mass fraction*

The chromatograms of the kinetic samples show an initial quantitative conversion of TG to FAME but after the first minutes the monoglycerides MG (1.29 % wt.) and diglycerides DG (0.17 % wt.) reappear. However, only MG are out of the specification (1.29 % wt., max. 0.80 % wt.), and consequently the total glycerol G (0.03 % wt., max. 0.02 % wt.)

The transesterification of used olive frying oil with methanol catalysed by sodium methoxide follows the mechanism outlined below:

1. $TG + CH_3O^- \leftrightarrow DG^- + FAME$
2. $DG^- + CH_3OH \leftrightarrow DG + CH_3O^-$
3. $DG + CH_3O^- \leftrightarrow MG^- + FAME$
4. $MG^- + CH_3OH \leftrightarrow MG + CH_3O^-$
5. $MG + CH_3O^- \leftrightarrow G^- + FAME$
6. $G^- + CH_3OH \leftrightarrow G + CH_3O^-$

In this mechanism we did not consider the formation of sodium methoxide, since it was already added as such to the reaction, that is, it was not formed by reaction of methanol with sodium hydroxide (like in many other transesterification processes) that produce water:-

$$CH_3OH + NaOH \leftrightarrow CH_3O^-Na^+ + H_2O$$

We did not consider either the formation of sodium salts of the free fatty acids contained in the oil, since the acidity index of the oils used were low, around 1,5°

$$R-COOH + NaOH \leftrightarrow R-COO^-Na^+ + H_2O$$

Since it is expected that reactions (2), (4) and (6) were much quicker than (1), (3) and (5) since DG^-, MG^- and G^- are much stronger bases than CH_3O^- we can add these reactions (1)+ (2) , (3) + (4) , (5) + (6):

$$TG + CH_3OH \underset{k_{-1}}{\overset{k_1}{\rightleftharpoons}} DG + FAME$$

$$DG + CH_3OH \underset{k_{-2}}{\overset{k_2}{\rightleftharpoons}} MG + FAME$$

$$MG + CH_3OH \underset{k_{-3}}{\overset{k_3}{\rightleftharpoons}} G + FAME$$

This constitutes a set of three consecutive equilibrium reactions and the rates of reaction for TG, DG, MG, G, methanol and FAME can be expressed as (12):

$$-\frac{dTG}{dt} = k_1 \cdot TG \cdot MeOH - k_{-1} \cdot DG \cdot FAME$$

$$-\frac{dDG}{dt} = k_{-1} \cdot DG \cdot FAME + k_2 \cdot DG \cdot MeOH - k_{-2} \cdot MG \cdot FAME - k_1 \cdot TG \cdot MeOH$$

$$-\frac{dMG}{dt} = k_3 \cdot MG \cdot MeOH + k_{-2} \cdot MG \cdot FAME - k_2 \cdot DG \cdot MeOH - k_{-3} \cdot G \cdot FAME$$

$$-\frac{dG}{dt} = k_{-3} \cdot G \cdot FAME - k_3 \cdot MG \cdot MeOH$$

$$-\frac{dMeOH}{dt} = +\frac{dFAME}{dt} = k_1 \cdot TG \cdot MeOH + k_2 \cdot DG \cdot MeOH + k_3 \cdot MG \cdot MeOH -$$
$$- k_{-1} \cdot DG \cdot FAME - k_{-2} \cdot MG \cdot FAME - k_{-3} \cdot G \cdot FAME$$

The % wt. of TG, DG, MG, G and FAME have been summarized in Table 18 and plotted against time (in minutes) in Figure 19. As it can be seen in this figure the transesterification reaction is very quick at 60 °C and almost all TG were converted after the first 5 minutes; MG and DG were transient intermediate species whose concentration was always very low. This data set made very difficult solving the system of differential equations outlined above, leading us to make a simplifying assumption: the transesterification reaction could be considered as an irreversible second order reaction (first order in TG and first order in methanol) which had been solved as follows:

The transesterification reaction had the general form:

$$A + bB \xrightarrow{k} products$$

In this case the function that expresses the rate of this reaction vs. time was (242):

$$k \cdot t \cdot b \cdot C_{A_0} (M - 1) = \ln \frac{C_B}{b \cdot M \cdot C_A}, \text{ where } M = \frac{C_{B0}}{bC_{Ao}}$$

The simplified reaction was:

$$TG + 3CH_3OH \xrightarrow{k} G + 3FAME$$

In this reaction C_A was the concentration of TG, C_B the concentration of methanol and

b = 3. In the reactor were introduced 760 mL (699.2 g) of waste olive oil with a mean molecular weight of 885.43 g mol^{-1}, and 255 mL (201.45 g) of methanol, which makes a total of 1015 mL in the reactor. Thus, the mol number *n* and the initial concentrations C_{I0} are:

$$n_{A0} = \frac{699.2g}{885.43g/mol} = 0.79mol$$

$$C_{A0} = \frac{0.79mol}{1.015L} = 0.78mol/L$$

$$n_{B0} = \frac{201.45g}{32g/mol} = 6.3mol$$

$$C_{B0} = \frac{6.3mol}{1015L} = 6.20mol/L$$

In consequence, the second order reaction equation remains as follows:

$$M = \frac{C_{B0}}{b \cdot C_{A0}} = \frac{6.20mol/L}{3 \cdot 0.78mol/L} = 2.65$$

$$k \cdot t \cdot 3 \cdot 0.78 \cdot (2.65 - 1) = \ln \frac{C_B}{3 \cdot 2.65 \cdot C_A}$$

$$3{,}9 \cdot k \cdot t = \ln \frac{C_B}{7.95 \cdot C_A}$$

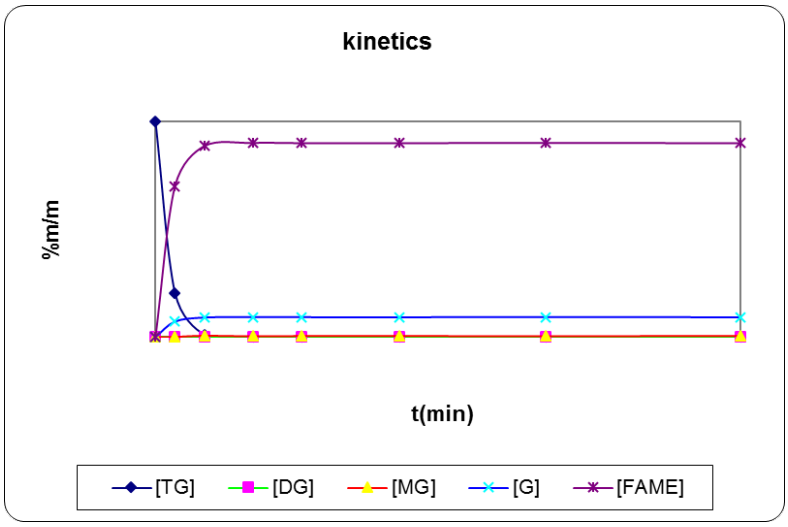

Figure 19. Concentration plots of mono-, di-triglycerides, FAME and glycerol vs. time in the kinetic experiments.

This second order kinetic equation had been solved using the mass fractions of TG and methanol. The mass fraction of methanol has been calculated in every point from the difference of the measured mass fractions of G, MG, DG, TG and FAME. The kinetic plot of $\ln(C_{MeOH}/aC_{TG})$ vs. time (minutes) gave a straight line (Figure 20). The 95% confidence limits for the intercept and slope of this straight line in Figure 20 are:

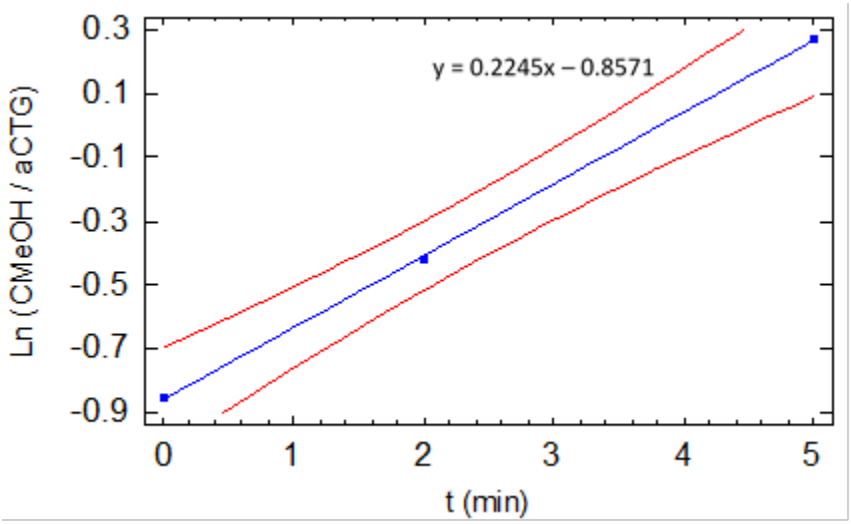

Figure 20. Kinetic plot of Ln (CMeOH / a CTG) vs. time for the second order kinetics transesterification reaction.

Slope: 0.2245 ± 0.0521

Intercept: -0.8571± 0.1621

The resulting rate constant *k* is 0,2245 L· mol^{-1} · min^{-1}·, and thus the transesterification reaction of used olive frying oil with methanol catalysed with sodium methoxide, follows the equation:

$$-r_{TG} = 0.2245[TG]\cdot[MeOH]\left(mol\cdot L^{-1}\cdot \min^{-1}\right)$$

2.4 Jojoba oil-wax

The transesterification of Jojoba oil-wax with methanol has been carried out by two alternative methods (chapter II section 3.2.4):

(a) acid catalysis, with acetyl chloride and methanol to yield anhydrous hydrogen chloride (95) . The conversion of the oil (measured by GC/MS) was 97% and the yield of crude isolated product was also 97%. However, the main drawbacks of this method are the work-up of the reaction product, that is time consuming and requires the use of a great amount of petroleum ether to extract the aqueous phase, and the formation of emulsions due to the free soaps formed in the neutralization step, that difficult the phase separation.

(b) With this precedent, we tried a basic catalyst, sodium methoxide (1wt% of the oil), freshly prepared from sodium metal and methanol, that has proven very successful in the transesterification reaction of triglyceride oils (4). In this method, the laborious steps of extraction were avoided but, although the GC/MS conversion was quantitative, only 90% of the crude mixture could be isolated, probably due to the adsorption of some polar components in the sodium sulphate used to dry the mixture after neutralization.

The transesterification reaction of jojoba oil wax is shown in scheme 3.

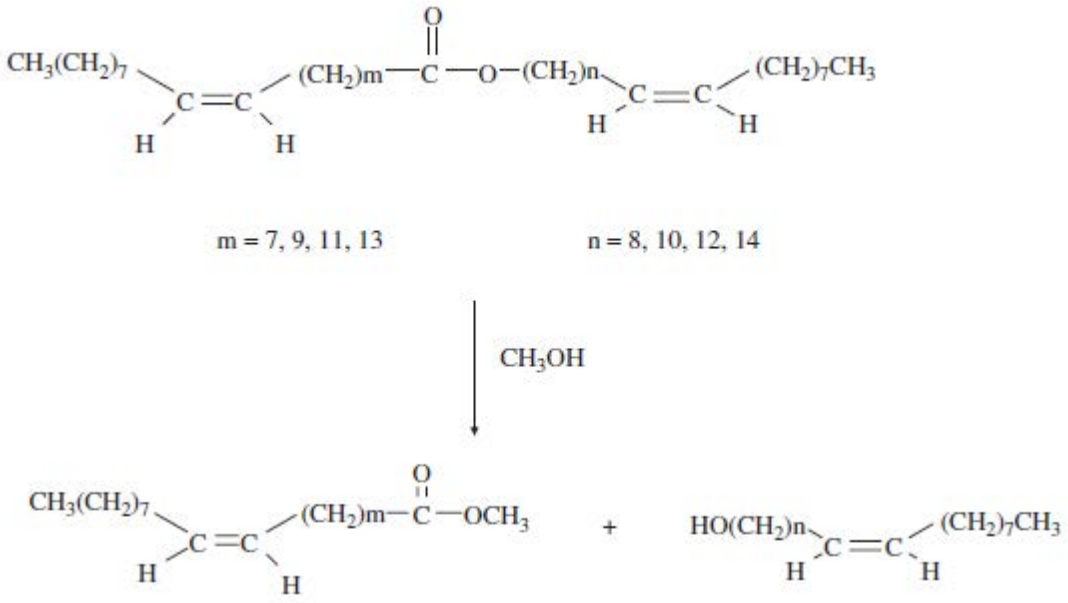

Scheme 3. Transesterification reaction of Jojoba oil-wax with methanol, showing a general structure for methyl jojoboate (bottom left) and jojobyl alcohol (bottom right).

The separation of jojobyl alcohol from methyl jojoboate was carried out following the procedure described in chapter II section 3.2.2. The crude product, mixture of methyl jojoboate and jojobyl alcohol, was analysed by GC-MS and FT-IR, showing good agreement with the molecular structure of the two fractions that shape it (Table 19, 3rd column).

Table 19: Composition of the products of the transesterification and separation of Jojoba oil-wax analysed by GC/MS.

Compound	*RT (min)*	*Crude Product (%)*	*Methyl jojoboate (%)*	*Jojobyl alcohol (%)*	*Residual Solids (%)*
Methyl palmitoleate C 16:1 *CAS No: 1120-25-8*	20.34	0.21			
Methyl palmitate C 16: 0 *CAS No: 112-39-0*	20.83	1.08	1.27	0.43	
Methyl 8,11-octadecadienate C 18:2, *CAS No: 56599-58-7*	24.09	0.04			
Methyl oleate C 18:1 *CAS No: 112-62-9*	24.29	7.22	9.51	3.39	
Methyl cis-11-eicosenoate C 20:1, *CAS No: 3946-08-5*	28.60	37.55	51.46	18.33	25.96
Methyl eicosanoate C 20:0 *CAS No: 1120-28-1*	28.87	0.23			
Methyl cis-13-docosenoate C 22:1, *CAS No: 1120-34-9*	34.45	11.15	14.49	5.02	5.30
Methyl docosanoate C 22:0 *CAS No: 929-77-1*	35.11	0.29			
Methyl 15-tetracosenoate C 24:1, *CAS No: 56554-33-7*	44.24	1.07	1.96	0.62	
Cis-9-octadecen-1-ol *CAS No: 143-28-2*	23.54	0.66	0.82	0.53	
Cis-11-eicosen-1-ol *CAS No: 629-96-9*	27.61	19.30	11.58	26.10	27.26
Cis-13-docosen-1-ol *CAS No: 629-98-1*	33.14	19.00	7.21	35.75	41.48
Trans-13-docosen-1-ol *CAS No: 23519-83-7*	33.82	0.88		1.36	
15-Tetracosen-1-ol *CAS No: cis-50995-29-4* *CAS No: trans-69521-46-6*	42.00	1.34	1.70	7.99	
			FAME = 79 %	*FAMEs = 28 %*	
			Alcoh. = 21 %	*Alcoh. = 72 %*	

As it will later be discussed in the characterization results (section 3 of this chapter), this mixture showed much better fluidity properties than the ones of the raw jojoba oil-wax, however they still do not meet the specifications. On the light of these preliminary results, a separation step was devised, since the poor fluidity properties are due mainly to the fatty alcohols that present strong intermolecular hydrogen bonds.

2.5 CASTOR OIL

Table 20 summarizes the main properties of the castor oil feedstock used in this study. As previously stated, the high water content (1920 mg/kg) is the only parameter that could cause a problem during the transesterification process.

Table 20: Characteristics of the castor oil feedstock

Test	*Value*	*Method*
Acidity index, º	0.56	ISO 660
Water content, mg/kg	1920	ISO 662
Saponification index, mg KOH/g	181.85	ISO 3657
Iodine index, gI_2/100 g	83.51	ISO 3961
Refraction index, at 20 ºC	1.4792	UNE 55015
Color, Gardner	2.7	AOCS Td 1a 64
Elemental analysis[1]		
% C, % m/m	80.52	
% H, % m/m	13.20	
S,mg/kg	< 5	

[1]*Mean value of four replicate analysis*

The transesterification of castor oil with methanol was carried out in two scales, 1.5 and 50.0 L reactors with basic catalysis. A commercial solution of sodium methoxide 25 % wt. in methanol was always used as the basic catalyst. The advance of the transesterification was followed by FT-IR spectroscopy (chapter II section 6.1.1) (227), taking aliquots every 2 minutes at the beginning of the reaction, later every 5-10 minutes and finally every 30 minutes. Usually, the transesterification was completed in 60 minutes with quantitative yield

- *Effect of the temperature of transesterification*

Table 21 (columns 2nd, 3rd and 4th) and Figure 21 summarize this transesterification procedure for castor oil at three different reaction temperatures in the 1.5 L reactor: from this data, it can be seen that the optimal reaction temperature and time are 40 ºC and 90 minutes respectively, since at higher reaction times the equilibrium of the transesterification reverses towards the reagents, as it has been observed by other authors (243). At 60 ºC the FAME solidifies due to the occurrence of 3.7 % w./w. of soap (see Figure 22 a) making impossible its purification by adsorption. There is not any obvious kinetic advantage in to heat at 50 ºC, since the formation of soaps is somewhat higher than at 40 ºC and the reaction does not proceed much quicker.

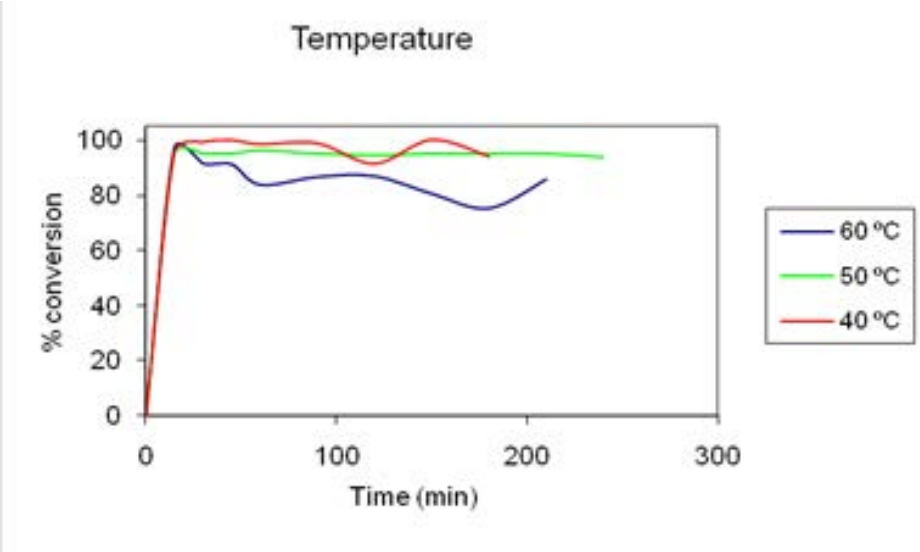

Figure 21. Conversion vs. time in the transesterification of castor oil: At three different reaction temperatures in the 1.5 L reactor.

Fig. 22a. Graphical summary of the experimental troubles found in the production of FAME from castor oil: FAME from castor oil obtained at 60 ºC: the FAME solidifies at room temperature due to the occurrence of soaps (3.7 % m/m)

Fig. 22b. *Graphical summary of the experimental troubles found in the production of FAME from castor oil: FAME from castor oil obtained with 2 % wt. of catalyst at 40 ºC: the G-phase solidifies at room temperature due to the occurrence of soaps (5.3 % m/m).*

- *Effect of the molar ratio methanol to castor oil and of the amount of catalyst*

Table 21(columns 5th, 8th and 9th) and Figure 23a summarize the transesterification procedure for castor oil at three different molar ratios methanol to oil in the 50 L reactor: all the results are very similar and we choose the lower molar ratio methanol to oil (5:1) as the optimal one to avoid the energy costs associated with the unnecessary recycling of alcohol. Table 21 (columns 5th, 6th and 7th) and Figure 23b summarize the transesterification procedure for castor oil with three different amounts of catalyst in the 50 L reactor: the lower amount of catalyst (0.5 % wt. of the oil) slows the reaction showing a clearly longer induction period, whereas the higher amount of catalyst (2 % wt. of the oil) produces an unsuitable FAME with 5.3 % m/m of soap, moreover rendering a solid G-phase (see Figure 22b). Thus, we choose 1 % wt. of the oil as the optimal amount of catalyst.

Table 21: Transesterification of castor oil at three different reaction temperatures in the 1.5 L reactor, and with three different amounts of catalyst and with three different molar ratios of methanol to oil, in the 50 L reactor.

Reactor volume	*1.5 L*	*1.5 L*	*1.5L*	*50 L*	*50 L*	*50L*	*50 L*	*50 L*
Castor oil, volume Temp., Molar ratio	1 L 40 ºC, , 7.5:1	1 L 50 ºC, , 7.5:1	1 L 60 ºC, , 7.5:1	30 L 40 ºC, 5:1	30 L 40 ºC, 5:1	30 L 40 ºC, 5:1	30 L 40 ºC, 7.5:1	30 L 40 ºC, 6:1
Methanol, L	0.30	0.30	0.30	6.4	6.4	6.4	9	7.7
Sodium Methoxide , L	0.0333 1 % wt. oil	0.0333 1 % wt. oil	0.0333 1 % wt. oil	1.0 1 % wt. oil	0.5 0.5 % wt. oil	2.0 2 % wt. oil	1.0 1 % wt. oil	1.0 1 % wt. oil
G-Phase1, L	0.035	0.034	0.036	1.82	1.75	1.75[4]	1.74	1.80
Wash	Dry[2], 2%	Dry[2], 4 %	Dry[2], 2 %	Dry[2],2%	Dry[3], 10%	Dry[2], 2%	Dry[2], 2%	Dry[2], 2%
FAME, L	0.69	0.80	0.96[4]	25.5	25.5	17	22.5	25.0
Yield, %	69	80	96	85	85	57	75	83

1 G-phase includes methanol.
b Dry wash with Magnesol (77 _C, 2–4 m/m%, stirring 30 min, filtered and inertized).
c Dry wash with Amberlite BD-10 (room temperature, 10 m/m%, stirring 120 min, filtered and inertized).
d The G-phase solidifies probably due to the occurrence of soaps (5.3 m/m%),

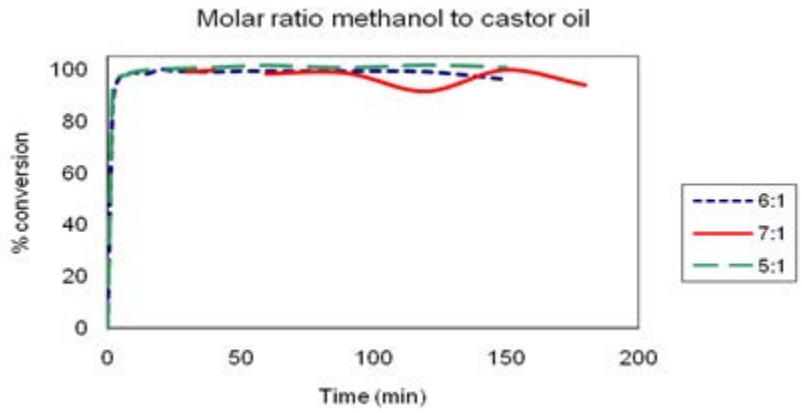

Figure 23a. Conversion vs. time in the transesterification of castor oil: At three different molar ratios methanol to oil in the 50 L reactor.

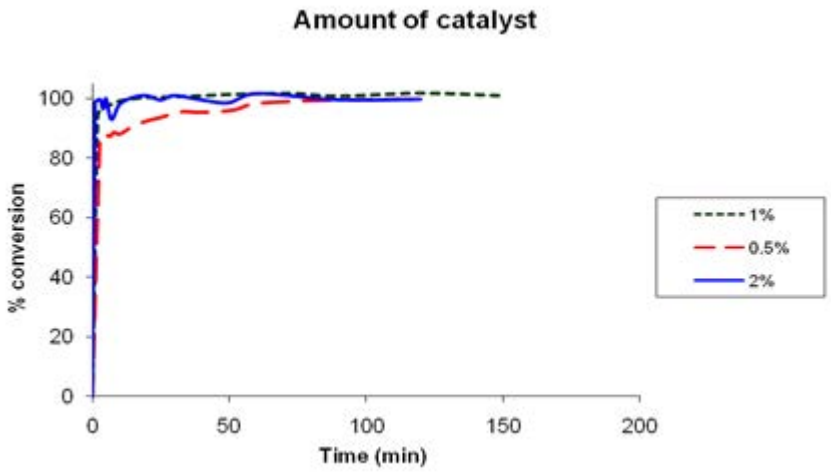

Figure 23b. Conversion vs. time in the transesterification of castor oil: With three different amounts of catalyst in the 50 L reactor.

The upper FAME phase was separated from the lower G-phase and two alternative ways of FAME purification were tried in this work: the "wet wash" and the "dry wash" (chapter II section 2.3.3).

A little better FAME quality was observed in the "dry" wash purification process using Amberlyte BD-10 with respect to the acidity index and the soap content, but the rest of the parameters were almost identical (see Table 29, section 3.2). When using solid adsorbents (magnesium silicate or Amberlyt e) for the purification process of FAME, a thorough filtration step through a 0.45 μm filter needs to be added to the production process scheme to account for the particle contamination problem.

The yield of FAME from castor oil in the 1.5 L reactor is somewhat irrelevant since the best yield of FAME (96 %) corresponds to a totally unsuitable FAME that solidifies at room temperature. In the 50 L reactor, the yields of FAME range from 57 % to 85 %, and this latest corresponds to the experimental conditions chosen as optimal, thus we could mention it as the yield of FAME from castor oil. The optimal conditions for the transesterification in the 50 L reactor resulted in 5:1 methanol/oil molar ratio and 40 °C (Table 29, 11th column, section 3.2).

3 FAME characterization

In this section, the properties of the biodiesel from animal fat/soybean oil mixture and castor oil are described in depth, depending on the aim of each study of this thesis, most of the properties are described on the correspondent section, however, in order to provide a quick comparison between the different properties of the FAME and FAEE obtained, some of the results shown in Tables 22a to 24.

Table 22a: FAME from edible oils characterisation

Property	*Standard-Method*	*Soybean FAME 1*	*Palm FAME*	*Soybean FAME 3*	*Rapeseed FAME*	*Coconut FAME 1*	*Peanut FAME*
Calcium, mg/kg		48.84					
Cloud point(°C)	ASTM D2500		+13	+1	-4	-4	+17
Cold Filter Plugging Point (CFPP, °C)	EN 116		+9	0	-9	-9	+10
Colour (Gardner)	AOCS Td 1a 64		0.5	0.5	0.5	0.5	0.5
Density at 15 °C (g/cm^3)	ASTM D1298	0.8905					
Density at 23 °C (kg/m^3)	EN ISO 3675		876.3	878.0	882.3	866.0	872.0
Higher heating value, MJ/kg	ASTM D240		40.49	40.33	39.53	38.63	40.64
Iodine value	fom FAME profile		69.9	120.0	100.8	11.3	100.0
Kinematic viscosity at 40 °C (mm^2/s)	ASTM D 445		4.45	4.16	4.32	2.55	4.69
Pour point(°C)	ASTM D2500		+12	-2	-13	-7	+12

Table 22b: FAME from edible oils characterisation

Property	*Standard-Method*	*Palm kernel distillate*	*Babassu distillate*	*Coconut distillate*	*Palm kernel bottom*	*Babassu bottom*	*Coconut bottom*
Acidity (mg KOH/g)	EN ISO 14104		0.033		0.78	0.310	
Cloud point(°C)	ASTM D2500		-7			7	
Cold Filter Plugging Point (CFPP, °C)	EN 116			-10		2	23
Colour and aspect	ASTM D1500	[x]Clear [a]	Clear [a]	Clear [a]	Yellow	yellow	yellow
Copper strip corrosion (class)	ASTM D 130		1a		1a	1a	1a
Density at 15 °C (g/cm^3)	ASTM D1298		874.5	870	882.0	874.8	879
Flash point (°C)	EN ISO 3679		50		82	45	
Freezing point (°C)	ASTM D2386	-15.3					
Higher heating value, MJ/kg	ASTM D240	37.57	37.41	37.66	37.85	39.29	39.38
Kinematic viscosity at 40 °C (mm^2 /s)	EN ISO 3104		2.13			3.65	
Lower heating value (MJ/kg)	ASTM D240*	34.89	34.93	35.06	35.33	36.78	36.73
Lower heating value (MJ/kg)	ASTM D4809	34.92	34.96	35.09			
Lubricity (mm), HFRR test	EN ISO 12156			0.3			
Oxidative stability (h)	EN 14112		>8	22.6			1.8
Pour point(°C)	ASTM D2500		-23			5	
Smoke point (mm)	ASTM D1322			22.8			
Water content (mg/kg)	ASTM D1774		343.5	278.9		480.3	111.1

aClear and colorless. bASTM D240

Table 23a: FAME from non-edible oils and fats characterisation

Property	*Standard-Method*	*Animal fat FAME*	*Animal fat mixed with soybean FAME*	*Jojoba oil-wax crude FAME*	*Methyl jojoboate*	*Castor FAME*
Acidity index (mg KOH/g)	EN ISO 660/2000	0.45-0.16	0.16			0.220
Calcium, mg/kg		n.d-4.5	4.5			
Cold Filter Plugging Point (CFPP, °C)	EN 116	+10	+4	+4	-14	-3
Copper strip corrosion (class)	ASTM D 130		1a			
Density at 15 °C (g/cm^3)	ASTM D1298	889.3				0.924
Density at 15 °C (kg/m^3)	ASTM D 4052	877.0	882.0	866.0	863.5	
Flash point (°C)	EN ISO 3679		179			
Higher heating value, MJ/kg	ASTM D 2382			43.47	41.52	35.86
Higher heating value, MJ/kg	ASTM D240	39.95	39.88			
iodine index, mg of I_2/100 g		55	98			
Iodine value	from FAME profile	58.1				
Kinematic viscosity at 40 °C (mm2 /s)	ASTM D 445	5.230	4.780	11.82	9.04	
Kinematic viscosity at 40 °C (mm2 /s)	EN ISO 3104		5.55			11.13
Lower Heating Value (LHV)(MJ/kg)	ASTM D4809					33.16
Lubricity (mm), HFRR test	EN ISO 12156					286
Oxidative stability (h)	EN 14112	5.11-3.86	3.8-5.4			3.18//3.11
Sulphur content, mg/kg	ASTM D4294	34.5-49.5	34.5-49.5			
Total contamination (mg/kg)	EN 12662	103.0-155.9	12.1			
Water content (mg/kg)	ASTM D1774	334-321	321			1029.9

Table 23b: FAME from non-edible oils and fats characterisation

Property	*Standard-Method*	*WFO FAME*	*Animal fat FAME*	*Lineseed FAME*	*Camelina FAME*
Cloud point(°C)	ASTM D2500	5	+13	-5	1
Cold Filter Plugging Point (CFPP, °C)	EN 116	-5	+10	+4	-5
Colour (Gardner)	AOCS Td 1a 64		3.0	4.0	Clear
Copper strip corrosion (class)	ASTM D 130	1a			
Density at 15 °C (kg /m^3)	ASTM D 4052	880			889.3
Density at 23 °C (kg/m^3)	EN ISO 3675			895.0	
Flash point (°C)	EN ISO 3679	141.9			
Freezing point (°C)	ASTM D2386				
Higher heating value, MJ/kg	ASTM D240	40.75	40.29	39.75	40
Iodine value	from FAME profile			176.7	150.7
Kinematic viscosity at 40 °C (mm2 /s)	EN ISO 3104	5.44		4.67	
Lower Heating Value (MJ/kg)	ASTM D240-modified				37.62
Lower Heating Value (MJ/kg)	ASTM D4809				37.65
Oxidative stability (h)	EN 14112				1.4
Pour point(°C)	ASTM D2500		+13	-8	-5

Table 24: FAEE characterisation

Property	*Standard- Method*	*Palm FAEE*	*Soybean FAEE*	*Rapeseed FAEE*
Cetane number	from FAME profile	61.9	51.1	58.1
Cloud point (°C)	ASTM D-2500	+9	-1	-5
Cold Filter Plugging Point (CFPP, °C)	EN 116	+10	-5	-11
Colour and aspect	ASTM D1500	0.5	0.5	0.5
Density at 15 °C (kg /m^3)	EN ISO 12185	870.2	878.0	870.0
Higher heating value, MJ/kg	ASTM D240	40.49	40.47	40.59
Iodine value	fom FAME profile	44.7	120.0	100.8
Kinematic viscosity at 40 °C (mm^2 /s)	EN ISO 3104	4.45	4.82	4.78
Oxidative stability (h)	EN 14112	7.73	0.71	4.12
Pour point(°C)	ASTM D2500	+9	-5	-16

3.1 Animal fat, soybean oil mixtures

- *Iodine index*

All the biodiesel samples checked give iodine indexes much lower than the upper value fixed by the EN14214 standard (120 mg/kg). The iodine index increases linearly with the soybean oil content in the feedstock, because of the most unsaturated character of the FAME of the latter when compared with the FAME derived from animal fats, see Figure 24.

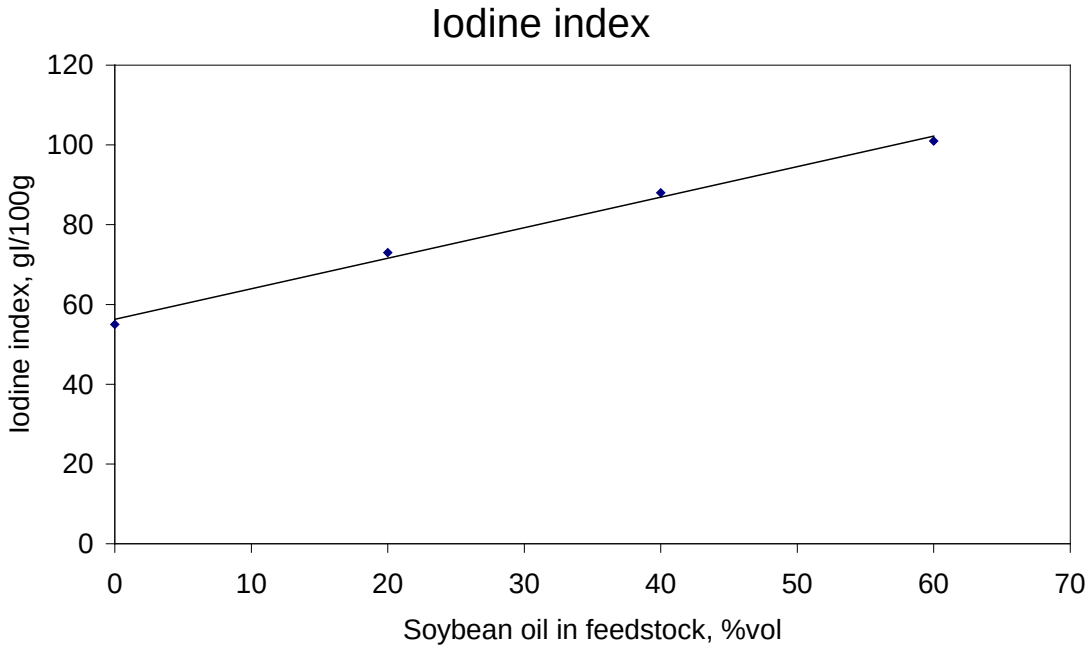

Figure 24. Iodine index of the biodiesel vs. soybean oil in the feedstock

- *Kinematic viscosity at 40 ºC*

Viscosity is the major reason why fats and oils are transesterified to biodiesel. The viscosity of biodiesel is approximately an order of magnitude lower than that of the starting oil or fat, leading to better atomization of the fuel in the combustion chamber of the engine.

All the samples of biodiesel are in the range established by the EN14214 (3.5 -5.0 mm^2/s) or the ASTM D6751 (1.9-6.0 mm^2/s) standards, and it is possible to correlate the biodiesel viscosity with the animal fat content of the feedstock: pure animal fat as feedstock gives the highest viscosity, slightly out of the specification EN 14214 (Figure 25). When using mixtures of animal fat and soybean oil as feedstock, the kinematic viscosity decreases with the increasing amount of soybean oil. Generally,

viscosity increases with the number of CH_2 groups in the FAME chain characteristic of the most saturated animal fat, and decreases with the increasing unsaturation of the soybean oil (244). The observed trend in Figure 25 agrees well with these two effects.

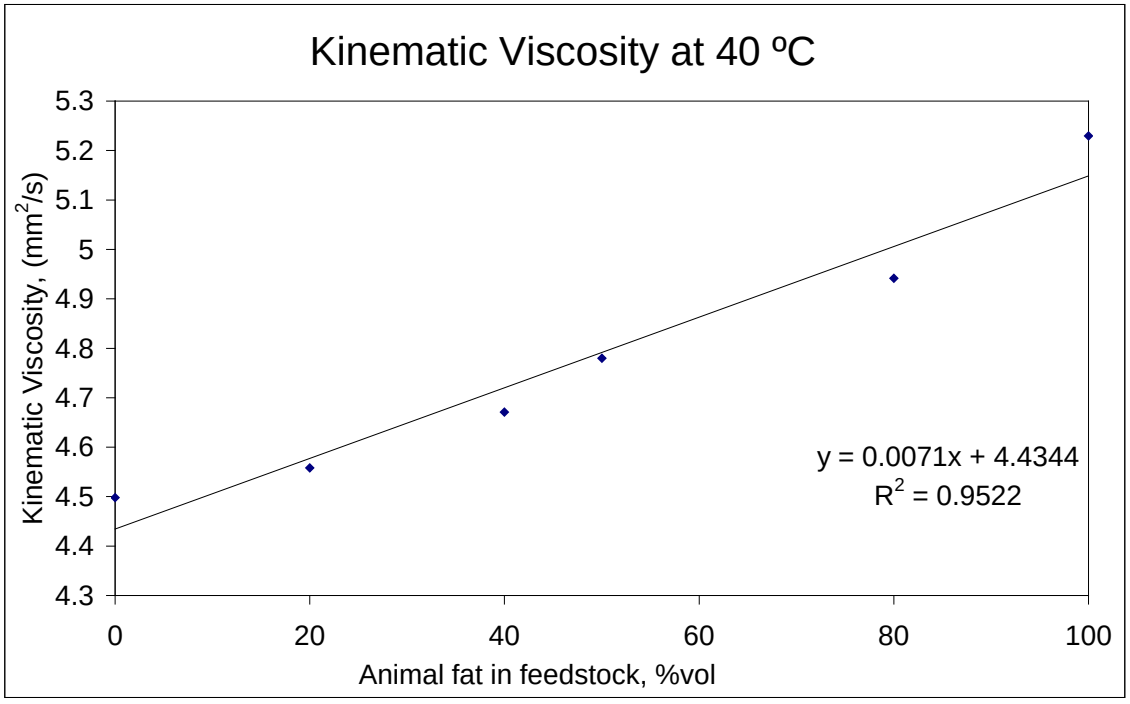

Figure 25. *Kinematic viscosity at 40 ºC of the biodiesel vs. feedstock composition.*

- *Density*

The density of all biodiesel samples is in the range of the EN 14214 standard, and increases smoothly with the amount of soybean oil in the feedstock.

- *Cold-filter plugging point*

The parameters such as the cloud point (CP, temperature at which the first solids become visible when cooling a diesel fuel), the pour point (PP, temperature at which fuel ceases to flow) and the cold-filter plugging point (CFPP, filterability test for cooled fuels already containing some solids) are used for assessing low temperature properties of the biodiesel. These parameters are determined by the amount of higher-melting saturated FAME or other higher melting minor components regardless of the nature of the unsaturated esters(245). However, cold flow is a "soft" specification, a "report to customer" being required in the EN 14214 or the ASTM D6751 standards, using limits depending on location and time of the year.

CFPP is of great interest when using animal fat as feedstock for biodiesel production, since the saturated FAME that characterize the biodiesel of this origin increases the CFPP in a substantial way. The CFPP results are plotted against the soybean oil content in the feedstock in the Figure 26. This CFPP correlates linearly with the soybean oil content in the raw material, since the FAME composing the soybean oil biodiesel are mostly unsaturated ones, and the predominant *cis* double bonds of these FAME greatly contribute to the lowering of the CFPP. Moreover, this biodiesel could be easily acceptable for winter template climates with very slight additivation (246).

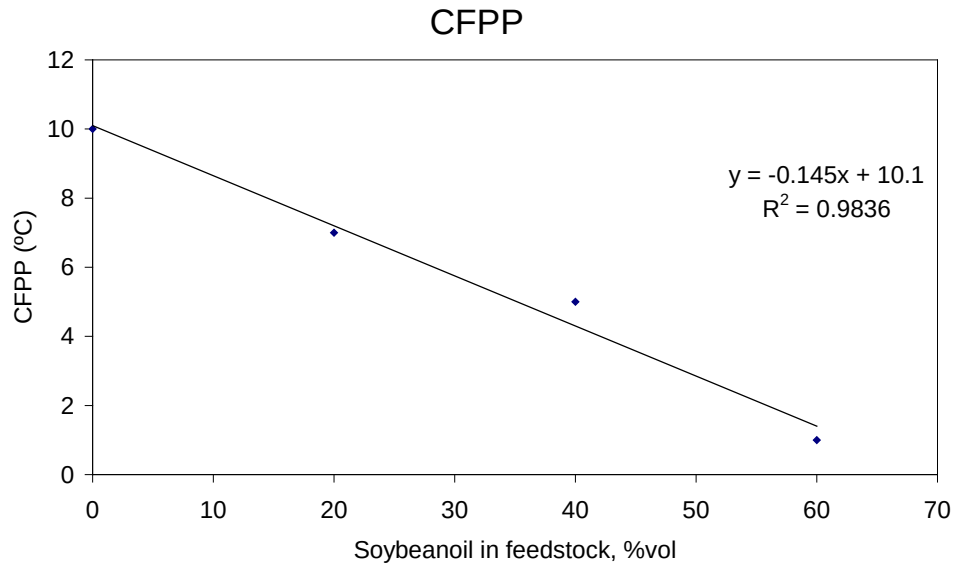

Figure 26. *Cold-filter plugging point of the biodiesel vs. soybean oil in the feedstock*

- *Higher heating value*

The higher heating value (HHV) is not specified in the EN 14214 or ASTM D6751 biodiesel standards. However, a European standard for using biodiesel as heating gasoil (EN 14213) specifies a minimum HHV of 35 MJ/kg. The HHV increases with increasing chain length and decreases with increasing unsaturation, and it is important for estimating the fuel consumption, the greater the HHV the lower the fuel consumption.

The HHV values are always lower than 43 MJ/kg, the typical value for the diesel fuel of fossil origin (247), and remain very close each other.

- *Elemental analysis*

The C and H contents are the usual ones for biodiesel, but it is noticeable in all the cases the appreciable N content, due to the contribution of the animal fat (see Table 13, section 2.2). The N content is not yet regulated by the EN 14214 or ASTM D6751 standards, but the presence of nitrogen compounds in fuels produce nocive NO_x gases in the combustion chambers and greatly contributes to the development of dark color in the biodiesel (another aspect still not regulated), due to the formation of oxidized nitrogen compounds, typically amine N-oxides.

Based in the above analyzed parameters, we have chosen the mixture of 50 %vol. of animal fat and soybean oil as the optimal feedstock for our biodiesel production process, and we have run many experiments in 1.5, 5.0 and 50.0 L reactors with very reproducible results using different batches of raw materials. Table 25 summarizes most of the properties of the biodiesel prepared by this process.

Table 25 Some Additional Properties of the Biodiesel from 50 vol % Animal Fat-Soybean Oil Feedstock

specification	*50/50 vol %*	*EN14214*
Flash point, °C	179	>120
Sulfur content, mg/kg	34.5-49.5	<10
Water content, mg/kg	321	<500
Copper corrosion, 3 h at 50 °C	1a	Class 1
Oxidative stability (Rancimat method), h	3.8-5.4	>8
Acidity index, mg of KOH/g	0.16	<0.5
Methanol content, % m/m	<0.01	<0.20
Total contamination, mg/kg	12.1	<24
Group I metals (Na), mg/kg	1.3	<5
Group II metals (Ca), mg/kg	4.5	<5
Phosphorus content, mg/kg	3.1	<10

The following parameters deserve special comments:

a) Sulfur content

The sulfur content of this biodiesel is out of specifications (34.5 - 49.5 mg/kg). The maximum values fixed by the standards are 10 mg/kg (EN14214) and 15 mg/kg (ASTM D6751). Although the production process used in this thesis is able to reduce the sulfur content from around 192 mg/kg in the feedstock (average value of 384 mg S/kg in the animal fat and less than 5 mgS/kg in the soybean oil) to the above values, a further reduction has not been possible with this animal fat. To lower this sulfur content to the level admitted by the standards, the animal fat should content less than 150 mg/kg of sulfur, if the desulfurization rate of our process keeps this sulfur reduction level, which is around the 85 %.

b) Oxidative stability (Rancimat method)

Saturated FAME are very oxidatively stable, while double bonds impart to FAME the susceptibility to react with oxygen. Especially FAME chains with methylene interrupted double bonds (linoleate and linolenate) are very susceptible to oxidation. The oxidative stability of the biodiesel ranges from 3.8 h to 5.4 h, depending of the batch of feedstock. These values are higher than the minimum fixed in ASTM D6751 standard (3 h) and very close to the minimum value of 8.0 h admitted by the EN14214 standard, which could be attained with very little additivation. The use of antioxidant additives is common to improve oxidative stability of biodiesel(248, 249, 250).

c) Group II metals (Ca + Mg)

The group II metal content (Ca + Mg) is still adequate but it is near the maximum value when CaO is used as the base for eliminating the reaction water and the acid catalyst in the esterification step. In this case, a final treatment of the biodiesel with the solid adsorbent magnesium silicate Magnesol D60 followed by two thorough filtration steps (0.45 μm) should be used to accomplish with this parameter.

3.2 Castor oil

- *Mono-, di- and triglycerides. Free and total glycerol*

The castor oil FAME prepared in the 50 L reactor at the optimal experimental conditions (Table 26, column 11th) is in the range established by the EN 14214 or ASTM D6751 standards with respect to the mono-, di- and triglycerides, indicating that the process described in this thesis reaches very good mono-, di- and triglyceride conversion values. However, the free and total glycerol are out of specifications showing that the purification process is insufficient to eliminate the glycerol from the FAME due to its hydrogen bond association with the methyl ricinoleate, the major constituent of the castor oil FAME.

- *FAME profile.*

Methyl ricinoleate is the major component (87.10 % wt.) of FAME from castor oil as expected from the composition of the parent oil. The FAME profile of castor oil is in accordance with the standard EN14214 as it is shown in Table 11. Saturated FAME (palmitate, 1.25 % wt. and stearate, 1.31 % wt.) have high advantageous cetane numbers and oxidative stability, but possess poor cold flow properties. Unsaturated, especially polyunsaturated FAME (oleate, 3.81 % wt., linoleate, 5.27 % wt.) have lower melting points, which are desirable for improved low-temperature properties, but also have low cetane numbers and reduced oxidative stability, which are undesirable for a diesel fuel.

Due to the presence of the OH- group the pure biodiesel of castor oil does not accomplish any property of the EN 14214 and it has to be blended with fossil diesel. The blends of castor biodiesel and fossil diesel have been characterized in this part of the thesis.

Table 26 Analysis of the FAME from castor oil produced in the reactors of 1 L and 50 L

Reactor volume (L)	1a	1b	1c	1	1	50	50	50a	50c	50	50	Standard
Castor oil volume (L)	1	1	1	1	1	30	30	30	30	30	30	EN 14214
Temperature (C)	40	40	40	50	60	40	40	40	40	40	40	
Catalyst amount, molar ratio	1% 7:1	1% 7:1	1% 7:1	1% 7:1	1% 7:1	1% 7:1	1% 6:1	1% 5:1	1% 5:1	0.5% 5:1	2% 5:1	
Acidity index (mg KOH/g)	1.45	1.43		1.26	1.36	1.5;1.57	1.57	1.6	1.45	Md=1.03; Ae=1.07	–	<0.50
Sulfur content (mg/kg)		0.4								0.4		<10.0
Total contamination (mg/kg)		160.5				385.9				160.5		<24
Soaps content (m/m% sodium oleate)	2.17	2.7		2.8	3.7	1.52;1.47	1.64	1.34	1.4	Md=1.0; Ae=0.62	5.3	
Monoglycerides (m/m%)	0.9									0.45		<0.80
Diglycerides (m/m%)	0.52									0.09		<0.20
Triglycerides (m/m%)	0.85									0.08		<0.20
Free glycerol (m/m%)	<0.005									**1.23**		<0.02
Total glycerol (m/m%)										**1.36**		<0.25
Water content (mg/kg)	1893		2000							353		<500
Oxidation stability (h) (Rancimat method)	4.78		1.7							7.9a;4.8c		>8.0
Methanol (m/m%)	0.32									0.23		<0.20
Density (kg/m3)		925.6	926.5									860–900
Kinematic viscosity at 40 C (mm2/s)		15.3	14.4			15.3;14.6	16.2	14.2	15.6	15.2		3.50–5.00
Higher heating value (MJ/kg)		38.32	37.27									
Cold-filter plugging point (C)			-3									
Elemental analysis												
%C										71.39		
%H										11.49		
%N										0.14		
Group I metals												
Na (mg/kg)		65				65	30	30		65		<5.0
Group II metals												
Ca (mg/kg)		3				3	4	4		1		<5.0
Mg(mg/kg)		28				28	29	29		7		
Sulfated ash (m/m%)		0.05										<0.02
Copper strip corrosion (class)		1a										Class 1
Flash point (C)		105										>120

a Analyzed at Biotel Fuels Ltd. b Analyzed at Universidad Politecnica de Madrid. c Analyzed at Universidad de Castilla La Mancha. d M: dry wash with Magnesol D-60. e A: dry wash with Amberlite BD-10. Replicate values are shown in the entries where more than a value appears for a parameter.

- *Kinematic viscosity at 40 ºC*

The kinematic viscosity at 40 ºC of the FAME from castor oil range from 14.2 to 16.2 mm^2/s and thus, any of the samples of castor oil FAME is in the range established by the EN14214 (3.5 -5.0 mm^2/s) or the ASTM D6751 (1.9-6.0 mm^2/s) standards. This high kinematic viscosity due to the intermolecular hydrogen bond association of the methyl ricinoleate molecules is the main obstacle for the use of pure castor oil FAME as fuel in internal combustion engines. Generally, viscosity increases with the number of CH_2 groups in the FAME chain and decreases with the increasing unsaturation of the oil (244).

Figure 27 shows the variation of the kinematic viscosity of FAME from castor oil and of pure methyl ricinoleate with the temperature, the first being always lower due to the contribution of other FAME.

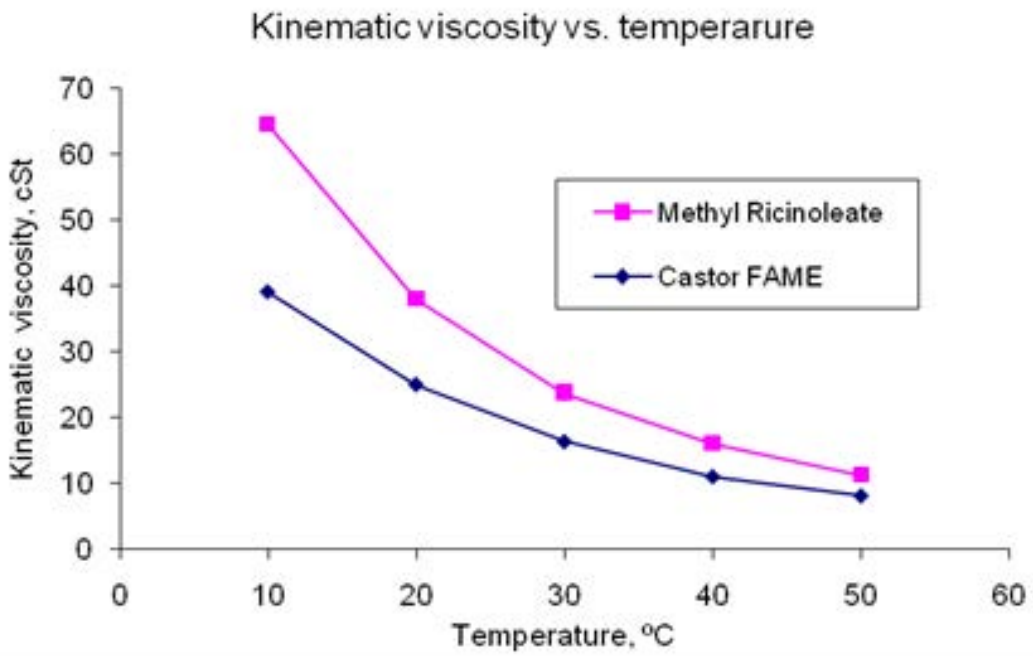

Figure 27 Variation of the kinematic viscosity with the temperature of the FAME from castor oil (diamonds) and of pure methyl ricinoleate (squares)

- *Density*

The density of the pure castor oil FAME is out of the range of the EN 14214 standard (Table 26, columns 3rd and 4th).

- *Cold-filter plugging point*

CFPP of pure castor FAME is - 3 ºC, which would enter the summer specification in Spain (0 ºC) but no the winter one (-10 ºC), Table 26 (column 4th).

- *Higher heating value*

The HHV of the pure castor FAME is summarized in Table 41 (columns 3th and 4th),

- *Elemental analysis*

The C and H contents of the pure castor FAME are the usual ones for biodiesel, but it is noticeable the appreciable N content (see Table 26, 11th column).

- *Oxidative stability (Rancimat method)*

The oxidative stability of the pure castor FAME ranges from 1.7 h to 7.9 h, depending of the batch of feedstock and of the measuring laboratory. Thus, for the same batch of castor FAME measured in two independent laboratories we have found very different values (Table 26, columns 2nd and 4th). Moreover, the batch of castor FAME prepared in the experimental conditions that we choose as optimal shows a very high oxidative stability of 7.9 h, measured in the laboratory that gives the higher values. This value is higher than the minimum fixed in ASTM D6751 standard (3 h) and closer to the minimum value of 8.0 h admitted by the EN14214 standard. The alternative laboratory gives for this sample a value of 4.83 h. Moreover, the use of antioxidant additives is common to improve oxidative stability of biodiesel (248, 249, 250).

- *Group I metals (Na + K)*

The sodium content of the castor FAME ranges from 30 to 65 mg/kg measured by atomic absorption spectrometry, and it is out of specification (Table 26). The impossibility to purify the FAME by washing with aqueous solutions produces this high sodium content that comes from the catalyst sodium methoxide.

- *Group II metals (Ca + Mg)*

The calcium content of the castor FAME is adequate (between 1 and 4 mg/kg) but it is near the maximum value (Table 26). On the other hand, the final treatment of the FAME with the solid adsorbent magnesium silicate Magnesol D60, although followed by two thorough filtration steps (0.45 μm) produces inacceptable magnesium contents of around 29 mg/kg. The "dry wash" purification method of the FAME with Amberlite BD-10 shows magnesium content of 7 mg/kg still out of specifications but near the maximum limit.

- *Total contamination*

The total contamination of castor FAME is very high, between 160.5 and 385.9 mg/kg, and out of specification EN 14214, although we carried out two filtration steps with 0.45 μm filter. This fact is probably due to the high soap content of the samples that ranges from 0.62 to 5.3 % m/m (Table 26). When this soap content is around or higher than 3 % m/m, the castor FAME solidifies as a whole (see Figure 22b, page 125, section 2.5). This elevated formation of soaps during the transesterification is due to the high water content of the raw castor oil (see Table 20, section 2.5) and to the hygroscopic character of this oil (226) that produces an unavoidable saponification side reaction.

- *Water content*

The water content of the castor FAME produced in the 1.5 L is around 2000 mg/kg, and reflects approximately the water content of the raw castor oil (1920 mg/kg). The drying of the oil before the transesterification would be inefficient due to its hygroscopic character (226). However, in one batch carried out in the 50 L reactor we could dry the castor FAME until 353 mg/kg, although it later also took some water. (Figure 28)

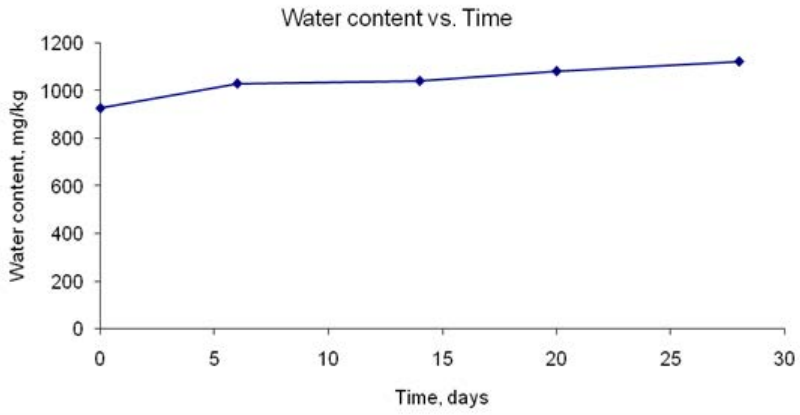

Figure 28 *Variation of the water content with time (in days) of castor oil FAME*

- *Acidity index*

The acidity index of the castor FAME ranges from 0.22 to 1.60 mg KOH/g. The "dry wash" purification procedure is insufficient to eliminate all the fatty acids since the adsorption mechanism of the magnesium silicate is to adsorb the polar OH groups of acids, alcohols and glycerol, but the presence in a big excess of the methyl ricinoleate creates a great competition for the active sites of the adsorbent that are practically all occupied by the OH group of the methyl ricinoleate. The adsorption with Amberlite BD-10 lowers slightly the acidity index, but also above specifications (Table 26).

- *Lubricity (wear scar)*

The fuel injection systems of diesel engines are preserved of a premature wear and damage by the lubricant power of the diesel fuel. This latter seems to decrease in a noticeable amount when the sulfur content of the gasoil lowers. Current and future regulations on the sulfur content of diesel fuel have led to a decrease of lubricity of these fuels. The lubricity of a fuel is usually measured by the High Frequency Reciprocating Rig (HFRR) test that gives the wear scar in μm of a fuel, after the ISO 12156-1 standard. The European standard for diesel fuel EN 590 fixes a maximum value for this wear scar of 460 μm. Biodiesel usually enhances lubricity when added to diesel fuel, this effect being particularly high for biodiesel from castor oil due to the high concentration of unsaturated hydroxyl fatty ester methyl ricinoleate (251) or to the presence of contaminants (free fatty acids or glycerol) which have been observed to behave as lubricity-imparting moieties (252).

- *Other parameters of the castor oil FAME*

The methanol content of the castor FAME is slightly higher than the limit value of 0.20 %m/m and varies from 0.23 to 0.32 % m/m since it is very difficult to eliminate this residual methanol due to its hydrogen bond association with the methyl ricinoleate. This elevated methanol content lowers the flash point of the castor FAME to only 105.0 ºC, out also of specification (Table 26).

The sulfated ash content is also high (0.05 5 % m/m) due to the high metallic content in sodium and magnesium, and the copper strip corrosion is within specification (class 1a).

4 BLENDS OF FAME AND FOSSIL FUELS CHARACTERIZATION

4.1 Castor FAME and regular diesel

- *Kinematic viscosity at 40 ºC*

Blends of castor FAME and reference fossil diesel have been prepared, (see Table 27 and Figure 29) only the blends with less than 40 % vol. of castor oil FAME could meet the specification of the EN 590 standard (< 4.50 mm^2/s) that is applicable at present for these blends;

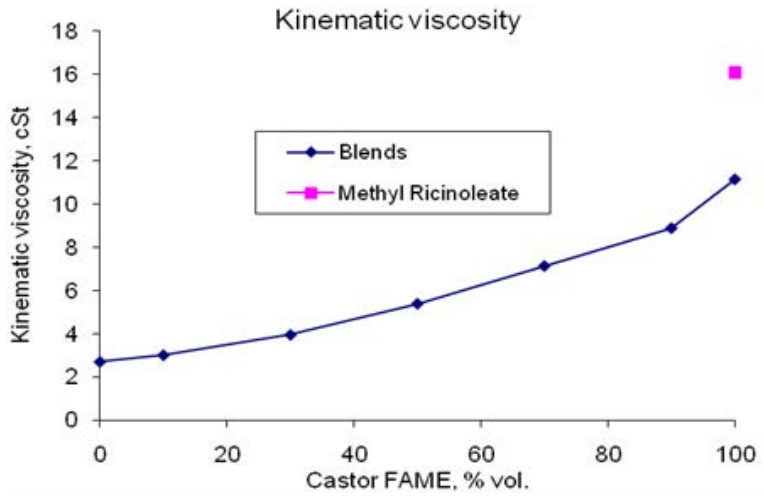

Figure 29 Kinematic viscosity at 40 ºC of the blends of castor oil FAME and reference diesel.

- *Density*

The blends with reference diesel until around 20 % vol. of castor FAME enter the technical specification EN 590 (see Table 27 and Figure 30).

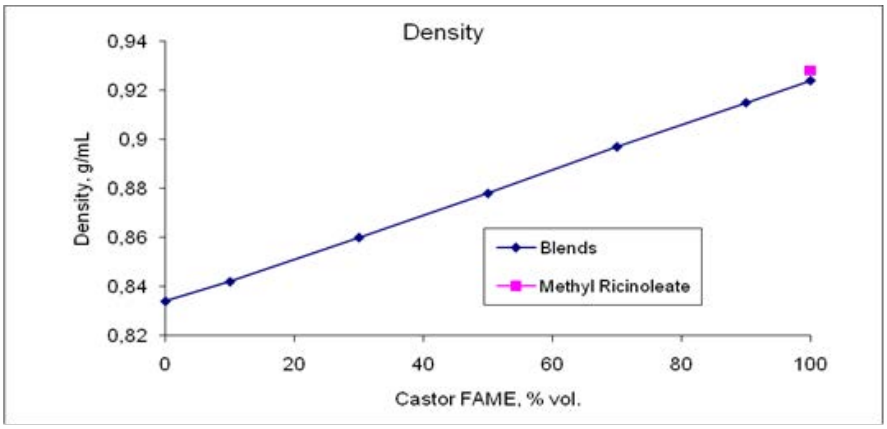

Figure 30. Density at 15 ºC of the blends of castor oil FAME and reference diesel

- *Cold-filter plugging point*

The CFPP results of the blends with reference diesel shown in Table 27 are plotted against the castor FAME content of the blend in the Figure 31. The cold filter plugging point of the blends shows also a singular effect, since the filterability remains identical to that of the reference diesel until around 50 % vol. of castor FAME has been blended with it. This fact could be explained because until around 50 % vol. of castor FAME the diluting effect of the hydrocarbons of the reference diesel avoid the approaching and crystallization at low temperature of the methyl ricinoleate molecules (the main constituent of castor FAME) ; when the castor FAME amount in the blends increases, the CFPP increases almost linearly. This explanation agrees well with the higher CFPP of pure methyl ricinoleate (see Figure 31), since the other ester components of castor FAME lower the CFPP as they lack the OH groups that attract each other by hydrogen bonds. These blends with reference diesel would enter the Spanish winter technical requirement until around 75 % vol. of castor FAME. Moreover, this castor FAME could be easily acceptable for winter template climates with very slight additivation (246).

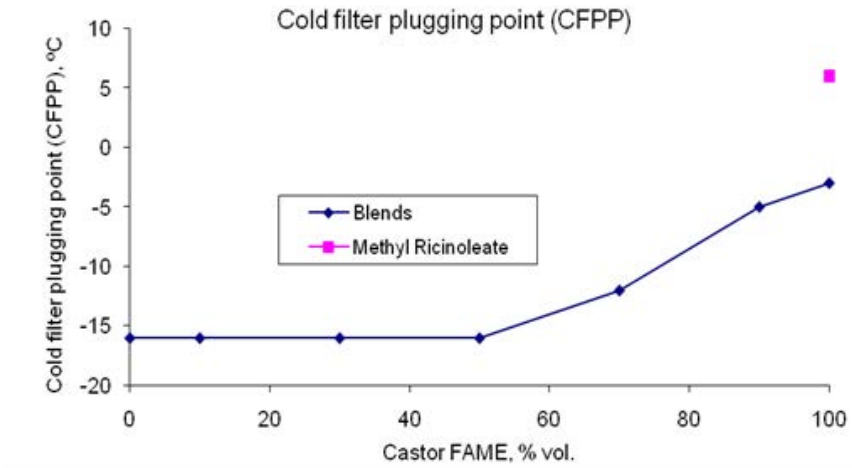

Figure 31. Cold-filter plugging point of the blends of castor oil FAME and reference diesel

- *Higher heating value*

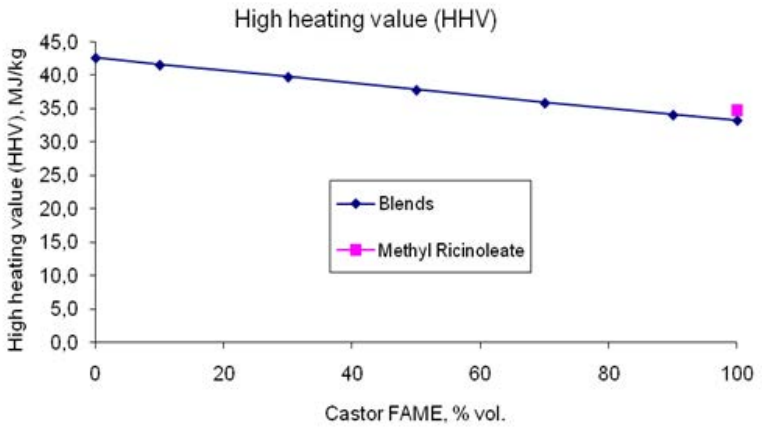

Figure 32 Higher heating value of the blends of castor oil FAME and reference diesel

Castor FAME and its blends with reference diesel (Table 27), all are above 35 MJ/kg. These values are always lower than 43 MJ/kg, the typical value for the diesel fuel of fossil origin (247), and decrease linearly with the amount of castor diesel in the blend, as shown in Figure 32.

Table 27. Analysis of the mixtures of FAME from castor oil and reference diesel.

	FAME Castor / Reference diesel, % vol.							
Specification	*0/100*	*10/90*	*30/70*	*50/50*	*70/30*	*90/10*	*100/0*	*Standard EN 590*
Density at 15 ºC, g/cm³	0.834	0.842	0.860	0.878	0.897	0.916	0.924	0.820-0.845
Kinematic viscosity at 40ºC, mm²/s (cSt)	2.68	2.99	3.93	5.37	7.12	8.87	11.13	2.00-4.50
Cold-filter plugging point,ºC	-16	-16	-16	-16	-12	-5	-3	-10; 0
Higher heating value, MJ/kg	45.67	44.61	42.67	40.66	38.61	36.80	35.86	
Lower heating value, MJ/kg	42.47	41.42	39.62	37.68	35.75	33.98	33.16	
Elemental analysis								
%C	85.11	83.85	79.95	78.89	76.15	72.96	72.10	
%H	14.58	14.53	13.87	13.55	13.03	12.85	12.29	
%N	0.20	0.13	0.15	0.13	0.15	0.15	0.14	
Aromatic hydrocarbons content, % m/m	26.6	23.9	18.6	13.3	7.98	2.7	0.00	
Water content, mg/kg	47.4	171.0	377.6	536.3	755.3	958.9	1029.9	< 200
Acidity Index, mg KOH/g	0.135	0.175	0.160	0.165	0.200	0.210	0.220	
Lubricity, Corrected print diameter, µm	413	209	214	-	230	-	286	< 460
Oxidative stability, h Rancimat method	11.18[1] 11.18[2]	1.25[1] 0.64[2]	1.66[1] 1.13[2]	- 1.64[2]	2.51[1] 2.21[2]	- 2.04[2]	3.18[1] 3.11[2]	20[3]

[1]Values measured on June 25th, 2008
[2]Values measured on July 23rd, 2008
[3]Method EN 15751

- *Elemental analysis*

The blends of castor FAME with reference diesel show in all cases also an appreciable nitrogen content, ranging from 0.13 to 0.20 % wt. The sulfur content of the castor FAME is within specifications (0.4 mg/kg, Table 26 columns 3rd and 11th) since the parent castor oil lacks of sulfur. The maximum values fixed by the standards are 10 mg/kg (EN14214) and 15 mg/kg (ASTM D6751).

- *Oxidative stability (Rancimat method)*

The oxidative stability of the blends of castor FAME and reference diesel shows an anti-synergistic effect, that is, the induction period in hours of all the blends is lower that that of the pure components separately (Table 27 and Figure 33). This anti-synergistic effect needs to be explained on the light of the oxidation mechanism of the unsaturated FAME. Saturated FAME are very oxidatively stable, while double bonds impart to FAME the susceptibility to react with oxygen. Especially FAME chains with methylene interrupted double bonds (linoleate and linolenate) are very susceptible to oxidation. One step of the oxidation mechanism of the unsaturated FAME is the attack of activated singlet oxygen to the allylic positions of the unsaturated fatty esters to form hydroperoxides (253, 254) (Scheme 4). The hydroperoxides are unstable species that evolved irreversibly to the formation of aldehydes, ketones and acids, sometimes with breaking of the fatty esters chain. In the case of blends with diesel fuels, which usually contain around 25% of aromatics (see Table 27), the presence of aromatic hydrocarbons enhance the light activation of the normally inactive form of oxygen (triplet oxygen $^3O_2$) to the photoactive form (singlet oxygen $^1O_2$), that is, the aromatic diesel hydrocarbons act as photosensitizers, probably through a charge transfer complex [HC$\cdots\cdots O_2$] (255). This effect decreases as the reference diesel amount in the blend lowers, the oxidative stability approaching that of the pure castor FAME. These oxidative stability measurements were repeated with a time difference of one month, the continuous red line in Figure 33 shows the initial measurements and the dashed blue line the second ones that obviously are lower due to the loss of stability. However, all these induction periods are lower than the minimum value of 20 h (method EN 15751) that the new standard will probably fix for the blends of biodiesel (until 7 % vol.) and fossil diesel, and thus the addition of antioxidants will be necessary.

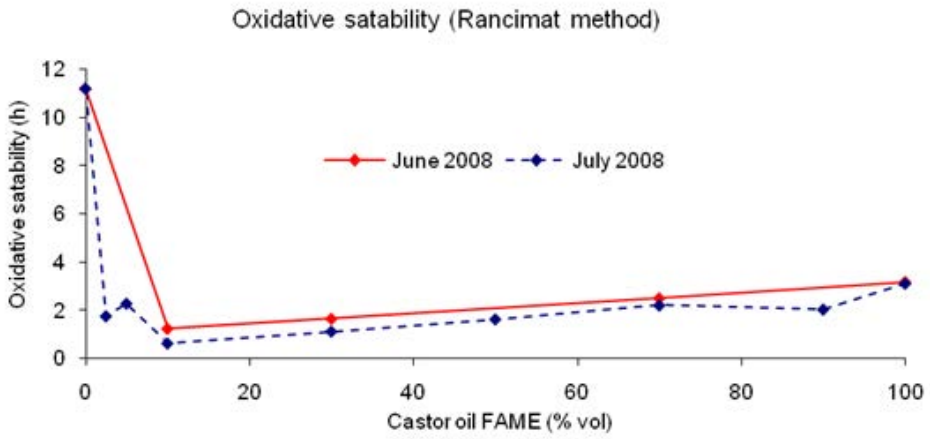

Figure 33. *Oxidative stability (Rancimat method) of the blends of castor oil FAME and reference diesel: values measured on June 2008 (continuous red line); values measured on July 2008 (dashed blue line), one month later.*

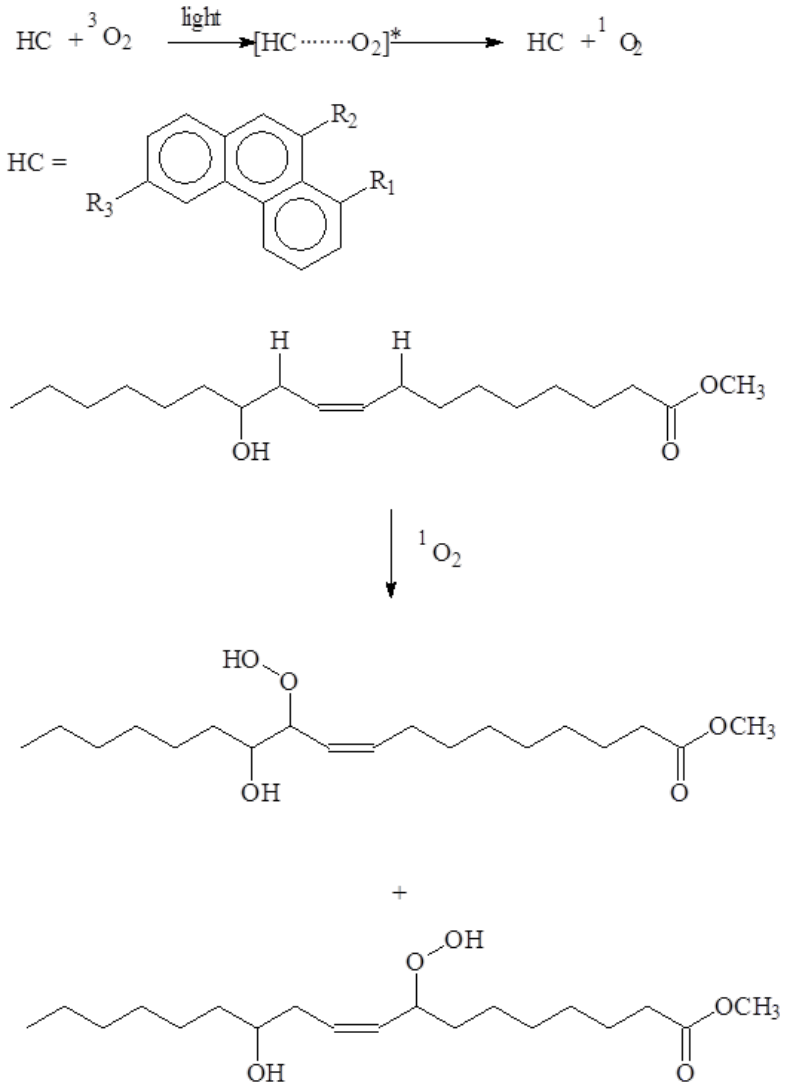

Scheme 4. *Mechanism (in part) of the oxidation of methyl ricinoleate by atmospheric oxygen.*

- *Water content*

The blends of castor FAME and reference diesel show water content that increases linearly with the amount of FAME in the blend since the fossil diesel has little water, see Figure 34. Moreover, when we measured the water content of castor FAME, this value increased irregularly from 925 to 1125 mg/kg in 28 days, showing also the hygroscopic character of this ester (Figure 28, previous section, page 142).

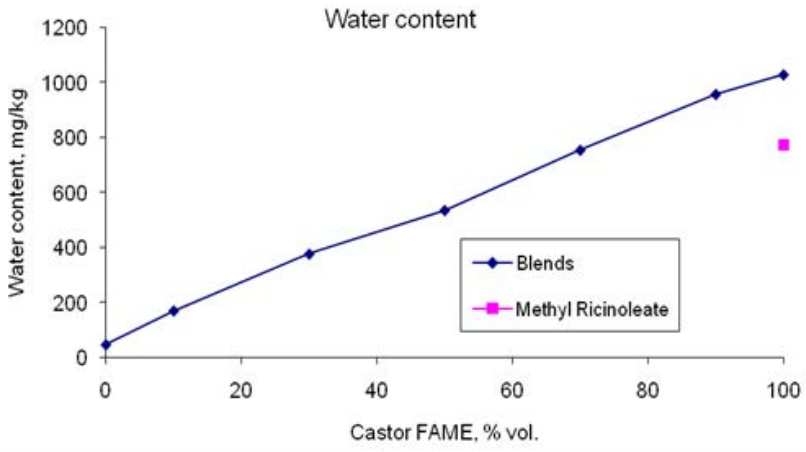

Figure 34. *Water content of the blends of castor oil FAME and reference diesel*

- *Acidity index*

The acidity index of the blends of castor FAME and reference diesel increases almost linearly with the amount of castor FAME in the blend (Figure 35).

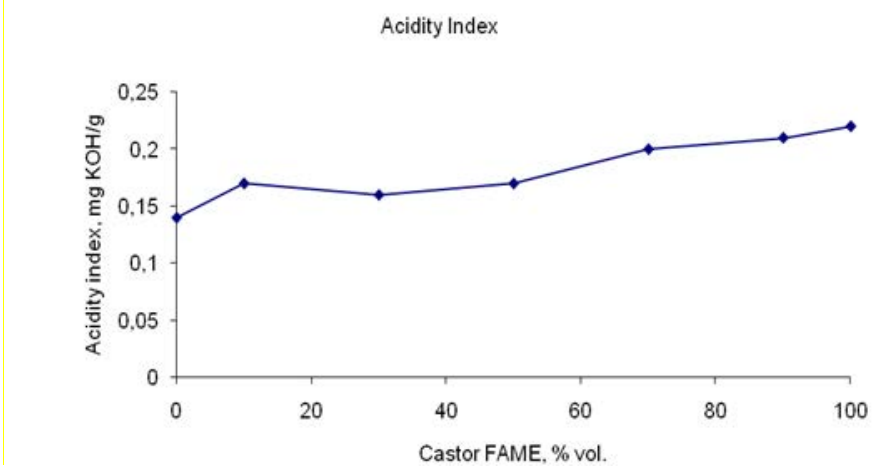

Figure 35. *Acidity index of the blends of castor oil FAME and reference diesel*

- *Lubricity (wear scar)*

The results obtained from the HFRR test of the blends of castor FAME and reference diesel (Figure 36) show a synergistic effect, that is, the values of the blends are always lower than those of the pure components. This synergistic effect has been observed rarely (251), since most of works have studied the effect of methyl esters as additives but not as blending components (252, 256).

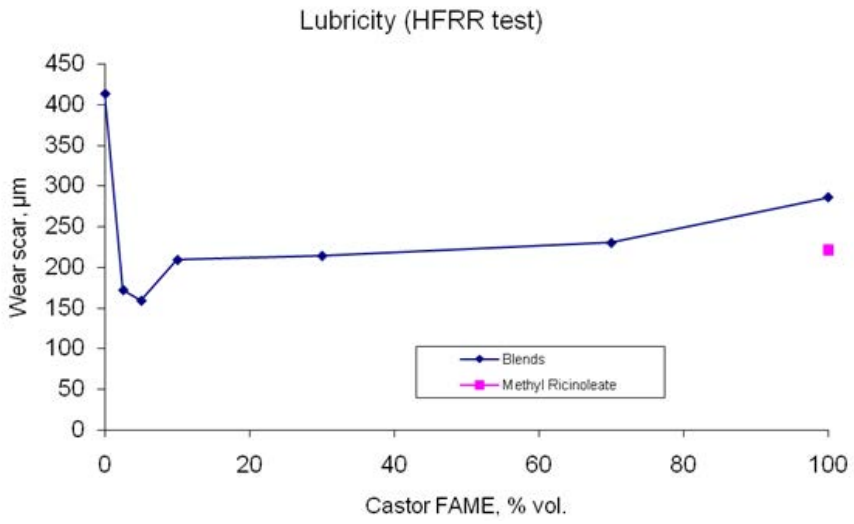

Figure 36. *Lubricity (wear scar) of the blends of castor oil FAME and reference diesel*

4.2 Jojoba FAME

The transesterification crude product, was a mixture of methyl jojoboate and jojobyl alcohol (section 2.3). However, although its density and higher heating value were adequate (866 kgm-3 and 42.17 kJ g-1, respectively), its fluidity properties were not: kinematic viscosity (11.82mm2 s-1) and cold filter plugging point (CFPP, +4°C). These fluidity properties were much better than that of the raw Jojoba oil-wax (Table 31), due to the breaking of the long molecular chains of the original wax into shorter chains of methyl jojoboate and jojobyl alcohol, but still they did not meet the specifications of biodiesel as defined in the European standard EN 14214.

Table 28 Properties of the biodiesel from Jojoba oil-wax

Sample	*Density at 15 ºC (kg · m-3) ASTM D 4052*		*Kinematic viscosity at 40 ºC (mm2 · s-1) ASTM D 445*		*Cold Filter Plugging Point (CFPP, ºC) EN 116*		*Higher heating value (cal · g-1) ASTM D 2382*	
Jojoba oil-wax	868.6		24.89		+ 14		10 390	
Crude product a	866.0		11.82		+4		10 072	
Methyl jojoboateb	863.5		9.04		-14		9 916	
Methyl jojoboatec	871.6		10.44		-10		10 099	
Reference values EN 14214	Min.	Max.	Min.	Max.	Winter	Summer		
	860	900	3.50	5.00	-10	0		

a Crude transesterification product.
b Methyl jojoboate obtained by crystallisation of the crude product.
c Methyl jojoboate obtained by elimination of the volatile compounds by distillation followed by crystallisation

In the work of Selim (96), the low molar ratio of methanol to raw oil used for the transesterification reaction (0.1) implied that a significant amount of the product was unreacted Jojoba oil-wax; as a proof of the above assertion, the kinematic viscosity at 40 °C of the biodiesel used (24.6mm^2 s^{-1}) is very close to that of the raw Jojoba oilwax (24.8mm^2 s^{-1}, Table 28) and very far from the limits marked by the European standard for biodiesel (3.5–5.0mm^2 s^{-1}).

After this relative success in the separation by a single crystallization step of the FAME mixture from the fatty alcohols (section 2.3), the physicochemical properties of the FAME mixture sought as biodiesel were analysed: density (863.5 kgm^{-3}), higher heating value (41.52 kJ g^{-1}) and cold filter plugging point (-14 °C) were now in good agreement with the European standard, although kinematic viscosity (9.0mm^2 s^{-1}) was still above the maximum allowed (5.0mm^2 s^{-1}).

A different separation method based in the vacuum distillation of the crude transesterification product was totally unsuccessful, since only a very small amount of light cracked products could be distilled. The bottom product was then separated by the single crystallization step and the properties of the FAME mixture fraction analysed, resulting poorer values of the CFPP (-10 °C) and the kinematic viscosity (10.4mm^2 s^{-1}) due to the evaporation of the lighter products in the distillation.

4.3 Biokerosene and fossil aviation fuel.

On 1st January 2012 the European Union set a Directive that included the aviation sector in its carbon dioxide tax emission system. Forcing all planes landing or taking off in EU Airports to pay a fare. This decision has been strongly criticized by many countries, and, the US, Russian and Indian Airlines had refused to pay the tax. However, this EU cap and trade system, the volatility of the Jet A1 prices and the insecurity of supplies has forced the airlines to seriously consider the incorporation of biofuels into Jet A1.

With this view, the author has focused a substantial part of his PhD thesis on the suitability of some FAME as blend components for Jet A1. In the two following publications of the author, distilled FAME from coconut, babassu and palm kernel and FAME from camelina have been blended with fossil kerosene and the most sensitive properties of the blends have been evaluated and discussed.

However it should be clearly stated that FAME are not allowed at present time as blends components for Jet A1, their amount being limited to 50 mg/kg under the denomination of "identified incidental material". The publication of these paper caused a controversy in the aviation fuel community, but from the author's opinion as discussed in this papers is that the issue of FAME in Jet A1 is far from having come to an end and it is at least worthy of a deeper research.

Fuel 102 (2012) 483–490

Contents lists available at SciVerse ScienceDirect

Fuel

journal homepage: www.elsevier.com/locate/fuel

Biokerosene from coconut and palm kernel oils: Production and properties of their blends with fossil kerosene

Alberto Llamas [a], María–Jesús García-Martínez [a], Ana-María Al-Lal [a], Laureano Canoira [a,*], Magín Lapuerta [b]

[a] Departament of Chemical Engineering & Fuels, ETS Ingenieros de Minas, Universidad Politécnica de Madrid, Ríos Rosas 21, 28003 Madrid, Spain
[b] Grupo de Combustibles y Motores, ETS Ingenieros Industriales, Universidad de Castilla La Mancha, Avenida Camilo José Cela, s/n, 13071 Ciudad Real, Spain

HIGHLIGHTS

- Coconut and palm kernel oils have been converted to FAME with basic catalyst.
- The FAME's have been subjected to fractional distillation at vacuum.
- The low boiling point fractions have been blended with two fossil kerosenes.
- Fossil kerosenes: straight-run atmospheric distillation cut and commercial Jet A1.
- The essential specifications required by ASTM D1655 were tested in these blends.

ARTICLE INFO

Article history:
Received 26 July 2011
Received in revised form 3 May 2012
Accepted 28 June 2012
Available online 17 July 2012

Keywords:
Biokerosene
Cononut
Palm kernel
Distillation
Blends with fossil kerosene

ABSTRACT

Coconut and palm kernel oils have been transesterified with methanol by the classical homogeneous basic catalysis method with good yields. The FAME's have been subjected to fractional distillation at vacuum, and the low boiling point fractions have been blended with two types of fossil kerosene, a straight-run atmospheric distillation cut (hydrotreated) and a commercial Jet A1.

The blends of palm kernel biokerosene and Jet A1 meet some specifications selected for study of the ASTM D1655 standard: smoke point, density, flash point, viscosity at −20 °C and freezing point and they do not comply with the low calorific value by a very narrow margin. On the other hand, the blends of palm kernel biokerosene and atmospheric distillation fossil kerosene only met the density and viscosity at −20 °C parameters. The blends of coconut biokerosene and atmospheric distillation fossil kerosene meet the following specifications: density, viscosity at −20 °C and lubricity.

It is especially noticeable that all the blends of 5 vol.% of biokerosene and fossil kerosenes do not meet the low calorific value by a very narrow margin, less than 1.0 MJ kg^{-1}. With these preliminary results, we can conclude that it would be feasible to blend coconut and palm kernel biokerosenes prepared in this way with commercial Jet A1 up to 10 vol.% of the former, if the IATA organization relaxes very slightly its standards.

1. Introduction

The world economy is strongly dependant of the oil prices, and the main oil reserves are located in social and politically unstable countries which causes great fluctuations in the crude oil and petroleum products prices. From January 2003 to July 2008, the jet fuel price increased a 462%, reaching $3.89/gallon. Due to the world economic crisis, the jet fuel price dropped to $1.26/gallon in February 2009, but since then this price has been steadily increasing, and it was $3.09/gallon in January 2012. These fluctuations and the very foreseeable future ones have led to many countries try to develop a diversified fuels market less dependant of the crude oil imports [1].

On the other hand, on December 20th 2006 the European Commission approved a law proposal to include the civil aviation sector in the European market of carbon dioxide emission rights [European Union Emissions Trading System, EUETS). On July 8th 2009, the European Parliament and Council agreed that all flights leaving or landing in the EU airports starting from January 1st 2012 should be included in the EUETS. On November 19th 2008, the EU Directive 2008/101/CE [2] included the civil aviation activities in the EUETS, and this directive was transposed by the Spanish law 13/2010 of July 5th 2010 [3]. Thus, in 2012 the aviation sector

* Corresponding author. Tel.: +34 91 336 7015; fax: +34 91 336 6948.
E-mail address: laureano.canoira.lopez@upm.es (L. Canoira).

0016-2361/$ - see front matter © 2012 Elsevier Ltd. All rights reserved.
http://dx.doi.org/10.1016/j.fuel.2012.06.108

should reduce their emissions to the 97% of the mean values registered in the period 2004–2006, and for 2013 these emission reductions should reach the 95% of the mean values for that same period. Trying to face this situation, the aviation companies are planning seriously the use of alternative jet fuels to reduce their greenhouse gas emissions and to lower their costs. However, the jet fuels should fulfil a set of extraordinarily sensitive properties to guarantee the safety of planes and passengers during all the flights.

The literature on the production and use of biofuels for the aviation sector is still scarce and in some cases contradictory. Dunn [4] studied the properties of a fuel obtained blending 10–30 vol.% of soybean FAME with JP-8 and JP-8 + 100. Dagault and Gail [5] examined the oxidation behaviour of a blend of 20 vol.% rapeseed FAME with Jet A1. Korres et al. [6] compared the behaviour of the jet fuel JP-5 against fossil diesel and animal fat biodiesel in a diesel engine. Wagutu et al. [7] prepared six biofuels from jatropha, croton, calodendrum, coconut, sunflower and soybean, and they concluded among other findings that the coconut FAME is the biofuel that approaches most closely to the fossil jet fuel properties.

Some other authors have approached the jet fuel alternatives from biological sources from a totally different perspective, that is, the use of the Fischer–Tropsch (FT) synthesis and the synthetic paraffinic kerosenes of biological origin (Bio-SPK). On the former issue, Hileman et al. [8] analyzed the chemical composition and the energetic content of different jet fuels, showing that the biokerosene obtained by FT synthesis or hydrotreating of renewable oils can reduce the energetic expenditure of the planes by 0.3%. Gill et al. [9] analyzed the theoretical aspects and the technology of the FT processes BTL, CTL and GTL. Cottineau [10] claimed that UOP has developed a biokerosene from jatropha that surpasses the properties of the actual jet fuel. World News [11] refers to the construction of two pilot plants in France based in the PRENFLO process from Udhe which are due to come on stream in 2012 to produce biodiesel and biokerosene from syngas, obtained from biomass by a FT technology.

On the Bio-SPK issue, Kinder and Rhams [12] reported the hydrotreating and isomerisation of vegetable oils to produce a kerosene range of hydrocarbons, which has a very similar chemical composition to the fossil jet fuel. In this technology, the oil, once refined, is hydrogenated to remove the oxygen atoms and to saturate the olefinic double bonds which increase the heating value of the fuel and its thermal and oxidative stability; the ulterior isomerisation and cracking of the diesel range paraffins yields a typical kerosene fraction called Bio-SPK. Some blends of 50 vol.% of Bio-SPK with Jet A1 have been tested in air flights of three different companies.

In this paper, a different approach has been followed. FAME from oils rich in shorter chain fatty acids, such as coconut and palm kernel, were synthesized [13], and then the fraction which approaches the distillation range of fossil kerosene, that is, from 175–185 °C to 240–275 °C at atmospheric pressure, was separated by vacuum distillation. Since this pure biokerosene did not meet the different aviation jet fuel standards, blends containing 5, 10 and 20 vol.% of biokerosene with fossil kerosene with and without additives, were tested together with pure biokerosene. The bottom fractions of the FAME distillation of coconut and palm kernel, which can reach up to 50% of the FAME, have also been tested in order to check if it accomplishes alone the EN 14213 standard for heating gasoil, or needs to be blended with other FAME to find this application.

2. Experimental

Refined coconut oil was purchased from Acros Organics (CAS No. 8001-31-8) and crude palm kernel oil was supplied by Combustibles Ecologicos Biotel SL. Kerosene of fossil origin has been used to prepare the blends with biokerosene: $K-1$ was a straight-run atmospheric distillation cut (hydrotreated) kerosene without any additives and $K-2$ was a commercial Jet A1 kerosene and it contains additives; both samples of fossil kerosene were obtained from the Spanish Company Logistica de Hidrocarburos (CLH). Jet fuel additives are used to prevent the formation of oxidation deposits in aircraft engines and fuel systems, to inhibit the corrosion of steel, to improve the fuel lubricity and oxidation stability, to increase the electrical conductivity of the fuel, to avoid microbiological contamination, to prevent the ice formation in fuel systems and to assist in detecting fuel leaks. The ASTM D1655–09a standard fixes the allowed additives in jet fuels.

2.1. Transesterification

Transesterification of coconut and palm kernel oils were carried out following our experimental procedure previously described in the literature [14]. Refined coconut oil has an acidity index of 0.6° (1° is equivalent to 1 wt.% of free oleic acid. In the units of acidity for biodiesel or kerosene, 1° is equivalent to 1.98 mg KOH/g, that is, to simplify the calculus, 1° = 2 mg KOH/g), and a water content of 411 ppm, and the previous esterification step was unnecessary with this feedstock. However, crude palm kernel oil has an acidity index of 2.18° and a water content of 442 ppm, and thus, the esterification step described in our previous paper was pertinent to reduce the acidity to 0.07°. The FAME profiles of the coconut and palm kernel biodiesels obtained with this procedure are reported in Table 1.

2.2. Distillation

The biokerosene fraction of the FAME's was obtained by fractional distillation of the coconut and palm kernel biodiesel fuels using a 41 cm long × 3.5 cm o.d. Vigreux column. The coconut biokerosene (CBK100) distilled between 47 and 114 °C at 2 torr (2.67 h Pa) with a yield of 81.8 wt.% based on the coconut FAME, and leaving 12.6 wt.%. yield of a bottom fraction (coconut bottom) that was also characterized. The palm kernel biokerosene (PBK100) distilled between 35 and 113 °C at 2 torr (2.67 h Pa) with a yield of 40.8% based on the palm kernel FAME, and leaving a 58.6% yield of a bottom fraction (palm kernel bottom) that was also analyzed.

Table 1 shows the FAME profile of the biokerosenes from coconut (CBK100) and palm kernel (PBK100), and also of the bottom fractions.

2.3. Blending

The blends of fossil kerosenes ($K1$ and $K2$) and 5, 10 and 20 vol.% of biokerosenes from coconut (CBK100) and palm kernel (PBK100) have been prepared by standard volumetric procedures.

Tables 2–4 list the values of the properties measured for all these blends, and also the properties of the undistilled (original) FAME's, the pure biokerosenes and the bottom fractions. In these tables, the standard procedures, the equipments used to measure each property and the experimental errors are also shown.

3. Results and discussion

3.1. Transesterification

The transesterification reaction of refined coconut oil was carried out following an experimental procedure that has been used in our research group since many years back, and whose experimental details have been reported previously [14]. The FAME

Table 1
FAME profiles of the biodiesels, biokerosenes and bottoms of coconut and palm kernel oils.[a]

FAME's (wt.%)	Boiling point (°C)	Coconut FAME	Palm kernel FAME	Coconut biokerosene	Palm kernel biokerosene	Coconut bottom	Palm kernel bottom
Methyl caprylate, C8:0	193^{760b}	8.3	Traces	17.3	3.6		
Methyl caprate, C10:0	224^{760b}	3.0	Traces	7.0	3.5	Traces	Traces
Methyl laurate, C12:0	262^{766b}	55.5	56.6	66.7	90.8	16.3	19.0
Methyl myristate, C14:0	295^{751b}	14.9	15.0	8.9	2.1	46.1	19.7
Methyl palmitate, C16:0	$415–8^{747b}$	6.4	8.5	0.1		26.0	9.9
Methyl stearate, C18:0	$442–3^{747b}$	2.5	1.7			2.2	12.8
Methyl oleate, C18:1	218.5^{20b}	7.5	17.1	Traces		8.7	32.7
Methyl linoleate, C18:2	215^{20b}	1.9	1.1			0.7	5.9

[a] All compositions were normalized to 100 wt.%
[b] Superscripts are the distillation pressures in mm Hg.

profile of this biodiesel (Table 1) shows that the main constituent is methyl laurate, followed by methyl myristate in a much lesser amount; the quantity of FAME's higher than C16 does not reach 20 wt.% and thus, this feedstock is very appropriate for the production of biokerosene.

The crude palm kernel oil was a different feedstock from the reactive point of view, since its high acidity index hindered the direct transesterification of the crude oil, making necessary a previous esterification step of the free fatty acids (FFA), and thus following exactly our previously reported procedure [14]. The FAME profile of this feedstock is very similar to that of coconut (Table 1), although in this case the amount of FAME's higher than C16 reached 28.4 wt.%, but the amounts of the main light constituents (methyl laurate and methyl myristate) were very similar to coconut and also appropriate for the production of biokerosenes.

3.2. Distillation

The coconut and palm kernel biodiesels have been distilled fractionally at vacuum, employing the usual laboratory equipment. The distillation was carried out at 2 torr (2.67 h Pa) using a rotary vacuum pump, and the boiling point ranges of the biokerosenes were converted to atmospheric equivalent temperature (AET) of distillation using the procedure recently described [15] .

The coconut biokerosene (CBK-100) distilled between 47 and 114 °C at 2 torr, which transformed to AET was between 273 and 349 °C. This boiling range is around 100 °C higher than that of fossil kerosene, which ranges between 175–185 °C and 240–275 °C. This situation also happens with biodiesel, which has much higher distillation temperature than fossil diesel. However, the ASTM D1655 standard fixes a final boiling point temperature for fossil kerosene of 300 °C (maximum) and thus, the coconut biokerosene produced here surpasses this point in around 50 °C. The distillation range of palm kernel biokerosene (PBK-100) was between 35 and 113 °C at 2 torr (2.67 h Pa), which transformed to AET was between 259 and 348 °C, again around 100 °C higher than the distillation range of fossil kerosene, and thus, the palm kernel biokerosene produced here would not meet the standard.

The boiling points of FAME's of interest have been also reported in Table 1. It can be observed that the boiling points of methyl laurate and methyl myristate are respectively 262^{766} and 295^{751} °C, and that of methyl palmitate $415–418^{747}$ °C (superscripts are the distillation pressures in mmHg). The coconut biokerosene produced here is mainly composed of the two former, with no significant amounts of the later, as can be corroborated by the ester profile. Although the AET distillation curve for biodiesel simulated from the individual FAME's boiling points presents lower values than the experimental one [15], in this case the opposite was obtained. In fact, it is surprising that although coconut biokerosene produced here has 17.0 wt.% of C8:0 FAME (b.p. 192.9^{760} °C) and 7.0 wt.% of C10:0 FAME (b.p. 224^{760} °C), the distillation stars at 273 °C, thus suspecting the formation of an azeotropic mixture of maximum boiling point. In the case of palm kernel biokerosene, the distillation starts earlier (259 °C), almost coinciding with the boiling point of methyl laurate (b.p. 262^{766} °C), but also finished at 348 °C, although no higher FAME's than C14:0 could be found in the ester profile, suspecting also the formation of azeotropic mixtures of maximum boiling point. This fact is again opposite to the finding that the AET distillation curve simulated from the FAME individual boiling points is lower than the experimental one [15].

3.3. Blending

Coconut and palm kernel biokerosene were blended at 5, 10 and 20 vol.% of biokerosene, with two types of fossil kerosene: a straight-run atmospheric distillation cut (hydrotreated) in the boiling range of kerosene, without any additives in it ($K-1$), and a commercial jet fuel Jet A1 ($K-2$). These amounts were established in order to foresee a progressive incorporation of this renewable fuel into the aviation jet fuels. Only the specifications considered essential among those required by the standard ASTM D1655-09a [16] were tested.

3.4. Thermal stability

Stability to oxidation at the operating temperatures found in jet aircrafts is an important performance requirement. For this measurement, the Rancimat method specified in the EN14214 European standard for biodiesel was used, and only the blends of coconut biokerosene and fossil kerosene $K-1$ were tested. All the blends showed an induction period higher than 8 h, and the pure coconut biokerosene showed 22.6 h. This fact agrees well with the strongly saturated character of the FAME constituents of the coconut biokerosene.

3.5. Combustion

Paraffinic hydrocarbons offer the most desirable combustion characteristics of cleanliness for jet fuels. On the contrary, aromatics, specially naphthalene and bicyclic aromatic hydrocarbons generally have the less appropriate combustion characteristics for aircraft turbine fuels, since their diffusion flames tend to produce much more soot [16].

3.5.1. Smoke point

This parameter is defined as the height in millimetres of the highest flame produced without smoking soot breakthrough when the fuel is burned in a specific test lamp. Previous studies [17,18]

Table 2
Properties of the blends of palm kernel biokerosene (PBK) and fossil kerosene without additives (*K*1).

	PBK_0/K1_100	PBK_5/K1_95	PBK_10/K1_90	PBK_20/K1_80	PBK_100/K1_0	Palm K.Bottom	Method	Equipment	Experimental error
Colour and aspect	Clear[a]	Clear[a]	Clear[a]	Clear[a]	Clear[a]	Yellow	ASTM D1500	–	±0.5 u.c.
Acidity (mg KOH/g)						0.78	EN ISO 14104	–	±0.02
Elemental composition									
C (%)	85.90	84.79	84.17	82.73	71.84	75.29	ASTM D5291	LECO CHN-600	±0.71
H (%)	13.88	13.10	13.82	13.13	12.51	11.76			±0.18
O (%)	0.22	2.11	2.01	4.14	15.65	12.95			
Density at 15 °C (kg/m^3)	793.0	800.0	804.2	812.0		882.0	ASTM D1298	Hydrometer	±0.3
FAME profile					Table 1	Table 1	EN 14103	Agilent GC 6890/MS7890	
High calorific value (MJ/kg)	47.40	45.31	45.08	44.01	37.57	37.85	ASTM D240	LECO AC-300	±0.25
Low calorific value (MJ/kg)	44.44	42.51	42.13	41.20	34.89	35.33	ASTM D240[b]	–	
CFPP[c] (°C)					−5.0	−2.0	EN ISO 116	ISL-ATPEM-11/86	±1.0
Viscosity at −20 °C (mm^2/s)	3.26	3.30	3.49	3.85	7.16	5.32[d]	EN ISO 3104	Cannon Fenske Proton 4378	±0.20%
Flash point (°C)	12.0	16.0	21.0	21.0		82.0	EN ISO 3679	Herzog 1088	±1.2
Freezing point (°C)	−42.5	−42.5	−43	−41	−15.3		ASTM D2386	M.Belenguer 528.01	±3.0
Smoke point (mm)	23.9	24.0	24.6	27.2			ASTM D1322	Analis 47551	±0.5
Copper strip corrosion, class	1a	1a	1a	1a	1a	1a	ASTM D130	M. Belenguer 534.01	

[a] Clear and colourless.
[b] ASTM D240 modified for oxygenated fuels.
[c] CFPP: Cold filter plugging point.
[d] Viscosity at 40 °C.

have shown that the sooting tendency of fuels and blends is inversely proportional to their smoke point. Consequently, a minimum value is required in jet fuel standards. All the blends of palm kernel biokerosene with Jet A1 ($K-2$) meet this specification (min. 25 mm), but in the blends with $K-1$, only the blend with 20 vol.% of PBK meets the specification. In all the blends the smoke point varies with the volume fraction of biokerosene (x) (Fig. 1) and it seems that it tends to follow a linear relationship, with increasing smoke points at higher biokerosene fractions:

$$\text{Smoke point}_{PBK/K1} = 23.42 - 17.20x \quad (1)$$

$$\text{Smoke point}_{PBK/K2} = 26.68 + 11.09x \quad (2)$$

this agrees with the explanation given above, since the saturated FAME's are very similar to the paraffinic hydrocarbons but very different to the aromatic hydrocarbons, and the increased volume fraction of the FAME increases the smoke point of the blends in a linear relationship.

3.6. Fuel metering and aircraft range

3.6.1. Density

This test is relevant for mass-volume relationships in most commercial transactions, and for the empirical assessment of the heating value, a low density meaning a low heating value per unit volume [16]. All the blends fitted within the limits fixed in the standard (775–840 kg m^{-3}), with a neat increase when the amount of biokerosene increases. These relationships seem to be linear (Fig. 2) for all the blends of fossil kerosene:

$$d_{PBK/K-1 \text{ and } K-2} = 794.25 + 94.00x \quad (3)$$

$$d_{CBK/K-1} = 802.20 + 49.14x \quad (4)$$

where x is the volume fraction of biokerosene. In all cases, it is very noticeable to observe that the $K-1$ fossil kerosene showed a different value with the pyknometer method and the hydrometer method, and that all densities converged at the same value (812 kg m^{-3}) at 20 vol.% of any biokerosene. Of course, the pure biokerosenes did not meet the density standard range. Also, the presence of additives did not affect the densities of the palm kernel biokerosene blends, since the equations were almost the same. Thus, we have combined all palm kernel biokerosene data into a single data set (Fig. 2 and Eq. (3)).

3.6.2. Low calorific value

This test provides knowledge of the energy amount obtainable from a fuel as power. The performance of any jet aircraft depends of the availability of a minimum amount of energy as heat. A reduction of this minimum amount of energy brings about an increase of fuel consumption and a reduction of the flight distance [16]. Any blend of fossil kerosene with biokerosene reached this minimum value of 42.8 MJ kg^{-1}, less the pure coconut (35.06 MJ kg^{-1}) or palm kernel (34.89 MJ kg^{-1}) biokerosenes. Only the 5 vol.% blends approached very closely to the specification, with values higher than 42.4 MJ kg^{-1}. The low calorific value (LCV) tends to decrease with the volume fraction of biokerosene x for all the blends (Fig. 3) following a second order polynomial regression:

$$LCV = 44.33 - 35.65x + 99.66x^2 \quad (5)$$

3.7. Viscosity

The viscosity of jet fuel is related to pumpability at the operating temperature (−20 °C) and also with the ability of lubricate the pump. All the blends of coconut biokerosene and fossil kerosene meet this specification (max. 8 mm^2 s^{-1}), and the viscosity of the

Table 3
Properties of the blends of coconut biokerosene (CBK) and fossil kerosene without additives (K1).

	CBK_0/ K1_100	CBK_5/ K1_95	CBK_10/ K1_90	CBK_20/ K1_80	CBK_100/ K1_0	Coconut bottom	Method	Equipment	Experimental error
Colour and aspect	Clear[a]	Clear[a]	Clear[a]	Clear[a]	Clear[a]	Yellow	ASTM D1500		±0.5 u.c.
Elemental composition									
C (%)	85.90	84.84	83.44	82.14	72.35	75.30	ASTM D5291	LECO CHNS-932	±0.71
H (%)	13.88	13.68	13.37	13.46	12.12	12.38			±0.18
O (%)	0.22	1.48	3.19	4.40	15.54	12.33			
Water content (mg/kg)	47.6	53.8	80.5	113.7	278.9	111.1	EN ISO 12937	Karl–Fischer 831KF	±6.7
Density at 23 °C (kg/m^3)					870.0		EN ISO 3675	Pyknometer	±0.3
Density at 15 °C (kg/m^3)	802.0	805.0	807.0	812.0	867.0	879.0	EN ISO 3675	Pyknometer	±0.3
Oxidative stability (h)	16.0	17.2	18.6	18.6	22.6	1.8	EN 14112	Rancimat 743 Methrom	±0,09 Mean value+0.16
Lubricity (mm), HFRR test	0.64	0.35	0.28	0.24	0.30		EN ISO 12156	PCS Instrument	±1.0 μm
FAME profile					Table 1	Table 1	EN 14103	Agilent GC 6890/ MS7890	
High calorific value (MJ/kg)	47.40	45.32	44.47	43.94	37.66	39.38	ASTM D240	Parr 1351	±0.25
Low calorific value (MJ/kg)	44.44	42.39	41.62	41.06	35.06	36.73	ASTM D240[b]	–	
CFPP[c] (°C)	−29.5	−33.0	−33.0	−31.0	−10.0	23.0	EN ISO 116	ISL FPP 5Gs	±1.0
Viscosity at −20 °C (mm^2/s)	3.26	3.64	3.81	4.18	8.26		ASTM D445	CannonFenske Afora 5354/2B	±0.20%
					2.27[d]				

[a] Clear and colourless.
[b] ASTM D240 modified for oxygenated fuels.
[c] CFPP: Cold filter plugging point.
[d] Viscosity at 40 °C.

Table 4
Properties of the blends of palm kernel biokerosene (PBK) and Jet A1 (K2).

	PBK_0/ K2_100	PBK_5/ K2_95	PBK_10/ K2_90	PBK_20/ K2_80	Method	Equipment	Experimental error
Colour and aspect	Clear[a]	Clear[a]	Clear[a]	Clear[a]	ASTM D1500		±0.5 u.c.
Elemental composition							
C (%)	84.12	84.47	84.17	82.57		LECO CHN-600	±0.71
H (%)	14.67	14.24	13.97	14.11	ASTM D5291		±0.18
O (%)	1.22	1.29	1.86	3.32			
Density at 15 °C (kg/m^3)	791.0	802.3	805.5	811.8	ASTM D1298	Hydrometer	±0.3
High calorific value (MJ/kg)	46.04	45.68	45.17	44.21	ASTM D240	LECO AC-300	±0.25
Low calorific value (MJ/kg)	42.90	42.64	42.18	41.19	ASTM D240[b]	–	
Flash point (°C)	43.0	43.5	45.0	45.5	EN ISO 3679	Herzog 1088	±1.2
Freezing point (°C)	−62.0	−60.0	−48.3	−41.5	ASTM D2386	M.Belenguer 528.01	±3.0
Smoke point (mm)	27.1	26.8	27.6	29.1	ASTM D1322	Analis 47551	±0.5
Copper strip corrosion, class	1a	1a	1a	1a	ASTM D130	M. Belenguer 534.01	
Viscosity at −20 °C (mm^2/s)	3.42	3.51	3.67	4.06	ASTM D445	Cannon Fenske Afora 5354/2B	±0.20%

[a] Clear and colourless.
[b] ASTM D240 modified for oxygenated fuels.

blends seems to be related with the volume fraction of fossil kerosene following the equation:

$$\ln \nu_{(blend)} = 1.17 \sum x_i \cdot \ln \nu_i - 0.22 \quad (6)$$

which is a general equation to calculate the kinematic viscosity of a blend, where x_i is the volume fraction of component i and ν_i is the kinematic viscosity of the ith component [19,20] (Fig. 4).

3.8. Fluidity at low temperature

3.8.1. Freezing point

This property is extremely important for jet fuels, and it should be enough low to avoid interferences with the jet fuel flow through filters at the temperature prevailing at high flying altitudes [16]. The use of pure biokerosenes was discarded because their FAME profiles anticipated high crystallization points. For this property, only the 5 and 10 vol.% blends of palm kernel biokerosene and $K-2$ meet the specification of Jet A1 (−47 °C); on the other hand, all the blends meet the specification of Jet A (−40 °C), although by a very narrow margin. The freezing point of the blends of palm kernel biokerosene and fossil kerosene without additives $K-1$ remains practically constant at around −43 °C independently from the amount of biokerosene added. However, the freezing point of the blends of this same biokerosene and fossil kerosene with additives $K-2$ increases with the volume fraction of biokerosene following a linear equation in the studied range of 0–20 vol.% of biokerosene (Fig. 5):

$$T_{PBK/K2} = -62.55 + 109.86x \quad (7)$$

where T is the freezing point temperature (°C) and x is the volume fraction of biokerosene in the blend. From this Fig. 5 it can be inferred that at low biokerosene fractions, the presence of additives in the fossil kerosene lowers the freezing point, but at higher fractions (20 vol.%), the presence of additives in the fossil kerosene does

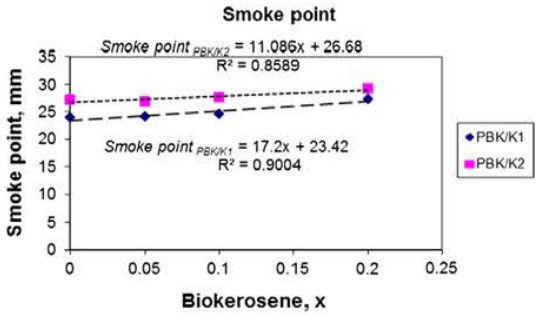

Fig. 1. Smoke point: variation with the volume fraction of biokerosene.

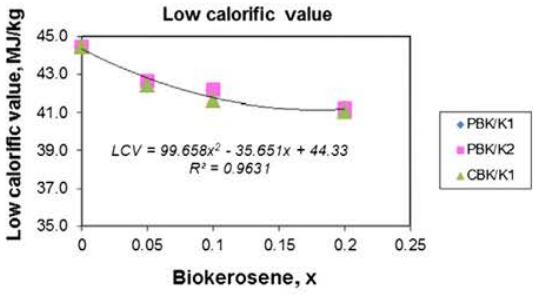

Fig. 3. Low calorific value: variation with the volume fraction of biokerosene.

not show any influence. Similar equations can be found in the literature for the cold flow behaviour of blends of biodiesel and fossil diesel, although these authors extend their study to ranges from 0 to 100% biodiesel, reaching second order polynomial regressions [21].

3.8.2. Cold filter plugging point (CFPP)

For the blends of coconut biokerosene and $K-1$ the automatic CFPP method was tested, which is more reliable than the manual freezing point method. CFPP is not a specific test for jet fuels, but it could give an indication of the cold flow properties of the blends [22].

The CFPP reveals essentially no change in the range 0–20 vol.% of coconut biokerosene (Fig. 6), although the value of pure biokerosene is higher (−10 °C). Moreover, the experimental error in the CFPP measurement is ±1 °C, and the temperature interval between filtrations in the tester is also 1.0 °C. Thus, the maximum difference observed of 3.5 °C in the measurement of the blends is of the same magnitude order than this error.

3.9. Compatibility with elastomers and metals in the fuel system and turbine: copper strip corrosion

A positive result for this test indicates that the jet fuel will not corrode copper or copper-based alloys in the different parts of the fuel system and turbine [16] All the blends of palm kernel biokerosene with $K-1$ and $K-2$ pass this test with the highest value (1a) (Tables 2 and 4).

3.10. Fuel lubricity: HFRR test

Lubricity is defined as the effectiveness of the fuel to lubricate the sliding parts in the aircraft/engine fuel systems. The failure of a jet fuel to meet this specification could cause reduction in the

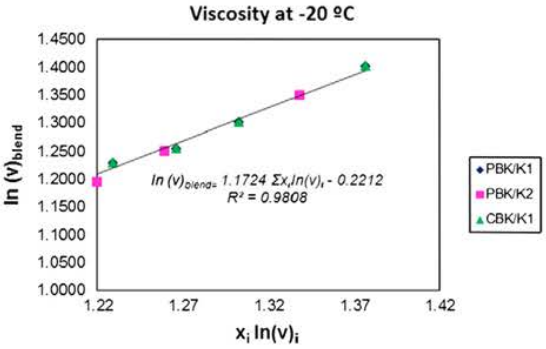

Fig. 4. Viscosity at −20 °C: regression with the volume fraction of biokerosene.

pump flow, or worse, severe mechanical failure leading to in flight engine shut down. The sensibility of the aircraft parts to jet fuel lubricity varies with their construction materials, and also the intrinsic lubricity of the jet fuel varies with its composition. The general physico-chemical properties of the jet fuel renders it a poor lubricating material, aggravated by the hydrodesulfurization process intended for reducing the sulphur content to ultra low sulphur levels, now required for all petroleum fuels [16]. Although the ASTM D1655 standard does not specify any limit for jet fuel lubricity, most modern aircraft fuel systems have been designed to operate on low lubricity fuel (wear diameter scar up to 0.85 mm). All the blends of coconut biokerosene and $K-1$ meet this limit, and these blends show also a synergistic effect, since the wear scar of the 10 and 20 vol.% blends have lower values than those of the pure components (Fig. 7). This synergistic effect has been observed in a previous work, related with blends of castor oil biodiesel and fossil diesel [23].

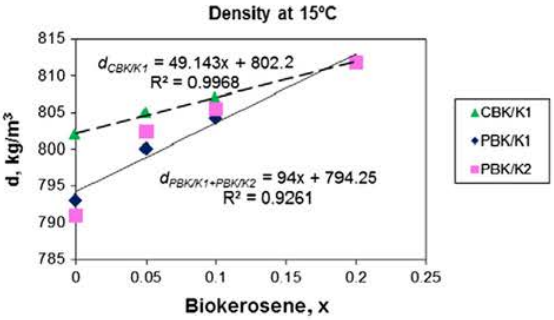

Fig. 2. Density at 15 °C: variation with the volume fraction of biokerosene.

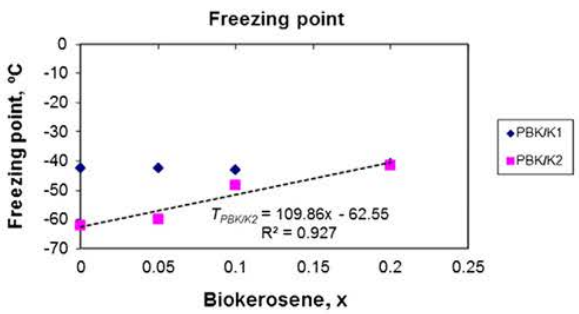

Fig. 5. Freezing point: variation with the volume fraction of biokerosene.

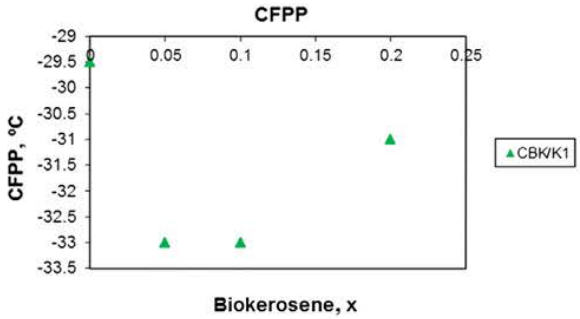

Fig. 6. Cold filter plugging point: variation with the volume fraction of biokerosene.

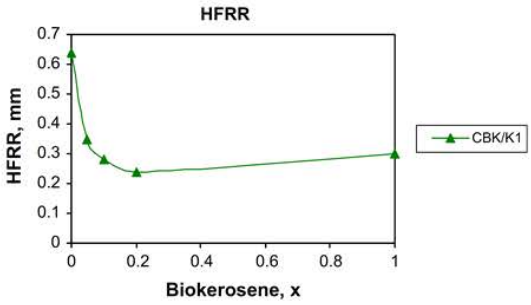

Fig. 7. Fuel lubricity: variation with the volume fraction of biokerosene.

3.11. Fuel handling: flash point

The flash point is defined as the lowest temperature at which a liquid produces enough vapours to ignite in the presence of a source of ignition, and it is one of the most significant properties of flammable liquids in industrial processes when evaluating process safety [24]. This test gives an indication of the maximum temperature for fuel shipment, storage and handling without serious fire hazard. ASTM D1655 fixes a minimum flash point for jet fuels of 38 °C, but the military aircrafts regulation establish a higher value of 60 °C for JP-5 [16]. All the blends of palm kernel biokerosene and $K-2$ meet the ASTM specification but not the JP-5 one, and any of the blends of PBK and $K-1$ meet any of both specifications. The flash point of mixtures of fossil diesel and biodiesel are strongly influenced by the flash point temperature of the fossil diesel when the biodiesel concentration was lower than 80 vol.% [24].

The flash point seems to be related with the blends composition by empirical linear regressions (Fig. 8):

$$T_{PBK/K1} = 13.60 + 44.57x \quad (8)$$

$$T_{PBK/K2} = 43.60 + 13.14x \quad (9)$$

where T is the flash point in °C and x is the volume fraction of biokerosene. These trends agree with the observation that the flash point of biodiesel is higher than that of fossil diesel.

3.12. Fuel cleanliness and contamination: water content

Water in a jet fuel onboard an aircraft represents a threat to the flight safety and can cause long term problems such as wear, corrosion and plugging of filters and other parts [16]. FAME is in general a highly hygroscopic material that when blended with fossil fuels increase the tendency of the latter to absorb water [23]. Thus, in the blends of coconut biokerosene and $K-1$ the water content

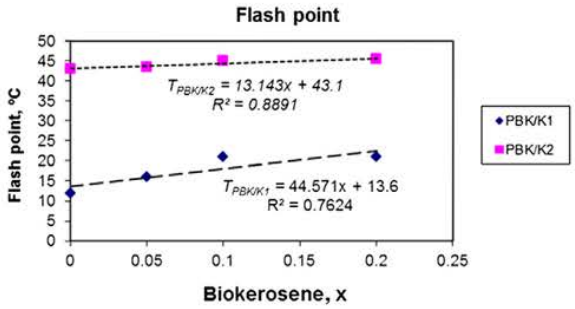

Fig. 8. Flash point: variation with the volume fraction of biokerosene.

increases with the volume fraction of biokerosene (Table 3), as it was expected, since this water comes from the "bio" fraction.

3.13. Miscellaneous

Colour could be an useful indicator of jet fuel quality, and specially, colour changes should be investigated to determine its cause. Jet fuel colour ranges from colourless (water white) to straw/pale yellow. All our blends are clear and colourless (Tables 2–4).

3.14. Bottom fractions

The bottom distillation fractions of coconut and palm kernel FAME's have been evaluated after the EN 14213 standard for heating biodiesel. Coconut bottom meets the following specifications: density, water content and low calorific value, but it did not accomplish the oxidative stability and the CFPP (Table 3).

On the other hand, palm kernel bottom only meets the density, low calorific value and CFPP specifications, but not all the rest of performed tests (Table 2). In conclusion, the possibility of use of these bottom fractions as heating fuel could only be accomplished if they are blended with other biodiesel or fossil diesel.

4. Conclusions

Coconut and palm kernel oils have been transesterified with methanol by the classical homogeneous basic catalysis method with good yields. The FAME have been subjected to fractional distillation at vacuum, and the low boiling point fractions have been blended with two types of fossil kerosene, a straight-run atmospheric distillation cut (hydrotreated, $K-1$) and commercial Jet A1 ($K-2$).

The blends of palm kernel biokerosene and Jet A1 meet some specifications selected for study of the ASTM D1655 standard: smoke point, density, flash point, viscosity at −20 °C and freezing point, and they do not comply with the low calorific value by a very narrow margin (−0.16 MJ kg^{-1} for 5 vol.% and −0.52 MJ kg^{-1} for 10 vol.% of biokerosene). On the other hand, the blends of fossil kerosene $K-1$ and palm kernel biokerosene only met the density parameter.

The blends of coconut biokerosene and $K-1$ meet the following specifications: density, viscosity at −20 °C and lubricity. It is especially noticeable that all the blends of 5 vol.% of biokerosene and fossil kerosenes $K-1$ and $K-2$ do not meet the low calorific value by a very narrow margin of less than −1.0 MJ kg^{-1}.

With these preliminary results, we can conclude that it would be feasible to blend coconut and palm kernel biokerosenes prepared in this way with commercial Jet A1 up to 10 vol.% of the former as partial substitutes of fossil jet fuels, if the IATA organization relaxes very slightly the standard of low calorific value, since this is

a property that depends of the feedstock and not of the performance of the biofuel production process.

Acknowledgements

We wish to thank to the Laboratory of Fuels and Petrochemistry of the Gómez-Pardo Foundation (Madrid), in special to Miguel Hernández, for its help in carrying out this work, and to Miguel Cobo, formerly with the company Combustibles Ecológicos Biotel SL, for the gift of palm kernel oil. We also thank Diego Koss, María Rodríguez de la Rubia and José Javier González Laguna for their technical contribution to this work.

References

[1] Biofuels International, <http://www.biofuels-news.com>. accessed November 8th, 2010.
[2] European Directive 2008/101/CE on Aviation Gas Emission.
[3] Spanish Law 13/2010. BOE 163: 59586–627, 6th July 2010.
[4] Dunn RO. Alternative jet fuels from vegetable oils. Trans ASAE 2001;44–6:1751–7.
[5] Dagaut P, Gail S. Kinetics of gas turbine liquid fuels combustion: jet A1 and biokerosene. Proc ASME Turbo Expo 2007;2:93–101.
[6] Korres DM, Karonis D, Lois E, Linck MB, Gupta AK. Aviation fuel JP-5 on a biodiesel engine. Fuel 2008;87:70–8.
[7] Wagutu AW, Chabra SC, Thoruwa CL, Thoruwa TF, Mahunnah RLA. Indigenous oil crops as a source for production of biodiesel in Kenya. Bull Chem Soc Ethiop 2009;3–3:359–70.
[8] Hileman JI, Stratton RW, Donohoo PE. Energy content and alternative jet fuel viability. J Propul Power 2010;26(6):1184–95.
[9] Gill SS, Tsolakis A, Dearn KD, Rodríguez-Fernández J. Combustion characteristics and emissions of Fischer–Tropsch diesel fuels in IC engines. Prog Energy Combust Sci 2011;37:503–23.
[10] Cottineau J. Green chemistry. bio motor fuels. The aviation industry unveils bio-kerosene. Info Chim Mag 2008;45(490):27.
[11] (a) World News: France. the BTL chain. Hydrocarbon Eng 2010;15(4):8.(b) Uhde's Prenflo process to be part of joint R&D project BioTfueL in France. Chem Eng 2010;117(4):79.
[12] Kinder JD, Rahmes T. In: Evaluation of Bio-Derived Synthetic Paraffinic Kerosene (Bio-SPK). The Boeing Company; June 2009. <www.boeing.com>.
[13] Pinzi S, Leiva D, Arzamendi G, Gandia LM, Dorado MP. Multiple response optimization of vegetable oils fatty acid composition to improve biodiesel physical properties. Bioresource Technol 2011;102:7280–8.
[14] Canoira L, Rodríguez-Gamero M, Querol E, Alcántara R, Lapuerta M, Oliva F. Biodiesel from low-grade animal fat: production process assessment and biodiesel properties characterization. Ind Eng Chem Res 2008;47:7997–8004.
[15] Lapuerta M, Canoira L, Raez J. Improved method for determining the atmospheric distillation curve of biodiesel fuels from reduced pressure. Ind Eng Chem Res 2011;50:7041–8.
[16] Standard specification for aviation turbine fuels. Standard ASTM D1655-09a. West Conshohocken, Pennsylvania: ASTM International; 2009.
[17] Clarke AE, Hunter TG, Garner FH. The tendency to smoke of organic substances on burning. J I Petrol 1946;32:627–42.
[18] Gill RJ, Olson DB. Estimation of soot thresholds for fuel mixtures. Combust Sci Technol 1984;5–6:307–15.
[19] Krisnagkura K, Yimsuwan T, Pairintra R. An empirical approach in predicting biodiesel viscosity at various temperatures. Fuel 2006;85:107–13.
[20] Freitas SVD, Pratas MJ, Ceriani R, Lima AS, Coutinho JAP. Evaluation of predictive models for the viscosity of biodiesel. Energy Fuel 2011;25:352–8.
[21] Tang H, Salley S, Ng KS. Fuel properties and precipitate formation at low temperatures in soy-, cottonseed- and poultry-fat based biodiesel blends. Fuel 2008;87:3006–17.
[22] Dunn RO. Effect of minor constituents on cold flow properties and performance of biodiesel. Prog Energy Combust Sci 2009;35:481–9.
[23] Canoira L, García- Galeán J, Alcántara R, Lapuerta M, García-Contreras, Fatty R. Acids methyl esters (FAME) from castor oil: production process assessment and synergistic effects in its properties. Renew Energy 2010;35:208–17.
[24] Lazzús J. Prediction of flash point temperature of organic compounds using a hybrid method of group contribution + neural network + particle swarm optimization. Chinese J Chem Eng 2010;18:817–23.

energy&fuels

Article

pubs.acs.org/EF

Biokerosene from Babassu and Camelina Oils: Production and Properties of Their Blends with Fossil Kerosene

Alberto Llamas,[†] Ana-María Al-Lal,[†] Miguel Hernandez,[‡] Magín Lapuerta,[§] and Laureano Canoira*[,†]

[†]Department of Chemical Engineering and Fuels, Escuela Técnica Superior de Ingenieros de Minas, Universidad Politécnica de Madrid, Ríos Rosas 21, 28003 Madrid, Spain

[‡]Laboratory of Fuels and Petrochemistry, Tecnogetafe Scientific Park, Universidad Politécnica de Madrid, Erik Kandel s/n, 28906 Getafe, Spain

[§]Grupo de Combustibles y Motores, Escuela Técnica Superior de Ingenieros Industriales, Universidad de Castilla La Mancha, Avda. Camilo José Cela s/n, 13071 Ciudad Real, Spain

ABSTRACT: Babassu and camelina oils have been transesterified with methanol by the classical homogeneous basic catalysis method with good yields. The babassu fatty acid methyl ester (FAME) has been subjected to fractional distillation at vacuum, and the low boiling point fraction has been blended with two types of fossil kerosene, a straight-run atmospheric distillation cut (hydrotreated) and a commercial Jet-A1. The camelina FAME has been blended with the fossil kerosene without previous distillation. The blends of babassu biokerosene and Jet-A1 have met some of the specifications selected for study of the ASTM D1655 standard: smoke point, density, flash point, cloud point, kinematic viscosity, oxidative stability and lower heating value. On the other hand, the blends of babassu biokerosene and atmospheric distillation cut only have met the density parameter and the oxidative stability. The blends of camelina FAME and atmospheric distillation cut have met the following specifications: density, kinematic viscosity at −20 °C, and lower heating value. With these preliminary results, it can be concluded that it would be feasible to blend babassu and camelina biokerosenes prepared in this way with commercial Jet-A1 up to 10 vol % of the former, if these blends prove to accomplish all the ASTM D1655-09 standards.

1. INTRODUCTION

The world economy is strongly dependent on oil prices, and the main oil reserves are located in social and politically unstable countries, which causes great fluctuations in the crude oil and petroleum products prices. From January 2003 to July 2008, the jet fuel price increased a 462%, reaching $ 3.89/gallon. Due to the world economic crisis, the jet fuel price dropped to $1.26/gallon in February 2009, but since then, this price has been steadily increasing, and it was $ 3.09/gallon in January 2012. These fluctuations and the very foreseeable future ones have led to many countries try to develop a diversified fuel market less dependent on crude oil imports.[1]

On the other hand, on December 20, 2006, the European Commission approved a law proposal to include the civil aviation sector in the European market of carbon dioxide emission rights (European Union Emissions Trading System, EUETS). On July 8, 2009, the European Parliament and Council agreed that all flights leaving or landing in the EU airports starting from January first 2012 should be included in the EUETS. On November 19, 2008, the EU Directive 2008/101/CE[2] included the civil aviation activities in the EUETS, and this directive was transposed by the Spanish law 13/2010 of July 5, 2010.[3] Thus, in 2012, the aviation sector should reduce their emissions by 3% of the mean values registered in the period 2004−2006, and for 2013, these emission reductions should reach 5% of the mean values for that same period. Trying to face this situation, the aviation companies are planning seriously the use of alternative jet fuels to reduce their greenhouse gas emissions and to lower their costs. However, some U.S. airlines have issued a lawsuit before the European Court of Justice based in that this EU action violates a long-standing worldwide aviation treaty, the Chicago convention of 1944, and also, the Chinese and Indian aviation companies have rejected to pay any EU carbon dioxide tax.[4] Moreover, the U.S.A. Departments of Agriculture and Energy and the Navy will invest a total of up to $150 million over three years to spur production of aviation and marine biofuels for commercial and military applications.[5] However, the jet fuels should fulfill a set of extraordinarily sensitive properties to guarantee the safety of planes and passengers during all the flights.

The literature on the production and use of biofuels for the aviation sector is still scarce and in some cases contradictory. Dunn[6] studied the properties of a fuel obtained blending 10−30 vol % soybean fatty acid methyl ester (FAME) with JP-8 and JP-8 + 100. Dagault and Gail[7] examined the oxidation behavior of a blend of 20 vol % rapeseed FAME with Jet-A1. Korres et al.[8] compared the behavior of the jet fuel JP-5 against fossil diesel and animal fat biodiesel in a diesel engine. Wagutu et al.[9] prepared six biofuels from jatropha, croton, calodendrum, coconut, sunflower, and soybean, and they concluded, among other findings, that the coconut FAME is the biofuel that approaches most closely to the fossil jet fuel properties.

Some other authors have approached the jet fuel alternatives from biological sources from a totally different perspective, that is, the use of the Fischer−Tropsch (FT) synthesis and the synthetic paraffinic kerosenes of biological origin (Bio-SPK).

Received: May 28, 2012
Revised: August 9, 2012
Published: August 21, 2012

dx.doi.org/10.1021/ef300927q | Energy Fuels 2012, 26, 5968−5976

Table 1. FAME Profiles of the Biokerosenes of Babassu and Camelina

FAME, wt %	boiling point[a], °C	camelina FAME (CAM100)	babassu FAME	babassu biokerosene (BBK100)	babassu bottom
methyl caprylate, C8:0	193		3.91	13.27	
methyl caprate, C10:0	224		3.30	11.27	
methyl laurate, C12:0	273	0.84	20.85	69.26	21.91
methyl myristate, C14:0	296	0.41	31.33	5.58	34.08
methyl palmitate, C16:0	338	5.83	18.00	0.61	19.84
methyl stearate, C18:0	352	2.97	5.51		6.18
methyl oleate, C18:1	349	15.83	12.54		13.25
methyl linoleate, C18:2	$192^{5.3}$	18.85	0.21		0.22
metil linolenate, C18:3	$182^{4.0}$	33.99	3.45		3.58
methylarachidate, C20:0	215.5[13]	1.54	0.19		0.19
methylcis-11-eicosenoate C20:1	-	16.03	0.72		0.75
methyl behenate, C22:0	240[13]	2.16			
metil eructate, C22:1	$174^{0.266}$	1.44			
iodine value, IV		148.8	20.7	0	21.7
mean formula		$C_{19.23}H_{34.97}O_2$	$C_{15.07}H_{29.75}O_2$	$C_{12.18}H_{24.36}O_2$	$C_{15.69}H_{30.94}O_2$
molecular weight, g mol^{-1}		298.153	242.980	202.860	251.579
stoichiometric air/fuel ratio		12.508	12.240	11.775	12.325
C[b], wt %		77.45	74.50	72.13	74.89
H[b], wt %		11.82	12.34	12.11	12.40
O[b], wt %		10.73	13.17	15.77	12.72

[a]Superscripts are the distillation pressures in hPa from references 21, 35, 36, and 37. [b]Calculated from the mean formula.

On the former issue, Hileman et al.[10] analyzed the chemical composition and the energy content of different jet fuels, showing that the biokerosene obtained by FT synthesis or hydrotreating of renewable oils can reduce the energy expenditure of planes by 0.3%. Cottineau[11] claimed that UOP has developed a biokerosene from jatropha that surpasses the properties of actual jet fuels. World News[12] referred to the construction of two pilot plants in France based in the PRENFLO process from Udhe, which were due to come on stream in 2012 to produce biodiesel and biokerosene from syngas, obtained from biomass by FT technology.[13]

On the Bio-SPK issue, Kinder and Rhams[14] reported the hydrotreating and isomerization of vegetable oils to produce a kerosene range of hydrocarbons, which had a very similar chemical composition to the fossil jet fuel. In this technology, the oil, once refined, was hydrogenated to remove the oxygen atoms and to saturate the olefinic double bonds, which increased the heating value of the fuel and its thermal and oxidative stability; the ulterior isomerization and cracking of the diesel range paraffins yielded a typical kerosene fraction called Bio-SPK. Some blends of 50 vol % Bio-SPK with Jet-A1 have been tested in air flights of three different companies.

The American Society for Testing Materials has published recently the approved methods for the production of alternative jet fuels that are basically the Fischer−Tropsch hydroprocessed synthesized paraffinic kerosene (FT-SPK) and the hydroprocessed esters and fatty acids (HEFA). FAME is not approved as an additive for jet fuel. The maximum allowable level is 5 mg/kg, which is accepted by approval authorities as the functional definition of "nil addition".[15] Moreover, a study has found that particulate matter emissions from a plane's engine can fall by almost 40% when researchers blend jet fuel with alternative fuels; plane's emissions at large airports are important sources of local air pollution including fine particulate matter, which can increase the people's risk of heart disease and asthma.[16]

In this paper, two different approaches have been followed. (a) A FAME from an oil rich in short chain fatty acids, such as babassu (*Orbygnya martiana*), a palm popular in Brazil, was synthesized,[17] and then, the fraction that approaches the distillation range of fossil kerosene, that is, from 175−185 °C to 240−275 °C at atmospheric pressure, was separated by vacuum distillation. Since this pure biokerosene did not meet the different aviation jet fuel standards, blends containing 5, 10, and 20 vol % biokerosene with fossil kerosene, with and without additives, were tested, together with pure biokerosene. The bottom fraction of the FAME distillation of babassu has also been tested in order to see if it accomplishes alone the EN 14213 standard for heating biodiesel or if it needs to be blended with other FAME to find this application. Another use for this bottom fraction could be as a marine transport biofuel. (b) A FAME from camelina oil (*Camelina sativa*), commonly known as gold of pleasure oil, very rich in unsaturated methyl esters (84.7 wt %), was blended without previous distillation at 5, 10, and 20 vol % with fossil kerosene without additives. The excellent cold flow behavior of these unsaturated methyl esters suggested direct blending without previous distillation.

2. EXPERIMENTAL SECTION

2.1. Materials. Camelina seeds were supplied by the Laboratory of Fuels and Petrochemistry of the Gomez-Pardo Foundation, and crude babassu oil was supplied by Combustibles Ecologicos Biotel SL. Kerosene of fossil origin was used to prepare the blends with biokerosene: K1 was a straight-run atmospheric distillation cut (hydrotreated) kerosene without any additives and K2 was commercial Jet-A1 kerosene, and it contains additives. Both samples of fossil kerosene were obtained from the Spanish Company Logistica de Hidrocarburos (CLH).

All reagents were of commercial grade and were used without any further purification. Dichloromethane was of technical grade, and it was purchased from Panreac. Methanol was of synthesis grade, and it was purchased from Scharlau. p-Toluensulphonic acid, used as catalyst for the esterification reaction of the crude oils, was of synthesis grade, and it was purchased from Scharlau. The molecular sieve was of technical purity, and it was purchased from Scharlau. The catalytic solution of sodium methoxide 25 wt % in methanol was purchased from Acros Organics. Magnesium silicate Magnesol D-60 was kindly supplied by The Dallas Group of America.

Table 2. Properties of the Blends of Babassu Biokerosene and Fossil Kerosene Cut (K1)

		BBK_0/K1_100	BBK_5/K1_95	BBK_10/K1_90	BBK_20/K1_80	BBK_100/K1_0	babasu bottom	method	equipment	exptl error
color and aspect		clear[a]	clear[a]	clear[a]	clear[a]	clear[a]	yellow	ASTM D1500	visual	±0.50 u.c.
acidity (mg KOH/g)			0.022	0.033	0.034	0.033	0.310	EN ISO 14104	manual	±0.02
water content									Karl Fischer	
(mg/kg_		595.2	202.0	197.2	95.35	343.5	480.3	ASTM D1774	Methrom 831KF	
(vol %)		0.047	0.016	0.016	0.007	0.030	0.042	ASTM D2907		<0.005
elemental composition, wt %	C	85.90	84.98	84.79	82.97	73.38	74.99			±0.71
	H	13.88	13.16	13.11	12.95	11.55	11.70	ASTM D5291	LECO	±0.18
	N	0.02	0.02	0.02	0.02	0.11	0.02		CHNS-932	±0.11
	S	0.17	0.16	0.13	0.13	0.10	0.02			±0.01 + 0.06 · mean
	O		1.68	1.95	3.93	14.86	13.27			
density at 15 °C (kg/m^3)		793.0	805.9	809.2	816.6	874.5	874.8	ASTM D1298	Digital DM48	±0.3
viscosity at 40 °C (mm^2/s)			1.15	1.46	1.24	2.13	3.65	EN ISO 3104	Cannon Fenske Proton 4378	±0.0013 · mean (0.20%)
FAME profile						Table 1	Table 1	EN 14103	Agilent GC 6890/MS7890	
higher heating value (MJ/kg)		47.70	45.63	45.16	44.66	37.41	39.29	ASTM D240	LECO AC300	±0.25
lower heating value (MJ/kg)		44.44	42.82	42.36	41.89	34.93	36.78	ASTM D240[b]		
flash point (°C)		12.0	27.5	30.0	27.1	50.0	45,0	EN ISO 3679	Petrotest PMA4	±1.2
cloud point (°C)		−42.5[c]	−28	−28	−31	−7	7	ASTM D2500	ATPM	<3.0
pour point (°C)			−38	−33	−30	−23	5	ASTM D2500	ATPM	<3.0
copper strip corrosion, class		1a	1a	1b	1b	1a	1a	ASTM D130	M. Belenguer 534.01	
CFPP[d], °C							2	EN ISO 116	ISL FPP 5Gs	±1.0
oxidative stability (h)			>8	>8	>8	>8		EN 14112	Rancimat Methrom 743	0.09 · mean + 0.16

[a]Clear and colorless. [b]ASTM D240 modified for oxygenated fuels. [c]Freezing point. [d]CFPP: Cold filter plugging point.

dx.doi.org/10.1021/ef300927q | *Energy Fuels* 2012, 26, 5968−5976

Table 3. Properties of the Blends of Camelina FAME and Fossil Kerosene Cut (K1)

		CAM_0/ K1_100	CAM_5/ K1_95	CAM_10/ K1_90	CAM_20/ K1_80	CAM_100/ K1_0	method	equipment	exptl error
color and aspect		clear[a]	clear[a]	clear[a]	clear[a]	clear[a]	ASTM D1500	visual	±0.50 u.c.
elemental composition, wt %	C	85.90	85.29	84.23	83.86	77.09			±0.71
	H	13.88	12.99	12.61	12.45	11.09			±0.18
	N	0.02	0.02	0.02	0.02	0.02	ASTM D5291	LECO	±0.11
	S	0.17	0.05	0.03	0.03	0.06		CHNS-932	±0.01 + 0.06 · mean
	O		1.65	3.11	3.64	11.74			
density at 15 °C (kg/m^3)		793.0	806.7	810.8	819.8	889.3	EN ISO 12185	Digital DM48	±0.3
viscosity at 40 °C (mm^2/s)			1.2591	1.3075	1.4539	4.3395	EN ISO 3104	Cannon Fenske	±0.0013 · mean (0.20%)
viscosity at 100 °C (mm^2/s)			0.6799	0.7053	0.7663	1.7077	ASTM D445	Cannon Fenske	±0.0013 · mean (0.20%)
viscosity at −20 °C (mm^2/s)			3.10	3.20	3.80	6.96	ASTM D341	estimated	±0.0013 · mean (0.20%)
FAME profile						Table 1	EN 14103	Agilent GC 6890/MS7890	
higher heating value (MJ/kg)		47.70	45.3	45.0	44.8	40.0	ASTM D240	LECO AC-300	±0.25
lower heating value (MJ/kg)		44.44	42.52	42.30	42.14	37.71	ASTM D240[b]		
CFPP[c] (°C)			−31	−29	−26	−5	EN ISO 116	ISL FPP 5Gs	±1.0
cloud point (°C)		−42.5[d]	−26	−26	−22	1	ASTM D2500	ATPEM	<3.0
pour point (°C)			−40	−32	−31	−5	ASTM D2500	ATPEM	<3.0
oxidative stability (h)			>8	>8	>8	1.4	EN 14112	Rancimat 743 Methrom	0.09 · mean + 0.16

[a]Clear and colorless. [b]ASTM D240 modified for oxygenated fuels. [c]CFPP: Cold filter plugging point. [d]Freezing point.

2.2. Extraction of Camelina Seeds. Camelina seeds are very small dark-yellow grains of elliptical shape (2.09 mm × 1.14 mm). Whole seeds of camelina were dried overnight at 105 °C in an oven, and the seeds were extracted with dichloromethane in a 1 L Soxhlet extractor for 24 h. After elimination of the solvent, the oil extracted amounts only to 6% wt of the dried seeds, and since higher oil yield have been reported for this seed in the literature,[18] the seeds were gently ground in an iron mortar, repeating the extraction procedure afterward. The amount of extracted oil from the grounded seeds increased to 31.4 wt %, closer to the reported values.

2.3. Esterification and Transesterification. Transesterification of babassu and camelina oils was carried out following the experimental procedure previously described in the literature.[19] Crude babassu and camelina oils needed a previous step of esterification, since their acidity numbers were 7.96 and 3.96 mg KOH/g oil, respectively; after the esterification, their acidity numbers decreased to 0.24 and 1.58 mg KOH/g oil, respectively. After the esterification step, babassu oil was dried over 4 Å molecular sieve (8 wt % of sieve based on the weight of oil) due to its high water content (984.1 ppm), which would produce the formation of soaps, and it was filtered prior to transesterification. Camelina oil was essentially dry due to the previous drying of the seeds.

The FAME profiles of the babassu and camelina biodiesels obtained with this procedure are reported in Table 1. The FAME profile of the babassu biokerosene shows that the main constituent is methyl laurate (69.3 wt %), followed by methyl caprylate and methyl caprate in much smaller amounts; the quantity of FAMEs higher than C16 does not reach 7 wt %, and thus, this feedstock is very appropriate for use as biokerosene.

The camelina oil was a different feedstock. The FAME profile of this feedstock is very unsaturated, since in this case the amount of unsaturated FAMEs reached 84.7 wt %, with 34 wt % of methyl linolenate (C18:3). The very good cold behavior of unsaturated FAMEs[20] makes this biodiesel (without distillation) appropriate for the production of biokerosenes.

2.4. Distillation. The biokerosene fraction of the babassu biodiesel fuel was obtained by fractional distillation using a 41 cm long × 3.5 cm outer diameter Vigreux column. The distillation was carried out at 2 Torr (2.67 hPa) using a rotary vacuum pump, and the boiling point range of the biokerosene was converted to atmospheric equivalent temperature (AET) of distillation using the procedure recently described.[21]

The babassu biokerosene (BBK100) distilled between 47 and 124 °C at 2 Torr, which transformed to AET was between 273 and 359 °C, gave a yield of 73.3 wt % with respect to the babassu biodiesel fuel and 19.4 wt % yield of a bottom fraction (babassu bottom), which was also characterized. This boiling range is around 100 °C higher than that of fossil kerosene, which ranges between 175−185 °C and 240−275 °C. This situation also happens with biodiesel, which has much higher distillation temperature than fossil diesel. However, the ASTM D1655 standard fixes a final boiling point temperature for fossil kerosene of 300 °C (maximum), and thus, the babassu biokerosene produced here surpasses this point in around 60 °C. The camelina biokerosene (CAM100) was used without previous distillation.

Table 1 shows the FAME profile of the biokerosenes from babassu (BBK100) and camelina (CAM100), and also of the bottom fraction of babassu. The boiling points of the FAMEs of interest have been also reported in Table 1. It can be observed that the standard boiling points of methyl caprylate and methyl caprate are respectively 193 and 224 °C, and those of methyl laurate, methyl myristate and methyl palmitate are respectively 273, 296, and 338 °C. The babassu biokerosene produced here is mainly composed of the four former, with no significant amounts of the latter (0.61 wt %), as can be corroborated by the ester profile. Although the AET distillation curve for biodiesel simulated from the individual FAME's boiling points presents lower values than the experimental one,[21] in this case, the opposite was obtained. In fact, it is surprising that although babassu biokerosene produced here has 13.3 wt % of C8:0 FAME (bp 193 °C) and 11.3 wt % of C10:0 FAME (bp 224 °C), the distillation starts at 273 °C, thus suspecting the formation of an azeotropic mixture of maximum boiling point

2.5. Blending. Babassu and camelina biokerosenes were blended at 5, 10, and 20 vol % of biokerosene, with two types of fossil kerosene: a straight-run atmospheric distillation cut (hydrotreated) in the boiling range of kerosene, without any additives in it (K1), and commercial jet fuel Jet-A1 (K2). The blends of fossil kerosenes (K1 and K2) and 5, 10, and 20 vol % of biokerosenes from babassu (BBK100) and camelina (CAM100) were prepared by standard volumetric

dx.doi.org/10.1021/ef300927q | Energy Fuels 2012, 26, 5968−5976

Table 4. Properties of the Blends of Babasu Biokerosene and Jet-A1 (K2)

		BBK_0/ K2_100	BBK_5/ K2_95	BBK_10/ K2_90	BBK_20/ K2_80	BBK_100/ K2_0	method	equipment	exptl error
color and aspect		clear[a]	clear[a]	clear[a]	clear[a]	clear[a]	ASTM D1500	visual	±0.50 u.c.
acidity (mg KOH/g)		0.0112	0.0112	0.0112	0.0336	0.0330	EN ISO 14104	manual	±0.02
water content,								Karl Fischer	
mg/kg			138.6	113.7	346.4	595.3	ASTM D1774	Methrom 831KF	
(vol %)			0.011	0.009	0.028	0.052	ASTM D2709		<0.005
elemental composition, wt %	C	84.12	85.81	84.13	78.35	73.38		LECO	±0.71
	H	14.67	13.25	13.08	12.64	11.55	ASTM D5291	CHNS-932	±0.18
	N		0.11	0.13	0.15	0.11			±0.11
	S		0.10	0.10	0.20	0.10			±0.01 + 0.06·mean
	O		0.73	2.56	8.66	14.86			
density at 15 °C (kg/m^3)		791.0	804.0	807.7	814.9	874.5	ASTM D1298	Digital DM48	±0.3
density at 23 °C (kg/m^3)			804.7	807.0	814.7	874.2	ASTM D1298	Digital DM48	±0.3
viscosity at 40 °C (mm^2/s)			1.27	1.31	1.32	2.13	ASTM D445	Cannon Fenske	±0.0013 · mean (0.20%)
higher heating value (MJ/kg)		46.04	45.95	45.54	44.75	37.41	ASTM D240	LECO AC-300	±0.25
lower heating value (MJ/kg)		42.90	43.12	42.74	42.04	34.93	ASTM D240[b]		
flash point (°C)		43.0	43	44	46	50	EN ISO 3679	Petrotest PMA4	±1.2
cloud point (°C)		−62.0[c]	−39	−38	−33	−7	ASTM D2500	ATPM	<3.0
pour point (°C)			−43	−42	−32	−23	ASTM D2500	ATPM	<3.0
smoke point (mm)		27.1	26.2	25.9	25.1	22.8	ASTM D1322	Analis 47551	±0.5
copper strip corrosion, class		1a	1a	1a	1a	1a	ASTM D130	M. Belenguer 534.01	
oxidative stability (h)			>8	>8	>8	>8	EN 14112	Rancimat Methrom 743	0.09 · mean + 0.16

[a]Clear and colorless. [b]ASTM D240 modified for oxygenated fuels. [c]Freezing point.

procedures. These amounts were established in order to foresee a progressive incorporation of this renewable fuel into the aviation jet fuels.

Jet fuel additives are used to prevent the formation of oxidation deposits in aircraft engines and fuel systems, to inhibit the corrosion of steel, to improve the fuel lubricity and oxidation stability, to increase the electrical conductivity of the fuel, to avoid microbiological contamination, to prevent the ice formation in fuel systems, and to assist in detecting fuel leaks. The ASTM D1655-09a standard fixes the allowed additives in jet fuels.[22]

Only the specifications considered essential among those required by the standard ASTM D1655-09a[22] were tested.

Tables 2, 3, and 4 list the values of the properties measured for all these blends, and also the properties of the undistilled FAMEs, the pure biokerosenes, and the bottom fraction of babassu. In these tables, the standard procedures, the equipment used to measure each property, and the experimental errors are also shown.

3. RESULTS AND DISCUSSION

3.1. Oxidation Stability. Stability to oxidation at the operating temperatures found in jet aircrafts is an important performance requirement. For this measurement, the Rancimat method specified in the EN14214 European standard for biodiesel was used. All the blends of babassu biokerosene and fossil kerosene K1 and K2 showed an induction period higher than 8 h, and also the pure babassu biokerosene. This fact agrees well with the strongly saturated character of the FAME constituents of the babassu biokerosene.

On the other hand, camelina FAME showed a very low induction period of 1.4 h due to its very unsaturated character, but the blends of camelina with fossil kerosene K1 showed induction periods higher than 8 h.

In summary, the addition of up to 20 vol % biokerosene to fossil kerosenes would not imply significant oxidative degradation during usual storage periods,[23] and thus, no specific storage limitation would be required.

3.2. Sooting Tendency. Paraffinic hydrocarbons offer the most desirable combustion characteristics of cleanliness for jet fuels. On the contrary, aromatics, although contributing to avoid leakages from seal swelling, generally have the less appropriate combustion characteristics for aircraft turbine fuels, since their diffusion flames tend to produce much more soot.[22]

The smoke point parameter is defined as the height in millimeters of the highest flame produced without smoking soot breakthrough when the fuel is burned in a specific test lamp. Previous studies[24,25] have shown that the sooting tendency of fuels and blends is inversely proportional to their smoke point. Consequently, a minimum value is required in jet fuel standards (min. 25 mm). All the blends of babassu biokerosene with Jet-A1 (K2) meet this specification.

3.3. Fuel Metering and Aircraft Range. *3.3.1. Density.* This test is relevant for mass−volume relationships in most commercial transactions, and for the empirical assessment of the heating value, a low density meaning a low heating value per unit volume.[22] All the blends fitted within the limits fixed in the standard (775−840 kg m^{-3}) (Figure 1a and b), except of course the pure babassu and camelina (BBK100 and CAM100), with a neat increase when the amount of biokerosene increases. These relationships seem to be linear for all the blends:

$$d_{BBK/K1} = 799.33 + 75.95x \quad (1)$$

$$d_{BBK/K2} = 797.39 + 77.88x \quad (2)$$

$$d_{CAM/K1} = 796.68 + 124.51x \quad (3)$$

where x is the volume fraction of biokerosene. Of course, the pure biokerosenes did not meet the density standard range.

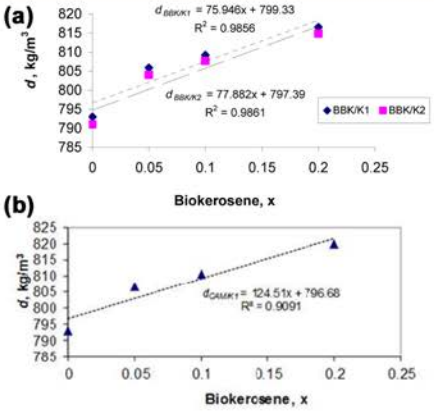

Figure 1. Density at 15 °C of (a) babassu blends and (b) camelina blends.

3.3.2. Lower Heating Value. This test provides knowledge of the energy amount obtainable from a fuel as power. The performance of any jet aircraft depends on the availability of a minimum amount of energy as heat. A reduction of this minimum amount of energy brings about an increase of fuel consumption and a reduction of the flight distance.[22] Only the blends of babassu biokerosene at 5 vol % with fossil kerosenes K1 and K2 reached the minimum value of 42.8 MJ kg^{-1}, and the 10% vol blend of babassu with Jet-A1 approached very closely to the specification with a value 42.74 MJ kg^{-1}, but not the pure babassu (34.93 MJ kg^{-1}) or camelina (37.71 MJ kg^{-1}) biokerosenes, nor any camelina blend (Tables 2, 3, and 4). The lower heating value shows a linear relationship with the mass fraction of biokerosene, thus assuring the absence of enthalpy excess in the blending.

3.4. Kinematic Viscosity. The viscosity of jet fuel is related to pumpability at the operating temperature (often below −20 °C) and also with the ability of lubricate the pump. The kinematic viscosity of the blends of babassu biokerosene and fossil kerosene cut K1 could not be regressed with the compositions since they remained almost constant at 1.2 mm^2 /s. The kinematic viscosity at 40 °C of the blends of babassu biokerosene and Jet-A1 K2 shows a linear relationship, see Figure 2,

$$\nu_{BBK/K2} = 1.265 + 0.30x \quad (4)$$

where x is the volume fraction of biokerosene.

The kinematic viscosity of the blends of camelina FAME and fossil kerosene cut K1 has been measured at 40 and 100 °C (Figure 2b), and extrapolated to −20 °C according to literature,[26] and the latter follows a linear relationship with the volume fraction of camelina FAME x:

$$\nu_{CAM/K1} = 2.498 + 6.87x \quad (5)$$

All the blends prepared meet the ASTM D1655 specification (<8 mm^2 s^{-1}). Also, the viscosity at −20 °C of the blends of camelina FAME and fossil kerosene cut K1 seems to follow the equation:

$$\ln \nu_{blends} = \sum x_i \ln \nu_i \quad (6)$$

which is a general equation to evaluate the kinematic viscosity of a blend, where x_i is the volume fraction of the ith component

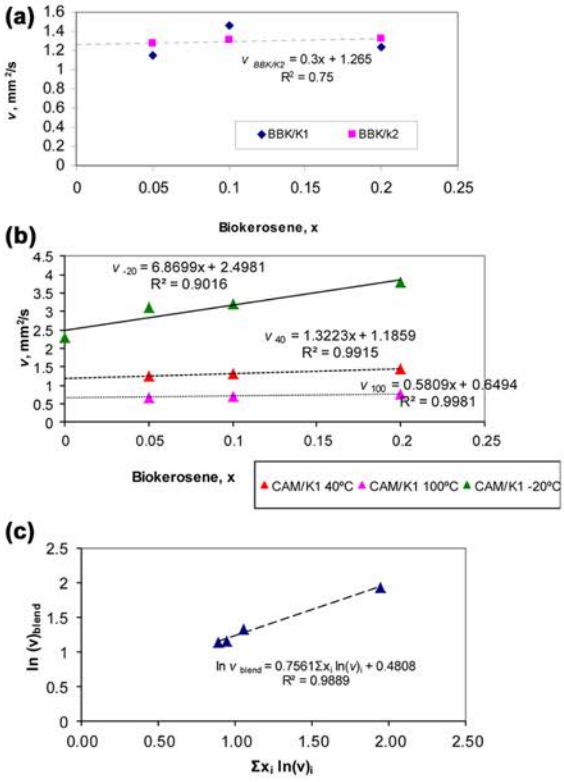

Figure 2. Kinematic viscosity of (a) the babassu blends at 40 °C and (b) camelina blends at 40, 100, and −20 °C. (c) Regression of the kinematic viscosity at −20 °C of the camelina blends.

and ν_i is the kinematic viscosity of the ith component (Figure 2c).[27,28] This equation would correspond to the Grunberg−Nissan equation with a zero value of the interaction term.[29]

3.5. Fluidity at Low Temperature. *3.5.1. Cloud Point and Pour Point.* These properties are extremely important for jet fuels, and they should be enough low to avoid interference with the jet fuel flow through filters at the temperature prevailing at high flying altitudes.[22] The test used to evaluate the cold flow behavior of kerosene is the manual freezing point method (ASTM D2386), which measures the temperature of apparition of the first crystals, with values of −40 °C for Jet-A and −47 °C for Jet-A1. However, in our own experience, this test has a low reproducibility and the results depend on a great extent of the ability of the operator. Thus, we have checked the cold flow behavior of the blends of babassu and camelina with fossil kerosene by the cloud point and the pour point test methods.

The cloud point test measures the temperature at which the solution becomes opaque to light by formation of the first crystals. If it is assumed that this property is similar to the freezing point, only the blends with 5 and 10 vol % of babassu biokerosene with Jet-A1 would meet the specification of Jet-A fuel (−40 °C) but not that of Jet-A1 (−47 °C). It is very interesting to observe (Figure 3) that the presence of additives in Jet-A1 K2 lowers the cloud point at 5 and 10 vol % of babassu biokerosene, but at 20 vol % of the latter, the influence of these additives disappears and both blends with K1 and K2 have the same value (−32 ± 1 °C). This same effect could be

dx.doi.org/10.1021/ef300927q | Energy Fuels 2012, 26, 5968−5976

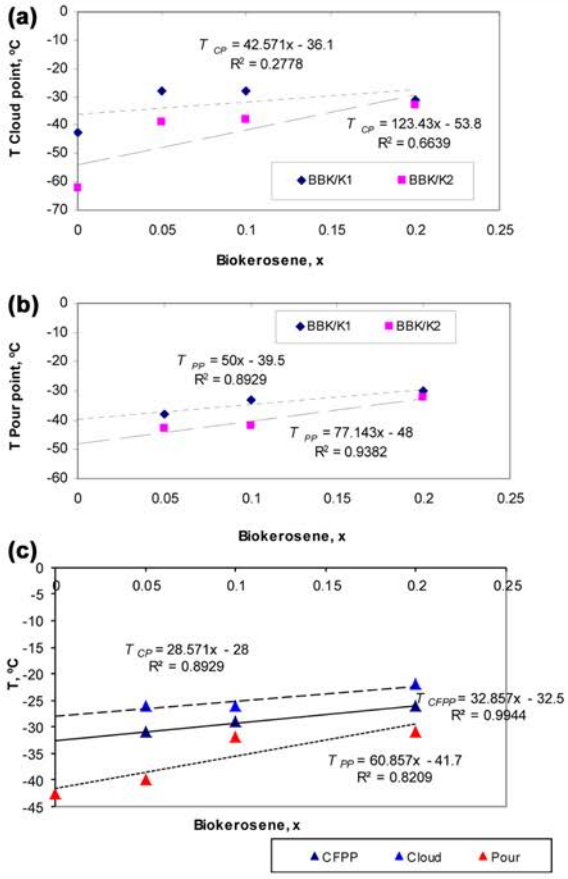

Figure 3. (a) Cloud point of the babassu blends. (b) Pour point of the babassu blends. (c) Cold flow behavior of the camelina blends.

observed with the pour point (−32 ± 1 °C). For all the blends, the cloud point increases following a linear relationship with the volume fraction of biokerosene x, either derived from babassu or from camelina (see Figure 3a and c):

$$T_{BBK/K1} = -36.1 + 42.57x \quad (7)$$

$$T_{BBK/K2} = -53.8 + 123.43x \quad (8)$$

$$T_{CAM/K1} = -28.0 + 28.57x \quad (9)$$

The pour point test measures the temperature at which the solution ceases to flow, and it is usually lower than the cloud point. The pour point of all the babassu and camelina blends shows also a linear relationship with the volume fraction of biokerosene x (Figure 3b and c):

$$T_{BBK/K1} = -39.5 + 50.0x \quad (10)$$

$$T_{BBK/K2} = -48.0 + 77.14x \quad (11)$$

$$T_{CAM/K1} = -41.7 + 60.86x \quad (12)$$

Similar relationships can be found in the literature for the cold flow behavior of blends of biodiesel and fossil diesel.[30]

3.5.2. Cold Filter Plugging Point (CFPP). For the blends of camelina biokerosene and fossil kerosene cut K1, the automatic CFPP method was used, which is more reliable than the manual freezing point method. CFPP is not a specific test for jet fuels, but it gives an indication of the cold flow properties of the blends.[31] The CFPP of the blends of fossil kerosene cut K1 and camelina can be adjusted to a linear equation (Figure 3c):

$$CFPP_{CAM/K1} = -32.5 + 32.86x \quad (13)$$

where x is the volume fraction of biokerosene. In this figure, it could be observed that the CFPP lies between the cloud point (higher) and the pour point (lower), and its variation is almost parallel to that of the cloud point.

3.6. Compatibility with Elastomers and Metals in the Fuel System and Turbine: Copper Strip Corrosion. A positive result for this test indicates that the jet fuel will not corrode copper or copper-based alloys in the different parts of the fuel system and turbine.[22] Most of the blends of babassu biokerosene with K1 and K2 passed this test with the highest value (1a) (Tables 2 and 4). Only the 10 and 20 vol % blends of babassu with fossil kerosene cut K1 show values of 1b. Further studies are in progress to check the compatibility of these blends with the composites of the tank and the seals of the Airbus A380.

3.7. Fuel Handling: Flash Point. The flash point is defined as the lowest temperature at which a liquid produces enough vapors to ignite in the presence of a source of ignition, and it is one of the most significant properties of flammable liquids in industrial processes when evaluating process safety.[32] This test gives an indication of the maximum temperature for fuel shipment, storage, and handling without serious fire hazard. ASTM D1655 fixes a minimum flash point for jet fuels of 38 °C, but the military aircraft regulation establishes a higher limit of 60 °C for JP-5.[22] All the blends of babassu biokerosene and Jet-A1 K2 meet the ASTM specification but not the JP-5 one (Figure 4), and any of the blends of BBK and K1 meet any of

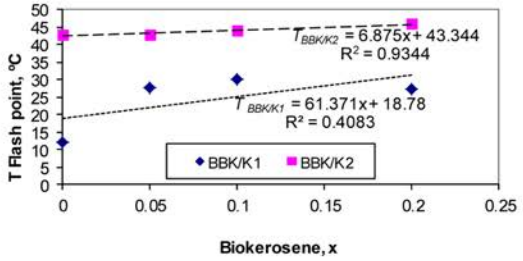

Figure 4. Flash point of the babassu blends.

both specifications. The flash point of mixtures of fossil kerosene and biokerosenes are strongly influenced by the flash point temperature of the fossil kerosene when the biokerosene concentration was lower than 80 vol %.[32]

The flash point seems to be related to the blends composition by the following equations:

$$T_{BBK/K1} = 18.78 + 61.37x \quad (14)$$

$$T_{BBK/K2} = 43.344 + 6.88x \quad (15)$$

where T is the flash point in °C and x is the volume fraction of biokerosene.

3.8. Fuel Cleanliness and Contamination: Acidity and Water Content. All the blends of babassu biokerosene with fossil kerosenes K1 and K2 meet the acidity specification (acidity lower than 0.10 mg KOH/g).

Water in a jet fuel onboard an aircraft represents a threat to the flight safety and can cause long-term problems such as wear, corrosion, and plugging of filters and other parts.[22] FAME is, in general, a highly hygroscopic material that when blended with fossil fuels increase the tendency of the latter to absorb water.[33] Thus, in the blends of babassu biokerosene with K1 and K2 the water content increases with the volumetric fraction of biokerosene. The observed results cannot be correlated since the storing conditions of the blends have not been exactly the same, but all the blends of babassu biokerosene met the requirement of ASTM D2709 (max. 0.05 vol %).[34]

3.9. Miscellaneous. Color could be a useful indicator of jet fuel quality, and specially, color changes should be investigated to determine their cause. Jet fuel color ranges from colorless (water white) to straw/pale yellow. All our blends are clear and colorless (Tables 2, 3, and 4).

3.10. Bottom Fraction of Babassu. The bottom distillation fraction of babassu FAME was evaluated after the EN 14213 standard for heating biodiesel. Babassu bottom meets the specifications of density, acidity, lower heating value, and copper strip corrosion, but not the cold flow properties.

In conclusion, the possibility of use of this bottom fraction as heating fuel could only be accomplished if it is blended with other biodiesel or fossil diesel. Thus, we have blended the bottom fraction of babassu oil biodiesel with camelina oil biodiesel at 50 vol % each, and we have measured the CFPP resulting an improvement of 7 °C (from +2 °C of the babassu bottom to −5 °C of the blend) .

5. CONCLUSIONS

Babassu and camelina oils have been transesterified with methanol by the classical basic homogeneous catalytic method. The babassu FAME has been distilled at vacuum, and the major low boiling point fraction (babassu biokerosene) has been blended with two types of fossil kerosene, fossil kerosene cut and Jet-A1. The blends of babassu biokerosene with fossil kerosene Jet-A1 meet the following ASTM D1655 specifications: color, acidity, density, lower heating value (5 and 10% vol blends), flash point, cloud point (not included in the standard), copper strip corrosion, oxidation stability, and smoke point.

The blends of babassu biokerosene and fossil kerosene cut K1 meet the following specifications of the ASTM D1655 standard: color, acidity, density, copper strip corrosion, oxidation stability, and lower heating value (only the 5 vol % blend).

The camelina FAME has been blended with fossil kerosene cut K1 avoiding the previous distillation step, and these blends meet the following specifications of the ASTM D1655 standard: color, density, viscosity at −20 °C, and oxidation stability.

With these preliminary results, we can conclude that it would be feasible to blend babassu and camelina biokerosenes prepared in this way with commercial Jet-A1, up to 10 vol % of the former, as partial substitutes of fossil jet fuels, if these blends prove to accomplish all the ASTM D1655-09 standards.

AUTHOR INFORMATION

Corresponding Author

*Telephone: +(34) 913367015. Fax: +(34) 913366948. E-mail: laureano.canoira.lopez@upm.es.

Notes

The authors declare no competing financial interest.

ACKNOWLEDGMENTS

We wish to thank the Laboratory of Fuels and Petrochemistry of the Gómez-Pardo Foundation (Technogetafe Scientific Park, Universidad Politécnica de Madrid) for its help in carrying out this work and for the supply of camelina seeds, Miguel Cobo, formerly with the company Combustibles Ecológicos Biotel SL, for the gift of babassu oil, and the Dallas Group of America, for the gift of Magnesol D-60. We also thank Emilia Mangue, Pedro Sanz (UPM), and José Javier González Laguna (UCLM) for their technical contribution to this work.

REFERENCES

(1) Biofuels International. http://www.biofuels-news.com (accessed Nov. 8, 2010).

(2) *European Directive 2008/101/CE on Aviation Gas Emission*; European Union: 2008.

(3) *Spanish Law 13/2010*, BOE; July 6,2010; Vol. *163*, pp 59586−59627.

(4) Hogue, C. Unfriendly skies. *Chem. Eng. News* **2011**, No. Oct. 17, 48−50.

(5) Administration pushes biofuels production. *Chem. Eng. News* **2011**, (Aug. 22), 30.

(6) Dunn, R. O. Alternative jet fuels from vegetable oils. *Trans. ASAE* **2001**, *44*−*6*, 1751−1757.

(7) Dagaut, P.; Gail, S. Kinetics of gas turbine liquid fuels combustion: Jet-A1 and biokerosene. *Proc. ASME Turbo Expo* **2007**, *2*, 93−101.

(8) Korres, D. M.; Karonis, D.; Lois, E.; Linck, M. B.; Gupta, A. K. Aviation fuel JP-5 on a biodiesel engine. *Fuel* **2008**, *87*, 70−78.

(9) Wagutu, A. W.; Chabra, S. C.; Thoruwa, C. L.; Thoruwa, T. F.; Mahunnah, R. L. A. Indigenous oil crops as a source for production of biodiesel in Kenia. *Bull. Chem. Soc. Ethiop.* **2009**, *3*−*3*, 359−370.

(10) Hileman, J. I.; Stratton, R. W.; Donohoo, P. E. Energy content and alternative jet fuel viability. *J. Propul. Power.* **2010**, *26* (6), 1184−1195.

(11) Cottineau, J. Green Chemistry. Bio motor fuels. The aviation industry unveils bio-kerosene. *Info Chim. Mag.* **2008**, *45* (490), 27.

(12) (a) World news: France: The BTL Chain. *Hydrocarbon Eng.* **2010**, *15* (4), 8. (b) Uhde's Prenflo process to be part of joint R&D project BioTfueL in France. *Chem. Eng.* **2010**, *117* (4), 79.

(13) Gill, S. S.; Tsolakis, A.; Dearn, K. D.; Rodríguez-Fernández, J. Combustion characteristics and emissions of Fischer−Tropsch diesel fuels in IC engines. *Prog. Energy Combust. Sci.* **2011**, *37*, 503−523.

(14) Kinder, J. D.; Rahms, T. *Evaluation of Bio-Derived Synthetic Paraffinic Kerosene (Bio-SPK)*; Ascension Publishing: Miami, FL, 2009.

(15) Standard specification for aviation turbine fuel containing synthesized hydrocarbons. *Standard ASTM D7566*; ASTM International: West Conshohocken, PA, 2011.

(16) Alternative jet fuels cut particulate emissions. *Chem. Eng. News* **2011**, (Nov. 21), 2.

(17) Pinzi, S.; Leiva, D.; Arzamendi, G.; Gandia, L. M.; Dorado, M. P. Multiple response optimization of vegetable oils fatty acid composition to improve biodiesel physical properties. *Bioresour. Technol.* **2011**, *102*, 7280−7288.

(18) Dorado, M. P. Raw materials to produce low-cost biodiesel. *Biofuels Refining and Performance*; Nag, A., Ed.; McGraw-Hill: New York, 2008; p 107.

(19) Canoira, L.; Rodríguez-Gamero, M.; Querol, E.; Alcántara, R.; Lapuerta, M.; Oliva, F. Biodiesel from low-grade animal fat: Production process assessment and biodiesel properties characterization. *Ind. Eng. Chem. Res.* **2008**, *47*, 7997−8004.

(20) Dunn, R. O.; Bagby, M. O. Low-temperature properties of triglyceride-based diesel fuels: Transesterified methyl esters and petroleum middle distillate/ester blends. *J. Am. Oil Chem. Soc.* **1995**, *72* (8), 895−904.

(21) Lapuerta, M.; Canoira, L.; Raez, J. Improved method for determining the atmospheric distillation curve of biodiesel fuels from reduced pressure. *Ind. Eng. Chem. Res.* **2011**, *50*, 7041−7048.
(22) Standard specification for aviation turbine fuels. *Standard ASTM D1655-09a*; ASTM International: West Conshohocken, PA, 2009.
(23) McCormick, R. L.; Westbrook, S. R. Storage stability of biodiesel and biodiesel blends. *Energy Fuels* **2010**, *24*, 690−698.
(24) Clarke, A. E.; Hunter, T. G.; Garner, F. H. The tendency to smoke of organic substances on burning. *J. Inst. Pet.* **1946**, *32*, 627−642.
(25) Gill, R. J.; Olson, D. B. Estimation of soot thresholds for fuel mixtures. *Combust. Sci. Technol.* **1984**, *5*−*6*, 307−315.
(26) Standard practice for viscosity temperature charts for liquid petroleum products. *Standard ASTM D341-09*; ASTM International: West Conshohocken, PA, 2009.
(27) Krisnagkura, K.; Yimsuwan, T.; Pairintra, R. An empirical approach in predicting biodiesel viscosity at various temperatures. *Fuel* **2006**, *85*, 107−113.
(28) Freitas, S. V. D.; Pratas, M. J.; Ceriani, R.; Lima, A. S.; Coutinho, J. A. P. Evaluation of predictive models for the viscosity of biodiesel. *Energy Fuels* **2011**, *25*, 352−358.
(29) Grunberg, L.; Nissan, A. M. *Nature* **1949**, *164*, 799−800.
(30) Tang, H.; Salley, S.; Ng, K. S. Fuel properties and precipitate formation at low temperatures in soy-, cottonseed-, and poultry-fat based biodiesel blends. *Fuel* **2008**, *87*, 3006−3017.
(31) Dunn, R. O. Effect of minor constituents on cold flow properties and performance of biodiesel. *Prog. Energy Combust. Sci.* **2009**, *35*, 481−489.
(32) Lazzús, J. Prediction of flash point temperature of organic compounds using a hybrid method of group contribution + neural network + particle swarm optimization. *Chinese J. Chem. Eng.* **2010**, *18*, 817−823.
(33) Canoira, L.; García-Galeán, J.; Alcántara, R.; Lapuerta, M.; García-Contreras, R. Fatty acids methyl esters (FAME) from castor oil: Production process assessment and synergistic effects in its properties. *Renewable Energy* **2010**, *35*, 208−217.
(34) Standard test method for water and sediment in middle distillate fuels by centrifuge. *Standard ASTM D2709-96*; ASTM International: West Conshohocken, PA, 2011.
(35) *NIST Chemistry WebBook*, NIST Standard Reference Database Number 69; National Institute of Standards and Technology (NIST): Gaithersburg, MD, 2005; available online: http://webbook.nist.gov./chemistry/ (accessed April 4, 2011).
(36) Sigma-Aldrich Catalog. http://www.sigmaaldrich.com/catalog/ (accessed April 4, 2011).
(37) Graboski, M. S.; McCormick, R. L. Combustion of fat and vegetable oil derived fuels in diesel engines. *Prog. Energy Combust. Sci.* **1998**, *24* (2), 125−164.

5 ADDITIVES DERIVED FROM BIODIESEL AND GLYCEROL

As a consequence of the big increase in the production of biodiesel in the first decade of the present century, the by-product of this production, bioglycerol has become a commodity that has exceeded the market demand, the pharmaceutical and cosmetics industries being unable to absorb the supply.

Thus, the biodiesel companies had no other choice than the energetic valorization of bioglycerol in their own factories, burning it with fuel oil or natural gas to produce electricity or steam. Resulting in the undervalorization of the by-product.

The most suitable solution would be to incorporate bioglycerol within the biodiesel, under a molecular form compatible with the fuel such as FAGE (Fatty Acid Glycerol Esters)(257).

In this paper of the author and others, a different approach aiming the same result has been followed: incorporating bioglycerol to diesel fuel as 1,3-ditert-butoxy-propan-2-ol as an additive that greatly improves the combustion properties of diesel and diesel-biodiesel blends.

Fuel 93 (2012) 632–637

Contents lists available at SciVerse ScienceDirect

Fuel

journal homepage: www.elsevier.com/locate/fuel

A new route to synthesize *tert*-butyl ethers of bioglycerol

Ana-María Al-Lal, Jerónimo-Emilio García-González, Alberto Llamas, Alfredo Monjas, Laureano Canoira *

Department of Chemical Engineering & Fuels, School of Mines, Universidad Politécnica de Madrid, Ríos Rosas 21, 28003 Madrid, Spain

ARTICLE INFO

Article history:
Received 3 February 2011
Received in revised form 23 September 2011
Accepted 27 September 2011
Available online 17 October 2011

Keywords:
Biodiesel components
Bioglycerol
Epichlorohydrin
1,3-Di-*tert*-butoxypropan-2-ol
Tert-butylation

ABSTRACT

The excess of bioglycerol from the production of biodiesel finds no profitable use in the already saturated glycerol market. In this paper, the synthesis of 1,3-di-*tert*-butoxypropan-2-ol as a component for fossil diesel/biodiesel is reported. This new application could add value to the bioglycerol at the same time that it could enhance the properties and environmental performance of biodiesel. The synthesis consists in a three-step process that starts by the transformation of epichlorohydrin, obtained by the transformation of bioglycerol by the new Solvay process. The results of the overall process are satisfactory in terms of selectivity, conversion and yield. A spectroscopic analysis has been carried out, which shows that among the resulting products of the process, 1,3-di-*tert*-butoxypropan-2-ol is the most abundant and only little amounts of by products are formed, making the overall process technically viable. Also a study of the net carbon dioxide emissions produced by the combustion of this component has been developed.

1. Introduction

Biodiesel is a renewable fuel whose production has increased exponentially in the last few years. Apart from several environmental advantages, biodiesel presents improved lubricity, higher flash point, reduction of most exhaust emissions, close heat combustion and viscosity to those of fossil diesel, and similar or even superior cetane number than fossil diesel.

The formula of biodiesel (monoalkylesters of vegetable oils and animal fats) includes the presence of oxygen, which along with the differences in the chemical structure of the mixture, impacts on the chemical reaction during ignition and combustion and decreases the soot formation [1].

Since 2000, the production of biodiesel has been increasing exponentially due to the aim of governments to meet Kyoto protocol and for other environmental reasons [2]. The rise in biodiesel production brought about a subsequent increase of that of bioglycerol, by-product from the former. The bioglycerol excess enters in an already saturated market, which has lead to a dramatic reduction on the economic value of glycerol as raw material [3].

The final destiny of the crude bioglycerol resulting from biodiesel production (usually called G-phase) has traditionally been energetic valorization [4] by joint combustion with methane to generate electrical power. This application is not considered to be optimum, as it does not generate a significant economic benefit and presents also important technical problems as emission of oxygenates, high sodium or potassium ash content, low heating value and high viscosity.

Alternative applications of bioglycerol are under investigation in industrial chemistry [5–7] for its conversion into valuable chemicals. One of the bioglycerol derivatives that has received much attention is glycerol carbonate [8–14]. Acrolein could also be obtained from bioglycerol on HZSM-5 zeolite [15]. Bioglycerol could be also a valuable feedstock for industrial microbiology [16].

One of these possible applications of bioglycerol is the transformation into oxygenated components for fuels, as 1,3-di-*tert*-butoxypropan-2-ol. Ether derivatives of glycerol are compatible with diesel and biodiesel fuels, and are also excellent components for these fuels. These components are mixed with biodiesel for different purposes, such as to increase the energetic efficiency of the fuel and its stability and to lower the emissions. [17–20]. A Japanese patent [21] has been issued on the use of 1,3-di-*tert*-butoxypropan-2-ol as diesel component in 0.2–10.0 vol.% to improve the combustion and to lower the particulate and VOC's emissions. Oxygenated components improve the diffusion-dominated combustion due to the availability of bonded oxygen in fuel rich regions of the non homogeneous mixture [22].

Tertbutylation of bioglycerol with isobutylene or *tert*-butanol has been referred in the literature using ion-exchange resins [23–28], zeolites [25,29], mesostructured silicas [30] and other catalysts [31–34]. According to these authors, the bioglycerol conversion producing *tert*-butyl oxygenated components using acidic catalysts reaches to about 50%. However, some years ago we tried to etherify bioglycerol with pure isobutylene over Amberlyst-15 catalyst in a fixed-bed experimental reactor without any success.

* Corresponding author. Tel.: +34 91 336 7015; fax: +34 91 336 6948.
E-mail address: laureano.canoira.lopez@upm.es (L. Canoira).

0016-2361/$ - see front matter © 2011 Elsevier Ltd. All rights reserved.
doi:10.1016/j.fuel.2011.09.055

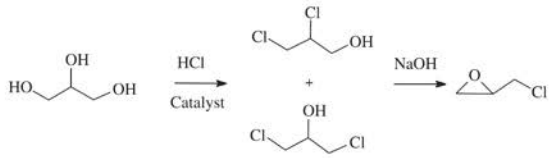

Scheme 1. Solvay process for the synthesis of epichlorohydrin from bioglycerol through dichloropropanols mixture.

We obtained only the trimerization of isobutylene with good yield and selectivity, but the bioglycerol was recovered totally unchanged [35].

The aim of this paper is to describe a new synthetic route for the production of 1,3-di-*tert*-butoxypropan-2-ol as a component for fossil diesel or biodiesel, different from the etherification process of glycerol with isobutylene or *tert*-butanol. Solvay has recently developed a process to obtain epichlorohydrin from bioglycerol instead of the classical route from propylene, and it is currently building two plants in China and Thailand due to come on line in 2013 based in this technology [36–38] (Scheme 1). Epichlorohydrin is a commodity chemical (production of around 700,000 tons/year) and it is mainly used in the reaction with bisphenol A to yield epoxy resins [39]. In this paper, we describe the synthesis of 1,3-di-*tert*-butoxypropan-2-ol in a three steps process, starting from epichlorohydrin and *tert*-butanol as raw materials (Scheme 2). Since *tert*-butanol is obtained by hydration of isobutylene, and epichlorohydrin is obtained from bioglycerol in the Solvay route, the process described in this paper could be considered as an alternative, however longer, to the direct etherification of bioglycerol with isobutylene to obtain 1,3-di-*tert*-butoxypropan-2-ol.

The first step consists in obtaining 1-chloro-3-*tert*-butoxypropan-2-ol (chlorohydrin ether) **1** by reaction of epichlorohydrin with *tert*-butanol, catalyzed by boron trifluoride etherate. The second step is the reaction of the chlorohydrin ether **1** with a strong basic solution of 50 wt.% sodium hydroxide to obtain 3-*tert*-butoxypropylene-1,2-oxide (glycidyl ether), **2**. Finally, the third step consists in the oxirane ring opening reaction of the glycidyl ether **2** with *tert*-butanol, testing different catalysts (perchloric acid, potassium hydroxide, sodium *tert*-butoxide and boron trifluoride etherate) to synthesize 1,3-di-*tert*-butoxypropan-2-ol, **3**.

2. Experimental

2.1. Apparatus

- A 2 L cylindrical glass tank reactor (22 cm height × 10 cm o.d.) equipped with: a 220 V heating jacket controlled by a Proportional Integral Derivative controller TC-10 from PID & Eng and a type K thermocouple, a mechanical KPG type Teflon stirrer powered by a Heidolph RZR 2050 engine, a water reflux condenser, two top B-29 inlets for a dropping funnel and a thermocouple and one bottom outlet for the discharge of products.
- A three necked 250 mL round bottomed glass flask, partially immersed in an oil bath heated by a magnetic stirring plate Bunsen MC-8, with temperature and stirring power regulations, was used for lower scale of reagents.
- *Vacuum equipment:* a Büchi 461 rotavapour was used for vacuum distillation of solvents. Vacuum distillation of products was performed with a 10 cm long Vigreux distillation column and liquid nitrogen trap mechanism. Vacuum was obtained by means of an Edwards vacuum pump E1M5.
- *Gas-chromatograph (GC):* a Hewlett Packard 5890 GC with a Carbowax 20 M capillary column (25 m × 0.32 mm × 0.3 μm) was used to analyze the reaction products. The detector was a FID. Helium was the carrier gas and the column head pressure was set to 6 psi (40.8 kPa). GC settings were as follows: initial temperature 100 °C; initial time 4 min.; heating rate 4 °C/min; final temperature 200 °C; final time 10 min.
- *Mass spectrometer VG AUTOSPEC:* Spectra of electronic impact: 70 eV; m/z scan from 50 to 800 Da; resolution 1000. Analytical column of the GC: Supelcowax: (30 m × 0.25 mm × 0.25 μm). Column head pressure: 22.4 psi (152.3 kPa) with helium flow of 2.16 mL/min. Sample Amount: 0.2 μL. GC settings were as follows: initial temperature 50 °C; initial time 1 min; medium temperature 200 °C; medium time 5 min; final temperature 250 °C; final time 20 min. Heating rate 10 °C/min.
- ^{1}H NMR spectra were recorded on a Bruker WP 200SY spectrometer at 200.13 MHz using $CDCl_3$ as solvent and $SiMe_4$ as internal standard.

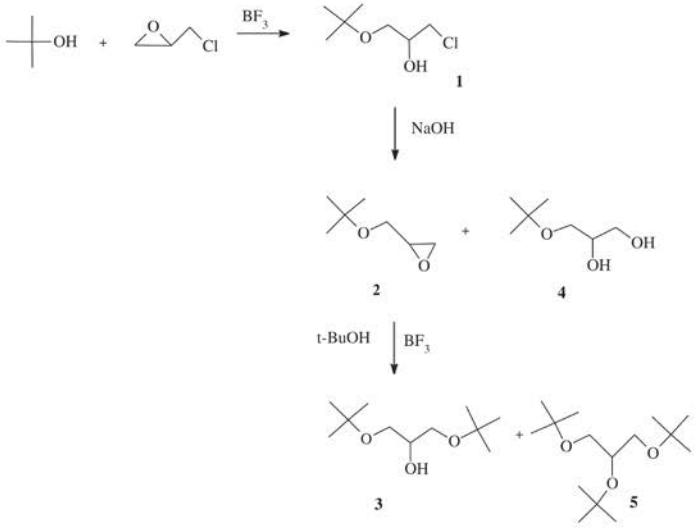

Scheme 2. Process for the synthesis of 1,3-di-*tert*-butoxypropan-2-ol from epichlorohydrin and *tert*-butanol.

2.2. Reagents

All the reagents used in this work were of commercial grade and were used without further purification.

2.3. Experimental procedures

2.3.1. 1-Chloro-3-tert-butoxypropan-2-ol synthesis **1** (chlorohydrin ether)

Tert-butanol (4 mol, 296 g) and 5 wt.%. of boron trifluoride etherate (0.104 mol, 14.2 g) were mixed in the stirred tank reactor. The mixture was maintained at ca. 80 °C. At this temperature, epichlorohydrin (1 mol, 92.5 g) was added dropwise to the reactor in a period of 2 h. After addition was finished, the reaction mixture was stirred for an additional 20 h until the reaction was completed, as observed by thin layer chromatography (TLC). The mixture was then cooled at room temperature and diluted with water. The solution was exhaustively extracted with dichloromethane. The combined extracts were washed with brine and dried with anhydrous sodium sulfate and finally, the dichloromethane was evaporated in vacuum. The crude 1-chloro-3-*tert*-butoxypropan-2-ol **1** (pure by GC and ^{1}H-NMR) was used without further purification (144.8 g, 87%, bp 56–7 °C^{80torr}). ^{1}H-NMR δ 1.17 (s, 9H); 2.67 (d, 1H) 3.4–4.0 (m, 5H).

2.3.2. 3-Tert-butoxypropylene-1,2-oxide **2** (tert-butyl glycidyl ether) synthesis

The chlorohydrin ether **1** obtained in the precedent procedure (1.03 mol, 172 g) was introduced in the reactor under N_2 atmosphere and cooled in an ice bath to approximately 5 °C. Addition of NaOH (50 wt.% aqueous, 1.275 mol) was carried out dropwise during a 1 h period, keeping the mixture stirred at 5 °C. Stirring at room temperature was kept until the reaction was complete by TLC (approximately 15 h). Water was added to the reaction mixture and the phases separated. The aqueous phase was exhaustively extracted with dichloromethane, and the combined organic phases were washed with water until neutral pH, then washed with brine and dried with anhydrous sodium sulfate. The solvent was removed by evaporation in vacuum. 3-*Tert*-butoxypropylene-1,2-oxide **2** was vacuum distilled as a colorless oil (102 g, 76.3%; 66–67 °C^{25torr}; lit. bp 152 °C^{760torr} [40]). ^{1}H-NMR: δ 1.17 (s, 9 H); 2.7 (m, 2H); 3.13 (m, 1H); 3.50 (m, 2H). 3-*Tert*-butoxypropane-1,2-diol **4** was also vacuum distilled as a colorless oil (36.1 g, 23.7%; 94.2–97.2 °C$^{0.075torr}$). ^{1}H-NMR: δ 1.14 (s, 9 H); 3.36 (dd, 1 H, J = 9.2 Hz, J = 5.8 Hz); 3.38 (dd, 1 H, J = 9.2 Hz, J = 4.4 Hz); 3.54 (s, 2H, OH); 3.56 (dd, 1 H, J = 11.3 Hz, J = 5.7 Hz); 3.63 (dd, 1 H, J = 11.3 Hz, J = 3.7 Hz); 3.74 (m, 1 H).

2.3.3. 1,3-Di-tert-butoxypropan-2-ol

Four different alternative catalysts have been checked:

(a) *Perchloric acid catalyst*: A mixture of *tert*-butanol (4 mol, 296 g) and 72 wt.% perchloric acid (0.01 mol, 1.00 g) was introduced in the 2 L reactor and heated at 80 °C. Once this temperature was reached, *tert*-butyl glycidyl ether **2** (1 mol, 130 g) was added dropwise during a 1 h period. The mixture was stirred for 15 additional hours, until all the reagent **2** was consumed as observed by GC. The resulting mixture was cooled and neutralized with aqueous 0.5 M sodium carbonate solution. The excess *tert*-butanol and water were evaporated in vacuum. 1,3-*Ditert*-butoxypropan-2-ol **3** was obtained in a 25.8% yield by GC.

(b) *Potassium hydroxide catalyst:* A mixture of *tert*-butanol (0.3 mol, 22.2 g) and potassium hydroxide (0.025 mol, 1.4 g) was placed in a magnetically stirred 250 mL three necked flask. The flask was heated to 80 °C in an oil bath. Once the temperature was reached and the potash lenses were dissolved, *tert*-butyl glycidyl ether **2** (0.1 mol, 13.0 g) was added dropwise during 1 h period. The mixture was kept stirred for an additional hour, until a conversion higher than 50% of the starting material **2** was observed by GC. The resulting mixture was cooled and neutralized with 0.6 mL of 1.12 M sulfuric acid. The excess *tert*-butanol and water were evaporated in vacuum. 1,3-Di-*tert*-butoxypropan-2-ol **3** was obtained only in a 3.8% yield by GC.

(c) *Sodium tert-butoxide catalyst*: A mixture of terbutanol (0.3 mol, 22.2 g) and metallic sodium (0.013 mol, 0.3 g) was placed in a magnetically stirred 250 mL three necked flask. The flask was heated to 80 °C until all sodium was dissolved. Later, *tert*-butyl glycidyl ether **2** (0.1 mol, 13.0 g) was added dropwise during 1 h period. The mixture was stirred at the same temperature for five additional hours, until the conversion of the starting compound **2** was quantitative as observed by GC. The resulting mixture was cooled and neutralized with 0.6 mL of 1.12 M sulfuric acid. The excess *tert*-butanol and water were evaporated in vacuum. 1,3-Di-*tert*-butoxypropan-2-ol **3** was obtained only in a 4.1% yield by GC.

(d) *Boron trifluoride etherate catalyst*: A mixture of *tert*-butanol (4 mol, 296 g) and boron trifluoride etherate (0.01 mol, 1.42 g) was placed in a mechanically stirred 2 L tank reactor. The reactor was heated at 80 °C. *Tert*-butyl glycidyl ether **2** (1 mol, 130 g) was added dropwise during 1 h period. Temperature and stirring were kept for an additional 15 h period, until the conversion of the compound **2** was quantitative by GC. The mixture was then cooled at room temperature and diluted with water. The solution was exhaustively extracted with dichloromethane. The combined extracts were washed with brine and dried with anhydrous sodium sulfate and finally, the dichloromethane was evaporated in vacuum. 1,3-Di-*tert*-butoxypropan-2-ol **3** was purified by vacuum distillation (107.3 g, 52.6%) ^{1}H-NMR: δ 0.98 (s, 18 H); 2.81 (s, 1H, OH); 3.16 (dd, 2 H, J = 9.0 Hz, J = 5.8 Hz); 3.20 (dd, 2H, J = 9.0 Hz, J = 5.3 Hz); 3.56 (m, 1 H, CH). MS (70 eV): 186 (M^+−18), 171 (M^+−18−15), 147 (M^+-57), 133, 117, 112, 100, 87, 75, 57 (base peak), 41, 29. A small impurity of 1,2,3-tri-*tert*-butoxypropane **5** was present in the distillate. ^{1}H-NMR: δ 1.15 (s, 18 H); 1.19 (s, 9 H); 3.16 (dd, 2 H, J = 9.2 Hz, J = 5.3 Hz); 3.36 (dd, 2 H, J = 9.2 Hz, J = 5.8 Hz); 3.59 (m, 1 H). MS (70 eV): 261 (M^+ + 1), 186, 173, 133, 130, 117, 87, 75, 57 (base peak). High calorific value = 32.503 MJ kg^{-1}; low calorific value = 29.955 MJ kg^{-1} [41].

3. Results and discussion

The synthesis of 1,3-di-*tert*-butoxypropan-2-ol **3** has been done in three steps, and conversion of the starting material, yield and selectivity of the desired products have been measured in each of them. Moreover, the experiments have been carried out at two different scales: in a 250 mL round bottomed glass reaction flask and in a 2 L stirred glass tank reactor (see experimental part 2). Table 1 summarizes the conversion, yield and selectivity in both reactors; these values are always lower for the 2 L reactor, due to the difficulties found in the distillation of a big amount of products.

The synthesis of compounds **1** and **2** were done following the procedure of Gokel et al. [40]. Conversion for the whole process, and yield and selectivity for the first stage, could be considered practically quantitative. The yield and selectivity for the synthesis of compounds **2** and **3** show ranges between values of about 70% and 50%, respectively. The reason for which these values are lower

Table 1
Conversion, yield and selectivity in the synthesis of 1,3-di-*tert*-butoxypropan-2-ol.

Reactor	Product	Conversion (%)	Yield (%)	Selectivity (%)
250 mL	1-Chloro-3-*tert*-butoxypropan-2-ol **1**	100	100	100
250 mL	3-*Tert*-butoxypropylene-1,2-oxide **2**	100	76.5	76.5
	3-*Tert*-butoxypropane-1,2-diol **4**		23.5	23.5
250 mL	1,3-Di-*tert*-butoxypropan-2-ol **3**	100	52.6	52.6
2 L	1-Chloro-3-*tert*-butoxypropan-2-ol **1**	96.6	87.3	90.4
2 L	3-*Tert*-butoxypropylene-1,2-oxide **2**		68.5	68.7
	3-*Tert*-butoxypropane-1,2-diol **4**	99.6	31.1	31.2
2 L	1,3-Di-*tert*-butoxypropan-2-ol **3**	100	48.9	48.9

could be explained by the fact that when these reactions take place, they generate oxygenated isomeric compounds of the desired product, of similar molecular weight. These products have to be separated from the desired compound by distillation, and this separation is not always totally successful as in the case of compound **3** (see below).

In the first step, the oxirane ring opening of epichlorohydrin was catalyzed by boron trifluoride etherate, which is a Lewis acid that coordinates with the oxygen atom of the oxirane ring; the nucleophilic attack of the voluminous *tert*-butanol was sterically hindered at the secondary carbon of the epichlorohydrin ring, and thus the attack occurs exclusively at the primary carbon atom, giving almost quantitative yield and selectivity of the chlorohydrin ether **1**. Boron trifluoride is a pungent, colorless corrosive gas (b.p. −101 °C), but its adduct with diethyl ether, boron trifluoride etherate, is a conveniently handled liquid that has found large scale applications for the acylation of vegetable oils [42], the synthesis of the conducting polymer poly-6-nitroindole [43] and the industrial production of polyacetals [44]. Moreover, boron trifluoride etherate is widely used as a Lewis acid reagent in industrial organic chemistry [45].

The second step was the synthesis of the glycidyl ether **2** by intramolecular ring closure of the compound **1**, catalyzed by concentrated aqueous sodium hydroxide. This is an E1 intramolecular elimination reaction in the very polar reaction medium (aqueous 50 wt.% NaOH) and, in this case, yield and selectivity are lower (68–76%) due to the competing reaction of nucleophilic substitution SN1 of the Cl atom by the OH^- reagent, giving 3-*tert*-butoxypropane-1,2-diol, **4**.

Four catalysts for synthesizing our interest compound **3** have been tried. The results obtained for this reaction using different catalysts are shown on Table 2. Any literature references exist for the oxirane ring opening of the glycidyl ether **2** with *tert*-butanol. We have tried two acid catalysts, conc. perchloric acid and boron trifluoride etherate; conc. perchloric acid was used by Gokel et al. [40] to hydrolyze the compound **2**. However, although the conversion of **2** was quantitative, the yield of **3** was very low (26%) probably because the strong acid produces besides the ring opening, the hydrolysis of the glycidyl ether, that is, the breaking of the t-Bu-O-C of the first *tert*-butyl moiety, by proton co-ordination with the oxirane oxygen atom. With boron trifluoride etherate as catalyst, the yield of **3** ranges between 48.9% and 52.6%, far away from the quantitative yield obtained in the ring opening of epichlorohydrin. One of the reasons for this decreasing of yield could be the absence of the electron-withdrawing effect of the chlorine atom of epichlorohydrin, which favors the co-ordination of the boron trifluoride to the oxirane ring atom, and the subsequent attack of *tert*-butanol. Thus, the lack of this electronic effect in the glycidyl ether **2** could account for the dramatic decreasing in yield. A by-product obtained is 1,2,3-tri-*tert*-butoxypropane **5**, from which a trace co-distilled with the compound **3**; the formation of compound **5** could be explained by the etherification of compound **3** with the excess *tert*-butanol in the acidic reaction medium. Higher poliols derived from the compound **2** and that are not characterized were also obtained, as can be observed in the chromatogram of the crude reaction product (Fig. 1).

Table 2
Conversion, yield and selectivity for the third step of the synthesis of 1,3-di-*tert*-butoxypropan-2-ol.

Catalyst	Conversion (%)	Yield (%)	Selectivity (%)
$HClO_4$	100	25.8	25.8
KOH	56.5	3.8	6.7
$NaCH_3O$	99.7	4.1	4.1
$BF_3\cdots Et_2O$	100	52.6	52.6

We have also tried the ring opening of compound **2** with basic catalysts, conc. potassium hydroxide and sodium *tert*-butoxide, Table 2, entries 3rd and 4th, with very poor results, since the yield of **3** never reached 10%.

The technical quality of the final product **3** has been tested by GC–MS and ^{1}H-NMR analytical techniques, and these data agree exactly with previously published data for 1,3-di-*tert*-butoxypropan-2-ol **3** [46].

Since a few years back, the environmental suitability of a chemical process has been measured by the environmental quotient factor *EQ* [47] where *E* represents the quotient between the weight of by-products and the weight of desired product, and *Q* represents the quality of the by-products (e.g., for neutralization salts such as sodium chloride or calcium sulfate $Q = 1$, but for heavy metals salts, *Q* ranges from 10^2 to 10^3 depending on the salt toxicity). The generally accepted values for *EQ* are less than 0.1 for the oil-refining industry (10^6–10^8 tons/year of production capacity), between 1 and 5 for the commodities industry (10^4–10^6 tons/year of production capacity), between 5 and 50 for the fine chemicals industry (10^2–10^4 tons/year of production capacity), and between 25 and 100 for the pharmaceutical industry (10–10^3 tons/year of production capacity). The *EQ* factor for the global production process of 1,3-di-*tert*-butoxypropan-2-ol from epichlorohydrin in the 2 L and 0.25 L reactors are:

$$C_3H_5OCl\ (\text{epichlorohydrin}) + 2C_4H_{10}O(\textit{tert}\text{-butanol}) + NaOH \rightarrow C_{11}H_{24}O_3(1,3\text{-di-}\textit{tert}\text{-butoxypropan-2-ol}) + NaCl + H_2O$$

$$E_{2L} = \frac{\sum M_w \text{ by products}}{M_w \text{ product} \times \text{yield}} = \frac{58.5+18}{204\times 0.292} = 1.284$$

$$E_{0.25L} = \frac{58.5+18}{204\times 0.402} = 0.933$$

$$E_{2L} \times Q = 1.284 \times 1.0 = 1.284$$

$$E_{0.25L} \times Q = 0.933 \times 1.0 = 0.933$$

The *Q* value is always 1 since the by-products lack toxicity. These values, although acceptable because the 1,3-di-*tert*-butoxypropan-2-ol could be considered a commodity, are higher than those of the oil-refining industry with which this component should be competitive.

Table 3 summarizes some representative properties of rapeseed–soybean–palm FAME (60:25:15 vol.%) with addition of 1 and 3 vol.% of compound **3**; higher amounts of compound **3** are hindered by the EN 14214 standard, which establish a minimum

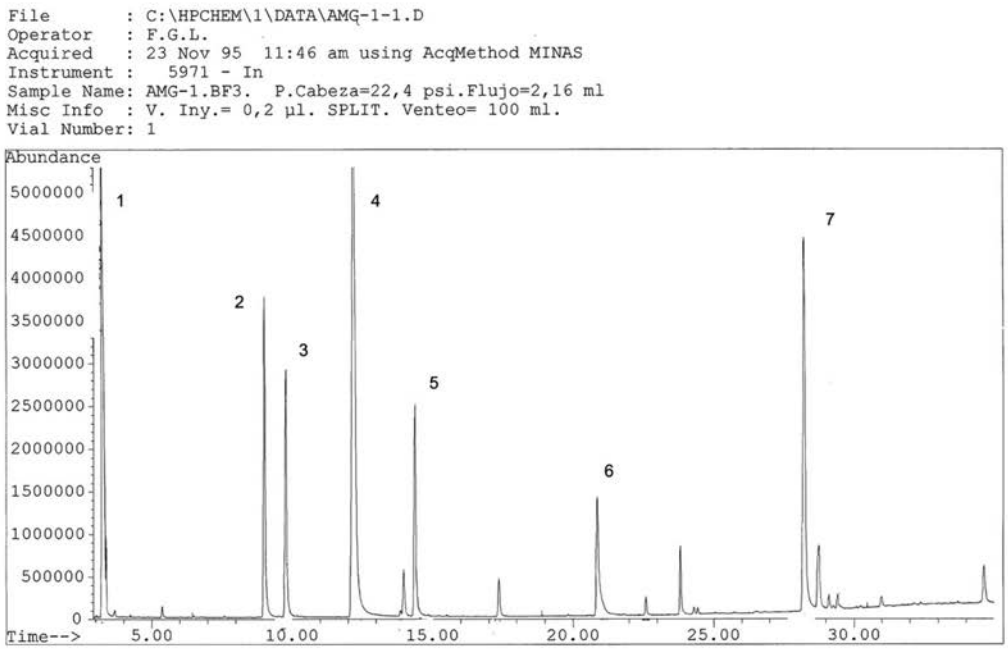

Fig. 1. Chromatogram of the crude product of the synthesis of 1,3-di-*tert*-butoxypropan-2-ol **3** catalyzed by boron trifluoride etherate. (1) *Tert*-butanol. (2) 1,2,3-Tri-*tert*-butoxypropane **5.** (3) 3-*Tert*-butoxypropane-1,2-diol **4.** (4) 1,3-Di-*tert*-butoxypropan-2-ol **3.** (5) 1,2-Di-*tert*-butoxypropan-1-ol. (6) 1-(2-Etoxypropoxy)-2-propanol. (7) Unidentified higher poliol.

Table 3
Properties[a] of rapeseed-soybean-palm FAME with 1 vol.% and 3 vol.% of 1,3-di-*tert*-butoxypropan-2-ol.

Sample	High calorific value (MJ kg^{-1})	Flash point (°C)	Cold filter plugging point (°C)	Kinematic viscosity at 40 °C (mm^2 s^{-1})	Density (kg m^{-3})
FAME	40.34	170.95	−5	4.33	883.6
FAME + 1% **3**	40.05	150.94	−8	4.35	884.0
FAME + 3% **3**	40.04	123.90	−9	4.35	884.2

[a] All the tests are the mean of two or three replicate values.

amount of 96.5 wt.% of FAME for biodiesel. The blend of rapeseed–soybean–palm FAME (60:25:15) chosen to test some representative properties with this component has been selected because most companies licensing transesterification processes guarantee that the biodiesel derived from this blend would satisfy the EN 14214 standard with very little or any additives. Moreover, glycerol ethers are reported to reduce the viscosity of biodiesel and to act as cold flow improvers [33]. In the amounts added to our samples, very slight increases in kinematic viscosity and density were observed, but still within the range of the EN 14214 standard. The cold filter plugging point (CFFP) improves as it has been reported in the literature [33]. The high calorific value decreases very slightly, and the main concern is about the flash point, which decreases from 170.9 °C to 123.9 °C, although still with the range of the standard but very close to the lower limit (min. 120 °C).

The net carbon dioxide emission of 1,3-di-*tert*-butoxypropan-2-ol could be calculated from the stoichiometric combustion equation and the low calorific value (29.955 MJ kg^{-1}) of the component **3**:

$$C_{11}H_{24}O_3 + 15.5O_2 \rightarrow 11CO_2 + 12H_2O$$

giving a carbon dioxide mass emission index (I_{CO_2}) of:

$$I_{CO_2} = \frac{mCO_2}{mfuel} = \frac{11 \times 44}{204} = 2.373 \text{ kg } CO_2 \text{ kg fuel}^{-1}$$

and a gross energetic emission index (IE_{CO_2}) of:

$$IE_{CO_2} = \frac{I_{CO_2}}{NHV} = \frac{2373 \text{ g } CO_2 \text{ kg fuel}^{-1}}{29.955 \text{ MJ kg fuel}^{-1}} = 79.219 \text{ g } CO_2 \text{ MJ}^{-1}$$

The net energetic emission index is defined as:

$$IE_{CO_2} \text{ (net)} = IE_{CO_2} \text{ (gross)}(1 - RF)$$

where *RF* is the mass fraction of renewable origin in the component 1,3-di-*tert*-butoxypropan-2-ol, that could be calculated from the chemical equation of synthesis resulting from the Schemes 1 and 2:

$$C_3H_8O_3 \text{ (bioglycerol, renewable origin)} + 2C_4H_{10}O(\textit{tert}\text{-butanol, fossil origin}) \rightarrow C_{11}H_{24}O_3(1,3\text{-di-}\textit{tert}\text{-butoxypropan-2-ol}) + 2H_2O$$

$$RF = \frac{\text{mass}_{\text{renewable}}}{\text{mass}_{\text{reagents}}} = \frac{92}{240} = 0.38$$

$$IE_{CO_2}(\text{net}) = 79.219 \text{ g } CO_2 \text{ MJ}^{-1}(1 - 0.38) = 49.116 \text{ g } CO_2 \text{ MJ}^{-1}$$

which is close to that of bioethyl *tert*-butyl ether (39.6 g CO_2 MJ^{-1}), and around 67% of the fossil diesel (72.79 g CO_2 MJ^{-1}), but far away from the rapeseed FAME (3.76 g CO_2 MJ^{-1}).

Further emissions and performance studies need to be carried out in order to definitively establish the beneficial effect of this component.

4. Conclusions

This paper describes the synthesis of 1,3-di-*tert*-butoxypropan-2-ol from epichlorohydrin, obtained from bioglycerol, in a three-step process: chlorohydrin ether, glycidyl ether and 1,3-di-*tert*-butoxypropan-2-ol synthesis respectively. Conversion is almost quantitative; however yield is decreasing about a 25% in each step. Among the four catalysts tested for the synthesis of compound **3**, boron trifluoride etherate provides the best results because it gives better yield and selectivity values, at the same quantitative conversion. The experiments determine that the product of interest, 1,3-di-*tert*-butoxypropan-2-ol, is obtained in major quantity. Moreover, the addition of this compound in 1–3 vol.% to a 60:25:15 blend of rapeseed–soybean–palm FAME does not affect the main properties of the biofuel. The investigated process has been shown to be technically viable, and it could represent an indirect way to incorporate bioglycerol to the biodiesel with the consequent economic benefit. Also a study of the net carbon dioxide emission produced by the combustion of this component has been developed.

Acknowledgements

The authors would like to show their gratitude to the late Dr. Juan Antonio Delgado Oyagüe, formerly with Repsol, for the scientific and technical support in the development of this work. Special thanks to the Technological Centre of Repsol for the GC–MS analysis and to the Laboratory de Fuels & Petrochemistry of the Gomez-Pardo Foundation for the tests of the FAME with 1,3-di-*tert*-butoxypropan-2-ol.

References

[1] Szybist JP, Song J, Alam M, Boehman AL. Biodiesel combustion, emissions and emission control. Fuel Process Technol 2007;88:679–91.
[2] Smith C. Biodiesel revolution gathering momentum; 2004. <http://www.straight.com/print/3568> [accessed 08.01.09].
[3] Noharsymi R, Ahmad ZA, Abdul RM. Recent progress on innovative and potential technologies for glycerol transformation into fuel additives: a critical review. Renew Sustain Energy Rev 2010;14:987–1000.
[4] Galan MI, Bonet J, Sire R, Reneaume JM, Plesu AE. From residual to useful oil: revalorization of glycerine from the biodiesel synthesis. Bioresour Technol 2009;100:3775–8.
[5] Zheng Y, Chen X, Shen Y. Commodity chemicals derived from glycerol, an important biorefinery feedstock. Chem Rev 2008;108(12):5253–77.
[6] Sabourin-Provost G, Hallenbeck PC. High yield conversion of a crude glycerol fraction from biodiesel production to hydrogen by photofermentation. Bioresour Technol 2009;100:3513–7.
[7] García E, Laca M, Pérez E, Garrido A, Peinado J. New class of acetal derived from glycerin as a biodiesel fuel component. Energy Fuel 2008;22:4274–80.
[8] Ochoa-Gómez JR, Gómez-Jiménez-Aberasturi O, Maestro-Madurga B, Pesquera-Rodríguez A, Ramírez-López C, Lorenzo-Ibarreta L, et al. Synthesis of glycerol carbonate from glycerol and dimethyl carbonate by transesterification: catalyst screening and reaction optimization. Appl Catal A – Gen 2009;366:315–24.
[9] Ilham Z, Saka S. Dimethyl carbonate as potential reactant in non-catalytic biodiesel production by supercritical method. Bioresour Technol 2009;100:1793–6.
[10] Kim SC, Kim YH, Lee H, Yoon DY, Song BK. Lipase-catalyzed synthesis of glycerol carbonate from renewable glycerol and dimethyl carbonate through transesterification. J Mol Catal B – Enzym 2007;49:75–8.
[11] Climent MJ, Corma A, De Frutos P, Iborra S, Noy M, Velty A, et al. Chemicals from biomass: synthesis of glycerol carbonate by transesterification and carbonylation with urea with hydrotalcite catalysts. The role of acid–base pairs. J Catal 2010;269:140–9.
[12] Aresta M, Dibenedetto A, Nocito F, Ferragina C. Valorization of bio-glycerol: new catalytic materials for the synthesis of glycerol carbonate via glycerolysis of urea. J Catal 2009;268:106–14.
[13] Aresta M, Dibenedetto A, Nocito F, Ferragina C. A study on the carboxylation of glycerol to glycerol carbonate with carbon dioxide: the role of the catalyst, solvent and reaction conditions. J Mol Catal A – Chem 2006;257:149–53.
[14] Fabbri D, Bevoni V, Notari M, Rivetti F. Properties of a potential biofuel obtained from soybean oil by transmethylation with dimethyl carbonate. Fuel 2007;86:690–7.
[15] Jia CJ, Liu Y, Schmidt W, Lu AH, Schüth F. Small-sized HZSM-5 zeolite as highly active catalyst for gas phase dehydration of glycerol to acrolein. J Catal 2010;269:71–9.
[16] Paulo da Silva G, Mack M, Contiero J. Glycerol: a promising and abundant carbon source for industrial microbiology. Biotechnol Adv 2009;27:30–9.
[17] Noureddini H, Dailey WR, Hunt BA. Production of ethers of glycerol from crude glycerol. Chem Eng Pap: Biomater 1998;18:1–14.
[18] Noureddini H. US patent no. 6174,501; 2001.
[19] Lipkin D. US patent no. 2221,839; 1940.
[20] Olah GA. US patent no. 5520,710; 1996.
[21] Kesling JR, Haven S, Karas LJ, Liotta FJ, Jr. Japanese patent JP07082576; 1995.
[22] Adi G, Hall C, Snyder D, Bunce M, Satkoski C, Kumar S, et al. Soy-biodiesel impact on NO_x emissions and fuel economy for diffusion-dominated combustion in a turbo-diesel engine incorporating exhaust gas recirculation and common rail fuel injection. Energy Fuel 2009;23(12):5821–9.
[23] Ozbay N, Oktar N, Dogu G, Dogu T. Conversion of biodiesel by-product glycerol to fuel ethers over different solid acid catalysts. Int J Chem React Eng 2010;8 [art. no. A18].
[24] Frusteri F, Arena F, Bonura G, Cannilla C, Spadaro L, Di Blasi O. Catalytic etherification of glycerol by *tert*-butyl alcohol to produce oxygenated additives for diesel fuel. Appl Catal A – Gen 2009;367(1–2):77–83.
[25] Klepáčová K, Mravec D, Kaszonyi A, Bajus M. Etherification of glycerol and ethylene glycol by isobutylene. Appl Catal A – Gen 2007;328(1):1–13.
[26] Kijeński J, Jamróz ME, Tęcza W. Studies of utilization of glycerol in organic synthesis. Part 2. Conversion of glycerol to its *tert*-butyl ethers (Badania nad wykorzystaniem glicerolu w syntezie organicznej. Cz. II. Konwersja glicerolu do jego tert-butylowych eterów). Przem. Chem. 2007;86(4):282–5.
[27] Klepáčová K, Mravec D, Bajus M. Etherification of glycerol with *tert*-butyl alcohol catalysed by ion-exchange resins. Chem Pap 2006;60(3):224–30.
[28] Klepáčová K, Mravec D, Bajus M. *Tert*-butylation of glycerol catalysed by ion-exchange resins. Appl Catal A – Gen 2005;294(2):141–7.
[29] Barsa EA, Steinmetz BM. US patent no. 20090240086; 2009.
[30] Melero JA, Vicente G, Morales G, Paniagua M, Moreno JM, Roldán R, et al. Acid-catalyzed etherification of bio-glycerol and isobutylene over sulfonic mesostructured silicas. Appl Catal A – Gen 2008;346:44–51.
[31] Boz N, Dogu T. Reflux-recycle-reactor for high yield and selectivity in TAME and TAEE production. AIChE J 2005;51(2):631–40.
[32] Dogu T, Boz N, Aydin E, Oktar N, Murtezaoglu K, Dogu G. DRIFT studies for the reaction and adsorption of alcohols and isobutylene on acidic resin catalyst and the mechanism of ETBE and MTBE synthesis. Ind Eng Chem Res 2001;40(23):5044–51.
[33] Behr A, Obendorf L. Development of a process for the acid catalyzed etherification of glycerine and isobutene forming glycerine tertiary butyl ethers. Eng Life Sci 2003;2(7):185–9.
[34] Macho V, Kavala M, Kolieskova Z. *Tert*-butyl ethers of polyhydric alcohols. Neftekhimiya (Pet Chem) 1979;19:821–7.
[35] Alcántara R, Alcántara E, Canoira L, Franco MJ, Herrera M, Navarro A. Trimerization of isobutene over Amberlyst-15 catalyst. React Funct Polym 2000;45:19–27.
[36] (a) Reisch MS, Tullo AH. Chem Eng News (C&EN); 2006 [December 18: 30–5; (b) C&EN 2009 [October 5: 22]; (c) C&EN 2010 [December 20: 23].
[37] Villorbina G, Tomás A, Escribá M, Oromí-Farrús M, Eras J, Balcells M, et al. Combining $AlCl_3\ 6H_2O$ and an ionic liquid to prepare chlorohydrin esters from glycerol. Tetrahedron Lett 2009;50(23):2828–30.
[38] Luo ZH, You XZ, Zhong J. Design of a reactive distillation column for direct preparation of dichloropropanol from glycerol. Ind Eng Chem Res 2009;48(24):10779–87.
[39] Wittcoff HA, Reuben BG. Industrial organic chemicals. New York: John Wiley & Sons; 1996.
[40] Dishong DM, Diamond CJ, Cinoman MI, Gokel GW. Crown cation complex effects. 20. Synthesis and cation binding properties of carbon-pivot lariat ethers. J Am Chem Soc 1983;105:586–93.
[41] Lapuerta M. Universidad de Castilla La Mancha, unpublished results; 2010.
[42] Sharma BK, Liu Z, Adhvaryu A, Erhan SZ. One-pot synthesis of chemically modified vegetable oils. J Agric Food Chem 2008;56(9):3049–56.
[43] Le Z, Zeng L, Xu J, Liu H, Ma M. Low-potential electrochemical polymerization of 6-nitroindole and characterization of its polymers. J Appl Poly Sci 2008;107(5):2793–801.
[44] Stasiński J, Krzyzanowski P, Cieślak J. The process of trioxane copolymerization and its industrial application (Przemysłowe zastosowanie procesu kopolimeryzacji trioksanu). Polimery/Polymers 1997;42(5):312–5.
[45] Brotherton RJ, Weber CJ, Guibert CR, Little JL. Boron compounds. Ullmann's encyclopedia of industrial chemistry. Weinheim: Wiley-VCH; 2005.
[46] Jamróz ME, Jarosz M, Witowska-Jarosz J, Bednarek E, Tecza W, Jamró MH, Dobrowolski JCZ, Kijeński J. Mono-, di-, and tri-*tert*-butyl ethers of glycerol. A molecular spectroscopic study. Spectrochim Acta Pt A – Mol Bio 2007;67(3–4):980–8.
[47] Sheldon RA. Consider the environmental quotient. CHEMTECH; 1994 [March 38–47].

6. COMBUSTION OF BIODIESEL

6.1 PAH Formation

One of the main concerns about the combustion of both fossil and renewable fuels is the production of particulate matter (PM) or soot. One of the most worrying components of the PM are the polycyclic aromatic hydrocarbons (PAH) since they are carcinogenic and mutagenic.

All combustion process may produce PAH including the cooking techniques in special at barbeque style. One of the main aims of this thesis (included in the title) is to characterize the PAH produced in the combustion of different types of biodiesel correlating it with the ester profile and type of alcohol (methanol and ethanol) used in its production. However in the laboratory we did not have any experimental engine. For this purpose, a method based in the combustion of biodiesel in a bomb calorimeter and the analysis of the PAH recovered from the bomb has been developed. This part of the thesis has been recently sent to publication in fuel and the manuscript submitted is included here.

Polycyclic aromatic hydrocarbons (PAH's) produced in the combustion of FAME and FAEE from different feedstocks: quantification and mechanisms of formation.

Authors: Alberto Llamas[1], Ana-María Al-Lal[1,2], María-Jesús García-Martínez[1], Marcelo F. Ortega[1], Juan Llamas[1], Magín Lapuerta[3] and Laureano Canoira[1*]

[1] Department of Energy & Fuels, ETS Ingenieros de Minas y Energía, Universidad Politécnica de Madrid. Ríos Rosas 21, 28003 Madrid, Spain.

[2] Laboratory of Fuels & Petrochemistry, Tecnogetafe Scientific Park, Universidad Politécnica de Madrid. Erik Kandel s/n, 28906 Getafe, Spain.

[3] Grupo de Combustibles y Motores, ETS de Ingenieros Industriales. Universidad de Castilla La-Mancha. Avda. Camilo José Cela s/n, 13071 Ciudad Real, Spain.

Corresponding author:

Prof. Laureano Canoira

E-mail: laureano.canoira.lopez@upm.es

Telephone: +(34) 913366949

Fax: +(34) 913366948

Abstract.

Polycyclic Aromatic Hydrocarbons (PAH) are pollutants of concern since they are known to be carcinogenic and mutagenic compounds. Their emissions are mainly related to combustion or pyrolysis of organic matter such as fossil fuels. In the current energy scenario where biofuels are growingly important, it is also necessary to characterize their PAH

emissions from combustion. There is a number of works concerning PAH emissions from biodiesel combustion in diesel engines, however, there are few regarding the difference between them depending on the feedstock and type of alcohol used in the transesterification. The authors have processed and characterized biodiesel from several feedstocks (i.e. yellow animal fat, palm, rapeseed, soy-bean, coconut, peanut, and linseed oils) to obtain FAME and FAEE and they have developed a method to measure the PAHs originated during their combustion in a bomb calorimeter. The tests have been carried out under different pure oxygen pressure conditions, and the samples have been obtained from the bomb after each one of these tests. The samples have been prepared for GC-MS analysis, where PAH quantities among some other combustion products have been analysed. This work shows statistical relationships obtained between the measured amounts of 16 PAHs of concern and the composition of the biodiesel, and also the oxygen pressure during combustion.

Keywords: Polycyclic aromatic hydrocarbons, combustion, biodiesel, quantification, mechanisms.

1. Introduction

PAH are produced in combustion processes from fossil and renewable fuels. It is important to understand the mechanisms that lead to the formation of these aromatic compounds during the combustion [1]. PAH are the compounds of most concern among the aromatic emissions from engines [2]. The combustion of fossil fuels is the main source of anthropogenic PAH emission [3] and specifically exhaust emissions are the most important contributors for PAH in urban areas [4,5].

PAH are hydrocarbons with a fused ring structure containing several benzene rings that may carry alkyl substituents, the 16 PAH of concern are shown in Table 1. PAH occurrence

in exhaust gases may be produced by (a) survival: the fuel PAH may survive the combustion process, retaining the original carbon skeleton; (b) pyrosynthesis during combustion from lower molecular weight aromatic compounds: the PAH isolated in the exhaust emissions could be produced when fragments of partially destroyed compounds could recombine to produce new PAH [1,6]; (c) pyrolysis of unburned fuel and lubricating oil: the pyrolysis products were shown to accumulate in the lubricant oil, raising the amount of PAHs from undetectable in fresh oil to substantial amounts in used oil (e.g., 190 μg g^{-1} of phenanthrene, 650 μg g^{-1} of methylphenanthrenes and 50 μg g^{-1} of chrysene) [7]

When the temperature exceeds 500 ºC, carbon–hydrogen and carbon–carbon bonds are broken to form free radicals. These radicals combine to form ethylene, acetylene and 1, 3-butadiene which further condense with aromatic ring structures, that are resistant to thermal degradation [4]. These same authors [4] discussed PAH source attribution and referred that three possible mechanisms are suggested of PAH formation during combustion, i.e. slow Diels–Alder condensations, rapid radical reactions, and ionic reaction mechanisms. However, the radical formation mechanism is favoured as the combustion process within the internal combustion engine occurs very rapidly. Gaseous hydrocarbon radicals rearrange quickly, providing the mechanism of PAH formation and growth. The addition of hydrocarbon radicals to lower molecular weight PAH then leads to the formation of higher PAH. Recently Lima *et al* [7]reviewed and discussed some of the factors (type of fuel, amount of oxygen, and temperature) that affect the production and environmental fate of combustion-derived PAH. While PAH are present at ambient temperature in air, both as gas and associated with particles, the lighter PAH, such as phenanthrene, are found almost

exclusively in gas phase whereas the heavier PAH, such as benzo[a]pyrene, are almost totally adsorbed on to particles.

Regarding PAH and biodiesel combustion, many literature works have been published [2,6,8–11], but few of them have studied its relation with the biodiesel composition [5,12–15], and none of them has compared the PAH emissions depending on the alcohol group, FAME or FAEE. Some previous works have compared regulated diesel emissions and particle size distributions from biodiesel fuels produced with different alcohols, but no analysis of PAH was included [16]

Moreover, in the last weeks, a great concern has been aroused by the information from the World Health Organisation (WHO) over the possible relationship between some types of cancer and the ingestion of processed meat in the human diet, especially if this meat has been cooked in barbecue style. In fact, when meat is cooked on a barbecue, fat drips onto the hot burning coals and forms PAH's [17]. Fats have a very similar molecular structure to biodiesel, and the internal combustion engine, the bomb calorimeter used in this work and the hot burning coals have in common a great oxygen excess, thus leading to PAH's formation by mechanisms that could be similar to those proposed in this work.

This work describes the production of PAH in the combustion of FAME and FAEE with different pure oxygen pressures in a bomb calorimeter, and it correlates the amount and type of PAH produced with the fatty acid profile of the biodiesel.

2. Experimental

2.1 Materials

Methanol and absolute ethanol were of commercial grade (Panreac) and were used without any further purification. Dichloromethane (Merck) was of HPLC grade. The catalytic

solution of sodium methoxide 25 % wt. in methanol was purchased from Across Organics. Magnesium silicate Magnesol D-60 was kindly supplied by The Dallas Group of America. Silica-gel 60 (Merck) was of 70-230 mesh ASTM (0.063-0.200 mm) size and was activated before use. Oxygen for the combustion bomb was of 99.99 % purity.

Rapeseed, soybean and palm oils and yellow animal fat were supplied by Combustibles Ecologicos Biotel SL. Coconut (Across Organics), peanut (Vitasia) and linseed (Fisher Scientific) oils were of commercial grade.

2.2 Synthesis Procedures

Degumming, esterification (if necessary) and transesterification of oils/fats have been carried out following a method previously described in the literature [18].

FAME and FAEE tests: Tables 2 and 3 show the results of some of the tests included in the EN14214 standard and carried out on the synthesized FAME and FAEE. These tables also indicate the standard procedure, the laboratory equipment used to perform the tests and the experimental errors. The EN14214 standard refers only to FAME but has been also applied to FAEE in this work, since not FAEE standard still exists.

2.3 Combustion

The higher heating values of FAME and FAEE were measured in an automatic bomb calorimeter LECO AC300, burning 1.0 g of biodiesel under different pure oxygen pressures: 689.5 kPa (100 psi), 1379.0 kPa (200 psi), 2068.4 kPa (300 psi) and 2757.9 kPa (400 psi). Once the combustion test has finished, the sample crucible and the bomb were thoroughly rinsed with dichloromethane and the combined dichloromethane extracts were passed through a Pasteur pipette half filled with silica-gel to eliminate soot particles.

In the test at 1379, 2068 and 2758 kPa of oxygen pressure, the test was repeated three times without changing nor cleaning the crucible and the bomb , in order to recover a higher amount of post-combustion products. In the test at 690 kPa the test was carried out only once, the crucible and the bomb were washed separately with dichloromethane, recovering the soot particles present in both devices, and the separated extracts were passed through silica-gel in the same way as described above. These recovering methods for PAH were taken into account when quantifying the total amount of PAH produced from each feedstock.

The cylindrical combustion bomb dimensions are 102 mm height x 59 mm inner diameter, which gives an internal volume of 0.279 L. Thus, when the internal oxygen pressure was 690 kPa, the weight of oxygen was 2.60 g and the corresponding mass of air was 10.90 g, which is almost the stoichiometric fuel / air mass ratio (see Table 4). As a consequence, the tests at 1379, 2068 and 2758 kPa were done practically with twice, three and four times the stoichiometric oxygen amounts.

2.4 PAH analysis

In this work, the post-combustion products of the biodiesel have been isolated and the PAH content has been analyzed, in order to check if there are differences between different feedstock and also between FAME and FAEE of the same feedstock with respect to the PAH formation during combustion.

All dichloromethane extracts were concentrated to 1 mL in a rotary evaporator, and they were analyzed without any further handling. Concentrated samples were charged with an internal standard (Decafluorobiphenyl, Supelco) and injected in the split mode (1 μL, three times) via automatic Agilent PTV injector in a gas chromatograph / mass spectrometer

system (GC-MS) Agilent GC 5975 - MS 7890, equipped with a capillary column HP5MS (30 m x 0.250 mm x 0.25 μm). The analytical program was: initial temperature 60 ºC, initial time 2 min, rate 5 ºC/min during 10 min, final temperature 110 ºC, final time 60 min. The column head pressure was 56.76 kPa and the analysis was carried out at constant flow (1 mL/min).

Mass spectrometer ionizing chamber was set at 70 eV in the electronic impact mode (EI), and the scan and simultaneous ion monitoring (SIM) modes of the software ChemStations from Agilent were used, scanning from 100 to 300 Da. The PAH analyzed and their characteristic ions were summarized in Table 1 and they are included in the EPA list of concern compounds; these PAH were quantified using calibration curves with standards of the 16 PAH of concern purchased from Chromlab.

Table 1: Polycyclic Aromatic Hydrocarbons analyzed

Compound	***Acronym***	***Characteristic ion***
Naphthalene	N	128
Acenaphthylene	ANI	152
Acenaphthene	ANE	154
Fluorene	FL	166
Phenanthrene	F	178
Anthracene	A	178
Fluoranthene	FLT	202
Pyrene	P	202
Benzo[a]anthracene	BA	228
Chrysene	C	228
Benzo[b]fluoranthene	BBF	252
Benzo[k]fluoranthene	BKF	252
Benzo[a]pyrene	BAP	252
Dibenzo[a,b]anthracene	DBA	278
Indeno[1,2,3-cd]pyrene	IN	276
Benzo[g,h,i]perylene	BPE	276

3. Results and discussion

3.1 Esterification and transesterification

Some oils need a previous step of esterification [18], since their acidity indexes were higher than 2 mg KOH g^{-1}; after the esterification, their acidity decreased to less than 0.2 mg KOH g^{-1}. The transesterification reaction of the oil/fat was carried out following the experimental procedure reported previously [18]. Table 2 shows the fatty ester profile of the FAME and FAEE synthesized in this work.

Table 2: Fatty ester profile of the FAME and FAEE.

Samples /methods	**C8:0** (%)	**C10:0** (%)	**C12:0** (%)	**C14:0** (%)	**C16:0** (%)	**C18:0** (%)	**C18:1** (%)	**C18:2** (%)	**C18:3** (%)	**C20:0** (%)	**C20:1** (%)	**IV**[1] $gI_2/100g$	**CN**[2]
FAME Peanut					10.1	2.9	57.6	26.3		1.4	1.7	100.0	60.3
FAME Camelina			1.1	0.5	6.2	3.1	17.5	19.1	33.6	1.6	17.3	150.7	52.7
FAME Coconut	0.1	8.8	32.2	20.5	10.9	2.9	8.3	2.4				11.3	55.3
FAME AnimalFat[3]				1.9	25.4	15.5	43.9	8.9	0.5		0.9	58.1	70.6
FAME Linseed				1.0	6.9	4.5	21.3	17.3	49.1			176.7	44.9
FAME Palm			0.3	1.0	46.0	9.7	33.5	9.1		0.3		44.7	69.9
FAEE Palm			0.3	1.0	46.0	9.7	33.5	9.1		0.3		44.7	61.9
FAME Rapeseed					5.1	9.2	59.6	17.7	6.6	0.5	1.4	100.8	58.1
FAEE Rapeseed					5.1	9.2	59.6	17.7	6.6	0.5	1.4	100.8	52.0
FAME Soybean					13.6	6.9	24.9	49.0	5.2	0.4		120.0	53.7
FAEE Soybean					13.6	6.9	24.9	49.0	5.2	0.4		120.0	51.1
FAME Soybean[4]					11.5	4.3	25.4	53.1	5.7			128.8	50.2
Standard method	EN14103											EN14214	[28]
Analytical equipment	Agilent GC6890N												

[1]Iodine value. [2]Cetane number. [3] FAME of Yellow Animal Fat has 2.9 % m/m of palmitoleic acid (C16:1), [4]FAME of reference.

3.2 Characterization of FAME and FAEE.

Several tests included in the EN 14214 standard have been carried out on the samples in order to characterize the biodiesel and they are shown in Table 3.

Table3: Properties of the FAME and FAEE.

Samples /methods	**Density** (kg m^{-3})	**Viscosity** (mm^2s^{-1})	**CP**[1] (º C)	**CFPP**[2] (º C)	**PP**[3] (º C)	**HHV**[4] ($MJkg^{-1}$)	**Colour**
FAME Peanut	872.0	4.69	+17	+10	+12	40.64	0.5
FAME Coconut	866.0	2.55	-4	-9	-7	38.63	0.5
FAME Animal Fat	889.3	5.55	+13	+10	+13	40.29	3.0
FAME Linseed	895.0	4.67	-5	+4	-8	39.75	4.0
FAME Palm	876.3	4.39	+13	+9	+12	39.61	0.5
FAEE Palm	870.2	4.45	+9	+10	+9	40.49	0.5
FAME Rapeseed	882.3	4.32	-4	-9	-13	39.53	0.5
FAEE Rapeseed	870.0	4.78	-5	-11	-16	40.59	0.5
FAME Soybean	878.0	4.16	+1	0	-2	40.33	0.5
FAEE Soybean	875.0	4.82	-1	-5	-5	40.47	0.5
Standard method	EN ISO12185	EN ISO 3104	ASTM D2500	EN ISO 116	ASTM D2500	ASTM D240	ASTM D1500
Analytical equipment	Digital DMA 48	Cannon-Fenske Proton4378	ATPMV0407	ISL FPP 5Gs	ATPM V0407	Leco AC-300	Lovibond AF 650
Experimental error	± 0.3	± 0.0013·mean (0.20 %)	< 3.0	± 1.0	< 3.0	± 0.25	± 0.50 u.c.

[1]Cloud point. [2]Cold filter plugging point. [3]Pour point. [4]Higher heating value. [5]FAME of reference.

3.2.1 Density.

Density is an important technical and economical parameter for fuels since they are usually measured by volume and sold by weight, and density relates both. Density has also influence, together with the heating value, on the fuel consumption, since the amount of fuel injected in the combustion chamber is delivered by volume. It has been reported previously [19–22]that the density of FAME and FAEE increases when (a) the chain length diminishes and (b) the number of double bonds increases. All the FAEE show density values lower than the corresponding FAME [22].

3.2.2 Kinematic viscosity at 40 ºC.

Fuel viscosity has influence over the injection and the combustion, especially at low engine operation temperatures. Biodiesel kinematic viscosity increases with the chain length of both the fatty acids and the alcohols [21]. Thus, all the FAEE show higher viscosities than the corresponding FAME without exception (Table 3), and the coconut FAME, very rich in C12:0 and C14:0 shows the lowest value of 2.55 $mm^2 s^{-1}$. Also, this property in inversely related with the number of double bonds, the higher saturation implying higher viscosities and hence, the FAME of yellow animal fat shows a value of 5.55 $mm^2 s^{-1}$ out of specification. However, the very unsaturated linseed FAME shows also a high value (4.67 $mm^2 s^{-1}$) very far from the reported value of 3.80 $mm^2 s^{-1}$ [23]. This observed fact could be due to the ageing of the biodiesel during storage, by formation of higher polymers induced by oxidative degradation [24]

3.2.3 Cold flow behaviour.

The measured properties chosen to evaluate the performance of these biodiesels at low temperature have been cloud point (CP), pour point (PP) and cold filter plugging point (CFPP). A bad performance of the biofuel at low temperatures may cause problems of handling, storage, injection and cool starting of the engine. Biodiesel shows in general poorer cold performance than fossil diesel, especially those esters with long saturated chains, which may cause problems either at ambient temperature, see the values for palm and yellow animal fat, always well above 0ºC (Table 3). The FAEE show in general better cold flow behaviour than the corresponding FAME's, as it has been reported previously [25]. The peanut FAME

shows exceedingly high values that do not match with its ester profile, probably due to the presence of food additives.

3.2.4 Higher heating value (HHV).

This property (not included in EN 14214 standard) is measured in a bomb calorimeter at constant volume, and it includes the energy released when the water vapour produced during the combustion condenses.

In general, the HHV of saturated FAME increases with the chain length [26] and it diminishes with the unsaturation degree [27]. These trends are accomplished by the most saturated FAME samples of this work: coconut (mainly C12:0 and C14:0, 38.63 MJ kg^{-1}), palm (mainly C16:0, 39.61 MJ kg^{-1}) and animal fat (mainly C18:0, 40.29 MJ kg^{-1}). And for the most unsaturated ones (between brackets the iodine value IV is given): linseed (IV 176.7, 39.75 MJ kg^{-1}), and soybean (IV 128.8, 40.30 MJ kg^{-1}).

However, all these values are lower than those of fossil diesel (around 42 MJ kg^{-1}) due to the presence of two oxygen atoms (around 11 % wt.) in the FAME and FAEE molecule; this detrimental effect is overweighed because the availability of bonded oxygen in the fuel-rich zone of the non-homogeneous mixture improves the diffusion combustion [28], specially under conditions of high charge and high fuel-air ratio.

FAEE show always higher HHV than the corresponding FAME due to the presence of an additional methylene group $–CH_2-$ in their molecules.

3.2.5 Cetane number (CN).

In this work, the cetane number of the FAME and FAEE reported has been estimated from the ester profile by the method of Lapuerta *et al* [29]. The CN increases with the chain length of both the fatty acid and the alcohol, decreases with the unsaturation degree (IV) [29,30]

and it is especially high for saturated esters. This work agrees with the literature since all FAEE show lower values than the corresponding FAME. All CN are well above the limit of 51 specified in the standard except linseed, the most unsaturated one (CN 44.9).

3.3 Combustion.

The molecular formula of FAME and FAEE was calculated from the ester profile, and their stoichiometric combustion equations are reported in Table 4 as well as the stoichiometric air / fuel mass ratio necessary for their complete combustion.

Table 4: Estimated ester molecular weight, combustion equations and stoichiometric air/fuel ratio

Samples	Mw g mol^{-1}	Combustion equation	Stoichiometric O_2/ fuel ratio
FAME Peanut	302.8	$C_{18.78}H_{35.29}O_{2.00} + 26.60\ O_2 \rightarrow 18.78\ CO_2 + 17.64\ H_2O$	2.63
FAME Coconut	233.8	$C_{14.40}H_{28.62}O_{2.00} + 20.56\ O_2 \rightarrow 14.40\ CO_2 + 14.31\ H_2O$	2.55
FAME Animal Fat	288.8	$C_{18.40}H_{35.52}O_{2.00} + 26.28\ O_2 \rightarrow 18.40\ CO_2 + 17.76\ H_2O$	2.64
FAME Linseed	292.4	$C_{18.87}H_{33.47}O_{2.00} + 26.24\ O_2 \rightarrow 18.87\ CO_2 + 16.73\ H_2O$	2.60
FAME Palm	284.1	$C_{18.06}H_{34.93}O_{2.00} + 25.79\ O_2 \rightarrow 18.06\ CO_2 + 17.47\ H_2O$	2.63
FAEE Palm	298.1	$C_{19.06}H_{36.94}O_{2.00} + 27.29\ O_2 \rightarrow 19.06\ CO_2 + 18.47\ H_2O$	2.65
FAME Rapeseed	294.3	$C_{18.89}H_{35.20}O_{2.00} + 26.69\ O_2 \rightarrow 18.89\ CO_2 + 17.61\ H_2O$	2.63
FAEE Rapeseed	308.3	$C_{19.89}H_{37.20}O_{2.00} + 28.19\ O_2 \rightarrow 19.89\ CO_2 + 18.61\ H_2O$	2.65
FAME Soybean	292.0	$C_{18.75}H_{34.55}O_{2.00} + 26.39\ O_2 \rightarrow 18.75\ CO_2 + 17.27\ H_2O$	2.62
FAEE Soybean	306.1	$C_{19.75}H_{36.55}O_{2.00} + 27.89\ O_2 \rightarrow 19.75\ CO_2 + 18.27\ H_2O$	2.64

The relative dosage Fr, defined as the ratio of the absolute dosage and the stoichiometric dosage (Equation 1), has been calculated for each test and it is around 0.28 (for the 2758 kPa tests), 0.37 (2068 kPa), and 0.57 (1379 kPa) which relate to usual partial load driving conditions in diesel engines (full load, between 0.70 and 0.80):

$$Fr = \frac{\frac{m_f}{m_a}}{\left(\frac{m_f}{m_a}\right)_{st}} \quad \text{(Equation 1)}$$

3.4 PAH analysis.

A detailed statistical analysis of the correlation between the amount of each individual PAH of concern included in the EPA list and the oxygen pressure during combustion has been carried out. Considering the tests at 1379, 2068 and 2758 kPa, A isometric logratio transformation, for compositional data [31], before to principal component analysis has been done. These Principal component analysis groups PAHs into two components or groups (Figure 1): Group 1: Fluorene, Anthracene, Fluoranthene, Crysene, Benzo[b]Perylene, Benzo[k]Perylene, Benzo[e]Pyrene, Perylene, Indene[1,2,3-cd]pyrene, Dibenzo[a,h]anthracene and Benzo[g,h,i]perylene and Group 2: Naphtalene, Phenantrene, Benzo[a]anthracene, Benzo[a]Pyrene and Pyrene.

FAME and FAEE molecules are not consumed on combustion by thermal decomposition to any appreciable degree, but primarily by abstraction of the H atoms by OH· and H· radicals [32]. The most labile H atoms are the α-hydrogen atoms respect to the ester group, because the resulting radicals are stabilized by resonance. This more stable radical decomposes later to a stable acrylic ester molecule and a (R-CH_2·) radical that can propagate the chain reaction by β-elimination process. The major PAH and soot precursors in the flame are acetylene, ethylene, propylene and 1,3-butadiene formed from the R-CH_2· radicals by the β-elimination mechanism. Scheme 1 shows this decomposition mechanism for methyl laurate C12:0, the major FAME in coconut biodiesel. Unfortunately the mass/charge ratio (m/z) in the mass spectra for alkyl acrylates is 86 Da (methyl) and 100 Da (ethyl) and the m/z ratio for the

dichloromethane solvent is 85 Da and thus the mass spectra start their scanning at 100 Da (Table 1) to avoid solvent interferences, making impossible the acrylates detection, the lighter compounds identified in the chromatograms are the xylene family, however they couldn't be quantified since no alkyl-PAH standards were introduced pior to the analysis. The formation of the acrylic ester in the initial fragmentation step could explain that there are no differences in the amount and type of PAH formed between FAME and FAEE as observed in this work.

The 1,3-butadiene and ethylene formed could explain the formation of benzene, naphthalene, anthracene and phenanthrene by Diels–Alder reaction and later aromatization (Scheme 2). The formation of higher PAH could also be explained by the Diels-Alder reaction of the precedent lighter PAH and ethylene coming from the β-elimination mechanism and subsequent aromatization of the naphthenic–aromatic hydrocarbon formed, having oxygen as the hydrogen acceptor to produce water in the combustion (Scheme 3). This mechanism could also explain that the main factor governing the PAH formation is the excess oxygen over the stoichiometric combustion value Fr [33]

The intermediate **1** (Scheme 2) 1, 4, 5, 6, 7, 8, 9, 10-octahydronaphthalene seems to be a key compound in the PAH's formation scheme. It can evolve towards naphthalene (the most abundant PAH in all experiments) but it can give alternatively anthracene (naphthalene and anthracene are at the far opposite ends of axes in Figure 1, -y and +x respectively). The compound **1** can also isomerize to 3, 4, 5, 6, 7, 8, 9, 10-octahydronaphthalene **2** that evolves later to phenanthrene which is a PAH placed in a third axis (+y) of Figure 1 but closer to the center, opposite to both naphthalene and anthracene. It is still unclear what is the reason that makes intermediate **1** evolve towards the +x, +y or –y axes of Figure 1, but it is clear from

the statistical analysis that they are alternative evolution pathways for PAH's formation, not simultaneous ones. .

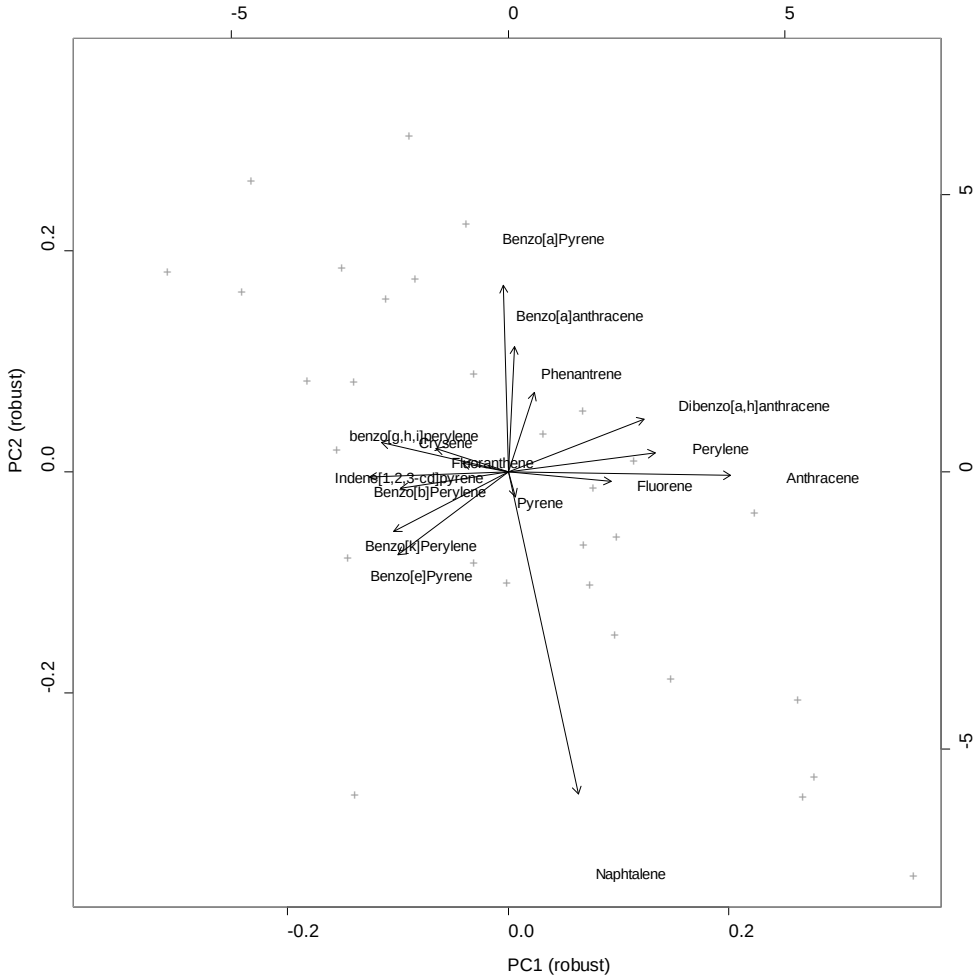

Figure 1 Component Analisys results

The tricyclic light PAH's anthracene and phenanthrene continue evolving towards the formation of heavier PAH's through Diels-Alder type cycloadditions. Phenanthrene and pyrene are in opposite axes of Figure 1 but closer to the origin. This behaviour could be explained because pyrene forms from phenanthrene by cycloaddition of ethylene; either phenanthrene remains or it reacts further to form pyrene.

The intermediate compound **3** 1,4-dihydrobenzo[a]anthracene seems also a key compound since it can oxidize to benzo[a]anthracene.(BaA) which reacts further with ethylene to form benzo[a]pyrene (Scheme 3); thus both compounds are placed in the same axis (+y) in a consecutive position and orthogonal to anthracene, that is, either anthracene persists (+x axis) or it reacts further (+y axis) to form benzo[a]anthracene and benzo[a]pyrene in this order. Dibenzo[a, h]anthracene (DBA) has as precursor benzo[a]anthracene (BaA) and both does not form simultaneously, although in this case the selectivity is not so great because DBA is in the bisector and not orthogonal to BaA. The same scheme happens with pyrene and benzo[e]pyrene, the second coming from the first by Diels-Alder cycloaddition, and thus pyrene is in the –y axis of Figure 1 and benzo[e]pyrene is in the bisector –x-y, not totally orthogonal to pyrene.

Another clear predominant direction in Figure 1 placed dibenzo[a, h]anthracene and perylene (bisector +x-y) opposite to benzo[k]perylene and benzo[e]pyrene (bisector –x-y). Perylene forms in a totally different way, by concerted cycloaddition of two naphthalene molecules through a 6-centers intermediate and of course it appears orthogonally (+x) to naphthalene (-y). Either perylene persists or it reacts with 1,3-butadiene to form benzo[k]perylene, so this latter and perylene appear in almost opposite bisector directions in Figure 1.

The total amount of PAH produced during combustion could be estimated from the following exponential equation:

$$Log(PAH_x) = -a \times Fr - b \times SAT - c \times Log(IV)$$

Where PAH_x is the total estimated amount of PAH, Fr is relative dosage in the combustion vessel during the combustion experiment as defined in equation 1, SAT is the percentage of

saturated fatty esters, IV is Iodine Value and a, b and c are the regression coefficients. The great difference between group 1 and group 2 is that in the group 1 the coefficients b and c are equal to zero or, in the same sense, there is not a significative influence of SAT and IV in this group of PAHs. While in the group 2 these coefficients aresignificantly different to zero. Table 5 summarizes the values of these coefficients and the R^2 and Fischer F-statistic for two models that have been tested. The models have significant values of the F-statistic and the most meaningful parameter is the Fr: the total amount of PAH decreases with this Fr value, that is, with the decreasing amounts of oxygen in the combustion vessel. Mainly in the model for group 1 where only the coefficient of this parameter is significantly different to zero. In model for group 2, the PAH amount produced decreases also with the percentage of saturated fatty esters, Finally, the third term of the equation indicates an inverse relationship between PAHs and IV or, rather, with increasing IV value decreases the total amount of PAHs of group 2.

Figure 2 shows the estimated amount of total heavy PAH (group 1) as a function of the relative dosage, Fr; this amount increases exponentially as explained above.

Figure 3 shows the total estimated amount of total light PAH less (group 2) as a function of the relative dosage, Fr and the iodine value, IV, the most significant variable that is also an exponential curve as explained above. In this figure, three groups of biodiesel types could be observed. The coconut FAME is the most PAH-producing biodiesel, clearly above the rest: the main distinctive characteristics of this FAME are its high saturation degree (IV = 11.3) and the short range of fatty acids chains (> 76.1 % m/m of FAME's with less than C14:0). The second group of most PAH-producing biodiesel includes palm FAME and palm FAEE: in these cases, the saturation degree is also high (IV = 44.7) but the fatty acids chains

are longer (palm, > 98.1 % m/m longer than C18:0). The group of least PAH-producing biodiesel includes all the most unsaturated biodiesel. No differences were found between FAME and FAEE for their capacity to produce PAH during combustion; this fact agrees well with the PAH formation mechanism described below, since the initial fragmentation breaks the ester group.

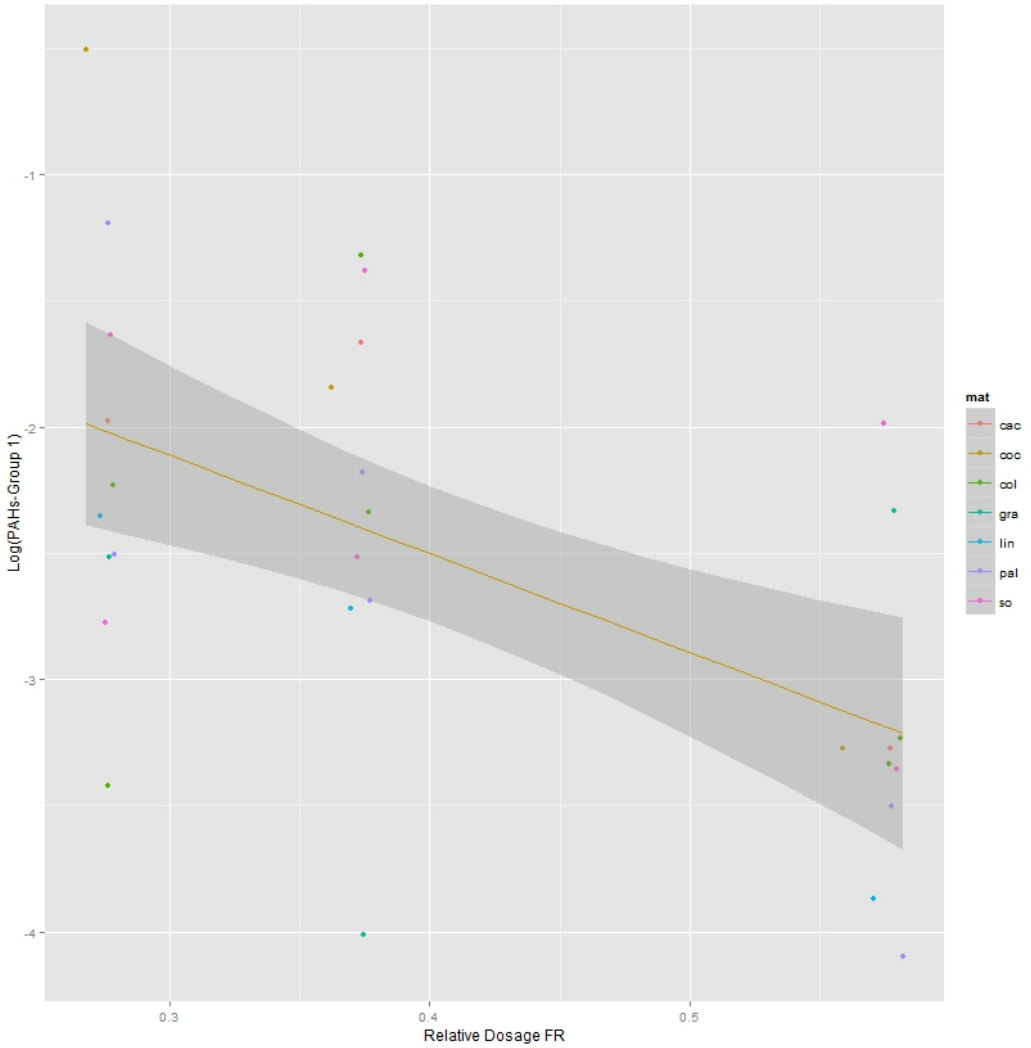

Figure 2 Total group 1 PAH concentration produced as a function of the relative dosage FR

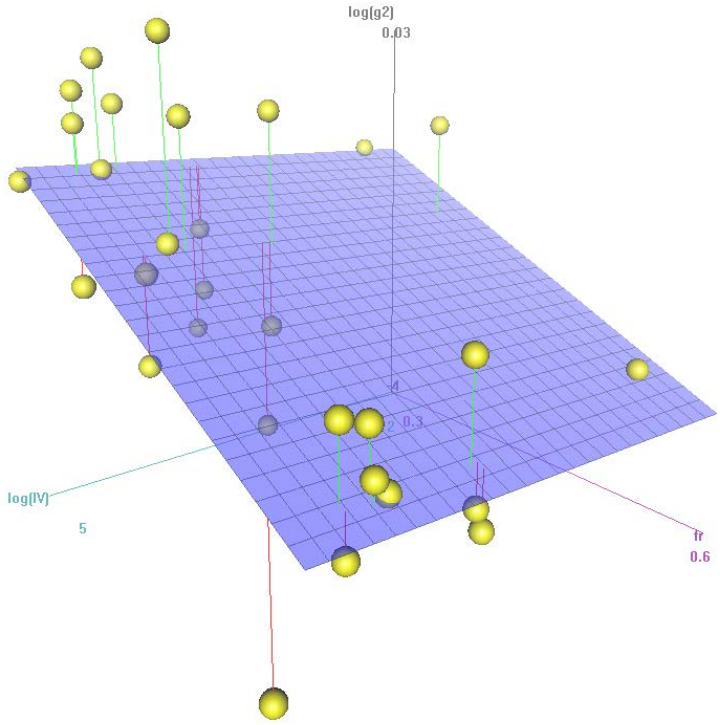

Figure 3 Total group 2 PAH concentration produced as a function of the Iodine Value IV and the relative dosage Fr.

Finally, Figure 4 summarizes the final factor in equation 2 that combines the two precedent ones Fr, IVb and SAT. Also three groups of PAH-producing biodiesel could be identified: a) coconut FAME; b) palm FAME and FAEE and finally c) the group of the least PAH-producing biodiesel split in various sub-groups because in these cases the different oxygen pressures are taken into account.

The mechanism outlined in Scheme 1 could explain also the formation and profile of n-alkanes observed in all the chromatograms by combination of two linear radicals R-CH_2· being n-$C_{29}H_{60}$ the most abundant n-alkane (around 9 x 10^6 counts) in all cases (Figure 5 shows this n-alkanes profile for the combustion of soybean FAEE under 2068 kPa of oxygen).

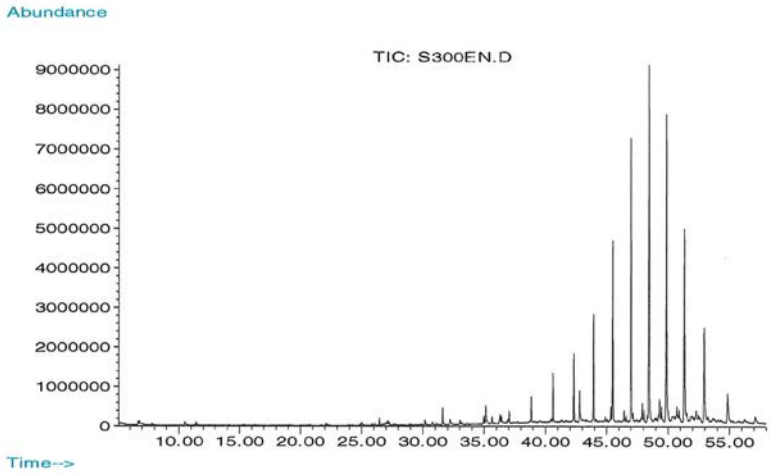

Figure 5 Total ion chromatogram of the combustion product of FAEE from soybean burnt at 2068 kPa oxygen pressure.

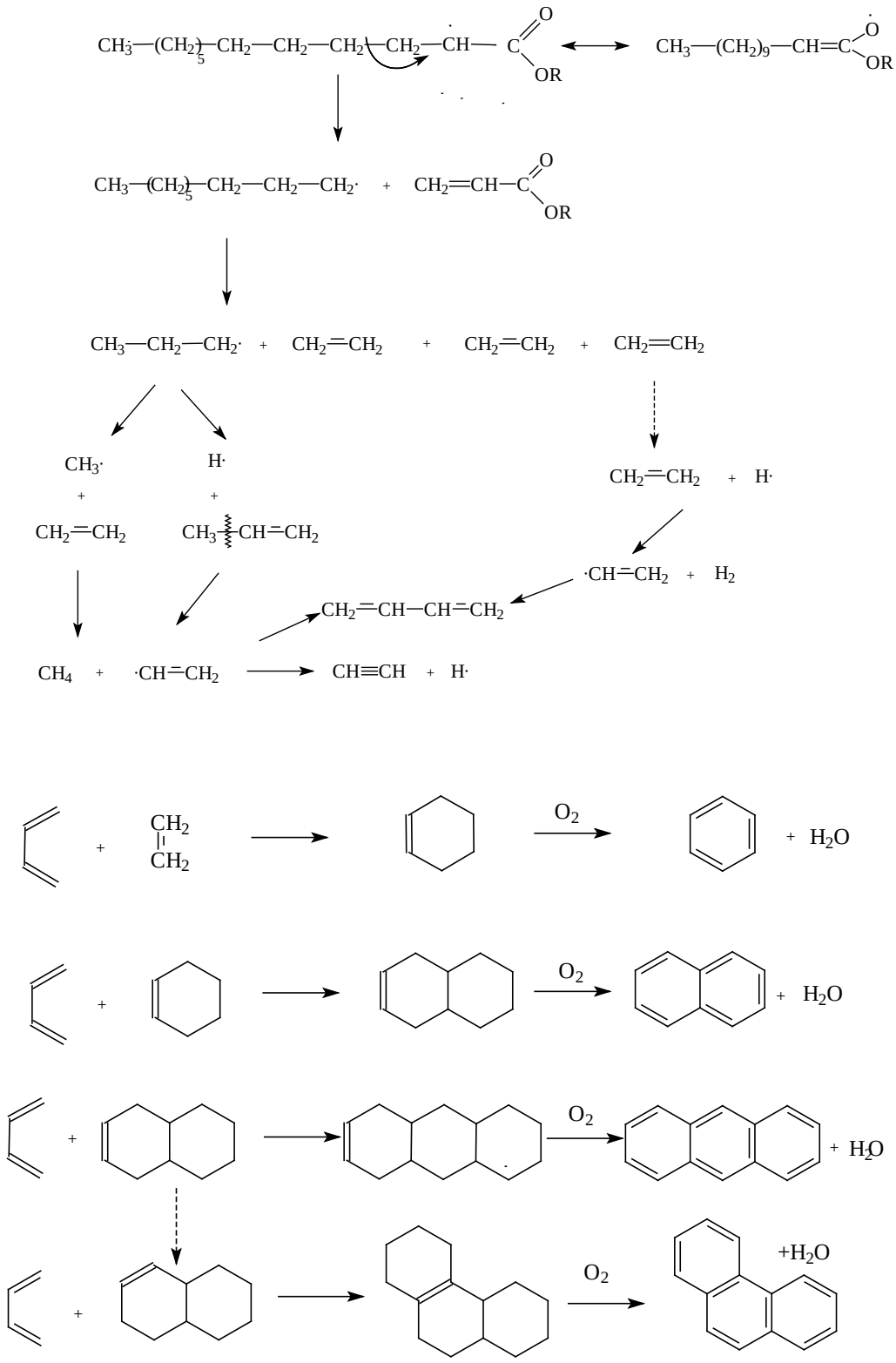

Scheme 1 and 2 Proposed decomposition mechanism of C12:0 saturated esters in the combustion process and proposed mechanism of formation of light PAH (benzene, naphthalene, anthracene and phe-nanthrene) by Diels-Alder reaction and aromatization.

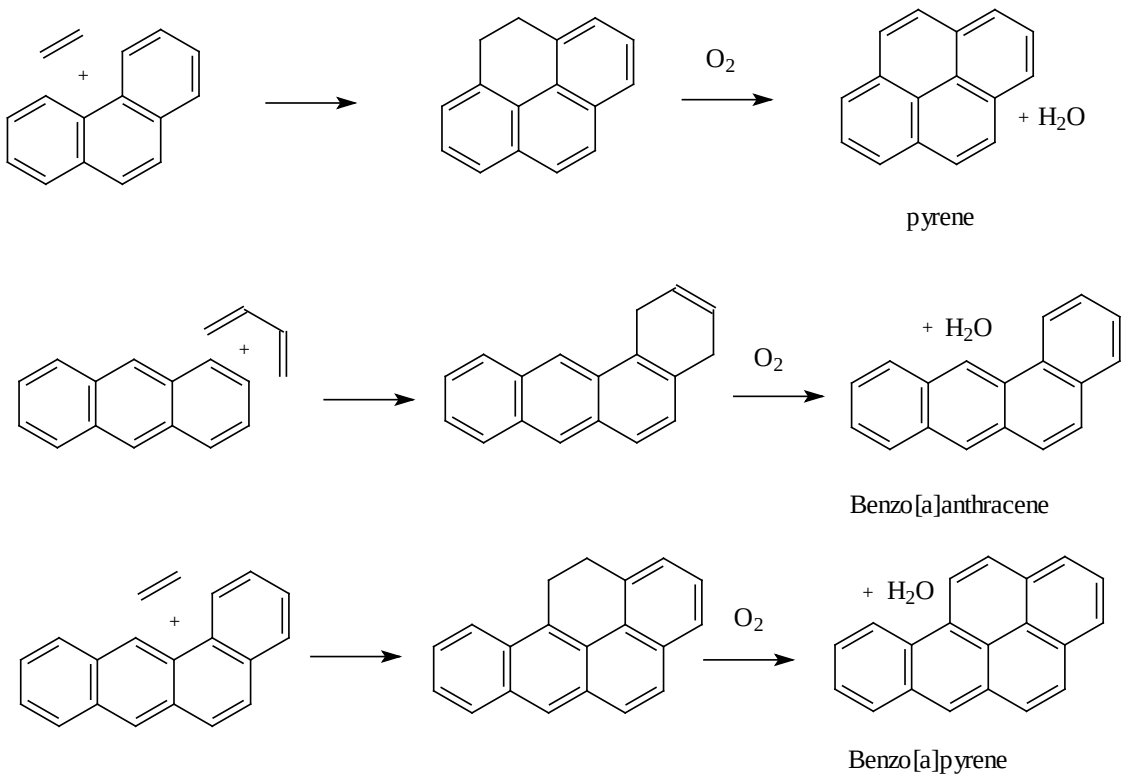

Scheme 3 Proposed mechanism of formation of heavy PAH (pyrene, benzo[a]anthracene and benzo[a]pyrene) by Diels-Alder reaction and aromatization.

The main ester components of the unsaturated biodiesel are alkyl oleate and alkyl linoleate. The structure of this last one is depicted in Scheme 4 to illustrate the changes in the mechanism outlined in Scheme 1 for this unsaturated esters: after the fragmentation of the acrylic ester and two ethylene molecules by β-elimination, the allylic radical formed is stabilized by resonance avoiding the propagation of the β-elimination mechanism and later the production of ethylene, essential compound as explained in Scheme 2 for the formation of higher PAH. This stable allyl radical could also decompose to give 1,3-butadiene but the unstable vinyl radical formed also makes this pathway less probable. This fact would explain the lower formation of PAH in the combustion of more unsaturated biodiesel by the term SAT in equation 2.

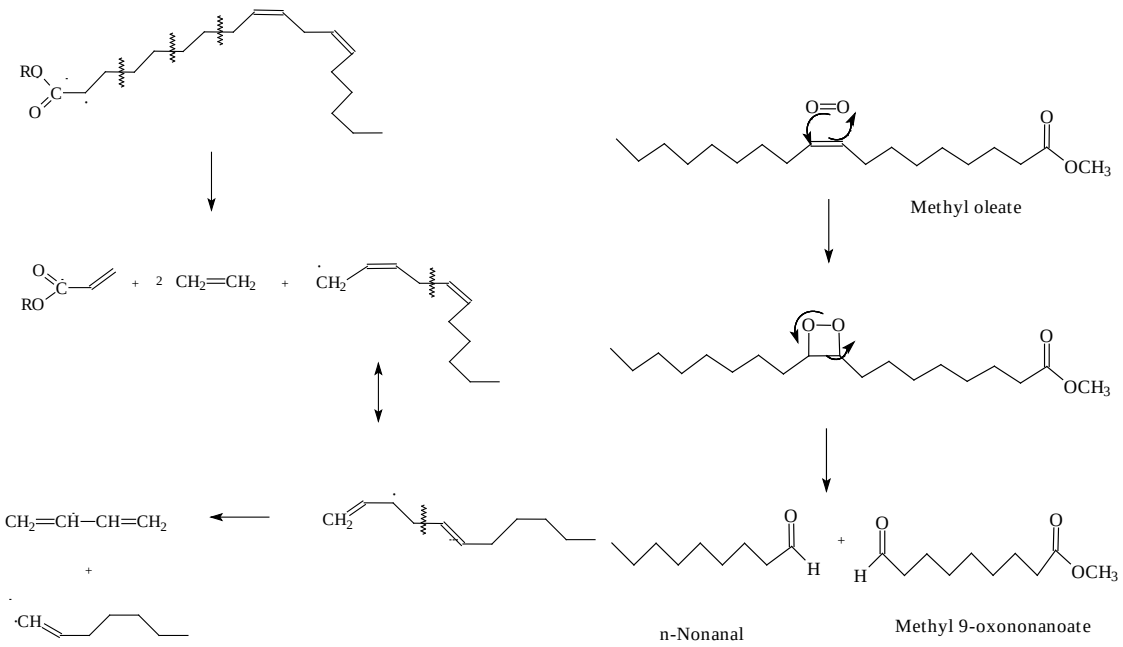

Scheme 4 and 5 Proposed decomposition mechanism of C18:2 unsaturated esters in the combustion process and proposed mechanism of oxygen cycloaddition to methyl oleate.

In reference [5]another Diels-Alder possible mechanism is proposed that may lead to PAH occurrence. This mechanism implies two FAME molecules that react to combine into a cyclohexene ring attached to four radicals forming a dimer FAME. However, the authors think that this mechanism is highly improbable because of the great size of the FAME or FAEE molecules and the low chance to adopt the six carbon atoms transition state necessary for the concerted Diels-Alder reaction. However, a more probable cycloaddition reaction is the 2 +2 cycloaddition of the abundant oxygen molecule to the unsaturated esters like oleate to form a dioxetane (Scheme 5). The breaking of this dioxetane led to n-nonanal and methyl 9-oxononanoate (around 18 x 10^3 counts in the GC-MS), both detected in the mass spectra (see Supplementary material).

4. Conclusions

In this work twelve different biodiesel have been burned in a bomb calorimeter in order to assess the PAH amounts formed depending on their sources and type of alcohol under four different oxygen abundance conditions.

An exponential model has been constructed to explain the formation of PAH where the most significant variables are the relative dosage, the iodine value and the percentage of saturated esters in the biodiesel. These PAH tend to show two different behaviors when statically grouped that may relate to heavy or light PAH formation.

No statistical differences were found between FAME and FAEE in their ability to produce PAH on combustion under these experimental conditions.

5. Acknowledgements

We wish to thank to the Laboratory of Fuels and Petrochemistry of the Gómez-Pardo Foundation (Technogetafe Scientific Park, Universidad Politécnica de Madrid), and to Miguel Cobo, formerly with the company Combustibles Ecológicos Biotel SL, for the gift of rrapeseed, soybean and palm oils. We also thank Marta del Campo Villanueva for their technical contribution to this work.

6. References

[1] Rhead, M. M.; Hardy, S. A. The sources of polycyclic aromatic compounds in diesel engine emissions. *Fuel* **2003**, *82*, 385–393.

[2] Borrás, E.; Tortajada-Genaro, L. A.; Vázquez, M.; Zielinska, B. Polycyclic aromatic hydrocarbon exhaust emissions from different reformulated diesel fuels and engine operating conditions. *Atmos. Environ.* **2009**, *43*, 5944–5952.

[3] Tavares, M.; Pinto. J. P.; Souza, A. L.; Scarminio, I. S.; Solci, M. C. Emission of polycyclic aromatic hydrocarbons from diesel engine in a bus station, Londrina, Brazil. *Atmos. Environ.* **2004**, *38,* 5039–5044.

[4] Ravindra, K.; Sokhi, R.; Van Grieken, R. Atmospheric polycyclic aromatic hydrocarbons: Source attribution, emission factors and regulation. *Atmos. Environ.* **2008**, *42*, 2895–2921.

[5] Karavalakis; G.; Deves, G.; Fontaras, G.; Stournas, S.; Samaras, Z.; Bakeas, E. The impact of soy-based biodiesel on PAH, nitro-PAH and oxy-PAH emissions from a passenger car operated over regulated and no regulated driving cycles. *Fuel* **2010**, *89(12),* 3876–3883.

[6] Karavalakis, G.; Bakeas, E.; Fontaras, G.; Stournas, S. Effect of biodiesel origin on regulated and particle-bound PAH (polycyclic aromatic hydrocarbon) emissions from a Euro 4 passenger car. *Energy* **2010**, *36 (8),* 5328–5337.

[7] Lima, A. L. C.; Farrington, J. W.; Reddy, C. M. Combustion Derived Polycyclic Aromatic Hydrocarbons in the Environment-A Review. *Environmental Forensics* **2005**, *6 (2),* 109 – 131.

[8] Correa, S. M.; Arbilla, G. Aromatic hydrocarbons emissions in diesel and biodiesel exhaust. *Atmos. Environ.* **2006**, *40*, 6821–6826.

[9] Fontaras, G.; Karavalakis, G.; Kousoulidou, M.; Tzamkiozis, T.; Ntziachristos, L.; Bakeas, E.; Stournas, S.; Samaras, Z. Effects of biodiesel on passenger car fuel consumption, regulated and non-regulated pollutant emissions over legislated and real-world driving cycles. *Fuel* **2009**, *88,* 1608–1617.

[10] Lai, J. Y.W.; Lin, K. C.; Violi, A. Biodiesel combustion: advances in chemical kinetic modelling. *Prog. Energ. Combust. Sci.* **2011**, *37 (1),* 1-14.

[11] Lin, Y.C.; Hsu, K.H.; Chen, C.B. Experimental investigation of the performance and emissions of a heavy-duty diesel engine fueled with waste cooking oil biodiesel/ultra-low sulphur diesel blends. *Energy* **2010**, *36(1)*, 241-248.

[12] Tsai, J.H.; Chen, S.J.; Huang, K.L.; Lin, Y.C.; Lee, W.J.; Lin, C.C.; Lin, W.Y. PM, carbon, and PAH emissions from a diesel generator fuelled with soy-biodiesel blends. *J. Hazard. Mater.* **2010**, *179*, 237–243.

[13] Karavalakis, G.; Bakeas, E.; Fontaras, G.; Stournas, S. An experimental study on the impact of biodiesel origin on the regulated and PAH emissions from a Euro 4 light-duty vehicle. *Fuel* **2011**, *90*, 3200–3208.

[14] Karavalakis, G.; Boutsika, V.; Stournas, S.; Bakeas, E. Biodiesel emissions profile in modern diesel vehicles. Part 2: Effect of biodiesel origin on carbonyl, PAH, nitro-PAH and oxy-PAH emissions. *Sci. Total Envir.* **2011**, *409 (4)*, 738-747.

[15] Ballesteros, R.; Hernández, J.J.; Lyons, L.L. An experimental study of the influence of biofuel origin on particle-associated PAH emissions. *Atmos. Environ.* **2010**, *44*, 930-938.

[16] Lapuerta, M; Herreros, J.M.; Lyons, L.L.; García-Contreras, R.; Briceño, Y. Effect of the alcohol type used in the production of waste cooking oil biodiesel on diesel performance and emissions. *Fuel* **2008**, *87*, 3161–3169.

[17] A. Brunning, Chemical & Engineering News, July 13th 2015, p.30

[18] Canoira, L.; Rodríguez-Gamero, M.; Querol, E.; Alcántara, R.; Lapuerta, M.; Oliva, F. Biodiesel from Low-Grade Animal Fat: Production Process Assessment and Biodiesel Properties characterization. *Ind. Eng. Chem. Res.* **2008**, *47*, 7997–8004.

[19] Worgetter, M.; Prankl, H.; Rathbauer, J. Eigenschaften von Biodiesel. Landbazforschung Volkenrode. Sonderhefl 190 (Biodiesel-Optimiemngspotentiale und Umwelteffekte). **1998**, 31-43.

[20] Mittelbach, M.; Worgetter, M.; Pernkopfy, J; Junek, H. Diesel fuel derived from vegetable oils: preparation and use of rape oil methyl ester. *Energy Agric.* **1983**, *2*, 369-384.

[21] Knothe, G. Einfluss der Struktur von Fettstiurealkylestern auf die Kraftstoffeigenschaften des Biodiesels. Biodiesel: Potenziale, Umweltwirkungen, Praxisetfahrungen. Braunschweig. Ed. Munack, A. and Krahl, J. Landbauforschung Volkenrode **2002**, 115-124.

[22] Lapuerta, M.; Rodriguez-Fernandez, J.; Armas, O. Correlation for the estimation of the density of fatty acid esters fuels and its implications. A proposed Biodiesel Cetane Index. Chemistry and Physics of Lipids **2010**, *163*, 720–727.

[23] Srivastava, A.; Prasad, R. Triglyceride-based diesel fuels. *Renew. Sustain. Energy Rev.* **2000**, *4*, 111-133.

[24] Canakci, M.; Monyem, A.; Van Gerpen, J. Accelerated Oxidation Processes in Biodiesel. *Trans. ASAE* **1999**, *42 (6)*, 1565-1572.

[25] Foglia, T.A.; Nelson, L.A.; Dunn, R.O.; Manner, W.N. Low-Temperature Properties of Alkyl Esters of Tallow and Grease. *J. Amer. Oil Chem. Soc.* **1997,** *74 (8)*, 951-955.

[26] Klopfenstein, W. E.; Walker, H.S. Efficiencies of Various Esters of Fatty Acids as Diesel Fuels. *J. Amer.Oil Chem. Soc.* **1983,** 60 (8), 1596-1598.

[27] Freedman, B.; Bagby, M. O. Heats of Combustion of Fatty Esters and Triglycerides. *J. Amer.Oil Chem. Soc.* **1989**, *66 (11)*, 1601-1605.

[28] Adi, G.; Hall, C.; Snyder, D.; Bunce, M.; Satkoski, C.; Kumar, S. *et al*. Soy-biodiesel impact on NOx emissions and fuel economy for diffusion-dominated combustion in a turbo-diesel engine incorporating exhaust gas recirculation and common rail fuel injection. *Energ. Fuel.* **2009,** *23(12),* 5821–5829.

[29] Lapuerta, M.; Rodriguez-Fernandez, J.; Font de Mora, E. Correlation for the estimation of the cetane number of biodiesel fuels and implications on the iodine number. *Energy Policy* **2009**, *37*, 4337–4344.

[30] Knothe, G.; Dunn, R. O.; Bagby, M. O. Biodiesel: The Use of Vegetable Oils and Their Derivatives as Altemative Diesel Fuels. **1997**. *www. biodiese/.org/resources!reportsdatahase/reportslgenl gen-162.pdf*

[31] Egozcue JJ, Pawlowsky-Glahn V, Mateu-Figueras G, Barceló-Vidal C. Isometric Logratio Transformations for Compositional Data Analysis. *Math. Geol.* 35(3), 279–300 (2003).

[32] Westbrook, C. K.; Pitz, W. J.; Curran, H. J. *J. Phys. Chem. A* **2006**, *110,* 6912–6922.

[33] Sánchez, N. Z.; Callejas, A.; Millera, A.; Bilbao, R.; Alzueta, M. U. Influence of the Oxygen Presence on Polycyclic Aromatic Hydrocarbon (PAH) Formation from Acetylene Pyrolysis under Sooting Conditions. *Energ. Fuel.* **2013**, *27*, 7081−7088.

6.2 Smoke point and oxygen extended sooting index of biokerosenes

With the same concern in mind, but following a different approach, the author has developed a method to evaluate the soot formation in the combustion of the blends of FAME with aviation kerosene that have been described in the previous papers.

Clearly, the presence of oxygen in the composition of a kerosene blend lowers the soot formation, this decrease is best shown with a new parameter developed by the research group to wich the autho belongs, the Oxygen Extended Sooting Index (OESI) than just with the result of the classical smoke point test.

Less soot involves les PAH formation that relates this paper with the scope of this thesis, focused in its last part on PAH.

energy&fuels

Article

pubs.acs.org/EF

Oxygen Extended Sooting Index of FAME Blends with Aviation Kerosene

Alberto Llamas,[‡] Magín Lapuerta,*[,†] Ana-María Al-Lal,[‡] and Laureano Canoira[‡]

[†]Grupo de Combustibles y Motores, Escuela Técnica Superior de Ingenieros Industriales, Universidad de Castilla La Mancha, Avda. Camilo José Cela s/n, 13071 Ciudad Real, Spain

[‡]Department of Chemical Engineering & Fuels, Escuela Técnica Superior de Ingenieros de Minas, Universidad Politécnica de Madrid, Ríos Rosas 21, 28003 Madrid, Spain

ABSTRACT: The use of biofuels in the aviation sector has economic and environmental benefits. Among the options for the production of renewable jet fuels, hydroprocessed esters and fatty acids (HEFA) have received predominant attention in comparison with fatty acid methyl esters (FAME), which are not approved as additives for jet fuels. However, the presence of oxygen in methyl esters tends to reduce soot emissions and therefore particulate matter emissions. This sooting tendency is quantified in this work with an oxygen-extended sooting index, based on smoke point measurements. Results have shown considerable reduction in the sooting tendency for all biokerosenes (produced by transesterification and eventually distillation) with respect to fossil kerosenes. Among the tested biokerosenes, that made from palm kernel oil was the most effective one, and nondistilled methyl esters (from camelina and linseed oils) showed lower effectiveness than distilled biokerosenes to reduce the sooting tendency. These results may constitute an additional argument for the use of FAME's as blend components of jet fuels. Other arguments were pointed out in previous publications, but some controversy has aroused over the use of these components. Some of the criticism was based on the fact that the methods used in our previous work are not approved for jet fuels in the standard methods and concluded that the use of FAME in any amount is, thus, inappropriate. However, some of the standard methods are not updated for considering oxygenated components (like the method for obtaining the lower heating value), and others are not precise enough (like the methods for measuring the freezing point), whereas some alternative methods may provide better reproducibility for oxygenated fuels.

1. INTRODUCTION

The aviation companies are facing two problems that argue in favor of biofuels: the rising cost and price volatility of traditional fuels and the environmental concerns. According to the International Air Transport Association (IATA), the global market for jet fuel represents a 10% slice of all transportation fuels (64 billion gallons/year). The conventional jet fuel's cost has been soaring; in 2010 airlines spent 139 billion US dollars ($) on jet fuel, an 11% increase over the previous years, but the fuel itself was 30% more expensive; however, gains in jet fuel hedging and efficiency overcome part of this increase. Jet fuel costs represent around 30% of operating expenses for airlines on average, up from 14% in 2003. A typical large airline consumes 11 million gallons a day, at a cost of $35 million/day ($25000/minute). An increase of one dollar in the crude barrel price costs this company some additional $100 million a year.[1]

Aircraft emissions of carbon dioxide, water and nitrogen, carbon monoxide, hydrocarbons, sulfur oxides, sulfates, and airborne particles have different effects depending of the height of emission. At ground level, aircraft emissions at large airports are important sources of local and regional air pollution including hydrocarbons and fine particulate matter which can increase the people's risk of heart disease and asthma.[2] At flight height these emissions have impacts in both tropospheric chemistry and global warming.[3,4] According to the Aerial Transport Action Group,[5] around 2000 world airlines transport actually more than 2 billion passengers per year in a fleet of around 23000 airplanes, with a prediction of doubling the number of passengers for the year 2031.[6] Transportation in general is responsible for 23% of world greenhouse gas emissions, and the aviation sector shares 12% of the total carbon dioxide emissions (670 Mt in 2012) while the road transport accounts for 74%. The emissions of an airplane turbine are the results of the combustion process of the jet fuel, and it is here where the use of renewable or more efficient fuels could diminish these emissions without the need to modify substantially the turbine design.

On the other hand, the European Parliament and Council agreed that all flights leaving or landing in EU airports starting from January 2012 should be included in the European Union Emissions Trading System (EUTS, EU Directive 2008/101/CE),[7] and this Directive was transposed by the Spanish law 13/2010.[8] Thus, in 2013 the aviation sector should reduce their emissions to 95% of the mean values registered in the period 2004−2006. However, some US airlines have issued a lawsuit before the European Court of Justice based on the fact that this EU action violates a long-standing worldwide aviation treaty, the Chicago convention of 1944, and also the Chinese, Indian, and Russian airlines have rejected paying the EU carbon dioxide tax.[9]

Received: August 13, 2013
Revised: October 3, 2013
Published: October 3, 2013

dx.doi.org/10.1021/ef401623t | *Energy Fuels* 2013, 27, 6815−6822

On September 22nd 2012, the US Senate passed unanimously a law (S. 1956) that would authorize the Transportation Department to prohibit US airlines from participating in the EU's cap-and-trade system for greenhouse gas emissions. Also, the House of Representatives passed a measure (H.R. 2594) similar to the above.[10]

The International Civil Aviation Organization (ICAO), a United Nations agency that regulates air travel, in its Global Framework Alternative Air Fuels (GFAAF) initiative and resolution A37-19 propose a 2% increase in the air fuel efficiency for 2020, and an additional 2% from 2020 to 2050, calculated on the basis of fuel volume per ton-km transported.[11]

In Spain, the Biokerosene Spanish Initiative proposed to produce 200000 t/year of biokerosene in 2020 (2−4% of total fuel consumption) [12] in the frame of the European program Enterprise 2020.

Trying to face this situation, the aviation companies are seriously considering the use of alternative jet fuels to reduce greenhouse gas emissions and to lower their costs. However, some of the properties of these alternative jet fuels should fulfill extraordinarily strict limits to guarantee the safety of passengers and planes during the flights.[13] The literature on the production and use of FAME for the aviation sector is still scarce and in some cases contradictory. The properties of a fuel obtained blending 10−30% vol. of soybean FAME with JP-8 and JP-8+100 were studied by Dunn.[14] The oxidation behavior of a blend of 20% vol. rapeseed FAME with Jet-A1 was examined by Dagault and Gail.[15] Korres et al.[16] compared the behavior of the jet fuel JP-5 against fossil diesel and animal fat biodiesel in a diesel engine. Six FAME's from jatropha, croton, calodendrum, coconut, sunflower, and soybean were prepared by Wagutu et al.,[17] and they concluded among other findings that the coconut FAME is the one that approaches most closely to the fossil jet fuel properties. Other alternative fuels from biological sources, such as Fischer−Tropsch (FT) and synthetic paraffinic kerosenes of biological origin (Bio-SPK), have also been used for blending with fossil kerosenes,[18−22] but not being related with FAME, they are not discussed here.

American Society for Testing Materials has recently published the approved methods for the production of alternative jet fuels that are basically the Fischer−Tropsch hydroprocessed synthesized paraffinic kerosene (FT-SPK) and the hydroprocessed esters and fatty acids (HEFA).[23] The actual situation of the production of renewable jet fuels, including the feedstock, the jet fuel input, and the technology used, has been clearly summarized recently,[1] with a predominance of the HEFA technology over the alcohol-to-jet or pyrolysis-to-jet and FT technologies. However, all these alternative jet fuels have a common drawback: they do not have any oxygen in their molecular structures since fatty acid methyl esters (FAME) are not approved as additives. The maximum allowable level is 5 mg/kg, which is accepted by approval authorities as the functional definition of "nil addition".[23] However, the presence of oxygen in a fuel has two main advantages: (a) it reduces the carbon content of the fuel, which in turn would reduce its carbon footprint, and (b) it reduces also the soot formation (emission) of the fuel. Numerous studies both experimental and numerical confirmed that oxygenated fuel additives reduce soot formation in engines.[24] Moreover, a study has found that particulate matter emissions from a plane's engine can fall by almost 40% when jet fuel was blended with oxygenated fuels.[2]

The objective of this paper is to quantify the potential of FAME blends to reduce the sooting tendency of kerosenes and to rebut a recent criticism[25] about the use of any type of FAME in any amount in the aviation fuels. The reduction in sooting tendency, together with other benefits derived from other properties reported in previous works,[26,27] makes FAME blends an option as aviation fuels, which is at least worthy to be considered.

2. EXPERIMENTAL SECTION

2.1. Materials. Camelina seeds were supplied by the Laboratory of Fuels & Petrochemistry of the Gomez-Pardo Foundation, refined coconut oil (CAS No. 8001-31-8) was purchased from Acros Organics, refined linseed oil (CAS No. 8001-26-1) was purchased from Fischer Scientific, and crude palm kernel and crude babassu oils were supplied by Combustibles Ecologicos Biotel SL. Two different kerosene fuels of fossil origin were used to prepare the blends with biokerosenes: K1 was a straight-run atmospheric distillation cut kerosene, subjected to hydrotreating to remove sulfur compounds, without any additives; K2 was a commercial Jet-A1 with additives, used for civil aviation. Both samples of fossil kerosene were obtained from the Spanish Compañía Logística de Hidrocarburos (CLH).

Additionally to the oils used in the studies presented in previous refs 26 and 27, linseed oil was also selected as an interesting feedstock for biokerosene production for its average low-chain acids together with its degree of unsaturation. Extraction of camelina oil and production of biokerosenes from camelina, coconut, palm kernel, and babassu through esterification (depending on the oil acidity), transesterification (in all cases), and distillation (except in the camelina and linseed cases) was described in previous refs 26 and 27. The procedure for linseed methyl ester was similar to that described for camelina oil, already described in ref 28, and, therefore, it will not be detailed here.

The biokerosene fractions of the biodiesel fuels were obtained by fractional distillation using a 41 cm long × 3.5 cm od Vigreux column. The distillation was carried out at 2 torr (2.67 hPa) using a rotary vacuum pump, and the boiling point ranges of the biokerosenes were converted to atmospheric equivalent temperature (AET) of distillation using the procedure recently described.[29] Table 1 shows the FAME profiles of the biokerosenes from babassu (BBK100), camelina (CAM100), coconut (CBK100), linseed (LIN100), and palm kernel (PBK100).

Table 1. FAME Profiles of the Biokerosenes

FAME, % wt	coconut	palm kernel	babassu	camelina	linseed
methyl caprylate, C8:0	17.3	3.6	13.3		
methyl caprate, C10:0	7	3.5	11.3		
methyl laurate, C12:0	66.7	90.8	69.3	0.8	
methyl myristate, C14:0	8.9	2.1	5.6	0.4	
methyl palmitate, C16:0	0.1		0.6	5.8	5.9
methyl stearate, C18:0				3.0	4.1
methyl oleate, C18:1				15.8	19.1
methyl linoleate, C18:2				18.9	17.2
methyl linolenate, C18:3				34.0	53.5
methylarachidate, C20:0				1.5	
methyl cis-11-eicosenoate C20:1				16.0	
methyl behenate, C22:0				2.2	
methyl eructate, C22:1				1.4	

The biokerosenes were blended at 5, 10, and 20% *v*/*v* of biokerosene, with the two types of fossil kerosene described above. In kerosene K2, additives are used to prevent the formation of oxidation deposits in aircraft engines and fuel systems, to inhibit the corrosion of steel, to improve the fuel lubricity and oxidation stability, to increase the electrical conductivity of the fuel, to avoid microbiological contamination, to prevent the ice formation in fuel

systems, and to assist in detecting fuel leaks. The ASTM D1655-09a standard fixes the allowed additives in jet fuels.[30]

To prepare the blends of fossil kerosene (K1 and K2) and 5, 10, and 20% *v*/*v* of FAME pipettes, beakers and volumetric flasks with the maximum precision (DIN 12600) were used. These amounts were established in order to evaluate a progressive incorporation of these renewable fuels into the aviation jet fuels.

Only the specifications considered essential among those required by the standard ASTM D1655-09a were tested, although of course all these standard specifications and the "fit for purpose" properties included in the "*Handbook of Aviation Fuel Properties*" published by the Coordinating Research Council (CRC)[31] should also be accomplished before any test flight.

2.2. Experimental Setup, Conditions, and Calibration. Smoke point is defined as the height in millimeters of the highest flame produced without smoking soot breakthrough when the fuel is burned in a specific test lamp.[32] Numerous studies[33−35] defined the sooting tendency of fuels and blends as inversely proportional to their smoke point. Consequently, a minimum value is required in jet fuel standards (min. twenty-five mm). A standard smoke point lamp as specified by ASTM D1322[32] was used for the smoke point measurements. A black-painted steel frame surrounding the apparatus was used to control air flow during the measurements. For each fuel, the smoke points were measured three times and averaged, and the standard deviation was obtained. Previously, the method was calibrated in accordance with ASTM D1322 using two standard reference fuel blends. The first blend, composed of 15% (*v*/*v*) toluene and 85% (*v*/*v*) 2,2,4-trimethylpentane (iso-octane), led to a smoke point of 25 mm, and the second blend, composed of 40% (*v*/*v*) toluene and 60% (*v*/*v*) 2,2,4-trimethylpentane, led to a smoke point of 15 mm. The comparison of the measured smoke points and those reported in the standard led to a correction factor of 1.006. The ambient temperature and relative humidity of the test site were monitored to make sure that fluctuations of environmental conditions did not affect the smoke points of the blends. The ambient temperature ranged from 21 to 25 °C, and the relative humidity ranged from 47 to 57%. All tests are performed at atmospheric pressure (around 93.5 kPa).

3. OXYGEN EXTENDED SOOTING INDEX

The inverse correlation between smoke point and sooting tendency of hydrocarbons was formulated by Calcote and Manos.[36] From this correlation, they defined the Threshold Sooting Index (*TSI*), which ranked arbitrarily the fuels from 0 to 100, with 0 being the lowest sooting value (assigned to ethane) and 100 the highest (assigned to naphthalene). The use of *TSI* permitted the use of all the literature data to interpret molecular structure effects and predict the sooting tendency of fuels under internal combustion engine conditions, and especially, of jet fuels in turbine combustors.[37] It was defined as

$$TSI = a\left(\frac{MW_f}{SP}\right) + b \tag{1}$$

where a and b are constants for any given experimental setup, MW_f is the molecular weight of the fuel, and SP is the measured smoke point. The inclusion of the molecular weight in the *TSI* correlation was justified by Calcote and Manos[36] because an increase in molecular weight requires more oxygen to diffuse into the flame to consume a unit volume of the fuel, which translates into an increased flame height. However, in case of oxygenated fuels, the molecular weight used in the *TSI* correlation is not a precise measure of the volumetric air to fuel ratio required by the flame for stoichiometric combustion. For a generic fuel with a mean formula $C_nH_mO_p$, this requirement is exactly quantified by $n + m/4 - p/2$, which is not proportional to $MW_f = 12n+m+16p$, especially in the case of oxygenates. Based on this evidence, a new Oxygen Extended Sooting Index (*OESI*) was recently proposed:[24]

$$OESI = a'\left(\frac{n + \frac{m}{4} - \frac{p}{2}}{SP}\right) + b' \tag{2}$$

OESI, similarly to *TSI*, permits comparing different sets of data obtained in different laboratories or different burners by scaling and adjusting the proportionality constants a' and b' of each data set. In this case, these constants were determined assigning the sooting index values proposed by Olson et al.[38] to toluene and isooctane (pure reference hydrocarbons used for the smoke point calibration in ASTM D1322) and the sooting index values obtained by mole-fraction weighting to the blends of both. This mixing rule was proposed by Gill and Olson,[35] who proved that the sooting tendency of blends in diffusion flames can be weighted proportionally to the molar fraction of their components. The identification of the *TSI* values proposed by Olson et al.[38] with the *OESI* values obtained here guaranties that the latter sooting index values remain in the same scale 0−100 with reference to ethane-naphthalene. The values finally obtained for the application of eq 2 were as follows: $a' = 43.588\ \text{mm}^{-1}$ and $b' = -5.7177$, Figure 1.

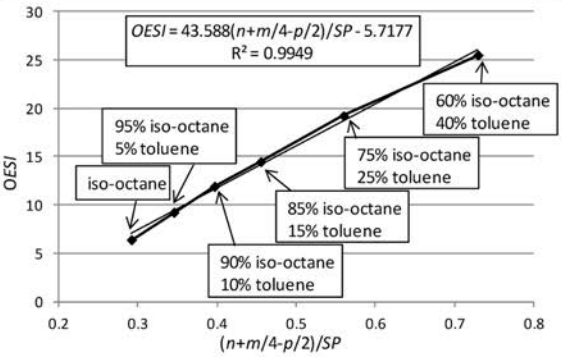

Figure 1. Calibration for the Oxygen Extended Sooting Index (*OESI*) with sooting index values of reference toluene/iso-octane blends.

4. RESULTS AND DISCUSSION

4.1. Smoke Point. As shown in Figure 2, none of the tested fossil kerosenes met the smoke specification. The commercial Jet A1 (here named as K2) showed a smoke point value very

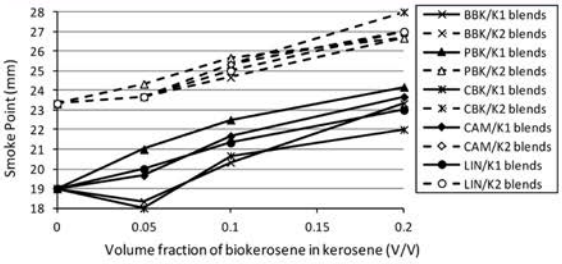

Figure 2. Smoke points of fossil kerosenes (K1 and K2) and blends with babassu biokerosene (BBK), palm kernel biokerosene (PBK), coconut biokerosene (CBK), camelina methyl ester (CAM), and linseed methyl ester (LIN)

dx.doi.org/10.1021/ef401623t | *Energy Fuels* 2013, 27, 6815−6822

close to the limit specified (*SP* > 25 mm) and also very similar to the smoke of other commercial jet fuels such as JP8, measured by other researchers under similar conditions.[37] However, kerosene K1, directly obtained from straight-run atmospheric distillation cut, was far from meeting specification, thus requiring significant, and therefore expensive, use of additives. Blending with selected and distilled (here termed as biokerosenes) or nondistilled fatty acid methyl esters is an effective alternative to reduce the soot formation and thus to increase the smoke point. In the case of FAME, the main mechanisms of formation of soot precursors (mainly acetylenes and aromatics[39]) are hindered by the formation of oxygenate intermediate species,[40] which are more stable than the products derived from the thermal decomposition of paraffinic, naphthenic, and aromatic hydrocarbons, typically composing the fossil kerosenes. In fact, the blends of coconut and palm kernel biokerosenes and camelina and linseed methyl esters with Jet A1 (K2) at 10% v/v met this specification. Only babassu biokerosene did not meet it although it was very close. Blends at 20% met the specification in all cases by far. In almost all cases the smoke point of the blends increased approximately linearly with the volume fraction of the biokerosene. In the case of kerosene K1, a linear extrapolation indicates that around 30% of most of the biokerosenes would be enough to reach the specification limit. Based on the mean standard deviation (0.425 mm), the described trends can be considered significant.

4.2. Sooting Tendency. The translation of the formerly presented smoke point results to sooting tendency, quantified with the *OESI*, leads to the results presented in Figure 3. These

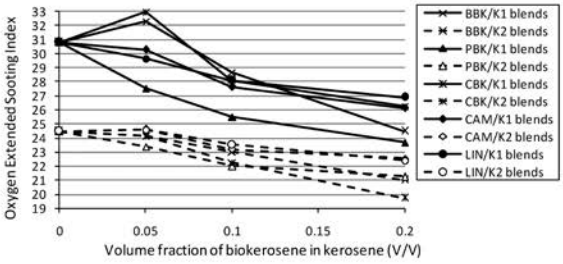

Figure 3. Oxygen Extended Sooting Index of fossil kerosenes (K1 and K2) and blends with babassu biokerosene (BBK), palm kernel biokerosene (PBK), coconut biokerosene (CBK), camelina methyl ester (CAM), and linseed methyl ester (LIN).

results are not exactly inverse to those presented in Figure 2 because the chemical composition of the biokerosenes was slightly different. However, these results provide a quantification of the ability of biokerosenes to reduce the sooting tendency of the kerosene fuels. All tested biokerosenes showed significant reductions of sooting tendency. Among them, that made from palm kernel oil was shown to be the most effective one (24% reduction when blended with K1 at 20% vol.), and nondistilled methyl esters (from camelina and linseed oils) showed, in general, lower effectiveness than distilled biokerosenes to reduce the sooting tendency. Distilled methyl esters have shorter carbon chains and, therefore, higher oxygen fraction as well as lower fraction of carbon−carbon bonds, which have a greater contribution to the formation of soot nuclei than those with higher concentration of carbon−hydrogen and carbon−oxygen bonds.[24] The latter conclusion is not observed from the smoke point data (Figure 2), demonstrating that the quantification through the *OESI* reveals some valuable additional information about the sooting tendency of the blends.

5. REBUTTAL OF RECENT CRITICISM TO FAME BASED BIOKEROSENES

5.1. Summary of Previous Work. In two recent papers[26,27] the authors have described the production of biokerosene from oils rich in short chain fatty acids, like coconut, palm kernel, and babassu, by transesterification and vacuum distillation of the FAME fraction of these oils, therefore entering the carbon range of fossil kerosene. Since these pure biokerosenes did not meet the different aviation jet fuel standards, blends containing 5, 10, and 20% *v*/*v* of biokerosene with fossil kerosene were tested together with pure biokerosene. Also the FAME from camelina oil and linseed oil (the latter with unpublished results so far), very rich in unsaturated methyl esters (84.7% wt and 89.8% respectively), were blended without previous distillation at 5, 10, and 20% *v*/*v* with fossil kerosene. The excellent cold flow behavior of these unsaturated methyl esters suggested direct blending without previous distillation. Table 2 shows the oxygen content, the energy density on a volume basis, and the smoke point for these blends and for Jet A1. The lower heating value (*LHV*), the density (*d*), and the energy density (*ED*) for the already ASTM approved renewable jet fuels are as follows: FT-SPK, *LHV* = 44.2 MJ/kg, *d* = 759 kg/m^3, and *ED* = 33.55 GJ/m^3; HEFA, *LHV* = 44.3 MJ/kg, *d* = 770 kg/m^3, and *ED* = 34.11 GJ/m^3.[1] It is true that the lower heating value of these biokerosene blends is lower than that of Jet A1, but as their density is also higher, the energy density (GJ/m^3 fuel) is always higher (or of the same magnitude, except for pure babassu and coconut biokerosenes) than Jet A1 and it is also higher than that of the biokerosenes approved by the ASTM, FT-SPK, and HEFA. This important fact could make these blends as suitable for commercial use as other biokerosenes but with the additional presence of oxygen that is always beneficial for fuels as explained above. Since fuels are injected in a volumetric dosage, the fact that the same volume of biokerosene blend injected produces the same amount of energy as Jet A1 could overcome some drawbacks of these new fuels.[41,42] Other properties of these blends have been extensively discussed in previous papers. Although some of the tested oils (babassu, coconut, and palm kernel) led to methyl esters which could be suitable for blending with aviation kerosene, a large commercial scale would probably make them environmentally unsustainable,[43] and, therefore, different production alternatives (e.g., via microbial processes) should be explored. However, the publication of one of these papers has aroused a controversy over the use of these FAME's as blend components for jet fuel.[25] After presenting the beneficial effects that the presence of oxygen in the biokerosene blends has on the sooting tendency of these alternative jet fuels, a second aim of this paper is to answer the comments mentioned in ref 25.

5.2. Oxidation Stability. Wilson et al.[25] recognize the following: "It is possible to produce FAME blends that will pass the standard test (they refer to ASTM D3241 Standard Test Method for Thermal Oxidation Stability of Aviation Turbine Fuels) but that would just open a new line of research to determine if the method provides suitable results with such a fuel". The aim of our papers was precisely to open new research lines in the field of biofuels.

Table 2. Properties of the Blends: Heating Values, Density, Composition, Energy Density, and Smoke Point

babassu	BBK_0/ K1_100	BBK_5/ K1_95	BBK_10/ K1_90	BBK_20/ K1_80	BBK_100/ K1_0	BBK_0/ K2_100	BBK_5/ K2_95	BBK_10/ K2_90	BBK_20/ K2_80	BBK_100/ K2_0
HHV, MJ/kg[26]	47.40	45.63	45.16	44.66	37.41	46.04	45.95	45.54	44.75	37.41
LHV, MJ/kg[26]	44.43	42.82	42.36	41.89	34.93	42.90	43.12	42.74	42.04	34.93
LHV, MJ/kg (ASTM D4809)	44.45	42.84	42.38	41.91	34.96	42.93	43.14	42.76	42.07	34.96
density at 15 °C, kg/m^3	793.0	805.9	809.2	816.6	874.5	791.0	804.0	807.7	814.9	874.5
C, % m/m	85.90	84.98	84.79	82.97	73.38	84.12	85.81	84.13	78.35	73.38
H, % m/m	13.88	13.16	13.11	12.95	11.55	14.67	13.25	13.08	12.64	11.55
N, % m/m	0.02	0.02	0.02	0.02	0.11		0.11	0.13	0.15	0.11
S, % m/m	0.17	0.16	0.13	0.13	0.10		0.10	0.10	0.20	0.10
O, % m/m	0.22	1.68	1.95	3.93	14.86	1.22	0.73	2.56	8.66	14.86
energy density, GJ/m^3	35.23	34.51	34.28	34.21	30.55	33.93	34.67	34.52	34.26	30.55
smoke point, mm	19.00	18.33	20.33	23.33	22.8	23.33	23.67	24.67	26.67	22.8
camelina	CAM_0/ K1_100	CAM_5/ K1_95	CAM_10/ K1_90	CAM_20/ K1_80	CAM_100/ K1_0	CAM_0/ K2_100	CAM_5/ K2_95	CAM_10/ K2_90	CAM_20/ K2_80	CAM_100/ K2_0
HHV, MJ/kg[26]	47.40	45.30	45.00	44.80	40.00	46.04				
LHV, MJ/kg[26]	44.43	42.52	42.30	42.14	37.62	42.90				
LHV, MJ/kg (ASTM D4809)	44.45	42.54	42.32	42.16	37.65	42.93				
density at 15 °C, kg/m^3	793.0	806.7	810.8	819.8	889.3	791.0				
C, % m/m	85.90	85.29	84.23	83.86	77.09	84.12				
H, % m/m	13.88	12.99	12.61	12.45	11.09	14.67				
N, % m/m	0.02	0.02	0.02	0.02	0.02					
S, % m/m	0.17	0.05	0.03	0.03	0.06					
O, % m/m	0.22	1.65	3.11	3.64	11.74	1.22				
energy density, GJ/m^3	35.23	34.30	34.30	34.55	33.46	33.93				
smoke point, mm	19.00	19.67	21.67	23.67		23.33	23.67	25.33	27.00	
coconut	CBK_0/ K1_100	CBK_5/ K1_95	CBK_10/ K1_90	CBK_20/ K1_80	CBK_100/ K1_0	CBK_0/ K2_100	CBK_5/ K2_95	CBK_10/ K2_90	CBK_20/ K2_80	CBK_100/ K2_0
HHV, MJ/kg[27]	47.40	45.32	44.47	43.94	37.66	46.04				
LHV, MJ/kg[27]	44.43	42.40	41.61	41.06	35.06	42.90				
LHV, MJ/kg (ASTM D4809)	44.45	42.42	41.63	41.08	35.09	42.93				
density at 15 °C, kg/m^3	802.0	805.0	807.0	812.0	867.0	791.0				
C, % m/m	85.90	84.84	83.44	82.14	72.35	84.12				
H, % m/m	13.88	13.68	13.37	13.46	12.12	14.67				
O, % m/m	0.22	1.48	3.19	4.40	15.54	1.22				
energy density, GJ/m^3	35.63	34.13	33.58	33.34	30.40	33.93				
smoke point, mm	19.00	18.00	20.67	22.00		23.33	23.67	25.33	28.00	
palm kernel	PBK_0/ K1_100	PBK_5/ K1_95	PBK_10/ K1_90	PBK_20/ K1_80	PBK_100/ K1_0	PBK_0/ K2_100	PBK_5/ K2_95	PBK_10/ K2_90	PBK_20/ K2_80	PBK_100/ K2_0
HHV, MJ/kg[27]	47.40	45.31	45.08	44.01	37.57	46.04	45.68	45.17	44.21	
LHV, MJ/kg[27]	44.43	42.51	42.13	41.20	34.89	42.90	42.64	42.18	41.19	
LHV, MJ/kg (ASTM D4809)	44.45	42.53	42.15	41.22	34.92	42.93	42.66	42.21	41.22	
density at 15 °C, kg/m^3	793.0	800.0	804.2	812.0		791.0	802.3	805.5	811.8	
C, % m/m	85.90	84.79	84.17	82.73	71.84	84.12	84.47	84.17	82.57	
H, % m/m	13.88	13.10	13.82	13.13	12.51	14.67	14.24	13.97	14.11	
O, % m/m	0.22	2.11	2.01	4.14	15.65	1.22	1.29	1.86	3.32	
energy density, GJ/m^3	35.23	34.01	33.88	33.45		33.93	34.21	33.98	33.44	
smoke point, mm	19.00	21.00	22.50	24.17		23.33	24.33	25.67	26.67	

On the other hand, being aware that the Rancimat method is not an approved method to measure the oxidation stability of jet fuels, in this test, the fuels are heated at 110 °C and to pass the test the induction time should be higher than 8 h, whereas in the ASTM 3241 test (JFTOT procedure), the duration of the heating at 260 °C (325 °C for SPK) is only 2.5 h., that is, the Rancimat temperature is lower but the test time is almost four times longer. The inverse relation between temperature and induction time, together with the evidence that lower temperature assures a better reproducibility of the test,[44] makes the Rancimat an appropriate test for comparing the oxidation stability of FAME-blended aviation fuels. Other methods such as the rapid small scale oxidation method[45] (which is not approved for jet fuels either) could be another alternative option.

dx.doi.org/10.1021/ef401623t | *Energy Fuels* 2013, 27, 6815−6822

5.3. Lower Heating Value. Wilson et al.[25] state that ASTM D240 is not an appropriate test for measuring the lower heating value of aviation turbine fuels and propose using ASTM D4809 instead. On the contrary, we believe that none of these methods is an appropriate one for oxygenated fuels. Both standard methods, ASTM D240 and ASTM D4809, use the same equation to calculate the lower heating value

$$LHV\ (\text{net},\ 25\ ^\circ\text{C}) = HHV\ (\text{gross},\ 25\ ^\circ\text{C}) - 212.2\ H \quad (3)$$

where *LHV* is the net heat of combustion at constant pressure (lower heating value) in kJ/kg, *HHV* is the gross heat of combustion at constant volume (higher heating value) in kJ/kg, and *H* is the mass % of hydrogen in the sample. Equation 3 was derived from simple combustion stoichiometry and considering the thermodynamic conversion from constant volume to constant pressure, but this equation does not consider the possibility of any oxygen content in the fuel. A similar combustion/thermodynamic approach leads, in the case of oxygenated fuels, to the following equation

$$LHV\ (\text{net},\ 25\ ^\circ\text{C}) = HHV\ (\text{gross},\ 25\ ^\circ\text{C}) - 213.65\ H - 0.77\ O \quad (4)$$

where *LHV* is the net heat of combustion at constant pressure (lower heating value) in kJ/kg, *HHV* is the gross heat of combustion at constant volume (higher heating value) in kJ/kg, and *H* and *O* are the mass % of hydrogen and oxygen respectively in the fuel sample. Equation 4 (and not eq 3) was used in our previous studies.[26,27] Nevertheless, both sets of values, resulting from both ASTM D4809 and from eq 4, are included in Table 2, and it is clear that the values obtained with eq 4 are always lower by −20 or −30 kJ/kg, and, therefore, they are more conservative than those obtained by the standard official method. As regards the accuracy of the experimental *HHV* values, those are the mean of three replicate results and the standard deviations ranged from 50.3 to 256.7 kJ/kg.

5.4. Kinematic Viscosity. We agree with the authors of ref 25 that the kinematic viscosity is a critical performance parameter for aviation jet fuels. Thus, the kinematic viscosity at −20 °C was measured for the 5, 10, and 20% vol. blends of coconut and palm kernel biokerosenes with fossil kerosenes,[27] whereas the kinematic viscosity of 5, 10, and 20% vol blends of camelina FAME with fossil kerosene was estimated by a linear extrapolation method, following ASTM D341 standard[46] from measurements at 40 and 100 °C.

5.5. Fluidity at Low Temperature. Wilson et al. stated[25] that "only freeze point tests, such as ASTM D2386, D5972, or D7153, are acceptable tests for determining conformance to D1655. The term "freeze point" actually describes the recovery temperature of the fuel, which is the temperature at which the fuel will be in the liquid phase regardless of how cold it has been".

In our opinion, this last sentence describes the "melting point" of the jet fuel, not the "freezing point". To clarify this point, additional Differential Scanning Calorimetric (DSC) analyses have been made on the palm kernel biokerosene blends with kerosene K1, going from ambient to low temperature (−90 °C) and coming back to ambient temperature. Always a hysteresis appears between the freezing point (temperature where the first crystals appear) and the melting point (temperature where all crystals disappear and the fuel returns to liquid phase), the freezing point being always lower than the melting point.

Moreover, in a paper previous to the one that has aroused this criticism,[27] the manual freezing point measured after ASTM D2386[47] was carried out for the blends of palm kernel biokerosene with fossil K1, showing almost no change from pure K1 to a blend with 20% vol. of biofuel (−42 ± 1 °C), while only the pure biofuel showed an important increase to −15.3 °C. This clearly indicates the difficulties of the measuring procedure already pointed out in our previous papers[26,27] that led us to use the cloud point,[48] the pour point,[49] and the cold filter plugging point[50] to check the cold flow behavior of those blends more precisely. On the contrary, both the DSC-measured freezing and melting points (shown in Figure 4) show the expected linear increase with the increasing concentration of biofuel, with the above-mentioned hysteresis in between, in agreement with other authors.[51−53]

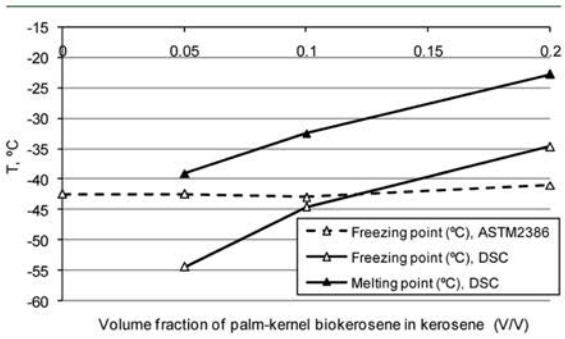

Figure 4. Freezing points of the blends of palm kernel biokerosene with fossil kerosene without additives, measured after ASTM D2386 and using Differential Scanning Calorimetry.

5.6. Fuel Gauging Performance and Other Performance Properties. Aircraft fuel tanks are filled by means of hoses with positive displacement sensors, and once filled, the tanks have pressure sensors that give information of the mass charged in the tank. In both cases, the measurement depends on the density of the fuel, but all the blends described in this paper satisfy the ASTM requirements for this property.

During flight, the measurement of fuel in the tank is carried out by means of capacitive type sensors that depend on the dielectric constant of the fuel. The scarce literature information about the value of the dielectric constant for blends of fossil diesel and biodiesel gives values between 2.0 for diesel and 3.1 for biodiesel.[54] Thus, in case the performance of these blends could be monitored in flight, the necessary adjustment of these instruments should be done.

6. CONCLUSIONS

Biokerosenes produced from transesterification and distillation favor the reduction in soot emissions (and thus particulate emissions) as a consequence of the presence of molecular oxygen. This fact should be considered, additionally to other benefits and drawbacks studied in previous work, when comparing this type of biokerosenes with other renewable options, such as hydroprocessed esters and fatty acids. The sooting tendency was quantified in this work with an oxygen-extended sooting index (*OESI*), based on smoke point measurements. Among the tested biokerosenes (derived from babassu, camelina, coconut, linseed, and palm kernel oils),

OESI results have shown that the biokerosene made from palm kernel oil was the most effective one, and nondistilled methyl esters (from camelina and linseed oils) showed lower effectiveness than distilled biokerosenes to reduce the soot formation tendency. This conclusion is not evident when smoke point results are directly observed, demonstrating that the quantification through the *OESI* reveals additional information about the sooting tendency.

A previous publication from these authors has aroused some controversy over the use of FAME as blending components with fossil kerosenes. Many of the arguments given are based on the evidence that the methods used in the previous work are not approved for jet fuels in the standard methods. The authors of the criticism conclude that the use of FAME in any amount is, thus, inappropriate, therefore discouraging any research on this field and any revision of the standard methods. However, some of the standard methods are not updated for considering oxygenated components. This is the case of lower heating value, for which an equation which does not consider the possibility of any oxygen content in the fuel is still used. Other methods have been shown to have low accuracy, such as the methods for measuring the freezing point, and some alternative methods, such as cold filter plugging point or differential scanning calorimetry for cold flow properties, or Rancimat, for oxidation stability of oil-derived kerosenes, may provide better reproducibility, at least in the case of oxygenated fuels.

■ AUTHOR INFORMATION

Corresponding Author

*Phone: +34-926295431. Fax: +34-926295361. E-mail: Magin.Lapuerta@uclm.es.

Notes

The authors declare no competing financial interest.

■ ACKNOWLEDGMENTS

We wish to thank Iván Cruz Plata for carrying out the smoke point tests, and the Petrochemistry & Fuels Laboratory of the Foundation Gómez-Pardo for technical help.

■ REFERENCES

(1) Bomgardner, M. M. Flying the green skies with biofuels. *Chem. Eng. News* **2012**, June *11th*, 18−20.

(2) O'Neil, K. Alternative jet fuels cut particulate emissions. *Chem. Eng. News* **2011**, Nov. *21st*, 2.

(3) Beck, J. P.; Reeves, C. E.; De Leeuw, F. A. A. M.; Penkett, S. A. The effect of aircraft emissions on tropospheric ozone in the northern hemisphere. *Atmos. Environ.* **1992**, *26A* (1), 17−29.

(4) Mahashabde, A.; Wolfe, P.; Ashok, A.; Dorbian, C.; He, O.; Fan, A.; Lukachko, S.; Mozdzanowska, A.; Wollersheim, C.; Barrett, S. R. H.; Locke, M.; Waitz, I. A. Assessing the environmental impacts of aircraft noise and emissions. *Prog. Aerospace Sci.* **2011**, *47*, 15−52.

(5) ATAG (Air Transport Action Group): "Beginner's Guide to Aviation biofuels" (May 2009).

(6) Airbus (2012): "Airbus global Market Forecast 2011-2031".

(7) European Directive **2008**/101/CE on Aviation Gas Emission.

(8) Spanish Law 13/2010, BOE 6th July 2010, *163*: 59586−59627.

(9) Hogue, C. Unfriendly skies. *Chem. Eng. News* **2011**, October *17th*, 48−50.

(10) *Chem. Eng. News* **2012**, September *30th*, 42.

(11) ICAO (International Civil Aviation Organization). http://www.icao.int/ (accessed October 15, 2013).

(12) Europa Press (online version July 8th 2012). http://europapress.es/ (accessed September 2012).

(13) ASTM International. ASTM D4054-09. *Standard Practice for Qualification and Approval of New Aviation Turbine Fuels and Fuel Additives*; ASTM International: West Conshohocken, PA, 2012.

(14) Dunn, R. O. Alternative jet fuels from vegetable oils. *Trans. ASAE* **2001**, *44−6*, 1751−1757.

(15) Dagaut, P.; Gail, S. Kinetics of gas turbine liquid fuels combustion: Jet A1 and biokerosene. *Proc ASME Turbo Expo* **2007**, *2*, 93−101.

(16) Korres, D. M.; Karonis, D.; Lois, E.; Linck, M. B.; Gupta, A. K. Aviation fuel JP-5 on a biodiesel engine. *Fuel* **2008**, *87*, 70−78.

(17) Wagutu, A. W.; Chabra, S. C.; Thoruwa, C. L.; Thoruwa, T. F.; Mahunnah, R. L. A. Indigenous oil crops as a source for production of biodiesel in Kenyia. *Bull. Chem. Soc. Ethiop.* **2009**, *3−3*, 359−370.

(18) Hileman, J. I.; Stratton, R. W.; Donohoo, P. E. Energy content and alternative jet fuel viability. *J. Propul. Power* **2010**, *26* (6), 1184−1195.

(19) Cottineau, J. Green Chemistry. Bio motor fuels. The aviation industry unveils bio-kerosene. *Info Chim. Mag.* **2008**, *45* (490), 27.

(20) (a) World news: France: The BTL Chain. *Hydrocarbon Eng.* **2010**, *15* (4), 8. (b) Uhde's Prenflo process to be part of joint R&D project BioTfueL in France. *Chem. Eng.* **2010**, *117* (4), 79.

(21) Gill, S. S.; Tsolakis, A.; Dearn, K. D.; Rodríguez-Fernández, J. Combustion characteristics and emissions of Fischer−Tropsch diesel fuels in IC engines. *Prog. Energy Combust. Sci.* **2011**, *37*, 503−523.

(22) Kinder, J. D.; Rahms, T. *Evaluation of Bio-Derived Synthetic Paraffinic Kerosene (Bio-SPK)*. The Boeing Company, June 2009. www.boeing.com (accessed October 15, 2013).

(23) ASTM International. ASTM D7566-11. *Standard specification for aviation turbine fuel containing synthesized hydrocarbons*; ASTM International: West Conshohocken, PA, 2011.

(24) Barrientos, E. J.; Lapuerta, M.; Boehman, A. L. Group additivity in soot formation for the example of C-5 oxygenated 4 hydrocarbon fuels. *Combust. Flame* **2013**, *160*, 1484−1498.

(25) Wilson, G. R., III; Edwards, T.; Corporan, E.; Freerks, R. L. Certification of alternative aviation fuels and blend components. *Energy Fuels* **2013**, *27*, 962−966.

(26) Llamas, A.; Al-Lal, A. M.; Hernandez, M.; Lapuerta, M.; Canoira, L. Biokerosene from babassu and camelina oils: production and properties of their blends with fossil kerosene. *Energy Fuels* **2012**, *26*, 5968−5976.

(27) Llamas, A.; García-Martínez, M. J.; Al-Lal, A. M.; Canoira, L. Biokerosene from coconut and palm kernel oils: Production and properties of their blends with fossil kerosene. *Fuel* **2012**, *102*, 483−490.

(28) Canoira, L.; Rodríguez-Gamero, M.; Querol, E.; Alcántara, R.; Lapuerta, M.; Oliva, F. Biodiesel from low-grade animal fat: production process assessment and biodiesel properties characterization. *Ind. Eng. Chem. Res.* **2008**, *47*, 7997−8004.

(29) Lapuerta, M.; Canoira, L.; Raez, J. Improved method for determining the atmospheric distillation curve of biodiesel fuels from reduced pressure. *Ind. Eng. Chem. Res.* **2011**, *50*, 7041−7048.

(30) ASTM International. ASTM D1655-09a. *Standard specification for aviation turbine fuels*; ASTM International: West Conshohocken, PA, 2009.

(31) Coordinating Research Council (CRC). *Handbook of Aviation Fuels Properties*; CRC: Alpharetta, GA, 2004; CRC Report 635.

(32) ASTM International. ASTM D 1322-08. *Standard Test Method for Smoke Point of Kerosine and Aviation Turbine Fuel*; ASTM International: West Conshohocken, United States, 2008.

(33) Minchin, S. T. Luminous stationary flames: the quantitative relationship between flame dimensions at the sooting point and chemical composition, with special reference to petroleum hydrocarbons. *J. Inst. Petrol. Technol.* **1931**, *17* (88), 102−120.

(34) Clarke, A. E.; Hunter, T. G.; Garner, F. H. The tendency to smoke of organic substances on burning. *J. Inst. Pet.* **1946**, *32*, 627−642.

(35) Gill, R. J.; Olson, D. B. Estimation of soot thresholds for fuel mixtures. *Combust. Sci. Technol.* **1984**, *5−6*, 307−315.

(36) Calcote, H. F.; Manos, D. F. Effect of molecular structure on incipient soot formation. *Combust. Flame* **1983**, *49*, 289−304.
(37) Yang, Y.; Boehman, A. L.; Santoro, R. J. A study of jet fuel sooting tendency using the threshold sooting index (TSI) model. *Combust. Flame* **2007**, *149*, 191−205.
(38) Olson, D. B.; Pickens, J. C.; Gill, R. G. The effects of molecular structure on soot formation II: diffusion flames. *Combust. Flame* **1985**, *62*, 43−60.
(39) Blanquart, G.; Pepiot-Desjardins, C.; Pitsch, H. Chemical mechanism for high temperature combustion of engine relevant fuels with emphasis on soot precursors. *Combust. Flame* **2009**, *156*, 588−607.
(40) Westbrook, C. K.; Pitz, W. J.; Curran, H. J. Chemical kinetic modeling study of the effects of oxygenated hydrocarbons on soot emissions from diesel engines. *J. Phys. Chem. A* **2006**, *110*, 6912−6922.
(41) Blakey, S.; Rye, L.; Wilson, C. W. Aviation gas turbine alternative fuels: A review. *Proc. Combust. Inst.* **2011**, *3*, 2863−2885.
(42) Rye, L.; Blakey, S.; Wilson, C. W. Sustainability of supply or the planet: a review of potential drop-in alternative aviation fuels. *Energy Environ. Sci.* **2010**, *3*, 17−27.
(43) Fargione, J.; Hill, J.; Tilman, D.; Polasky, S.; Hawthorne, P. Land clearing and the biofuel carbon debt. *Science* **2008**, *319* (5867), 1235−1238.
(44) Lapuerta, M.; Rodríguez-Fernández, J.; Ramos, A.; Alvarez, B. Effect of the test temperature and anti-oxidant addition on the oxidation stability of commercial biodiesel fuels. *Fuel* **2012**, *93* (1), 391−396.
(45) European Committee for Standarization. EN 16091:2011. Liquid petroleum products. Middle distillates and fatty acid methyl ester (FAME) fuels and blends. Determination of oxidation stability by rapid small scale oxidation method. European Committee for Standarization 2011, Brussels, Belgium.
(46) ASTM International. ASTM D341-09. *Standard practice for viscosity temperature charts for liquid petroleum products*; ASTM International: West Conshohocken, PA, 2009.
(47) ASTM International. ASTM D2386-06. *Standard Test Method for Freezing Point of Aviation Fuels*; ASTM International: West Conshohoken, PA, 2006.
(48) ASTM International. ASTM D2500-02. *Standard Test Method for Cloud Point of Petroleum Products*; ASTM International: West Conshohoken, PA, 2002.
(49) ASTM International. ASTM D97-07. *Standard Test Method for Pour Point of Petroleum Products*; ASTM International: West Conshohoken, PA, 2007.
(50) ASTM International. ASTM D6371-05. *Standard Test Method for Cold Filter Plugging Point of Diesel and Heating Fuels*; ASTM International: West Conshohoken, PA, 2005.
(51) Dunn, R. O.; Bagby, M. O. Low-temperature properties of triglyceride-based diesel fuels: transesterified methyl esters and petroleum middle distillate/ester blends. *J. Am. Oil Chem. Soc.* **1995**, 72 (8), 895−904.
(52) Tang, H.; Salley, S.; Ng, K. S. Fuel properties and precipitate formation at low temperatures in soy-, cottonseed- and poultry-fat based biodiesel blends. *Fuel* **2008**, *87*, 3006−3017.
(53) Dunn, R. O. Effect of minor constituents on cold flow properties and performance of biodiesel. *Prog. Energy Combust. Sci.* **2009**, *35*, 481−489.
(54) Vazquez-Gay, R. A. Design, construction and calibration of an equipment to measure the dielectric constant of lubricants diluted with different fuels. B.Sc. Thesis No. 10-10-200930, Universidad De Castilla-La Mancha, ETS Ingenieros Industriales, Ciudad Real, Spain.

6 REFERENCES

237. SHELDON, R.A. *Consider the Environmental Quotient. CHEMTECH . ,* 1994, (March), 38, 1994.

238. SCHOBER, S., SEIDL, I. and MITTELBACH, M. Ester Content Evaluation in Biodiesel from Animal Fats and Lauric Oils. *European Journal of Lipid Science and Technology*, 2006, vol. 108, no. 4. pp. 309-314.

239. KINNEY, A.J. and CLEMENTE, T.E. Modifying Soybean Oil for Enhanced Performance in Biodiesel Blends. *Fuel Processing Technology*, 6/25, 2005, vol. 86, no. 10. pp. 1137-1147.

240. BRINGE, N.A. The Biodiesel Handbook; G. KNOTHE, J. VAN GERPEN and J. KRAHL eds., Champaign, IL,: AOCS, 2005; *Soybean Oil Composition for Biodiesel.*, pp. 161-164.

241. FREEDMAN, B., PRYDE, E.H. and MOUNTS, T.L. Variables Affecting the Yields of Fatty Esters from Transesterified Vegetable Oils. *Journal of the American Oil Chemists Society*, 1984, vol. 61, no. 10. pp. 1638 - 1643.

242. MENEGHETTI, S.P., et al. Ethanolysis of Castor and Cottonseed Oil: A Systematic Study using Classical Catalysts, 2006, vol. 83, no. 9 ISSN 0003-021X.

243. LEVENSPIEL, O. *Chemical Reaction Engineering.* 3rd ed. ed. New York,: John Wiley and Sons, 1999.

244. KNOTHE, G. Dependence of Biodiesel Fuel Properties on the Structure of Fatty Acid Alkyl Esters. *Fuel Processing Technology*, 6/25, 2005, vol. 86, no. 10. pp. 1059-1070.

245. IMAHARA, H., MINAMI, E. and SAKA, S. Thermodynamic Study on Cloud Point of Biodiesel with its Fatty Acid Composition. *Fuel*, 9, 2006, vol. 85, no. 12–13. pp. 1666-1670.

246. DUNN, R. Thermal Analysis of Alternative Diesel Fuels from Vegetable Oils, 1999, vol. 76, no. 1 ISSN 0003-021X.

247. DEMIRBAS, A. Importance of Biodiesel as Transportation Fuel. *Energy Policy*, 9, 2007, vol. 35, no. 9. pp. 4661-4670.

248. OLLETT, L. Assuring Quality and Consistency Of biodiesel. *Annual Fuels and Lubes Asia Conference and Exhibition*, 2007. pp. 18.

249. DUNN, R. Oxidative Stability of Soybean Oil Fatty Acid Methyl Esters by Oil Stability Index (OSI), 2005, vol. 82, no. 5 ISSN 0003-021X.

250. MONYEM, A. and H. VAN GERPEN, J. The Effect of Biodiesel Oxidation on Engine Performance and Emissions. *Biomass and Bioenergy*, 4, 2001, vol. 20, no. 4. pp. 317-325.

251. GOODRUM, J.W. and GELLER, D.P. Influence of Fatty Acid Methyl Esters from Hydroxylated Vegetable Oils on Diesel Fuel Lubricity. *Bioresource Technology*, 5, 2005, vol. 96, no. 7. pp. 851-855.

252. KNOTHE, G. and STEIDLEY, K.R., 2005, vol. 19, no. 3. pp. 1200 ISSN 0887-0624.

253. GARCÍA-MARTÍNEZ, M.J., et al. Continuous Photodegradation of Naphthalene in Water Catalyzed by TiO2 Supported on Glass Raschig Rings. *Chemical Engineering Journal*, 6/1, 2005, vol. 110, no. 1–3. pp. 123-128.

254. GARCÍA-MARTÍNEZ, M.J., et al. Photodegradation of Polycyclic Aromatic Hydrocarbons in Fossil Fuels Catalysed by Supported TiO2. *Applied Catalysis B: Environmental*, 10/5, 2006, vol. 67, no. 3–4. pp. 279-289. Available from:

255. ALCÁNTARA, R., et al. Photoxidation of Ethylbenzene with Air Catalyzed by a Polymer Supported Rose Bengal Photosensitizer. *Journal of Photochemistry and Photobiology A: Chemistry*, 5/8, 2000, vol. 133, no. 1–2. pp. 27-32.

256. GELLER, D.P. and GOODRUM, J.W. Effects of Specific Fatty Acid Methyl Esters on Diesel Fuel Lubricity. *Fuel*, 12, 2004, vol. 83, no. 17–18. pp. 2351-2356.

257. LAPUERTA, M., RODRÍGUEZ-FERNÁNDEZ, J., ESTEVEZ, C. and BAYARRI, N. Properties of Fatty Acid Glycerol Formal Ester (FAGE) for use as a Component in Blends for Diesel Engines. *Biomass and Bioenergy*, 5, 2015, vol. 76. pp. 130-140.

TABLE OF CONTENTS

1 CONCLUSIONS

- FAME from non-edible sources production and characterization.

- *Biodiesel from waste materials*

1 Low-grade animal fat, a cheap feedstock without any other use, was transformed into biodiesel. Due to its high content on FFA a previous esterification was required. Several mixtures of this feedstock and soybean oil were submitted to transesterification. The viscosity of pure animal fat biodiesel is slightly out of the specification.

2 Soy-bean oil, waste frying oil (50% mixture of olive and sunflower oil) and tallow were transformed into biodiesel by transesterification reaction with methanol.

The transesterification reaction of waste frying oil with methanol, catalysed with sodium methoxide, to produce biodiesel follows a first order kinetics (FOK) in methanol and also a FOK in triglycerides, with a rate constant of k = 0.2245 L mol-1 min-1.

- *FAME from non-edible plants.*

3 This thesis shows the successful production of a Jojoba-based FAME biodiesel which is close to meet the biodiesel standard EN 14214. Acid catalysis was dismissed since the basic catalysist products were easier to treat.
This was achieved through the use of sodium methoxide as a catalyst and a cryogenic separation of the products. While FAME from Jojoba can be produced in 55% yield, its use as a fuel will be dependant on the co-production of value added products from the fatty alcohols.

4 The optimal transesterification via basic catalysis from castor oil conditions have been found, being: 1 % wt. catalyst and 5:1 molar ratio of methanol to oil, temperature was set on 40 °C. Due to the alcohol group present in methyl ricinoleate, some of the castor oil FAME properties render it unsuitable in pure state for its direct use as fuel in internal combustion engines. Thus, blends with reference diesel have been prepared and their properties have been evaluated.. The blends of castor FAME and reference diesel until approximately 40 % vol. of castor FAME meet most of the specifications of the EN 590 standard.

- **Production of biokerosenes.**

5 Coconut, palm kernel and babassu oils have been transesterified with methanol by homogeneous basic catalysis with good yields. The FAME have been subjected to fractional distillation at vacuum, and the low boiling point fractions have been blended with two types of fossil kerosene, a straight-run atmospheric distillation cut (hydrotreated, K - 1) and commercial Jet A1 (K - 2).

The blends of babassu biokerosene and fossil kerosene cut K1 meet the following specifications of the ASTM D1655 standard: color, acidity, density, copper strip corrosion, and lower heating value (only the 5 vol % blend). While its blends of with Jet-A1 meet: lower heating value (10% vol blends), flash point, and smoke point as well.

The blends of fossil kerosene K-1 and palm kernel biokerosene only met the density parameter. Its blends with Jet A1 meet some specifications selected for study of the ASTM D1655 standard: smoke point, flash point and freezing point, and they do not comply with the lower heating value by a very narrow margin.

The blends of coconut biokerosene and K - 1 meet the density and lubricity specifications.

None of the blends of 5 % vol. of biokerosene and fossil kerosenes K - 1 and K - 2 meet the lower heating value by a very narrow margin of less than -1.0 MJ kg^{-1}.

- **PAH and soot emissions.**

6 In this thesis twelve different biodiesel have been burned in a bomb calorimeter in order to assess the PAH amounts formed depending on their sources and type of alcohol under four different oxygen abundance conditions.

An exponential model has been constructed to explain the formation of PAH where the most significant variables are the relative dosage, the iodine value and the percentage of saturated esters in the biodiesel. These PAH tend to show two different behaviors when statically grouped that may relate to heavy or light PAH formation. No statistical differences were found between FAME and FAEE in their ability to produce PAH on combustion under these experimental conditions.

7 Biokerosenes produced from transesterification and distillation favor the reduction in soot emissions (and thus particulate emissions) as a consequence of the presence of molecular oxygen.. The sooting tendency was quantified in this work with an oxygen extended sooting index (OESI), based on smoke point measurements. Among the tested biokerosenes (derived from babassu, camelina, coconut, linseed, and palm kernel oils), OESI results have shown that the biokerosene made from palm kernel oil was the most effective one, and nondistilled methyl esters (from camelina and linseed oils) showed lower effectiveness than distilled biokerosenes to reduce the soot formation tendency. However, some of the standard methods are not updated nor considering oxygenated components.

- **Production of additives from glycerine**

8 This thesis describes the synthesis of 1,3-di-tert-butoxypropan- 2-ol from epichlorohydrin, obtained from bioglycerol, in a three step process: chlorohydrin ether, glycidyl ether and 1,3-di-tertbutoxypropan- 2-ol synthesis respectively. Conversion is almost quantitative; however yield is decreasing about a 25% in each step. Among the four catalysts tested for the synthesis of ,3-di-tertbutoxypropan- 2-ol, boron trifluoride etherate provides the best results because it gives better yield and selectivity values, at the same quantitative conversion.